

Notice 1

Under the Copyright Act 1968, this thesis must be used only under the normal conditions of scholarly fair dealing. In particular no results or conclusions should be extracted from it, nor should it be copied or closely paraphrased in whole or in part without the written consent of the author. Proper written acknowledgement should be made for any assistance obtained from this thesis.

Notice 2

I certify that I have made all reasonable efforts to secure copyright permissions for third-party content included in this thesis and have not knowingly added copyright content to my work without the owner's permission.

Protective actions of phosphoinositide
3-kinase (p110 α) in a setting of
cardiomyopathy

Lynette Pretorius

B.Sc. (Hons).

Submitted in total fulfilment of the requirements for the degree of
Doctor of Philosophy

Faculty of Medicine, Nursing, and Health Sciences,
Department of Medicine (Alfred Hospital), Monash University
Cardiac Hypertrophy Laboratory, Baker IDI Heart & Diabetes Institute

December 2010



MONASH University
Medicine, Nursing and Health Sciences



Baker IDI
HEART & DIABETES INSTITUTE

Table of contents

<i>Table of contents</i>	<i>ii</i>
<i>Index of figures</i>	<i>ix</i>
<i>Index of tables</i>	<i>xiii</i>
<i>Summary of thesis</i>	<i>xv</i>
<i>Declaration</i>	<i>xvii</i>
<i>Acknowledgements</i>	<i>xviii</i>
<i>Prizes, publications and presentations during PhD candidature</i>	<i>xx</i>
<i>Dedication</i>	<i>xxvii</i>
<i>Abbreviations</i>	<i>xxviii</i>
<i>Chapter 1 – General introduction</i>	<i>1</i>
<i>1.1. Heart failure</i>	<i>1</i>
1.1.1. Impact of cardiovascular disease and heart failure.....	<i>1</i>
1.1.2. Association between cardiac hypertrophy and heart failure.....	<i>2</i>
1.1.3. Complications associated with hypertrophy and heart failure	<i>4</i>
<i>1.2. Normal cardiac structure and function</i>	<i>4</i>
1.2.1. Cellular structure of the cardiac myocyte.....	<i>4</i>
1.2.2. Energy metabolism in the normal heart.....	<i>7</i>
1.2.3. Structural scaffolding of the cardiac myocyte	<i>7</i>
1.2.4. Cardiac contractile function.....	<i>8</i>
1.2.4.1. The Frank-Starling mechanism	<i>8</i>
1.2.4.2. Excitation-contraction coupling.....	<i>8</i>
1.2.5. Electrophysiology.....	<i>9</i>
<i>1.3. Cardiac remodelling</i>	<i>11</i>
1.3.1. Cardiac hypertrophy.....	<i>11</i>
1.3.1.1. Physiological and pathological cardiac hypertrophy.....	<i>11</i>
1.3.1.2. Concentric and eccentric cardiac hypertrophy.....	<i>13</i>
1.3.1.3. Distinct features of physiological and pathological cardiac hypertrophy	<i>13</i>
1.3.2. Fibrosis	<i>16</i>
1.3.3. Cell death.....	<i>17</i>
1.3.4. Alterations in myocardial energy metabolism	<i>17</i>

1.3.5. Alterations in cardiac myocyte calcium homeostasis.....	18
1.3.6. Expression of embryonic genes and genes encoding contractile proteins in cardiac hypertrophy	19
1.3.7. Gender differences in cardiac hypertrophy and remodelling	21
1.4. Heart failure therapy	25
1.4.1. Current therapeutics	25
1.4.1.1. Drug therapy for heart failure and arrhythmia.....	25
1.4.1.2. Non-drug therapy	26
1.4.2. Limitations of current treatments and the need for new and effective medications	27
1.5. Triggers and signalling pathways that induce cardiac hypertrophy and remodelling ..	27
1.5.1. The IGF1-PI3K-Akt pathway	31
1.5.1.1. IGF1.....	31
1.5.1.2. PI3Ks	32
1.5.1.3. Akt	34
1.5.1.4. Benefits of IGF1-PI3K (p110 α)-Akt signalling in cardiac disease.....	37
1.5.2. G-protein coupled receptor pathways	37
1.5.3. MAPK and downstream pathways	39
1.5.3.1. ERK 1/2 pathway	40
1.5.3.2. JNKs.....	40
1.5.3.3. p38-MAPKs.....	41
1.5.4. Calcium signalling pathway.....	43
1.5.5. Mammalian sterile 20-like kinase 1.....	44
1.5.6. Crosstalk between PI3K and GPCR regulated signalling pathways in the heart.....	44
1.5.7. Signalling mechanisms that mediate gender differences	46
1.5.7.1. Gender differences in genetic mouse models.....	50
1.5.7.2. Crosstalk between PI3K and estrogen-receptor mediated signalling	51
1.5.8. Signalling and atrial fibrillation	51
1.6. Outline of PhD project.....	58
1.6.1. Project rationale	58
1.6.1.1. Benefits of PI3K (p110 α) signalling in a model of dilated cardiomyopathy.....	58
1.6.1.2. PI3K (p110 α) and atrial fibrillation.....	59
1.6.1.3. The role of PI3K (p110 α) in estrogen-mediated cardioprotection.....	60
1.6.2. Aims of PhD project.....	61
1.6.3. Hypotheses of PhD project	61
Chapter 2 – Materials and methods.....	62
2.1. Ethics approval for animal and human care and experimentation	62

2.1.1. Ethics approval and animal care for mouse studies.....	62
2.1.2. Ethics approval for human studies.....	62
2.2. Generation of cardiac-specific transgenic mouse models.....	62
2.2.1. Constitutively active PI3K transgenic mice.....	62
2.2.2. Dominant negative PI3K transgenic mice.....	63
2.2.3. Mst1 transgenic mice.....	63
2.2.4. Kinase dead Akt transgenic mice.....	63
2.2.5. Double-transgenic mice.....	63
2.2.6. Triple-transgenic mice.....	64
2.3. Genotyping.....	66
2.3.1. Mouse tail DNA digestion and extraction.....	66
2.3.2. PCR.....	66
2.4. Measurement of cardiac function and electrophysiology.....	68
2.4.1. Echocardiography.....	68
2.4.2. Catheterisation.....	70
2.4.3. Electrocardiography.....	73
2.4.4. Intracardiac electrocardiography catheterisation.....	73
2.4.5. Telemetry.....	76
2.5. Ovariectomy and hormone replacement therapy.....	77
2.6. Tissue harvesting and tibia length measurement.....	80
2.7. Protein expression analysis.....	81
2.7.1. Heart homogenisation.....	81
2.7.2. Protein extraction.....	81
2.7.3. Measurement of protein concentration – Bradford assay.....	82
2.7.4. Western blotting.....	82
2.7.5. Immunoprecipitation.....	86
2.7.6. PI3K activity assay.....	87
2.7.6.1. Mouse ventricular tissue.....	87
2.7.6.2. Human atrial tissue.....	88
2.7.7. Gelatin Zymography.....	89
2.8. Gene expression analysis.....	90
2.8.1. RNA extraction.....	90
2.8.2. Measurement of RNA concentration and quality.....	90
2.8.3. Northern gel preparation and transfer.....	91
2.8.4. Northern blotting.....	94

2.8.5. Microarray gene expression analysis	96
2.9. Plasminogen assays	97
2.10. Histology and fibrosis examination	98
2.11. TUNEL staining for apoptosis	100
2.12. Sample Analysis and Statistics	101
Chapter 3 – The role of PI3K (p110α) in a mouse model of dilated cardiomyopathy	104
3.1. Introduction	104
3.2. Methods	104
3.2.1. Techniques used in this chapter	104
3.2.2. Animals.....	105
3.2.2.1. Inheritance pattern of transgenic mice.....	105
3.3. Results	108
3.3.1. Lifespan of double-transgenic mice	108
3.3.2. Characterisation of the cardiac phenotype of the transgenic mice	111
3.3.2.1. Cardiac dimensions.....	111
3.3.2.2. Systolic function	114
3.3.2.3. Gender differences in cardiac dimensions and systolic function.....	114
3.3.3. Morphology	120
3.3.3.1. Organ weights	120
3.3.3.2. Gender differences in organ weights.....	123
3.3.3.3. Bulging of eyes associated with severe cardiac dysfunction.....	123
3.3.4. Histopathology.....	129
3.3.4.1. Measurement of cardiac chamber dilation and fibrosis	129
3.3.4.2. Examination of lung congestion in transgenic mice	133
3.3.4.3. Measurement of apoptosis in transgenic mice	134
3.3.5. Gene expression in transgenic heart tissue	134
3.3.5.1. Gene expression in Mst1 mice at 8 months of age.....	134
3.3.5.2. Gene expression in transgenic mice at 4.5 months of age.....	134
3.3.6. Protein expression in transgenic heart tissue.....	138
3.3.7. Akt contributes to the cardioprotective properties of PI3K (p110 α)	138
3.3.7.1. Cardiac dimensions and systolic function of triple-transgenic mice.....	140
3.3.7.2. Morphology of triple-transgenic mice	140
3.4. Discussion.....	144
3.4.1. Summary of major findings.....	144

3.4.2. Impact of manipulating PI3K (p110 α) in the stressed heart: PI3K (p110 α) is critical for cardiac function and survival, and protects the heart against heart failure	144
3.4.3. Molecular mechanisms responsible for the cardioprotective properties induced by caPI3K	146
3.4.4. Decreased PI3K (p110 α) activity in a setting of cardiac stress induces more severe disease in females	149
3.4.5. Future directions.....	149
3.5. Conclusion	150
<i>Chapter 4 – Reduced PI3K (p110α) activity increases the heart’s susceptibility to atrial fibrillation</i>	<i>151</i>
4.1. Introduction	151
4.2. Methods	152
4.2.1 Techniques used in this study.....	152
4.2.2. Animals.....	152
4.3. Results	153
4.3.1. PI3K (p110 α) activity in dnPI3K-Mst1 mice.....	153
4.3.2. Extended characterisation of the cardiac phenotype of the dnPI3K-Mst1 mice	153
4.3.2.1. Haemodynamic characteristics of the dnPI3K-Mst1 mice.....	153
4.3.2.2. Left atrial and ventricular enlargement in dnPI3K-Mst1 mice.....	156
4.3.2.3. Increased fibrosis in left atria of dnPI3K-Mst1 mice	156
4.3.2.4. Expression of fibrotic genes in atria of dnPI3K-Mst1 mice.....	156
4.3.2.5. Atrial thrombi formation in dnPI3K-Mst1 mice	160
4.3.2.6. Mechanisms responsible for atrial thrombi formation	160
4.3.3. Changes in cardiac conduction in dnPI3K-Mst1 transgenic mice.....	163
4.3.3.1. Electrical conduction abnormalities in dnPI3K-Mst1 mice	163
4.3.3.2. Location of the conduction blockade in dnPI3K-Mst1 mice.....	167
4.3.3.3. dnPI3K-Mst1 mice are more susceptible to atrial fibrillation.....	168
4.3.3.4. ECG characteristics of aged dnPI3K and Mst1 mice.....	170
4.3.4. Gene expression profiles in mouse atrial samples.....	170
4.3.5. Reduced PI3K (p110 α) activity in atrial appendages of patients with atrial fibrillation	173
4.3.6. Increased PI3K (p110 α) activity protects against abnormalities in Mst1 mice	176
4.4. Discussion.....	178
4.4.1. Summary of major findings.....	178
4.4.2. Reduced PI3K (p110 α) activity induces cardiac conduction abnormalities and makes the heart more susceptible to atrial fibrillation	178

4.4.3. Advantages of the atrial fibrillation mouse model.....	181
4.4.4. Potential role of PI3K (p110 α) in human atrial fibrillation.....	181
4.4.5. Increased PI3K (p110 α) activity can protect the stressed heart from cardiac conduction abnormalities	182
4.5. Conclusion	183
Chapter 5 – Role of PI3K (p110α) in estrogen mediated cardioprotection	184
5.1. Introduction	184
5.2. Methods	185
5.2.1 Techniques used in this study.....	185
5.2.2. Animals.....	185
5.3. Results	186
5.3.1. Interaction between the regulatory subunit of PI3K (p110 α) and estrogen receptor α in the heart	186
5.3.2. Effectiveness of ovariectomy surgery	186
5.3.3. Phenotype of ovariectomised mice.....	188
5.3.3.1. Cardiac chamber dimensions and systolic function.....	188
5.3.3.2. Morphology.....	188
5.3.4. Protein expression in heart tissue following ovariectomy.....	194
5.3.5. Effect of estrogen replacement following ovariectomy	196
5.3.5.1. Effectiveness of estrogen replacement.....	196
5.3.5.2. Unexpected adverse effect of estrogen replacement therapy.....	197
5.3.5.3. Cardiac chamber dimensions and fractional shortening following estrogen replacement	198
5.3.5.4. Morphology of ovariectomised mice with or without estrogen replacement	199
5.4. Discussion.....	202
5.4.1. Summary of major findings.....	202
5.4.2. Interaction between estrogen receptor α and PI3K (p110 α) in the adult heart	202
5.4.3. Impact of ovariectomy and estrogen replacement in Mst1 mice with or without manipulation of PI3K (p110 α)	203
5.5. Limitations and future studies.....	204
5.6. Conclusion	205
Chapter 6 - General discussion	206
6.1. Research approaches leading to the experimental findings	208

6.2. PI3K (p110α) as a potential therapeutic target.....	209
6.3. Conclusion	213
<i>References</i>.....	214
<i>Appendix 1</i>	313
<i>Appendix 2</i>	314
<i>Appendix 3</i>	315

Index of figures

Figure 1. Cardiac hypertrophy can be associated with HF and arrhythmia.....	3
Figure 2. Cellular organisation of cardiac myocytes.....	6
Figure 3. Electrical conduction of impulses through the heart.....	10
Figure 4. The mechanical events of the cardiac cycle.	12
Figure 5. Differences between concentric and eccentric hypertrophy.	14
Figure 6. Signalling pathways associated with cardiac hypertrophy and remodelling.	29
Figure 7. Physiological and pathological cardiac hypertrophy.....	30
Figure 8. PI3K (p110 α) is necessary and sufficient for physiological postnatal heart growth.	33
Figure 9. PI3K (p110 α) is critical for physiological exercise-induced cardiac hypertrophy.....	35
Figure 10. Transgenic mice with cardiac-specific over-expression of Mst1 develop dilated cardiomyopathy characterised by chamber dilation, wall thinning, fibrosis and apoptosis.	45
Figure 11. Proposed signalling cascades involved in estrogen-mediated effects in the heart.....	49
Figure 12. Mechanisms involved in the development and maintenance of atrial fibrillation.	53
Figure 13. PCR of Ntg, caPI3K, dnPI3K, kdAkt and Mst1 mice, showing respective base pair sizes.....	67
Figure 14. PCR of double-transgenic mice, showing positive bands for both the Mst1 and dnPI3K genes.....	69
Figure 15. M-mode echocardiographic trace of a mouse heart, showing the measurement of chamber dimensions and wall thicknesses.....	71
Figure 16. Catheterisation of the mouse heart.	72
Figure 17. Parameters measured by ECG in the mouse heart.....	74
Figure 18. Intracardiac ECG catheter recordings of the mouse heart.....	75
Figure 19. ECG of the mouse heart recorded by telemetry.....	76
Figure 20. Ovariectomy surgery in mice.	78
Figure 21. Measurement of tibia length using a vernier caliper.....	80

Figure 22. Western blotting to examine protein expression in tissue.	83
Figure 23. Examination of 28S and 18S bands to determine RNA quality.....	91
Figure 24. Northern gel transfer apparatus enabling upward capillary transfer of RNA from northern gel to Hybond-N membrane.....	93
Figure 25. Masson’s Trichrome stained cardiac tissue sections.	99
Figure 26. TUNEL staining of a cardiac tissue section.....	102
Figure 27. Survival of caPI3K-Mst1 and dnPI3K-Mst1 mice compared with Mst1 mice.....	109
Figure 28. Female dnPI3K-Mst1 mice have a significantly shorter lifespan compared with their male counterparts.....	110
Figure 29. Systolic function of transgenic mice at 4.5 months of age.....	115
Figure 30. Systolic function of transgenic mice at 8 months of age.....	116
Figure 31. Gender-associated differences in systolic function in the transgenic mice at 4.5 months of age.	118
Figure 32. Atrial weight measurements of female and male mice at 4.5 months of age.....	126
Figure 33. Lung weight measurements of female and male mice at 4.5 months of age.....	127
Figure 34. Bulging of the eyes in a dnPI3K-Mst1 mouse compared with a Ntg mouse.....	128
Figure 35. Increased atrial dilation and fibrosis in dnPI3K-Mst1 mice.	130
Figure 36. Ventricular chamber dilation and wall thinning in the dnPI3K-Mst1 mice compared with both Ntg and Mst1 mice at 4.5 months of age.	130
Figure 37. Atrial fibrosis in transgenic mice at 4.5 months of age.	131
Figure 38. Ventricular fibrosis in transgenic mice at 4.5 months of age.	132
Figure 39. Examination of lung congestion in transgenic mice at 4.5 months of age..	133
Figure 40. Apoptosis in hearts of transgenic mice measured by TUNEL staining.	135
Figure 41. Gene expression of embryonic genes and genes associated with calcium handling in the hearts of Mst1 mice at 8 months of age.....	136
Figure 42. Gene expression of embryonic genes and genes associated with calcium handling in the hearts of transgenic mice at 4.5 months of age.....	137
Figure 43. Protein expression in hearts from transgenic mice at 4.5 months of age. .	139

Figure 44. Fractional shortening in triple transgenic mice at 4.5 months of age.	142
Figure 45. Proposed molecular mechanism responsible for the anti-apoptotic action of PI3K (p110 α) in the Mst1 mice.	148
Figure 46. Role of PI3K (p110 α) in a setting of dilated cardiomyopathy.	150
Figure 47. PI3K activity and phosphorylation of Akt in mouse ventricular samples. ...	154
Figure 48. Assessment of cardiac chamber dimensions in transgenic mice.	157
Figure 49. dnPI3K-Mst1 mice have more severe fibrosis in the left atrium compared with the right atrium.	158
Figure 50. Gene expression changes of extracellular matrix- and fibrosis-related genes in the atria from transgenic mice.	159
Figure 51. Atrial thrombus formation in dnPI3K-Mst1 mice.	160
Figure 52. Global fibrinolytic activity in plasma from transgenic mice.	161
Figure 53. MMP-2 activity in ventricular tissue from transgenic mice.	162
Figure 54. Representative surface ECG traces from Ntg, dnPI3K, Mst1, and dnPI3K-Mst1 mice.	165
Figure 55. Atrial-ventricular conduction blockade in dnPI3K-Mst1 mice.	166
Figure 56. ECG trace and measurements obtained from an intracardiac electrophysiology catheter located in the right ventricle.	167
Figure 57. ECG from dnPI3K-Mst1 showing episodes of atrial fibrillation.	168
Figure 58. ECG telemetry traces from dnPI3K-Mst1 mice showing episodes of atrial tachycardia and atrial fibrillation.	169
Figure 59. Surface ECG recordings of aged dnPI3K compared with aged Ntg mice. ...	171
Figure 60. Changes in gene expression of connexin proteins in the atria from transgenic mice.	172
Figure 61. Expression changes of potassium channels and metabolic genes in atria of transgenic mice.	174
Figure 62. PI3K (p110 α) activity in human atrial samples from patients with either acute or chronic AF compared with patients who did not develop AF post-operatively.	175
Figure 63. Atrial fibrosis in Ntg, Mst1 and caPI3K-Mst1 mice.	177
Figure 64. Mechanism of increased susceptibility to AF induced by the reduction of PI3K (p110 α) activity.	183

Figure 65. Estrogen receptor α is associated with the regulatory subunit of phosphoinositide 3-kinase (p110 α) in the heart.	186
Figure 66. Uterus weight of ovariectomised and sham-operated mice.	187
Figure 67. Fractional shortening in transgenic mice at 4-4.5 months of age that underwent ovariectomy or a sham operation.	190
Figure 68. Body weight gain in mice following ovariectomy.	191
Figure 69. Mst1 mice show an improved cardiac phenotype following ovariectomy.	193
Figure 70. Protein expression in hearts from transgenic mice that underwent ovariectomy or a sham operation.	195
Figure 71. Uterus weight/tibia length in sham-operated mice that received placebo pellets compared with ovariectomised mice that received estrogen pellets.	196
Figure 72. Mst1 mice show improved cardiac function following ovariectomy, which appears to be reversed by estrogen replacement.	198
Figure 73. Mst1 mice show an improved cardiac phenotype following ovariectomy, which appears to be reversed by estrogen replacement.	201
Figure 74. Possible mechanism via which an interaction between ER α and PI3K (p110 α) mediates cardioprotection in females.	203
Figure 75. Summary of the novel findings from my PhD project.	207

Index of tables

Table 1. Distinct structural and functional features of physiological and pathological cardiac hypertrophy.....	15
Table 2. Differential expression of genes in pathological and physiological cardiac hypertrophy.....	19
Table 3. Differential responses to physiological and pathological hypertrophic stimuli in females and males.....	23
Table 4. Animal studies showing that the IGF1R-PI3K (p110 α)-Akt pathway is critical for physiological cardiac hypertrophy.....	36
Table 5. Mouse models that highlight the protective effects of the IGF1-PI3K (p110 α)-Akt signalling cascade or exercise in settings of heart disease.....	38
Table 6. Electrophysiological and histopathological changes seen in AF mouse models (paroxysmal or induced AF).....	57
Table 7. Genotypes generated by crossing PI3K and Mst1 transgenic mice.....	64
Table 8. Genotypes generated by crossing caPI3K-Mst1 and kdAkt mice.....	65
Table 9. Primer sequences for genotyping using PCR.....	67
Table 10. Comparison of the nutritional content of the soy-free and control diets.....	79
Table 11. Antibodies used for western blotting.....	85
Table 12. Northern probe band sizes.....	95
Table 13. Inheritance pattern of caPI3K mice crossed with Mst1 mice.....	106
Table 14. Inheritance pattern of dnPI3K mice crossed with Mst1 mice.....	106
Table 15. Inheritance pattern of triple-transgenic mice.....	107
Table 16. Left ventricular wall thicknesses and chamber dimensions in transgenic mice at 4.5 months of age.....	112
Table 17. Left ventricular wall thicknesses and chamber dimensions in transgenic mice at 8 months of age.....	113
Table 18. Gender differences in left ventricular chamber dimensions and wall thicknesses in transgenic mice at 4.5 months of age.....	117
Table 19. Gender differences in left ventricular chamber dimensions and wall thicknesses in transgenic mice at 8 months of age.....	119
Table 20. Organ weights of transgenic mice at 4.5 months of age.....	121
Table 21. Organ weights of transgenic mice at 8 months of age.....	122

Table 22. Gender-associated differences in organ weights of transgenic mice at 4.5 months of age.....	124
Table 23. Gender-associated differences in organ weights of transgenic mice at 8 months of age.....	125
Table 24. Left ventricular wall thicknesses and chamber dimensions in triple-transgenic mice at 4.5 months of age.....	141
Table 25. Organ weights of female triple-transgenic mice at 4.5 months of age.....	143
Table 26. Haemodynamic analyses from transgenic mice at 4.2-4.9 months of age. .	155
Table 27. ECG analyses from transgenic mice at 4.5 months of age.....	164
Table 28. Parameters derived from ECG of aged transgenic mice.....	171
Table 29. Effect of ovariectomy on cardiac chamber dimensions and left ventricular wall thicknesses at 4-4.5 months of age.	189
Table 30. Effect of ovariectomy on organ weights of transgenic mice at 4-4.5 months of age.....	192
Table 31. Effect of estrogen replacement on organ weights of ovariectomised transgenic mice.....	200
Table 32. Effect of ovariectomy on organ weights of transgenic mice at 4-4.5 months of age (complete statistics presented).....	313
Table 33. Effect of estrogen replacement on organ weights of ovariectomised transgenic mice (complete statistics presented).	314
Table 34. Cardiac chamber dimensions of transgenic mice following ovariectomy and estrogen replacement.	315

Summary of thesis

Heart failure affects approximately 1-3% of Western society. There is currently no cure and treatments largely delay disease progression. Consequently, there is great interest in identifying strategies that can improve cardiac function and reverse some of the negative consequences associated with heart failure. This thesis investigates the cardioprotective properties of a gene activated in the athlete's heart [phosphoinositide 3-kinase (PI3K), p110 α] in a setting of heart failure.

Two double-transgenic mouse models were generated to assess the role of PI3K in a setting of cardiac stress (dilated cardiomyopathy, DCM). Mice either expressing a constitutively active mutant of PI3K (p110 α) (caPI3K) or a dominant negative mutant of PI3K (p110 α) (dnPI3K) were crossed with a transgenic mouse model of DCM [due to over-expression of mammalian sterile 20-like kinase 1 (Mst1)]. Increasing PI3K activity in the DCM model (caPI3K-Mst1) improved lifespan and cardiac function, whereas decreasing PI3K activity in the DCM model (dnPI3K-Mst1) had an adverse effect. The cardioprotective properties of PI3K (p110 α) were mediated, at least in part, by the kinase Akt.

Using the dnPI3K-Mst1 model, I was able to show that reduced PI3K (p110 α) activity increases the heart's susceptibility to atrial fibrillation (AF, the most common arrhythmia in cardiology departments worldwide). dnPI3K-Mst1 mice displayed overt atrial remodelling, varying degrees of conduction blockade and developed spontaneous AF. To assess a possible link between PI3K activity and AF in humans, PI3K (p110 α) activity was measured in atrial appendages of patients with AF (acute or chronic) and compared to patients without AF. PI3K (p110 α) activity was lower in patients with AF compared to patients in sinus rhythm. These results suggest that reduced PI3K (p110 α) makes the heart more susceptible to the development of AF. Thus, strategies or agents that can activate PI3K (p110 α) specifically in the heart may represent a useful therapeutic approach for AF.

An unanticipated but novel finding was the observation that female dnPI3K-Mst1 mice showed faster disease progression than males. Prior to menopause, females are normally protected against cardiovascular disease compared with males. In contrast, in settings of aging, diabetes or hypertension [associated with depressed or defective PI3K (p110 α) activity] females are more prone to cardiac disease than males.

Taken together with my results, this suggests that there may be an interaction between PI3K (p110 α) and estrogen, and that this interaction is essential for the cardioprotection seen in pre-menopausal women. Data obtained from dnPI3K-Mst1 mice suggests that PI3K (p110 α) plays an important role in mediating cardioprotection in females. Unexpectedly, ovariectomy had a beneficial effect on the cardiac phenotype of Mst1 mice, but no significant effect in caPI3K-Mst1 or dnPI3K-Mst1 mice. The mechanisms responsible for these phenotypes will require further investigation.

In summary, this thesis presents compelling evidence to support investigation into therapeutics that activate components of the PI3K (p110 α) signalling pathway in a setting of cardiac stress.

Declaration

The work presented in this thesis has been carried out by myself, except where due acknowledgement has been made. No part of this thesis has been submitted for the award of any other degree or diploma. This thesis is not longer than 100,000 words excluding references and tables.

Lynette Pretorius

Acknowledgements

This thesis would not have been possible without the following people who provided their expertise and support throughout my PhD candidature. I would like to express my sincere gratitude for their efforts.

- 1) First, and foremost, I would like to thank my supervisors **Dr. Julie R. McMullen** and **Associate Professor Xiao-Jun Du**, without whom this project would not have been possible. Their support and feedback throughout my PhD candidature have not only been invaluable in the preparation of this thesis, but have also made the learning process enjoyable and interesting. Additionally, **Dr. Julie R. McMullen** assisted with echocardiography and electrocardiography experiments, as well as mice dissections. **Associate Professor Xiao-Jun Du** assisted with the ovariectomy surgery, as well as both electrocardiography and intra-coronary catheter experiments.
- 2) I would like to thank the Cardiac Hypertrophy laboratory (consisting of **Mr. Joon Win Tan, Mrs. Nelly Cemerlang, Mrs. Kate L. Weeks, Ms. Somayeh E. Nasr-Esfahani, Mr. Yow Keat Tham, Dr. Bianca C. Bernardo, Mr. Russel D. Bouwman** and **Mrs. Geeta Sapra**) for their assistance with experimental protocols, as well as helpful discussions throughout the course of my PhD candidature. **Mr. Joon Win Tan** and **Mrs. Nelly Cemerlang** also performed the PI3K activity assays of human atrial tissue samples. **Mr. Joon Win Tan** also performed the ovariectomy surgery and hormone replacement.
- 3) For their assistance with the echocardiography, electrocardiography, telemetry and intra-coronary catheter experiments I would like to thank **Dr. Helen Kiriazis, Dr. Ziqui Ming** and **Miss Nicole L. Jennings**.
- 4) I would like to thank the members of my PhD advisory committee (consisting of **Dr. Rebecca H. Ritchie, Dr. Xiaoming Gao, Dr. Paul Gregorevic, Associate Professor Elizabeth A. Woodcock, Associate Professor Walter G. Thomas**, and **Associate Professor Marie A. Bogoyevitch**) for helpful discussions throughout the course of my candidature. **Dr. Xiaoming Gao** also assisted with the development of the TUNEL staining protocol.

- 5) For assistance with the development of the real-time PCR protocol and the performance of the matrix metalloproteinase gelatin zymography analysis I would like to thank **Dr. Yi-Dan Su**.
- 6) I would like to thank **Dr. Ruby C.Y. Lin** (from the Ramaciotti Centre for Gene Function Analysis, University of New South Wales) who performed the microarray experiments.
- 7) The PI3K and Mst1 transgenic mice strains were kindly provided by **Professor Seigo Izumo** (from Beth Israel Deaconess Medical Centre, Harvard Medical School) and **Professor Junichi Sadoshima** (from the University of Medicine and Dentistry of New Jersey).
- 8) I would like to thank **Dr. Silvana Marasco** and **Dr. Anthony M. Dart** (from the Alfred Hospital, Melbourne) for the recruitment of patients and tissue harvesting of the human atrial tissue samples.
- 9) I would like to thank **Associate Professor Geoffrey A. Head** and **Dr. Elena Lukoshkova** (from the National Cardiology Research Centre, Moscow) for the development of the telemetry analysis software. **Associate Professor Geoffrey A. Head** also assisted with the interpretation of telemetry results.
- 10) I would like to thank **Associate Professor Robert L. Medcalf** and his laboratory for the performance of the plasminogen assays.
- 11) Experiments in this thesis were funded by National Health and Medical Research Council Project grants and a National Heart Foundation of Australia Grant-In-Aid to Dr. Julie McMullen.
- 12) I was supported by an Australian Postgraduate Award, as well as the Baker IDI Heart and Diabetes Institute Bright Sparks Top Up Scholarship.
- 13) Finally, and most importantly, I would like to thank **my family** for their faith and support throughout my candidature. They were with me every step of the way, and without their love and support, this thesis would not have been possible.

Prizes, publications and presentations during PhD candidature

Prizes during PhD candidature

The following awards were received by Lynette Pretorius during her PhD candidature:

1. Commonwealth Australian Postgraduate Award (2007-2010)
2. Baker IDI Heart & Diabetes Institute Bright Sparks Scholarship (2007-2010)
3. International Society for Heart Research (ISHR) Postgraduate Travel Award to attend the Cardiac Society of Australia and New Zealand (CSANZ) Annual Scientific Meeting and the ISHR Australasian Section Annual Scientific Meeting in Adelaide, Australia (2008)
4. Baker IDI Heart & Diabetes Institute Bright Sparks Postgraduate Travel Scholarship to attend the CSANZ Annual Scientific Meeting and the ISHR Australasian Section Annual Scientific Meeting in Adelaide, Australia (2008)
5. 2nd Place, Rod Andrews Poster Prize Presentation, Baker IDI Heart & Diabetes Institute (2008, 2009)
6. ISHR Postgraduate Travel Award to attend the CSANZ Annual Scientific Meeting and the ISHR Australasian Section Annual Scientific Meeting in Sydney, Australia (2009)
7. Baker IDI Heart & Diabetes Institute Bright Sparks Postgraduate Travel Scholarship to attend the CSANZ Annual Scientific Meeting and the ISHR Australasian Section Annual Scientific Meeting in Sydney, Australia (2009)
8. ISHR Student Investigator Award for Best Mini-Oral Presentation at the ISHR Australasian Section 33rd Annual Scientific Meeting, Sydney, Australia (2009)
9. Baker IDI Heart & Diabetes Institute Research Prize for Best Monthly Publication (September, 2009)
10. Monash University Award for Outstanding Contribution to the Faculty of Medicine, Nursing, and Health Sciences (2009)
11. ISHR Postgraduate Travel Award to attend the XXth ISHR World Congress in Kyoto, Japan (2010)
12. National Heart Foundation Travel Award to attend the XXth ISHR World Congress in Kyoto, Japan (2010)
13. 1st Place, Monash University Central Clinical School PhD Symposium (2010)

Publications during PhD candidature

Peer reviewed manuscripts

Pretorius, L.*, Du, X.J.*, Woodcock, E.A., Kiriazis, H., Lin, R.C.Y., Marasco, S., Medcalf, R.L., Ming, Z., Head, G.A., Tan, J.W., Cemerlang, N., Sadoshima, J., Shioi, T., Izumo, S., Lukoshkova, E., Dart, A.M., Jennings, G.L., and McMullen, J.R. (2009). **Reduced phosphoinositide 3-kinase (p110 α) activation increases the susceptibility to atrial fibrillation in a model of dilated cardiomyopathy.** *American Journal of Pathology* 175(3), 998-1009. * Authors contributed equally to this work.

Bernardo, B.C., Weeks, K.L., **Pretorius, L.**, and McMullen, J.R. **Molecular mechanisms of cardiac hypertrophy and heart failure.** In *Advances in Experimental Medicine and Biology Series*. E. Bittar, ed. (Springer). *Chapter submitted to editor December 2009.*

Bernardo, B.C., Weeks, K.L., **Pretorius, L.**, and McMullen, J.R. (2010). **Molecular distinction between physiological and pathological cardiac hypertrophy: experimental findings and therapeutic strategies.** *Pharmacology and Therapeutics* 128(1), 191-227.

Owen, K.L., **Pretorius, L.**, and McMullen, J.R. (2009). **The protective effects of exercise and phosphoinositide 3-kinase (p110 α) in the failing heart.** *Clinical Science* 116(5), 365-375.

Pretorius, L.*, Owen, K.L.*, and McMullen, J.R. (2009). **Role of phosphoinositide 3-kinases in regulating cardiac function.** *Frontiers in Bioscience* 14, 2221-2229.

* Authors contributed equally to this work

Pretorius, L., Owen, K.L., Jennings, G.L., and McMullen J.R. (2008). **Promoting physiological hypertrophy in the failing heart.** *Clinical and Experimental Pharmacology and Physiology* 35(4), 438-441.

Published abstracts

Pretorius, L., Du, X.J., Woodcock, E.A., Kiriazis, H., Lin, R.C.Y., Marasco, S., Head, G., Dart, A., Jennings, G.L., and McMullen, J.R. (2009). **Cardiac insulin resistance due to reduced phosphoinositide 3-kinase (p110 α) activation increases the heart's susceptibility to atrial fibrillation.** Heart, Lung and Circulation 18 Suppl 3, S131.

Pretorius, L., Kiriazis, H., Ming, Z., Cemerlang, N., Tan, J., Du, X.J., and McMullen, J.R. (2009). **Identification of the molecular mechanisms responsible for the cardioprotective properties of phosphoinositide 3-kinase (p110 α).** Heart, Lung and Circulation 18 Suppl 3, S302.

Pretorius, L., Kiriazis, H., Ming, Z., Sadoshima, J., Izumo, S., Jennings, G.L., Du, X.J., and McMullen, J.R. (2008). **Phosphoinositide 3-kinase (p110 α) [PI3K (p110 α)] is critical for the maintenance of cardiac function and survival in a setting of heart failure.** Heart, Lung and Circulation 17 Suppl 3, S222.

Du, X.J., Woodcock, E.A., Kiriazis, H., **Pretorius, L.**, Ming, Z., Sadoshima, J., Shioi, T., Izumo, S., Dart, A.M., Jennings, G.L., and McMullen, J.R. (2007). **Atrial fibrillation and conduction blockade in a mouse model of dilated cardiomyopathy with reduced phosphoinositide 3-kinase activity.** From the American Heart Association Scientific Sessions 2007 Orlando, Florida November 4-7, 2007. Circulation Research 101(11), 3.

Pretorius, L., Kiriazis, H., Ming, Z., Bouwman, R.D., Sadoshima, J., Izumo, S., Jennings, G.L., Du, X.J., and McMullen, J.R. (2006). **Activation of physiological hypertrophic signalling: new strategy for the treatment of heart failure.** Proceedings of the Australian Health and Medical Research Congress 2006, ISSN 1447-6010, page 189.

Oral and poster presentations during PhD candidature

All orals and posters presented by Lynette Pretorius are marked with an asterisk (*).

Invited oral presentation

Pretorius, L. (2010). **Role of the IGF1-PI3K pathway in the heart: Identifying and targeting genes in the athlete's heart to treat heart failure.** Kyoto Prefectural University of Medicine, Kyoto, Japan. *

Oral presentations

Pretorius, L. **Protective actions of phosphoinositide 3-kinase (p110 α) in a setting of cardiomyopathy.** Monash University Postgraduate Symposia, October 2010. *

Pretorius, L. Tan, J.W., Cemerlang, N., Kiriazis, H., Jennings, G.L., Du, X.J., and McMullen, J.R. **Akt mediates the cardioprotective properties of phosphoinositide-3-kinase (p110 α) in a setting of heart failure.** Rod Andrews Prize Presentation, 2009. *

Pretorius, L. Du, X.J., Woodcock, E.A., Kiriazis, H., Lin, R.C.Y., Marasco, S., Head, G., Dart, A., Jennings, G.L., and McMullen, J.R. (2009). **Cardiac insulin resistance due to reduced phosphoinositide 3-kinase (p110 α) activation increases the heart's susceptibility to atrial fibrillation.** Cardiac Society of Australia and New Zealand Annual Scientific Meeting and the International Society for Heart Research Australasian Section Annual Scientific Meeting 2009, Sydney, Australia, August 2009. *

Pretorius, L. Kiriazis, H., Ming, Z., Cemerlang, N., Tan, J., Du, X.J., and McMullen, J.R. (2009). **Identification of the molecular mechanisms responsible for the cardioprotective properties of phosphoinositide 3-kinase (p110 α).** Cardiac Society of Australia and New Zealand Annual Scientific Meeting and the International Society for Heart Research Australasian Section Annual Scientific Meeting 2009, Sydney, Australia, August 2009. *

Pretorius, L., Kiriazis, H., Ming, Z., Sadoshima, J., Izumo, S., Jennings, G.L., Du., X.J., and McMullen, J.R. (2008). **Phosphoinositide 3-kinase (p110 α) [PI3K (p110 α)] is critical for the maintenance of cardiac function and survival in a setting of heart failure.** Cardiac Society of Australia and New Zealand Annual Scientific Meeting and the International Society for Heart Research Australasian Section Annual Scientific Meeting 2008, Adelaide, Australia, August 2008. *

Pretorius, L., Kiriazis, H., Ming, Z., Bouwman, R.D., Sadoshima, J., Izumo, S., Jennings, G.L., Du., X.J., and McMullen, J.R. (2006). **Activation of physiological hypertrophic signalling: new strategy for the treatment of heart failure.** Australian Health and Medical Research Congress, Melbourne, Australia, December 2006. *

Poster presentations

Pretorius, L., Tan, J.W., Cemerlang, N., Kiriazis, H., Jennings, N.L., Du, X.J., and McMullen, J.R. (2010). **Phosphoinositide 3-kinase (p110 α) reduces the pathological consequences of heart failure via activation of Akt.** International Society for Heart Research XXth World Congress, Kyoto, Japan. *

Pretorius, L., Du, X.J., Woodcock, E.A., Kiriazis, H., Lin, R.C.Y., Marasco, S., Medcalf, R.L., Ming, Z., Head, G.A., Tan, J.W., Cemerlang, N., Sadoshima, J., Shioi, T., Izumo, S., Lukoschkova, E., Dart, A.M., Jennings, G.L., and McMullen, J.R. (2009). **Reduced phosphoinositide 3-kinase (p110 α) activation increases the heart's susceptibility to atrial fibrillation.** Monash University Higher Degree by Research Student Poster Exhibition 2009. *

Pretorius, L., Kiriazis, H., Ming, Z., Sadoshima, J., Izumo, S., Jennings, G.L., Du, X.J., and McMullen, J.R. (2008). **Phosphoinositide-3 kinase (p110 α) is critical for the maintenance of cardiac function and survival in a setting of heart failure.** Rod Andrews Poster Prize Exhibition. *

Pretorius, L. Du, X.J., Woodcock, E.A., Kiriazis, H., Lin, R.C.Y., Marasco, S., Head, G.A., Tan, J.W., Cemerlang, N., Sadoshima, J., Shioi, T., Izumo, S., Lukoschkova, E., Dart, A.M., Jennings, G.L., and McMullen, J.R. (2008). **Phosphoinositide 3-kinase (p110 α) protects the heart against cardiac dysfunction, fibrosis, and atrial fibrillation.** International Heart Forum, Beijing, September 2008.

Pretorius, L. Du, X.J., and McMullen, J.R. (2008). **Phosphoinositide 3-kinase (p110 α) is critical for the maintenance of cardiac function and survival in a setting of heart failure.** Monash University Higher Degree by Research Student Poster Exhibition 2008. *

Pretorius, L. Du, X.J., Woodcock, E.A., Kiriazis, H., Lin, R.C.Y., Marasco, S., Head, G.A., Tan, J.W., Cemerlang, N., Sadoshima, J., Shioi, T., Izumo, S., Lukoschkova, E., Dart, A.M., Jennings, G.L., and McMullen, J.R. (2008). **Phosphoinositide 3-kinase (p110 α) protects the heart against cardiac dysfunction, fibrosis, and atrial fibrillation.** Alfred Medical Research Week 2008. *

Pretorius, L. Kiriazis, H., Ming, Z., Sadoshima, J., Izumo, S., Jennings, G.L., Du, X.J., and McMullen, J.R. (2007). **Phosphoinositide-3 kinase (p110 α) is critical for the maintenance of cardiac function and survival in a setting of heart failure.** Alfred Medical Research Week 2007. *

Pretorius, L. Kiriazis, H., Ming, Z., Bouwman, R.D., Sadoshima, J., Izumo, S., Jennings, G.L., Du., X.J., and McMullen, J.R. (2006). **Activation of physiological hypertrophic signalling: new strategy for the treatment of heart failure.** Australian Health and Medical Research Congress 2006. *

Pretorius, L. Kiriazis, H., Ming, Z., Bouwman, R.D., Sadoshima, J., Izumo, S., Jennings, G.L., Du., X.J., and McMullen, J.R. (2006). **Activation of physiological hypertrophic signalling: new strategy for the treatment of heart failure.** Baker Scientific Symposium 2006. *

Pretorius, L., Kiriazis, H., Ming, Z., Bouwman, R.D., Sadoshima, J., Izumo, S., Jennings, G.L., Du, X.J., and McMullen, J.R. (2006). **Activation of physiological hypertrophic signalling: new strategy for the treatment of heart failure.** Alfred Medical Research Week 2006. *

Dedication

This thesis is dedicated to my parents Colin and Maggie, who had the incredible courage and wisdom to leave their homeland so that their children could follow their passions in a safe country. Throughout my life they have provided me with more love, support, encouragement, guidance, and praise than any one person could ask for. They never doubted my dreams and are an inspiration in everything I do.

Abbreviations

A

ACE: Angiotensin-converting enzyme, 25

AF: Atrial fibrillation, 4

Akt. *See* PKB

Ang II: Angiotensin II, 25

ANP: Atrial natriuretic peptide, 19

APS: Ammonium persulfate, 84

AR: Androgen receptor, 46

ARBs: Angiotensin receptor blockers, 25

AT₁: Angiotensin type-1, 25

ATPase: Adenosinetriphosphatase, 20

AV node: Atrioventricular node, 9

AVB: Atrial-ventricular conduction blockade, 163

AW/TL: Atrial weight to tibia length ratio, 120

B

BNP: B-type natriuretic peptide, 19

bpm: Beats per minute, 73

BSA: Bovine serum albumin, 82

C

CaMKII: Calcium/calmodulin-dependent protein kinase II, 28

caPI3K: Constitutively active PI3K(p110alpha), 32

caPI3K-kdAkt: caPI3K crossed with kdAkt, 64

caPI3K-Mst1: caPI3K crossed with Mst1, 64

caPI3K-Mst1-kdAkt: caPI3K crossed with both Mst1 and kdAkt, 64

CDC: Centers for Disease Control and Prevention, 1

D

DAB: 3,3'-diaminobenzidine, 101

DAG: Diacylglycerol, 39

DEPC: Diethylpyrocarbonate, 90

dnPI3K: Dominant negative PI3K(p110alpha), 32

dnPI3K-Mst1: dnPI3K crossed with Mst1, 64

dP/dt_{Max}: Maximum rate of rise of left ventricular pressure, 70

dP/dt_{Min}: Maximum rate of fall of left ventricular pressure, 70

DTT: Dithiotreitol, 84

E

ECG: Electrocardiography, 11

ECM: Extracellular matrix, 4

ER: Estrogen receptor, 46

ERK: Extracellularly responsive kinases, 28

ET-1: Endothelin-1, 28

F

FoxO: Forkhead Box O, 147

G

gp-130: Glycoprotein 130, 28

GPCR: G protein-coupled receptor, 28

GPER: G protein coupled estrogen receptor, 47

GSK-3: Glycogen synthase kinase 3, 37

H

HEPES: 4-(2-hydroxyethyl)-1-piperazineethanesulfonic acid, 87

HF: Heart failure, 1

HLB: Heart lysis buffer, 81

Hsp70: Heat shock protein 70, 59

HW/TL: Heart weight to tibia length ratio, 120

I

IGF-1: Insulin-like growth factor 1, 28

IGF-1R: Insulin-like growth factor 1 receptor, 31

Ins(1,4,5)P₃: Inositol-1,4,5-triphosphate, 39

IVS: Interventricular septal width, 70

I

JAK: Janus kinase, 28

JNK: c-Jun N-terminal kinases, 28

K

Kcnd3: Potassium voltage-gated channel Shal-related family member 3, 173

Kcnj2: Potassium inwardly rectifying channel subfamily J member 2, 173

Kcnt2: Potassium channel subfamily T member 2, 173

Kcnv2: Potassium channel subfamily V member 2, 173

kdAkt: Kinase dead Akt, 63

KXA: Ketamine/Xylazine/Atropine, 70

L

LVEDD: Left ventricular end-diastolic dimension, 70

LVEDP: Left ventricular end-diastolic pressure, 70

LVESD: Left ventricular end-systolic dimension, 70

LVPW: Left ventricular posterior wall thickness, 70

LVSP: Left ventricular systolic pressure, 70

LW/TL: Lung weight to tibia length ratio, 120

M

MAPK: Mitogen-activated protein kinase, 28

MAPKK: Mitogen activated protein kinase kinase, 40

MHC: Myosin heavy chain, 19

MMP: Matrix metalloproteinase, 8

Mst1: Mammalian sterile 20-like kinase 1, 28

Mst1-kdAkt: Mst1 crossed with kdAkt, 64

mTOR: Mammalian target of rapamycin, 37

N

NPRA: Natriuretic peptide receptor A, 20

Ntg: Non-transgenic, 32

O

OVX: Ovariectomy, 77

P

pAkt: Phosphorylated form of Akt, 138

PCR: Polymerase chain reaction, 66

pERK: Phosphorylated form of ERK, 138

PFA: Paraformaldehyde, 80

PGC1: PPAR α -activated γ coactivator-1, 48

PI3K: Phosphoinositide 3-kinase, 28

PKA: Protein kinase A, 28

PKB: Protein kinase B, also referred to as Akt, 28

PKC: Protein kinase C, 28

pp38: Phosphorylated form of p38, 138

PPAR: Peroxisome proliferator-activated receptor, 48

PR: Progesterone receptor, 46

R

RT: Room temperature, 66

S

SA node: Sino-atrial node, 9

SDS: Sodium dodecyl sulfate, 82

SERCA-2a: Sarcoplasmic reticulum Ca²⁺ ATPase 2a, 9

SR: Sarcoplasmic reticulum, 9

STAT: Signal transducer and activator of transcription, 28

T

TCA: Tricarboxylic acid cycle, 173

TEMED: Tetramethyl-ethylenediamine, 84

TIMP: Tissue inhibitor of metalloproteinases, 8

TLC: Thin-layer chromatography, 88

TnC: Troponin C, 9

TNF: Tumour necrosis factor, 50

TnI: Troponin I, 8

TnT: Troponin T, 8

TRPC: Transient receptor potential channels, 39

TUNEL: Terminal deoxynucleotidyl transferase nick end labeling, 45

U

UW/TL: Uterus weight to tibia length ratio, 186

Chapter 1 – General introduction

1.1. Heart failure

1.1.1. Impact of cardiovascular disease and heart failure

In Western societies, cardiovascular disease rates have reached epidemic proportions. Cardiovascular disease affects more than 3.7 million Australians (1 in 5 Australians) and kills one Australian nearly every 11 minutes (AIHW, 2008; NHF, 2005; NHF, 2007). In the United States of America, nearly 1 in 3 people are affected by cardiovascular disease (Lloyd-Jones *et al.*, 2010). Nearly half of all deaths in the developed world are attributed to cardiovascular disease and it is estimated that it will claim 25 million lives annually by 2020 (Lloyd-Jones *et al.*, 2010; Zipes *et al.*, 2005). While the Centers for Disease Control and Prevention (CDC) reported that rates of cardiovascular disease mortality declined by 16% since 2000, it is still the leading cause of both morbidity and mortality across all age groups (CDC, 2006). The decline in mortality rates has been attributed to improved control of risk factors (including smoking, physical inactivity, high cholesterol, and high blood pressure), improved early detection methods (including non-invasive imaging and blood tests), better treatment (including lifestyle changes and drug therapy), and more specialised care facilities (AIHW, 2004; Nissen *et al.*, 2004; Rose *et al.*, 2001).

A major contributor to cardiovascular disease mortality is the development of heart failure (HF), which affects approximately 1-3% of the Western population (1.3% of Australians - approximately 263,000 people) (AIHW, 2008; Davies *et al.*, 2001; Lloyd-Jones *et al.*, 2010; Mosterd and Hoes, 2007; Thom *et al.*, 2006; Zannad *et al.*, 2009). The heart is responsible for the maintenance of blood pressure, the perfusion of all organs in the body with oxygenated blood, as well as the removal of deoxygenated blood through the cardio-pulmonary system (Kumar *et al.*, 2005; Lilly, 2007). HF occurs when the heart becomes unable to provide sufficient blood perfusion to meet the metabolic demands of the body, or when it is only able to do so through elevation of the filling pressure of the heart (Kumar *et al.*, 2005). The progressive loss of cardiac function seen in HF causes pulmonary congestion and peripheral oedema and can induce a variety of symptoms including a lack of energy, breathlessness, drowsiness, numbness or tingling of the hands and feet, insomnia, cough, anorexia, anxiety and

depression (Blinderman *et al.*, 2008). HF can result from a variety of diseases that impair or overload the heart such as hypertension, myocardial infarction, coronary artery disease, valvular diseases or a variety of cardiomyopathies, and is frequently present as the most severe manifestation of end-stage cardiac diseases (Clark *et al.*, 2004; Lilly, 2007).

The incidence of HF increases with age, with approximately 15% of people over the age of 80 affected (Lloyd-Jones *et al.*, 2010). HF contributes significantly to the worldwide economic disease burden of cardiovascular disease, currently estimated to be as high as US \$149 billion per year (Zannad *et al.*, 2009). In Australia, the economic cost of HF is \$4 billion per year (AIHW, 2008). In contrast with other cardiovascular diseases such as stroke and coronary heart disease, the incidence of HF continues to increase (Lloyd-Jones *et al.*, 2010; Roger *et al.*, 2004; Zannad *et al.*, 2009). This has been attributed to an aging population, as well as the availability of interventions that prolong survival following a cardiac insult such as myocardial infarction (AIHW, 2004; Schocken *et al.*, 2008; Stewart *et al.*, 2003; Zannad *et al.*, 2009). Currently there is no satisfactory cure for HF, and long term survival following HF remains poor with only one-third of patients surviving after 5 years (Bleumink *et al.*, 2004; Levy *et al.*, 2002; Roger *et al.*, 2004; Zannad *et al.*, 2009).

1.1.2. Association between cardiac hypertrophy and heart failure

Growth of the adult heart is closely matched to the functional load placed upon it (Zak, 1984). In response to an increased workload (for example in a setting of hypertension), the heart compensates for the increased haemodynamic burden placed upon it by increasing cardiac cell size and mass (Cooper, 1987; Hunter and Chien, 1999; Sugden and Clerk, 1998) through a process known as cardiac hypertrophy. Cardiac hypertrophy can be defined as the increase of the cardiac muscle mass of the heart through either increased wall thickness and/or dilation of cardiac chambers (McMullen and Jennings, 2007). Cardiac hypertrophy is a key event in the progression from a cardiac insult to the development of HF (Figure 1). Initially hypertrophy of the heart following a cardiac insult is considered a compensatory response. Enlargement of cardiac myocytes and formation of additional sarcomeres is associated with an increase in wall thickness

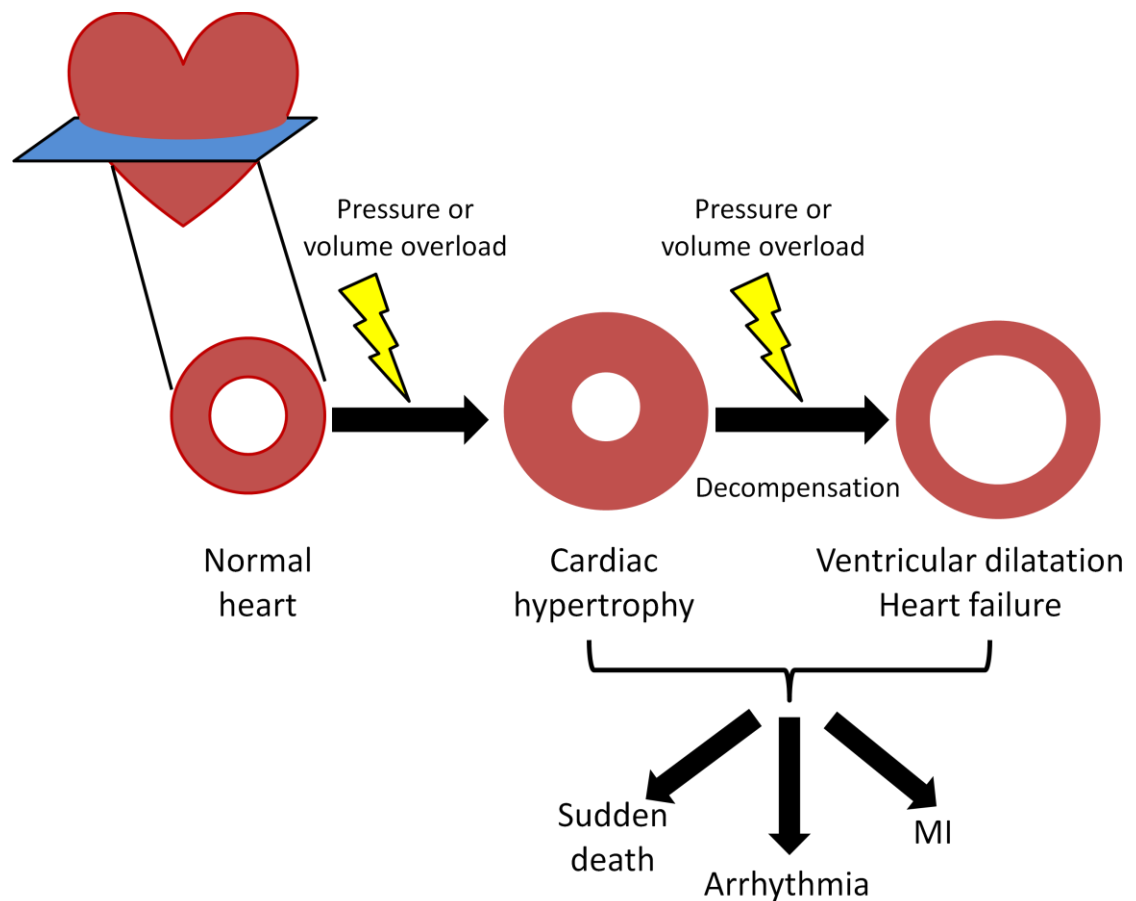


Figure 1. Cardiac hypertrophy can be associated with HF and arrhythmia.

Following a chronic pressure or volume overload stimulus, the heart hypertrophies as a compensatory response. Sustained pressure or volume overload leads to decompensation of the hypertrophied heart, inducing dilated cardiomyopathy and heart failure (HF). HF can increase the risk of myocardial infarction (MI), cardiac arrhythmia, or sudden death.

that reduces wall tension associated with the insult (such as pressure or volume overload), thereby improving muscle oxygen consumption and increasing contractile force (Frey *et al.*, 2004). Following a prolonged exposure to a pathological stimulus however, the heart decompensates, increasing the risk of arrhythmia, myocardial infarction or sudden death (Figure 1).

1.1.3. Complications associated with hypertrophy and heart failure

Cardiac hypertrophy is a well-established and independent risk factor for myocardial infarction, arrhythmia or sudden death, and hypertrophy has been found in nearly all forms of HF (Benjamin *et al.*, 1994; de Simone *et al.*, 2001; de Simone *et al.*, 2008; Dogan *et al.*, 2007; Heist and Ruskin, 2006; Levy *et al.*, 1990; Mureddu *et al.*, 2001; Osranek *et al.*, 2005). Ventricular arrhythmias are more frequent in the presence of cardiac hypertrophy (Adabag *et al.*, 2008; Du *et al.*, 2000b; Klein and Horowitz, 1988; Maron *et al.*, 2000; McKenna and Behr, 2002; Monserrat *et al.*, 2003; Mulrow *et al.*, 1986; Saumarez *et al.*, 1992; Saxon and De Marco, 2002; Spirito *et al.*, 1987; Umana *et al.*, 2003), and atrial fibrillation (AF) is frequently associated with a variety of cardiomyopathies (Ammash *et al.*, 2000; Cecchi *et al.*, 1995; Fananapazir *et al.*, 1989; Maron *et al.*, 1999; Maron *et al.*, 2002; Olivotto *et al.*, 2001; Pretorius *et al.*, 2009). AF is also a significant risk factor for sudden death, as it is associated with stroke and progressive congestive HF (Heist and Ruskin, 2006; Olivotto *et al.*, 2001). Left ventricular mass is also a predictor of myocardial infarction, even when no previous coronary heart disease can be identified (de Simone *et al.*, 2008).

1.2. Normal cardiac structure and function

1.2.1. Cellular structure of the cardiac myocyte

The pathophysiology of HF is complex, and consequently an understanding of normal cardiac structure and function is essential. The heart is composed of cardiac muscle cells (known as cardiac myocytes), fibroblasts, endothelial cells, mast cells, vascular smooth muscle cells, neurons, as well as the surrounding extracellular matrix (ECM) (Nag, 1980; Zak, 1984). Cardiac myocytes account for approximately 75% of the cell volume of the myocardium, but only 25% of the cell number (Jugdutt, 2003; Miner and

Miller, 2006; Nag, 1980; Popescu *et al.*, 2006; Weber, 1989; Zak, 1984). Postnatal cardiac growth occurs largely due to an increase in myocyte size as it is generally believed that the majority of myocytes cannot re-enter the cell cycle after the perinatal period (Soonpaa *et al.*, 1996; Sugden and Clerk, 1998). It is generally accepted that only a small proportion of cardiac myocytes can proliferate (cardiac progenitor cells), as DNA labelling studies indicate that DNA synthesis only takes place in a very small number of cardiac myocytes (MacLellan and Schneider, 2000; Nakagawa *et al.*, 1988; Pasumarthi and Field, 2002; Soonpaa *et al.*, 1996).

Myocytes are composed of myofibril bundles consisting of sarcomeres (Figure 2), the basic contractile unit of the heart (Kumar *et al.*, 2005; Zipes *et al.*, 2005). The sarcomere of the cardiac myocyte is composed of two groups of overlapping contractile filaments – actin and myosin (Figure 2). Myosin is tethered to the sarcomere Z-line (Figure 2), which provides elasticity to the contractile process (Lewinter *et al.*, 2010; Trombitas *et al.*, 2000; Watanabe *et al.*, 2002). The Z-lines are connected to the outside of the cell by specialised junctions known as costameres, containing membrane-spanning receptors known as integrins that connect the ECM to the intracellular contractile cytoskeleton (Figure 2) (Hannigan *et al.*, 2007; Srivastava and Yu, 2006). Actin filaments are arranged in an alpha-helix composed of two strands that branch out to interdigitate between the myosin filaments [Figure 2, (Kumar *et al.*, 2005; Zipes *et al.*, 2005)].

Cardiac myocytes are able to transmit contractile force through intercalated discs that are present at the ends of the cardiac myocytes (Bourne, 1953; Noorman *et al.*, 2009). Intercalated discs consist of three types of protein complexes known as the adherens junctions, desmosomes, and gap junctions (Figure 2). Adherens junctions mechanically connect myocytes by linking them to the actin cytoskeleton (Niessen, 2007; Tepass *et al.*, 2000), providing an anchor-point for the myofibrils and enabling cell to cell transmission of contractile force (Ferreira-Cornwell *et al.*, 2002). Desmosomes provide structural support between myocytes through interaction with intermediate filaments (Gutstein *et al.*, 2003; Noorman *et al.*, 2009). Gap junctions allow passive diffusion of metabolites, water and ions in order to mediate direct

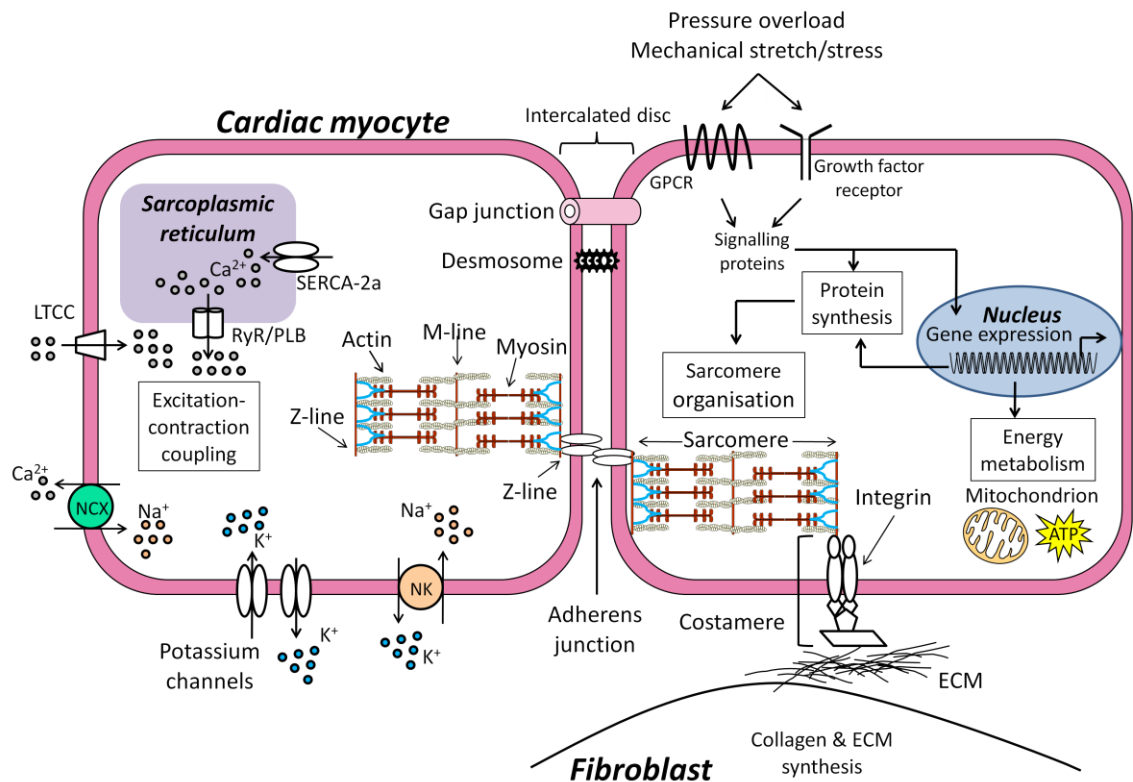


Figure 2. Cellular organisation of cardiac myocytes.

A cardiac myocyte is composed of sarcomeres (the area between two Z-lines), consisting of actin and myosin filaments. Contraction of sarcomeres is triggered by increases in free calcium (Ca^{2+}) via (1) influx and (2) release from the sarcoplasmic reticulum through the action of the L-type Ca^{2+} channels (LTCC), the ryanodine receptors (RyR) and phospholamban (PLB). Free Ca^{2+} is then sequestered back into the sarcoplasmic reticulum through sarcoplasmic reticulum Ca^{2+} ATPase 2a (SERCA-2a). Cytosolic Ca^{2+} can also be removed by ion exchange with sodium (Na^+) using the sodium-calcium exchanger (NCX) [Na^+ can also enter the cell through the sodium-potassium ATPase pump (NK). Potassium ions (K^+) enter and leave the cardiac myocyte through a variety of potassium channels on the cardiac myocyte cell membrane]. Communication between cardiac myocytes is accomplished through the intercalated disc, consisting of gap junctions, desmosomes, and adherens junctions. The extracellular matrix (ECM) proteins are synthesised in the fibroblasts and provide structural scaffolding within the heart. Structural proteins such as integrins play a role in linking the ECM and sarcomeres in the heart. Cardiac function is highly dependent on oxidative energy (ATP) which is generated in the mitochondria. Molecular signalling pathways, including G protein-coupled receptor (GPCR) pathways and growth factor receptor pathways, as well as changes in gene expression mediate protein synthesis. Figure adapted from Bernardo, B.C., Weeks, K.L., Pretorius, L., and McMullen, J.R. (2010). Molecular distinction between physiological and pathological cardiac hypertrophy: experimental findings and therapeutic strategies. *Pharmacology & Therapeutics* 128, 191-227, and Olson, E.N. (2004). A decade of discoveries in cardiac biology. *Nature Medicine* 10, 467-474.

Used with permission of Elsevier. Adapted by permission from Springer Nature Customer Service Centre GmbH: Springer Nature, Nature Medicine, A decade of discoveries in cardiac biology, Olson, E.N., COPYRIGHT 2004

electrical and metabolic communication between adjacent myocytes (Elfgang *et al.*, 1995; Kumar and Gilula, 1996; Noorman *et al.*, 2009), and ensure sequential and coordinated cardiac myocyte contraction (Bernstein and Morley, 2006; Gutstein *et al.*, 2003; Rohr, 2004).

1.2.2. Energy metabolism in the normal heart

The heart utilises more energy than any other organ, with approximately 30% of energy used for basic cellular metabolism and 70% for contraction [particularly the action of the sarcoplasmic reticulum Ca^{2+} ATPase 2a (SERCA-2a) and other ion pumps] (Stanley *et al.*, 2005). It acquires energy by converting chemical energy stored in fatty acids and glucose into mechanical energy necessary for the actin-myosin interaction of myofibrils (Neubauer, 2007). In the embryonic heart oxygen supply is limited and fatty acid transport and metabolism are still not fully matured, and consequently glucose is the primary substrate for ATP generation (Girard *et al.*, 1992; Lopaschuk *et al.*, 1992; Ostadal *et al.*, 1999; Stanley *et al.*, 2005). Soon after birth however, there is a 10-fold increase in fatty acid uptake and oxidation together with a marked decrease in glycolysis (Itoi and Lopaschuk, 1993; Lopaschuk *et al.*, 1991; Stanley *et al.*, 2005). Adult cardiac myocytes contain a large proportion of mitochondria that are almost exclusively dependent on fatty acid oxidation (Kumar *et al.*, 2005; Neubauer, 2007; Stanley *et al.*, 2005; van der Vusse *et al.*, 1992). The healthy adult myocardium utilises fatty acid oxidation as the main substrate for energy metabolism, accounting for up to 70% of ATP production (Stanley *et al.*, 2005; van der Vusse *et al.*, 1992). In contrast, glucose and lactate metabolism only account for approximately 30% of ATP synthesis (approximately 15% each) (Stanley *et al.*, 2005). The adult heart is able to alter its dependence on a particular energy substrate in order to adapt to altering workloads particularly under diseased conditions (Stanley *et al.*, 2005; van der Vusse *et al.*, 1992). This will be discussed in further detail in Section 1.3.4.

1.2.3. Structural scaffolding of the cardiac myocyte

Cardiac myocytes are enveloped in a dense matrix of collagen fibrils, elastin, cells and macrophages, macromolecules (such as glycoproteins) and other molecules (such as

growth factors, cytokines, and proteases) (Brown, 2005; Miner and Miller, 2006) collectively known as the ECM (Figure 2) which forms the structural scaffolding of the heart. As part of the ECM, the fibrillar collagen network (composed mainly of type I and type III collagen) maintains the structural integrity of cardiac myocytes, enabling myofibrillar alignment and the transmission of contractile force during contraction (Gunasinghe and Spinale, 2004; Janicki and Brower, 2002). The quantity of collagen in the ECM is determined by a balance between synthesis and degradation through the opposing actions of matrix metalloproteinases (MMPs) and tissue inhibitors of metalloproteinases (TIMPs) (Levick and Brower, 2008; Spinale, 2007; Wilson and Spinale, 2001).

1.2.4. Cardiac contractile function

1.2.4.1. The Frank-Starling mechanism

The ability of the heart to adapt to different rates of blood flow is referred to as the Frank-Starling mechanism. This mechanism is critical for linking changes in venous return (the rate at which blood flows back to the heart) with changes in stroke volume (the volume of blood pumped by the ventricles in a heartbeat) (Guyton and Hall, 2000; Shiels and White, 2008; Zipes *et al.*, 2005). Utilising the Frank-Starling mechanism, the heart is able to induce greater stroke volume through increased stretch on the myofibers of the heart within a certain range, thereby increasing the contractile force of the heart (Guyton and Hall, 2000; Lilly, 2007; Lorell and Carabello, 2000; Shiels and White, 2008).

1.2.4.2. Excitation-contraction coupling

Cardiac contraction occurs due to a process of electrical excitation of the myocytes, referred to as excitation-contraction coupling (Bers, 2002). Activation of the myofilaments to initiate contraction is regulated by Ca^{2+} . In the inactive state of the sarcomere, tropomyosin molecules are attached to the active site between actin thin filaments and myosin thick filaments thus inhibiting contraction. Along the actin molecule, troponin subunits are arranged – troponin T (TnT) subunits link troponin to the actin-tropomyosin complex, troponin I (TnI) subunits inhibit myosin ATPase activity

and stabilises the activated state of the actin-tropomyosin complex, and troponin C (TnC) subunits bind calcium ions (Ca^{2+}) which are required for contraction (Galinska *et al.*, 2010; Lilly, 2007).

During the cardiac action potential, the L-type Ca^{2+} channels are depolarised, leading to the activation of the calcium release channels (collectively known as the ryanodine receptors) to induce Ca^{2+} release from the sarcoplasmic reticulum (SR) [Figure 2, (Bers, 2002; Olson, 2004)]. While this initial influx of Ca^{2+} is not sufficient to induce contraction, it is able to trigger a significantly greater amount of Ca^{2+} release from the SR calcium stores (Olson, 2004), a mechanism referred to as calcium-induced calcium release. Combined, the release and influx of Ca^{2+} provides sufficient Ca^{2+} to bind to TnC, resulting in the exposure of the active site between actin and myosin, enabling contraction (Bers, 2002). Contraction proceeds as the myosin heads bind to the actin filaments, causing the filaments to move past each other in an ATP-dependent reaction (Lilly, 2007).

Following contraction, free Ca^{2+} concentration declines, allowing disassociation of the Ca^{2+} -troponin complex leading to relaxation, as the active site between the actin-myosin filaments is no longer exposed (Bers, 2002; Lilly, 2007). Inactivation of the L-type Ca^{2+} channels (and resultant inactivation of the ryanodine receptors) abolishes the influx of Ca^{2+} into the cells, thereby inhibiting calcium-induced calcium release. Cytosolic Ca^{2+} is sequestered back into the SR primarily by the activity of SERCA-2a (Figure 2), which is regulated by phospholamban (Asahi *et al.*, 2003).

1.2.5. Electrophysiology

The heart conducts electrical signals through specialized cells to initiate the heart beat and electrically co-ordinate contraction (Guyton and Hall, 2000; Zipes *et al.*, 2005). The electrical signal (referred to as the action potential) is initiated by the sino-atrial (SA) node, and then is conducted throughout the heart through a conduction system of specialized cells including the atrioventricular (AV) node, the Bundle of His, and the Purkinje fibers (Figure 3). As the impulse is conducted, the atria depolarise and

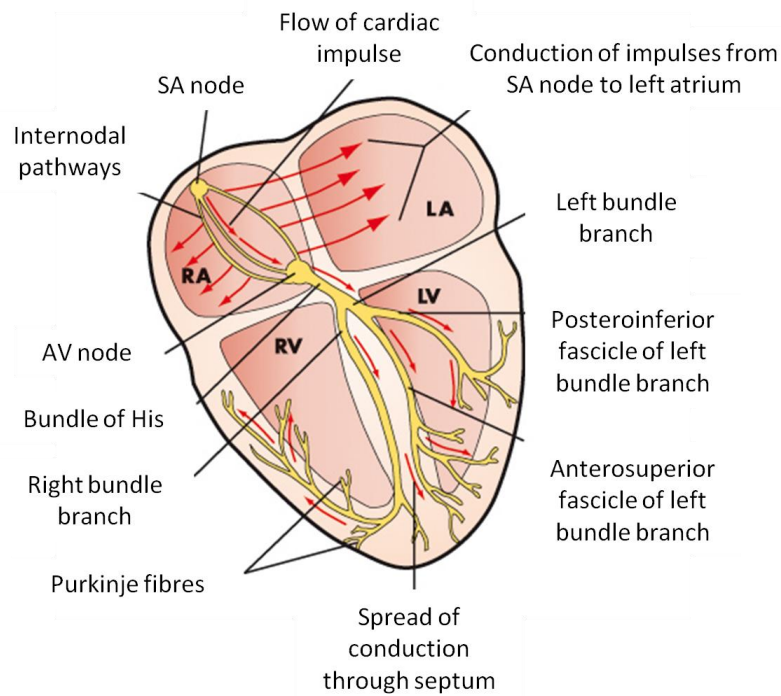


Figure 3. Electrical conduction of impulses through the heart.

The heart beat is initiated at the SA node, after which it is conducted throughout the heart via the internodal pathways, AV node, the bundle of His and bundle branches, towards the Purkinje fibers. RA: right atrium, LA: left atrium, RV: right ventricle, and LV: left ventricle. Figure adapted from Harris, P., Nagy, S., and Vardaxi, N. (2006). *Mosby's Dictionary of Medicine, Nursing & Health Professions*. (Sydney, Elsevier Australia).

Used with permission of Elsevier Science & Technology Journals, from Mosby's Dictionary of Medicine, Harris P., Nagy S., and Verdaxi, N., 3rd edition, 2006; permission conveyed through Copyright Clearance Center, Inc.

contract, pumping the blood into the ventricles (Guyton and Hall, 2000; Zipes *et al.*, 2005). Consequently, the ventricles depolarise and contract to pump the blood through the body. The relaxation period during which the heart fills with blood is referred to as the diastole phase, while the period of contraction is referred to as the systole phase. The period of diastole and systole is referred to as the cardiac cycle. The events during the cardiac cycle are easily identifiable using electrocardiography (ECG) [(Zipes *et al.*, 2005), Figure 4].

1.3. Cardiac remodelling

Ventricular remodelling refers to changes in cardiac mass (hypertrophy), volume and shape that occur to compensate for an increased load placed upon the heart (Cohn *et al.*, 2000). The process of cardiac remodelling can include molecular changes, alterations in collagen deposition (e.g. fibrosis), cell death, energy metabolism and calcium homeostasis. Of note, remodelling can be physiological or pathological in nature. Physiological remodelling can occur in response to chronic aerobic exercise and is associated with compensatory changes in heart dimensions and function (Atchley and Douglas, 2007). In contrast, pathological remodelling may occur in response to disease and ultimately leads to depressed cardiac function (Zipes *et al.*, 2005).

1.3.1. Cardiac hypertrophy

1.3.1.1. Physiological and pathological cardiac hypertrophy

Cardiac hypertrophy can broadly be classified as either physiological or pathological. Physiological cardiac hypertrophy includes normal postnatal growth, pregnancy-induced growth and exercise-induced growth and is considered beneficial, as it is associated with preserved or enhanced cardiac function (Atchley and Douglas, 2007; Fagard, 1997; Ferrans, 1984; Pluim *et al.*, 2000; Scheuer and Buttrick, 1987). Pathological hypertrophy occurs in response to chronic pressure or volume overload and is detrimental to patient health as it is associated with increased fibrosis and apoptosis, as well as depressed cardiac function and increased mortality (Cohn *et al.*, 1997; Levy *et al.*, 1990; Weber *et al.*, 1993).

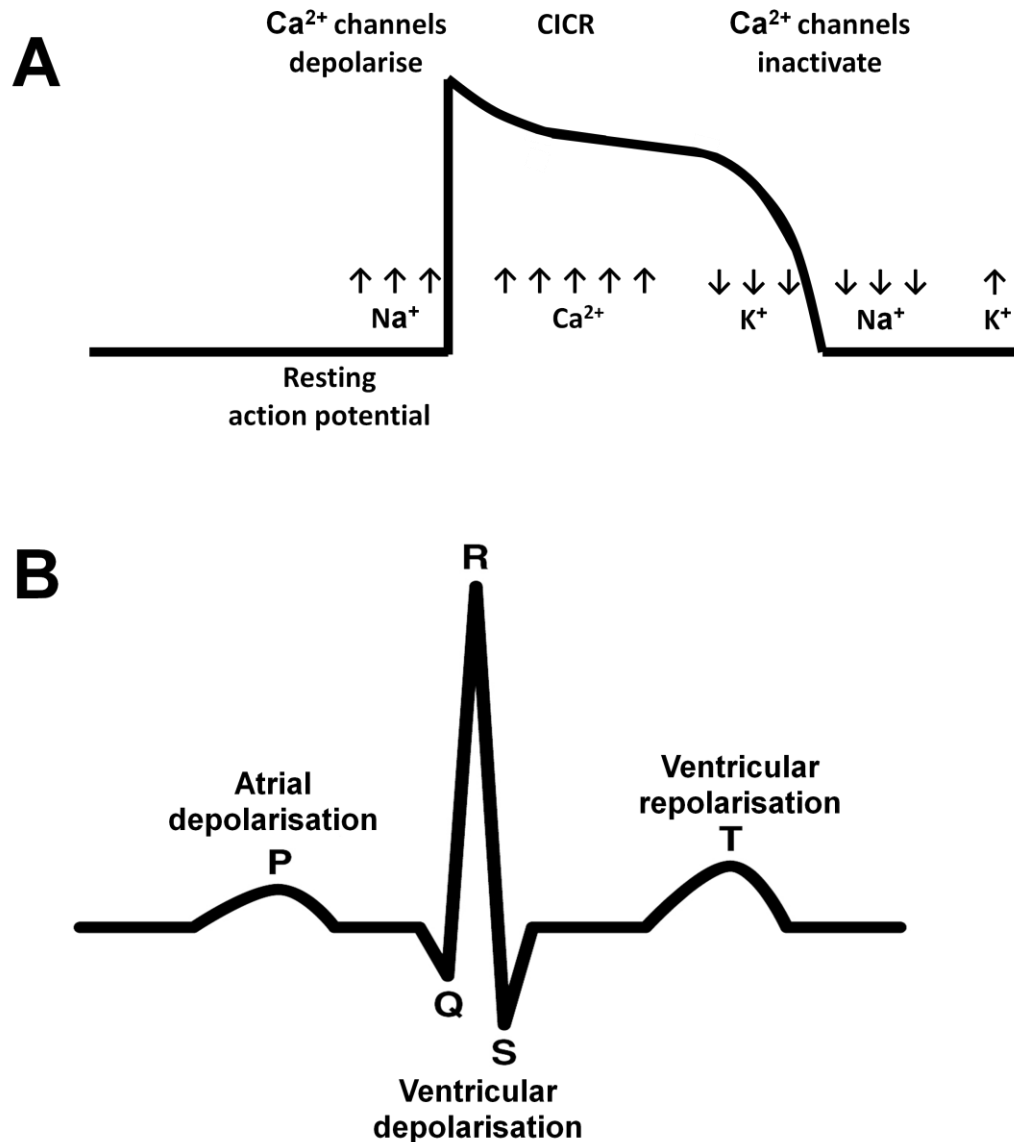


Figure 4. The mechanical events of the cardiac cycle.

A: A diagrammatic representation of the ventricular action potential. Sodium ions (Na^+) enter the cell through ion exchange with potassium ions (K^+). This allows calcium ion (Ca^{2+}) influx inducing the calcium release channels to depolarise, leading to sustained Ca^{2+} ion release from intracellular calcium stores through a process known as calcium-induced calcium release (CICR). Inactivation of the calcium channels reduces Ca^{2+} ion concentration, returning the action potential to rest. **B:** A diagrammatic representation of an electrocardiography trace showing atrial depolarisation followed by atrial contraction, as well as ventricular depolarisation followed by ventricular contraction and repolarisation. The p wave represents atrial depolarisation followed by atrial contraction (Rhoades and Bell, 2009). The QRS complex represents ventricular depolarisation followed by ventricular contraction, while the T wave represents ventricular repolarisation (Rhoades and Bell, 2009). Figure adapted from Rhoades, R.A., and Bell, D.R. (2009). *Medical physiology: principles for clinical medicine* 3rd edition. (Philadelphia, Lippincott Williams & Wilkins) and Borlak, J., and Thum, T. (2003). *Hallmarks of ion channel gene expression in end-stage heart failure*. *FASEB Journal* 17, 1592-1608.

Used with permission of Wolters Kluwer Health, Inc. and John Wiley and Sons. Figure B Copyright © FASEB

1.3.1.2. Concentric and eccentric cardiac hypertrophy

Physiological cardiac hypertrophy can be either concentric or eccentric depending on the type of exercise undertaken. Isotonic exercise (such as running or swimming) produces eccentric cardiac hypertrophy characterised by a series pattern of sarcomere addition, leading to an increase in myocyte cell length (Ferrans, 1984; Hunter and Chien, 1999; Schaible and Scheuer, 1984). Isometric exercise (such as weight lifting) leads to concentric cardiac hypertrophy, which is characterised by a parallel pattern of sarcomere addition and an increase in myocyte cell width (Ferrans, 1984; Hunter and Chien, 1999; Schaible and Scheuer, 1984). Similarly, pathological hypertrophy can also be either concentric or eccentric, depending on aetiology. Chronic pressure overload (for example in hypertension) leads to concentric ventricular hypertrophy, phenotypically evident as an increase in wall thickness (Ferrans, 1984). In contrast, chronic volume overload (for example aortic regurgitation) results in eccentric ventricular hypertrophy visible as an increase in ventricular cavity size and thinning of ventricular walls (Ferrans, 1984). Hypertrophy following myocardial infarction bears characteristics of both concentric and eccentric hypertrophy. Usually the increase in myocyte size accompanying pathological hypertrophy is also accompanied by a decrease in capillary density per cross-sectional area, and an increase in the deposition of fibrous tissue (Kumar *et al.*, 2005). The differences between concentric and eccentric cardiac hypertrophy are illustrated in Figure 5.

1.3.1.3. Distinct features of physiological and pathological cardiac hypertrophy

Even though physiological and pathological hypertrophy can be associated with similar increases in heart size, they are associated with distinct structural, functional, and metabolic characteristics (Table 1), as well as distinct molecular signalling pathways (as described in Section 1.5.). An understanding of the underlying mechanisms involved in these different forms of hypertrophy may provide an experimental basis for therapeutic strategies which can block pathological hypertrophy while stimulating physiological hypertrophy.

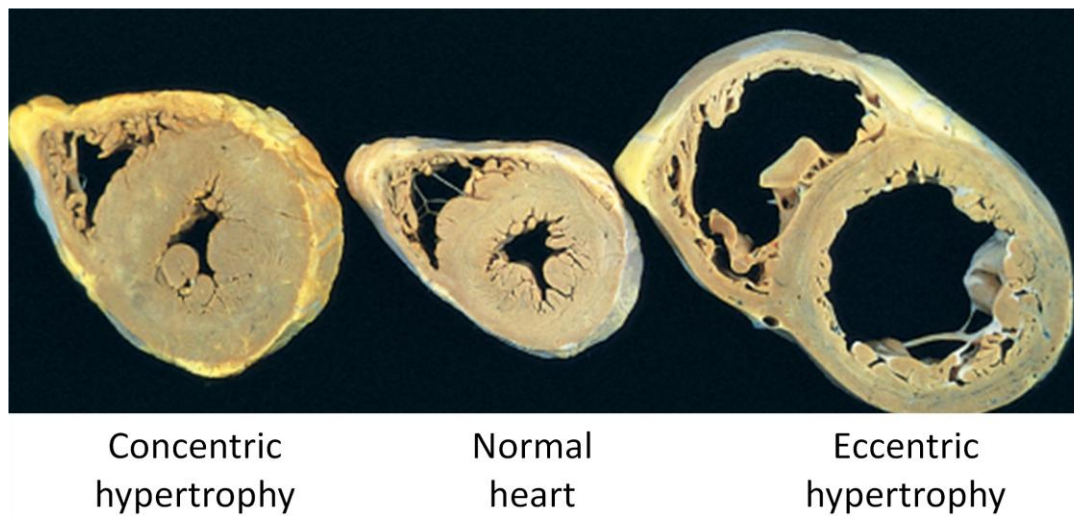


Figure 5. Differences between concentric and eccentric hypertrophy.

Concentric hypertrophy (left) and eccentric hypertrophy (right) compared to the normal human heart (centre). Figure adapted from Kumar, V., Abbas, A.K., and Fausto, N. (2005). Robbins and Cotran's Pathologic Basis of Disease (Philadelphia, Elsevier/Saunders).

Used with permission of Elsevier Science & Technology Journals, from Robbins & Cotran's Pathologic Basis of Disease, Kumar V., Abbas A.K., and Fausto, N., 2005; permission conveyed through Copyright Clearance Center, Inc.

Table 1. Distinct structural and functional features of physiological and pathological cardiac hypertrophy.

	Physiological Hypertrophy	Pathological Hypertrophy
Stimuli	- Exercise - Postnatal growth - Pregnancy	- Pressure or volume overload - Various cardiomyopathies - Genetic mutations
Cardiac morphology	↑ heart size ↑ myocyte volume Formation of new sarcomeres	↑ heart size ↑ myocyte volume Formation of new sarcomeres
Cardiac function	Cardiac function normal or enhanced	Depressed cardiac function during the later phase
Cardiac fibrosis	No fibrosis	Increased fibrosis
Cell death	No apoptosis	Increased apoptosis
Embryonic gene expression	Relatively normal pattern of gene expression	Activated pattern of embryonic gene expression
Metabolism	↑ fatty acid oxidation ↑ glucose metabolism	↓ fatty acid oxidation ↑ glucose metabolism
Angiogenesis	Normal or increased capillary density	Reduced capillary density
Reversible	Yes	Not usually
Association with heart failure	No	Yes

The association between pathological cardiac hypertrophy and HF is linked to alterations in myocardial structure including increased fibrosis, apoptosis, and myocardial stiffness, with progressive loss of cardiac function (de Simone *et al.*, 2004; de Simone *et al.*, 2008; Di Napoli *et al.*, 2003; Maceira *et al.*, 2002; Namba *et al.*, 1997; Weber *et al.*, 1988; Weber *et al.*, 1993; Zile *et al.*, 2001). In contrast, physiological cardiac hypertrophy represents a physiological adaptation to chronic exercise without pathology. Media reports of sudden death in young athletes have led to questions regarding whether highly trained athletes develop pathological conditions (Maron and Pelliccia, 2006). The risk of sudden death in athletes has not been comprehensively assessed but appears relatively low (1: 200,000 per year in a US state) and is usually linked to mutations of cardiac genes (Maron *et al.*, 1998; Semsarian and Maron, 2002). Therefore it is generally accepted that exercise-induced physiological cardiac hypertrophy in the healthy population does not have adverse consequences.

1.3.2. Fibrosis

Physiological cardiac hypertrophy is associated with a normal fibrillar collagen network, which facilitates efficient cardiac contraction (Gunasinghe and Spinale, 2004). In contrast, pathological hypertrophy is often associated with increased synthesis and deposition of collagen in the heart (known as cardiac fibrosis) which leads to mechanical stiffness, impairment of excitation-contraction coupling, and is associated with the progression to heart failure (Daniels *et al.*, 2009; Gunasinghe and Spinale, 2004; Jalil *et al.*, 1989; Janicki and Brower, 2002; Khan and Sheppard, 2006; Manabe *et al.*, 2002; Rossi, 1998; Wynn, 2008). Fibrosis can be classified as either reparative (replacement of degenerating myocardial cells with collagen leading to scar formation) or reactive (expanded ECM proteins in the interstitial space between cardiac myocytes without myocyte degeneration) (Burstein and Nattel, 2008).

Evidence suggests that increased fibrosis is a key substrate for the development of cardiac arrhythmias such as AF (Falk, 1998; Frustaci *et al.*, 1997; Mathew *et al.*, 2009; Pretorius *et al.*, 2009; Roberts, 2006), as it disrupts electrical conduction between cardiac myocytes (Daniels *et al.*, 2009). Fibrosis also increases the barrier for diffusion of gases and nutrients (Corradi *et al.*, 2004; Corradi *et al.*, 2005). This negatively influences myocardial energy balance and likely contributes to the

transition from hypertrophy to HF (Brown et al., 2005; Daniels et al., 2009; Gunasinghe and Spinale, 2004; Manabe et al., 2002).

1.3.3. Cell death

Myocyte cell death due to apoptosis is considered as a key feature of HF (Di Napoli *et al.*, 2003; Hayakawa *et al.*, 2003; Narula *et al.*, 1996; Olivetti *et al.*, 1997; Sharov *et al.*, 1996; Wencker *et al.*, 2003). Cardiac myocyte apoptosis reduces the number of myocytes available for contraction, and as such contributes to the progressive loss of contractile function in the failing heart (Kang and Izumo, 2000; Teiger *et al.*, 1996; Wencker *et al.*, 2003). Pathological cardiac hypertrophy is usually associated with increased apoptosis, whereas physiological hypertrophy is not. Therefore it is likely that differential activation of pro-apoptotic and pro-survival signals in these two forms of hypertrophy may be an important factor contributing to the distinct phenotypes observed in pathological and physiological cardiac hypertrophy.

1.3.4. Alterations in myocardial energy metabolism

To adapt to an increased workload, the adult heart is capable of switching energy metabolism in order to produce a continuous supply of ATP (van Bilsen *et al.*, 2009; van der Vusse *et al.*, 1992). Early pathological hypertrophy is typically characterised by decreased fatty acid uptake and oxidation and increased glucose metabolism (Akki *et al.*, 2008; Allard *et al.*, 1994; Christe and Rodgers, 1994; Davila-Roman *et al.*, 2002; el Alaoui-Talibi *et al.*, 1992; Osorio *et al.*, 2002; Recchia *et al.*, 1998). This change in substrate metabolism may initially be beneficial because it allows for faster production of ATP (van Bilsen *et al.*, 2009). However, as cardiac disease progresses (decompensated hypertrophy and failure) the heart becomes insulin resistant and hypoxic, which reduce the efficacy of glucose metabolism (Neubauer, 2007), and this is considered detrimental to cardiac function. It is thought that impaired glucose uptake may contribute to cardiac dysfunction through its effects on excitation-contraction coupling (Ritchie and Delbridge, 2006). A reduction in ATP synthesis through creatine kinase in human heart failure has also been reported, demonstrating a deficit in energy

supply (Weiss *et al.*, 2005). However, whether these changes are a cause or a consequence of HF is yet to be determined.

Unlike pathological cardiac hypertrophy, physiological hypertrophy is not associated with a switch to glucose metabolism. Exercise training increases the oxidative capacity of the heart, which is considered cardioprotective (Burelle *et al.*, 2004; Rimbaud *et al.*, 2009). The expression of genes important for fatty acid oxidation was significantly increased in the hearts of trained rats, but tended to decrease in hypertensive rat hearts (Rimbaud *et al.*, 2009).

1.3.5. Alterations in cardiac myocyte calcium homeostasis

Several abnormalities involving excitation-contraction coupling and the contractile proteins have been identified in the hypertrophied and failing heart. As previously noted, Ca^{2+} plays an essential role in the regulation of myocardial contraction [see Section 1.2.4.2.]. Mishandling of Ca^{2+} transients is a major cause of contractile dysfunction and arrhythmias in pathophysiological conditions (Bers, 2002; Olson, 2004). Patients with end-stage heart failure display prolonged action potentials with impaired relaxation, which is associated with prolonged elevation of the intracellular Ca^{2+} transient during relaxation (Piacentino *et al.*, 2003). Abnormal Ca^{2+} transients can also lead to delayed after-depolarisation of the cardiac action potential leading to the formation of re-entry circuits and predisposing the heart to arrhythmias (discussed further in Section 1.5.8) (Nishida *et al.*, 2010). Additionally, leakage of Ca^{2+} from the ryanodine receptor further contributes to the development of cardiac arrhythmias and contractile dysfunction as it results in increased Ca^{2+} during diastole (Chelu and Wehrens, 2007).

HF has also been associated with a decrease in calcium uptake by the SR, which consequently depletes SR calcium and decreases the amount of SERCA-2a and phospholamban (Flesch *et al.*, 1996; Frank *et al.*, 1998; Hobai and O'Rourke, 2001; Munch *et al.*, 2000). Abnormalities of the sodium-calcium exchanger in the cell membrane have also been demonstrated in HF, and may be a compensatory response to the reduction of Ca^{2+} uptake by SERCA-2a as augmentation of the sodium-calcium exchanger improves the removal of Ca^{2+} from the cytoplasm (Hasenfuss and Pieske, 2002; Studer *et al.*, 1994). There is also abnormal function of the ryanodine receptor,

which has been shown to decrease the rate of contraction and increase diastolic tension (Marks *et al.*, 2002; Shannon *et al.*, 2002).

1.3.6. Expression of embryonic genes and genes encoding contractile proteins in cardiac hypertrophy

Pathological hypertrophy and HF in humans and animal models have been associated with the re-expression of embryonic genes including atrial natriuretic peptide (ANP), B-type natriuretic peptide (BNP), β -myosin heavy chain (MHC), and α -skeletal actin, as well as down-regulation of α -MHC and SERCA-2a expression [Table 2, (Arai *et al.*, 1992; Arai *et al.*, 1993; Arai *et al.*, 1996; Chien *et al.*, 1993; Hasenfuss *et al.*, 1994; Izumo *et al.*, 1988; Matsui *et al.*, 1995; McMullen *et al.*, 2003; Mercadier *et al.*, 1990; Schiaffino *et al.*, 1989a)]. In contrast, mice that undergo exercise training generally show mild or no changes in their embryonic gene expression profile [Table 2, (Allen *et al.*, 2001; Iemitsu *et al.*, 2001; Kong *et al.*, 2005; McMullen *et al.*, 2003)].

Table 2. Differential expression of genes in pathological and physiological cardiac hypertrophy.

Gene	Pathological Cardiac Hypertrophy	Physiological Cardiac Hypertrophy
Atrial Natriuretic Peptide	↑	↔
B-type Natriuretic Peptide	↑	↔
α -Myosin Heavy Chain	↓	↔
β -Myosin Heavy Chain	↑	↔
α -skeletal actin	↑	↔
SERCA-2a	↓	↔

* Data obtained from animal models of cardiac hypertrophy.

The functional consequences of re-expression of embryonic genes in the adult heart are not completely understood. Studies in genetic mouse models suggest

that ANP and BNP have anti-hypertrophic and anti-fibrotic properties (Ogawa *et al.*, 2001; Oliver *et al.*, 1997; Patel *et al.*, 2005). Mice with global deletion of the natriuretic peptide receptor A (NPRA) for ANP and BNP develop marked pathological hypertrophy with significant interstitial fibrosis under basal conditions (Oliver *et al.*, 1997). However, interpretation of this data is confounded by the development of hypertension in these mice (Oliver *et al.*, 1997). Cardiac-specific dominant negative NPRA mice displayed exacerbated cardiac hypertrophy and fibrosis following pressure overload, but did not develop increased blood pressure under basal conditions (Patel *et al.*, 2005). Targeted disruption of cardiac BNP resulted in increased fibrotic lesions without an increase in blood pressure under basal conditions, as well as markedly greater fibrotic lesions and increases in ECM proteins following pressure overload (Ogawa *et al.*, 2001).

The genes that encode α -MHC and β -MHC (Hoh *et al.*, 1978) are developmentally and hormonally regulated (Lompre *et al.*, 1984). β -MHC is predominant in the mouse embryonic heart, but becomes down-regulated soon after birth where α -MHC is predominantly expressed (Chien *et al.*, 1993; Lyons *et al.*, 1990; Morkin, 2000; Siedner *et al.*, 2003; Tardiff *et al.*, 2000). This is mainly attributable to the fact that β -MHC has reduced adenosine triphosphatase (ATPase) catalytic activity compared with α -MHC, which results in decreased levels of contraction, but improved cardiac energy efficiency (Alpert and Mulieri, 1982; Barany, 1967; Dorn *et al.*, 1994; Holubarsch *et al.*, 1985; Lyons *et al.*, 1990; Schwartz *et al.*, 1981). In disease settings however, β -MHC is re-expressed while α -MHC is reduced (Chien *et al.*, 1993; Izumo *et al.*, 1987). It has been clearly demonstrated that the MHC isoforms switch in models of pathological cardiac hypertrophy. Following pressure overload-induced pathological cardiac hypertrophy, rat ventricles show marked mRNA accumulation of β -MHC within two days of the onset of hypertrophy (Izumo *et al.*, 1987; Schiaffino *et al.*, 1989b). Pathological stress (due to aortic banding) lead to a 15-fold increase in β -MHC expression, with a concomitant down-regulation of α -MHC (McMullen *et al.*, 2003). By contrast, β -MHC was not different in swim trained mice compared with non-trained mice (McMullen *et al.*, 2003).

Two isoforms of actin have been identified in the heart – α -cardiac actin and α -skeletal actin (Bertola *et al.*, 2008; Mayer *et al.*, 1984; Vandekerckhove and

Weber, 1979; Vandekerckhove *et al.*, 1986), and these actin isoforms are developmentally regulated (Hewett *et al.*, 1994; Swynghedauw, 1986). During early development α -cardiac actin and α -skeletal actin are co-expressed (Bertola *et al.*, 2008; Gunning *et al.*, 1983). In the adult heart, α -cardiac actin becomes the main actin isoform (Bertola *et al.*, 2008; Boheler *et al.*, 1991; Carrier *et al.*, 1992; Ilkovski *et al.*, 2005; Mayer *et al.*, 1984; Schwartz *et al.*, 1986). Several studies have shown increased α -skeletal actin expression during pathological cardiac hypertrophy (McMullen *et al.*, 2003; Schwartz *et al.*, 1986; Suurmeijer *et al.*, 2003; Winegrad *et al.*, 1990). Chronic pressure overload induced rapid accumulation of α -skeletal actin mRNA in rat ventricles (Izumo *et al.*, 1988; Schiaffino *et al.*, 1989a; Schwartz *et al.*, 1986) and aortic banding of mice induced a 9-fold increase in α -skeletal actin expression (McMullen *et al.*, 2003).

SERCA-2a is the most important Ca^{2+} handling pump in the SR of cardiac muscle (Wuytack *et al.*, 2002), and is essential for normal contractile function of the heart (Hasenfuss, 1998; Periasamy and Huke, 2001; Periasamy and Kalyanasundaram, 2007). Studies have shown that reductions in SERCA-2a are associated with cardiac disease (Aoyagi *et al.*, 1999; Periasamy and Kalyanasundaram, 2007; Prasad *et al.*, 2004; Wankerl and Schwartz, 1995). Double-knockout of the SERCA-2a gene was embryonically lethal, while heterozygous gene expression induced a reduction in contractility, cardiac function, and Ca^{2+} homeostasis during excitation-contraction coupling (Ji *et al.*, 2000; Periasamy *et al.*, 1999; Prasad *et al.*, 2004). Reduced SERCA-2a levels also resulted in marked cardiac hypertrophy and chamber dilation with increased prevalence and faster progression to HF (Schultz *et al.*, 2004). SERCA-2a expression has also been shown to decrease in hearts from patients with end-stage HF (Arai *et al.*, 1993; Hasenfuss *et al.*, 1994; Hasenfuss, 1998; Mercadier *et al.*, 1990). Serca-2a gene therapy has been tested experimentally to restore myocyte contractile function or cardiac function in animal models of cardiac disease (Byrne *et al.*, 2008; del Monte *et al.*, 1999; Hajjar *et al.*, 1998; Kawase *et al.*, 2008; Miyamoto *et al.*, 2000).

1.3.7. Gender differences in cardiac hypertrophy and remodelling

It has become increasingly apparent that gender has a role in regulating heart size and remodelling in a setting of disease [extensively reviewed by (Du *et al.*, 2006) and

(Luczak and Leinwand, 2009)]. Prior to adolescence, there are no significant differences in heart size between males and females, suggesting a similar number of cardiac myocytes at birth, as myocytes are terminally differentiated (de Simone *et al.*, 1995; Sugden and Clerk, 1998; Zak, 1974). Following puberty however, males have approximately 30% larger hearts than females (associated with a greater increase in body size), suggesting a significantly larger level of physiological hypertrophy in males (de Simone *et al.*, 1995). Men lose approximately 1 gram of cardiac mass per year following puberty, which leads to compensatory hypertrophy to maintain adequate cardiac mass. Females, however, maintain their myocyte number and size with aging (Grandi *et al.*, 1992; Olivetti *et al.*, 1995).

In general, pre-menopausal women tend to be protected against cardiovascular disease compared with age-matched men, but this protection is abolished following menopause (Lloyd-Jones *et al.*, 2010; Mikkola and Clarkson, 2002; Sullivan, 2003). Of note, recent Australian figures indicate the prevalence of cardiovascular disease and HF is higher in females than in males but this is associated with females living longer (AIHW, 2008). In studies of either human cardiovascular disease or animal models of pathological hypertrophy females generally fare better than their male counterparts (see Table 3). Female patients with aortic valve stenosis showed smaller left ventricular chamber sizes, whereas the men developed left ventricular chamber dilation (Aurigemma and Gaasch, 1995; Du *et al.*, 2006). Pressure overload due to aortic constriction in animals induced a worse phenotype in the males, with marked diastolic dysfunction, chamber dilation and transition to HF (Douglas *et al.*, 1998; Skavdahl *et al.*, 2005). Similarly, in humans or rats following myocardial infarction, progression to HF was worse in males than females (Giuberti *et al.*, 2007; Smith *et al.*, 2000; Vaccarino *et al.*, 2001). Male mice subjected to myocardial infarction displayed increased cardiac rupture and hypertrophy with poorer ventricular function compared with females (Cavasin *et al.*, 2004). Studies on the spontaneously hypertensive rat model also show cardioprotection in females compared with males, as HF occurred earlier in males than females in response to chronic hypertension (Gerdes *et al.*, 1996; Tamura *et al.*, 1999) and males developed more cardiac

Table 3. Differential responses to physiological and pathological hypertrophic stimuli in females and males.

Physiological/ Pathological	Model	Female	Male
Physiological	Voluntary Cage Wheel Running (Mice) (Konhilas <i>et al.</i> , 2004)	↑↑ Hypertrophy ↑ Exercise capacity	↑ Hypertrophy
	Swim Training (Rats) (Schaible and Scheuer, 1979; Schaible and Scheuer, 1981)	↑↑ Hypertrophy	↑ Hypertrophy
Pathological	Transverse Aortic Constriction (Mice) (Skavdahl <i>et al.</i> , 2005)	↑ Hypertrophy	↑↑ Hypertrophy
	Ascending Aortic Constriction (Rats) (Douglas <i>et al.</i> , 1998)	↑ Hypertrophy	↑↑ Hypertrophy ↑ Progression to Heart Failure ↑ Chamber Dilation
	Ascending Aortic Stenosis (Rats) (Weinberg <i>et al.</i> , 1999)	↑ Hypertrophy ↑ Fetal gene expression ↔ Contractile reserve	↑ Hypertrophy ↑↑ Fetal gene expression ↓ Contractile reserve
	Dahl Salt-Sensitive Hypertensive Rats (Podesser <i>et al.</i> , 2007)	↑ Hypertrophy (concentric) ↑ Septal thickness	↑ Hypertrophy (eccentric) ↑ Posterior wall thickness
	Spontaneously Hypertensive Heart Failure Rats (Tamura <i>et al.</i> , 1999)	↑ Myocyte Cross-Sectional Area ↔ Cardiac Function	↑↑ Myocyte Cross-Sectional Area ↓ Cardiac Function ↑ Progression to Heart Failure ↑ Mortality

* Table adapted from Bernardo, B.C., Weeks, K.L., Pretorius, L., and McMullen, J.R. (2010). Molecular distinction between physiological and pathological cardiac hypertrophy: experimental findings and therapeutic strategies. *Pharmacology & Therapeutics* 128, 191-227.

Used with permission of Elsevier.

hypertrophy (Tamura *et al.*, 1999). Salt-sensitive Dahl rats on a high-salt diet developed significant hypertrophy, but only males developed significant chamber dilation, while females showed improved contractile function (Jain *et al.*, 2002; Podesser *et al.*, 2007).

The prevalence of cardiac disease is declining in men, but not women (Lloyd-Jones *et al.*, 2010; Zipes *et al.*, 2005), suggesting a need for a more comprehensive understanding of the impact gender-related differences have on the development and severity of cardiac disease. Interestingly, however, in settings of diabetes or hypertension women have a greater risk than men to develop cardiovascular disease (Regitz-Zagrosek, 2006), though the reasons for this remain unclear. Clinical trials are often biased towards the male gender (Heiat *et al.*, 2002; Kim *et al.*, 2010; Lee *et al.*, 2001; Melloni *et al.*, 2010), but gender-related differences in drug effects have previously been established. For example, in women ACE inhibitors and β -blockers are less effective and show more side effects compared with male counterparts (Regitz-Zagrosek, 2006; Wing *et al.*, 2003). It has also been shown that digitalis – a common treatment for heart disease – causes more deaths in women (Regitz-Zagrosek, 2006).

Differences in physiological cardiac hypertrophy between genders have not been examined widely. It is however clear that there is differential cardiac remodelling following aerobic exercise between the genders (Table 3) (Higginbotham *et al.*, 1984; Sullivan *et al.*, 1991). Treadmill training in rats induced cardiac hypertrophy in both males and females but only males showed enhanced cardiac performance (Schaible and Scheuer, 1979; Schaible *et al.*, 1981). In contrast, female rats that underwent chronic swim training showed an increased hypertrophic response compared with their male counterparts (Luczak and Leinwand, 2009; Schaible and Scheuer, 1979; Schaible and Scheuer, 1981). Female mice have increased exercise capacity for both voluntary wheel or treadmill running, with females running more on a cage wheel than males independent of the strain or age (Luczak and Leinwand, 2009). Moreover, female mice perform better in endurance tests, indicative of increased cardiovascular performance (Luczak and Leinwand, 2009). While cage wheel running induces significant cardiac hypertrophy in both genders, females show greater cardiac hypertrophy (Konhilas *et al.*, 2004).

1.4. Heart failure therapy

1.4.1. Current therapeutics

Current treatments for HF focus on disease management, and include drug therapy, implantable devices, as well as surgery (including cardiac transplantation) (Krum and Abraham, 2009). Pharmacologic approaches to treat HF largely focus on improving systolic dysfunction, in order to enhance survival, delay disease progression, minimize the symptoms and disability associated with HF, restore organ perfusion, and return cardiac filling pressure to optimal levels (Krum and Abraham, 2009; Zipes *et al.*, 2005). Despite the vast array of pharmacological treatments for HF that are available, approximately 20% of patients still progress to more severe cases of HF that ultimately end in the implantation of devices that can assist the mechanical efficiency of the heart, or surgery (Dec, 2004; Hunt *et al.*, 2009).

1.4.1.1. Drug therapy for heart failure and arrhythmia

First-line treatment of HF includes angiotensin-converting enzyme (ACE) inhibitors and angiotensin receptor blockers (ARBs), which are able to improve survival and reduce blood pressure and left-ventricular remodelling associated with HF (ACE-Inhibitor-Myocardial-Infarction-Collaborative-Group, 1998; Adorasio *et al.*, 2006; Cohn and Tognoni, 2001; Hunt *et al.*, 2009; McMurray and Pfeffer, 2002; Packer and Cohn, 1999; Packer *et al.*, 1999). These drugs act by reducing the remodelling mediated by renin-angiotensin system signalling through the Angiotensin II (Ang II) - angiotensin type-1 (AT₁) receptor signalling pathway (Burnier, 2001; Greenberg *et al.*, 1995; Mehta and Griendling, 2007; Pfeffer *et al.*, 1982; Pfeffer *et al.*, 1988). ACE inhibitors have also been shown to reduce the risk of developing AF (Ducharme *et al.*, 2006; Healey *et al.*, 2005; Maggioni *et al.*, 2005; Pedersen *et al.*, 1999; Vermes *et al.*, 2003).

β -Adrenergic receptor blockers (commonly referred to as β -blockers) are often used in conjunction with ACE inhibitors or ARBs (Dec, 2004; Zipes *et al.*, 2005). β -blockers blunt peripheral vasoconstriction, abnormal renal sodium excretion, cardiac hypertrophy, arrhythmias, and apoptosis through reduced signal transduction via β -adrenergic receptors (Bristow, 2000a; Bristow, 2000b; CIBISII-Investigators, 1999; Dec, 2004; Packer *et al.*, 2001; Willenheimer *et al.*, 2005). Additionally, long-term β -blocker

treatment has been shown to reduce HF symptoms, improve cardiac function, improve survival, and reduce hospitalisation (Bristow, 2000a; CIBISII-Investigators, 1999; McNamara *et al.*, 2001; Packer *et al.*, 1996; Packer *et al.*, 2001; Willenheimer *et al.*, 2005).

Diuretic treatment is used to improve the congestive symptoms associated with HF (Hunt *et al.*, 2009). Acutely, diuretic treatment is able to decrease the left ventricular filling pressure of the heart (Zipes *et al.*, 2005). Chronic treatment enhances the delivery of sodium chloride, small ions, and water into urine, promoting increased urinary production and decreased water and solute reabsorption by the kidneys (Zipes *et al.*, 2005). Anti-coagulation therapy can be provided to HF patients that are at risk of the development of arrhythmia, thromboembolism, or stroke (Baker and Wright, 1994; De Caterina, 2009; Hunt *et al.*, 2009; Lip and Gibbs, 1999; Mathew *et al.*, 2009; Zipes *et al.*, 2005). Additionally, anti-arrhythmic agents (for example Amiodarone) are used to treat HF patients that have already developed arrhythmic complications (Amiodarone-Investigators, 1997; Deedwania *et al.*, 1998; Doval *et al.*, 1994; Heist and Ruskin, 2006; Hunt *et al.*, 2009; Nanas *et al.*, 2001; Poole-Wilson *et al.*, 2003; Singh *et al.*, 1995).

1.4.1.2. Non-drug therapy

Implantable devices significantly improve lifespan, but are expensive, and as such are only used in patients with end-stage HF (Boehmer, 2003; Cleland *et al.*, 2005; Eapen and Rogers, 2009; John *et al.*, 2008; Starling *et al.*, 2007). Surgical interventions for severe end-stage HF include coronary revascularisation (such as CABG surgery), cardiomyoplasty to assist myocardial contraction (Furnary *et al.*, 1996), partial resection of the left ventricle (the “Batista” procedure) (Batista *et al.*, 1997), circular patch plasty (the “Dor” procedure) (Dor *et al.*, 1998), mitral valve repair or replacement (Bolling *et al.*, 1998), external ventricular constraint devices [such as the Acorn CorCap device (Eapen and Rogers, 2009; Konertz *et al.*, 2001; Starling *et al.*, 2007)], mechanical circulatory support (Hunt and Frazier, 1998) and cardiac transplantation (Dec, 2004; Hunt *et al.*, 2009).

1.4.2. Limitations of current treatments and the need for new and effective medications

While the above-mentioned strategies have some benefits in HF, these treatments largely delay disease progression. There is currently no cure for HF and mortality in these patients remains high with one-third dying within a year of diagnosis (Bleumink *et al.*, 2004; Cowie *et al.*, 2000; Zannad *et al.*, 1999). Therefore there is need for novel therapies to treat HF and improve function of the failing heart. Several strategies have been considered, including stem cell therapy, cardiac regeneration, and the induction of physiological hypertrophy (Owen *et al.*, 2009; Pretorius *et al.*, 2008; Schachinger *et al.*, 2004; Stamm *et al.*, 2003; Strauer *et al.*, 2002; Taylor *et al.*, 1998).

As previously noted, exercise is a potent stimulus for the development of physiological hypertrophy (McMullen *et al.*, 2003), and it has been shown that regular physical activity protects against a range of cardiovascular diseases. Exercise can also reverse some of the molecular and functional abnormalities found in patients and animal models of cardiac disease (Coats, 2000; Jennings *et al.*, 1986; Konhilas *et al.*, 2006; McMullen *et al.*, 2003; McMullen *et al.*, 2007; Nelson *et al.*, 1986; Scheuer *et al.*, 1982). In animal studies it has been demonstrated that exercise induces physiological hypertrophy, and inhibits pathological hypertrophy (Konhilas *et al.*, 2006; McMullen *et al.*, 2003; McMullen *et al.*, 2007). Exercise training regimes are used as a non-pharmacological approach to alleviate symptoms and improve quality of life in patients with HF (Flynn *et al.*, 2009; Hunt *et al.*, 2009). However, HF patients may have limited exercise capacity, particularly due to pulmonary congestion that induces dyspnea due to lack of oxygen to the muscles (Pina *et al.*, 2003; Zipes *et al.*, 2005). Whether it would be possible to selectively activate signalling pathways responsible for physiological cardiac hypertrophy in order to improve outcomes of patients with HF is currently unknown.

1.5. Triggers and signalling pathways that induce cardiac hypertrophy and remodelling

An understanding of signalling cascades that mediate distinct forms of hypertrophy and remodelling may provide new opportunities to treat HF. Hypertrophy of cardiac

myocytes is associated with an increase in protein synthesis and organisation of contractile proteins into sarcomeric units, as well as stimulation of the hypertrophic gene expression program (Aoki and Izumo, 2001; Chien *et al.*, 1993; Izumo *et al.*, 1988; Sugden and Clerk, 1998). There are various stimuli that activate signal transduction pathways mediating cardiac hypertrophy, including mechanical stimuli, humoral factors (e.g. Ang II), growth factors, cytokines, hormones and changes in energy metabolism (Bernardo *et al.*, 2010; Hunter and Chien, 1999; McMullen *et al.*, 2005). These hypertrophic signals are transduced via signalling pathways which in turn activate transcription factors and transcriptional co-factors to promote or suppress transcription of a specific gene promoter (Akazawa and Komuro, 2003).

Signalling cascades responsible for the induction of hypertrophy are complex and there is extensive crosstalk (Figure 6). However, studies utilising genetic mouse models suggest that physiological and pathological cardiac hypertrophy can be induced by distinct stimuli/triggers and signalling pathways. Pathological cardiac hypertrophy is mediated, at least in part, via the G_q/G₁₁ protein-coupled receptor (GPCR) pathways [Figure 7, (Akhter *et al.*, 1998; Sakata *et al.*, 1998; Wettschureck *et al.*, 2001)], while physiological cardiac hypertrophy appears to be mediated largely via the insulin-like growth factor 1 (IGF-1)-phosphoinositide 3-kinase (PI3K, p110 α)-Akt pathway [Figure 7, (DeBosch *et al.*, 2006b; Luo *et al.*, 2005; McMullen *et al.*, 2003; McMullen *et al.*, 2004; Shioi *et al.*, 2000)]. In support of this hypothesis, human studies have shown that hypertension induced increased cardiac release of GPCR agonists [e.g. Ang II and endothelin-1 (ET-1)], while the cardiac formation of IGF1, but not Ang II and ET-1, was increased in the athlete's heart (Neri Serneri *et al.*, 2001a; Neri Serneri *et al.*, 2001b). Other signalling pathways involved in cardiac remodelling include the glycoprotein 130 (gp-130)-Janus Kinase (JAK)-Signal Transducer and Activator of Transcription (STAT) pathway, mitogen- activated protein kinases [MAPKs, including the extracellularly responsive kinases (ERK 1/2/5/7), the c-Jun N-terminal kinases (JNK 1/2/3), and the p38 MAPKs], protein kinase A, B and C (PKA, PKB and PKC, respectively), calcium signalling proteins [calcineurin and calcium/ calmodulin-dependent protein kinase II (CaMKII)], and stress-activated signalling pathways [such as mammalian sterile 20-like kinase 1 (Mst1)] (see Figure 6). Signalling cascades relevant to this thesis are discussed in detail below.

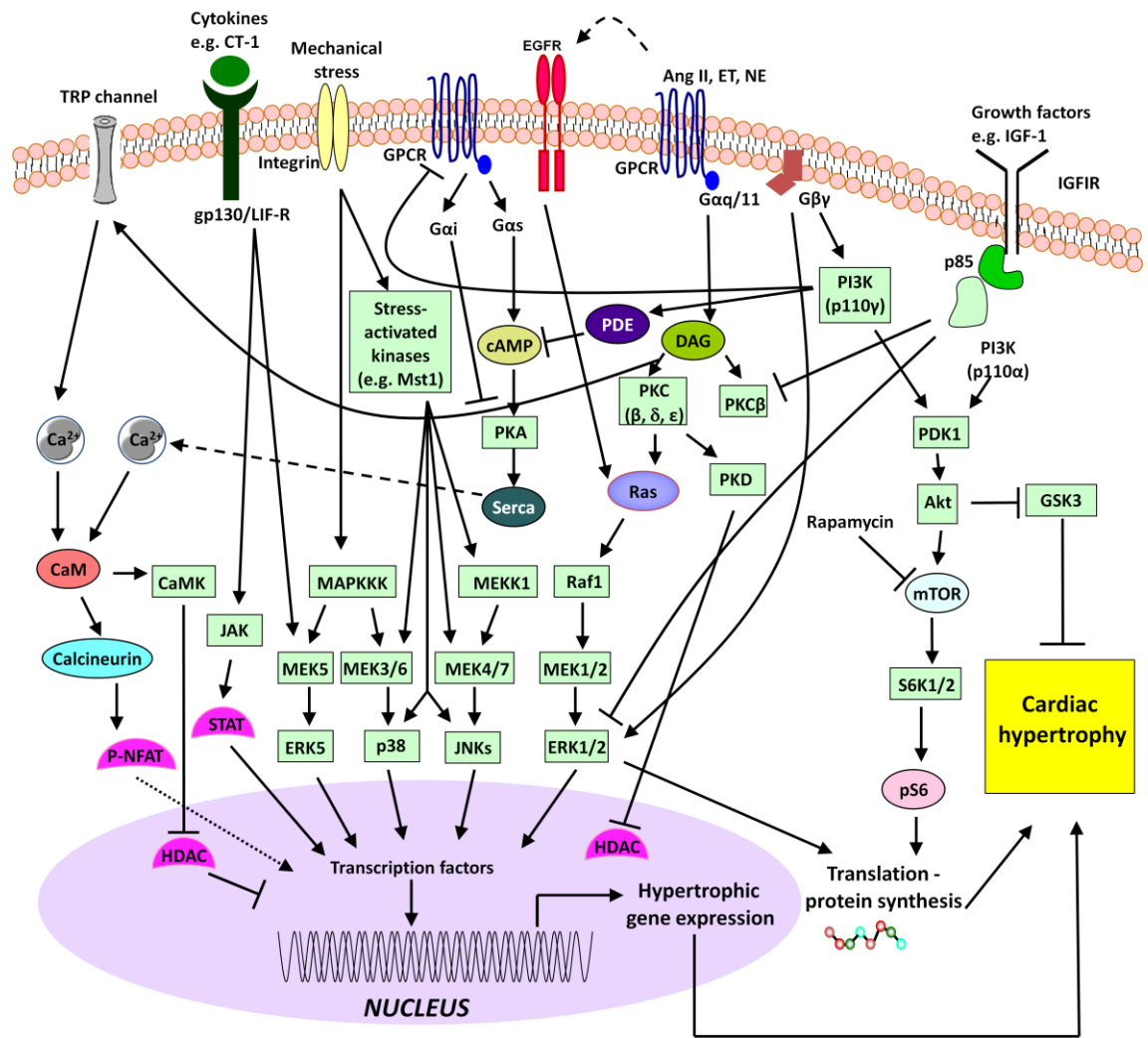


Figure 6. Signalling pathways associated with cardiac hypertrophy and remodelling.

A schematic representation of some key signalling pathways involved in cardiac hypertrophy. For simplification, not all signalling cascades and crosstalk are shown. IGF1: insulin-like growth factor 1; IGF1R: IGF1 receptor; PI3K: phosphoinositide 3-kinase; PDK1: phosphoinositide-dependent kinase 1; Akt: protein kinase B; mTOR: mammalian target of rapamycin; GSK3: glycogen synthase kinase 3; Ang II: angiotensin II, ET-1: endothelin 1; NE: norepinephrine; PDE: phosphodiesterase; cAMP: cyclic AMP; GPCR: G protein coupled receptor; DAG: diacylglycerol; PKA, PKC, PKD: protein kinase A, C, D; MEKK: mitogen/ extracellular-signal-regulated kinase kinase; MEK: mitogen/extracellular-signal-regulated kinase; MAPKKK: mitogen-activated protein kinase kinase kinase; Mst1: mammalian sterile 20-like kinase 1; SERCA: sarcoplasmic reticulum Ca^{2+} ATPase 2a.; ERK: extracellular regulated kinase; EGFR: epidermal growth factor receptor; JNK: c-Jun N-terminal kinase; TRP: transient receptor potential; gp130/LIF-R: glycoprotein 130 receptor-low affinity leukaemia factor; caM: calmodulin; CaMK: Ca^{2+} /calmodulin-dependent protein kinase; JAK/STAT: Janus Kinase/Signal transducers and activators of transcription; HDAC: histone deacetylase; and NFAT: Nuclear factor of activated T-cells. Figure adapted from Bernardo, B.C., Weeks, K.L., Pretorius, L., and McMullen, J.R. (2010). Molecular distinction between physiological and pathological cardiac hypertrophy: experimental findings and therapeutic strategies. *Pharmacology & Therapeutics* 128, 191-227. Used with permission of Elsevier.

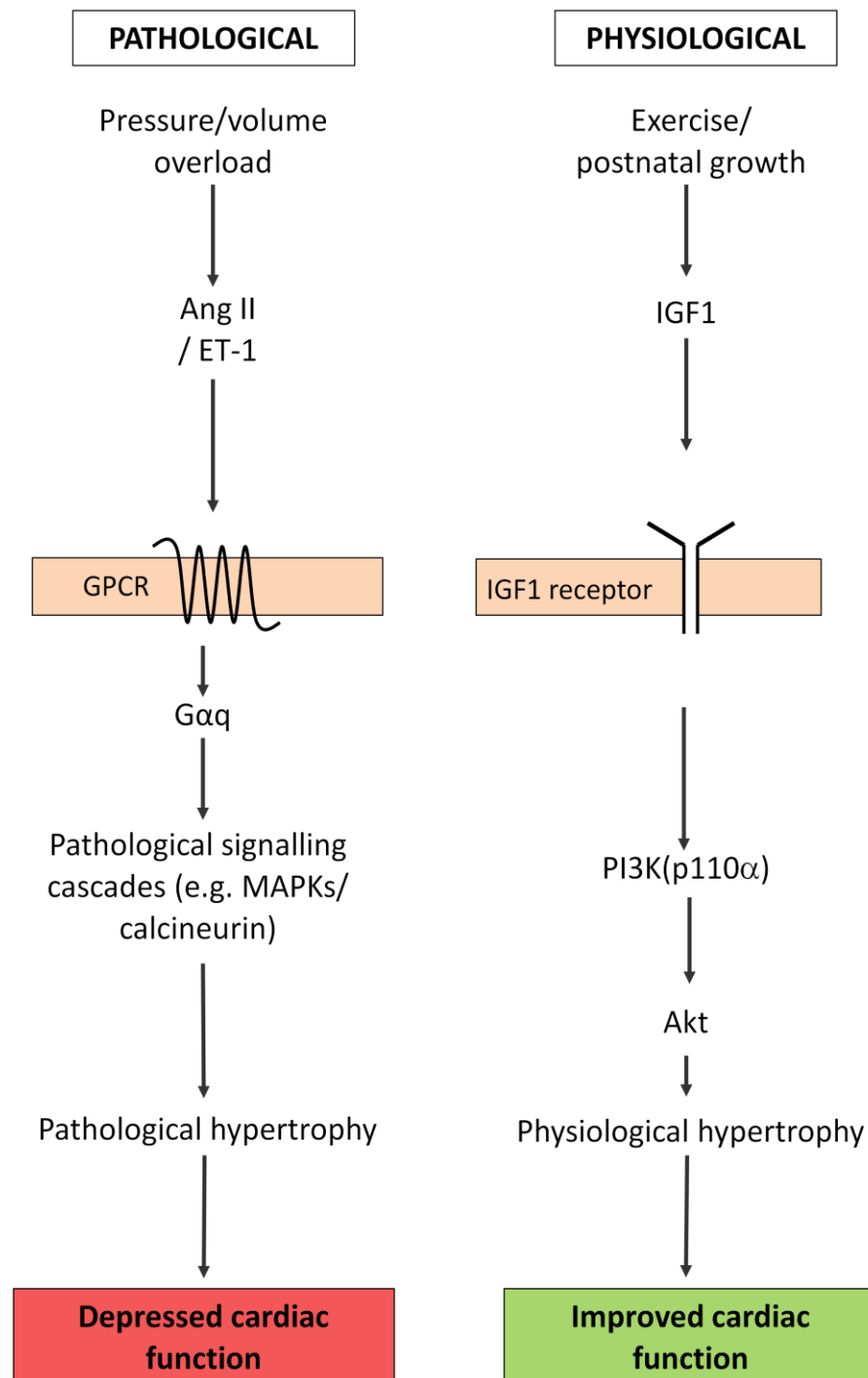


Figure 7. Physiological and pathological cardiac hypertrophy.

Pathological hypertrophy is mediated by the G protein-coupled receptor (GPCR) pathway and is detrimental. In contrast physiological hypertrophy is mediated via the Insulin-like growth factor 1 (IGF1) – phosphoinositide 3-kinase [PI3K] (p110α) – Akt pathway and is considered beneficial. AngII: Angiotensin II; ET-1: endothelin 1; and MAPKs: mitogen activated protein kinases. Figure adapted from Owen, K.L., Pretorius, L., and McMullen, J.R. (2009). The protective effects of exercise and phosphoinositide 3-kinase (p110alpha) in the failing heart. *Clinical Science* 116, 365-375.

Used with permission of Portland Press.

1.5.1. The IGF1-PI3K-Akt pathway

Studies from genetic mouse models suggest that the IGF1-PI3K (p110 α)-Akt pathway is a critical mediator of physiological hypertrophy and is protective in settings of cardiac stress.

1.5.1.1. IGF1

IGF1 is produced mainly by the liver in response to growth hormone stimulation, and has a critical role in normal growth and development (Adams *et al.*, 2000). IGF1 acts via the insulin-like growth factor 1 receptor [IGF-1R, (Adams *et al.*, 2000)], a receptor tyrosine kinase that in turn activates downstream signalling proteins such as PI3K (p110 α). Several studies have examined the importance of IGF1 and IGF-1R in the heart. Transgenic mice with over-expression of IGF1 in both skeletal and cardiac muscle displayed cardiac hypertrophy with enhanced systolic function up to 10 weeks of age, but progressed to pathological cardiac hypertrophy by 12 months of age (Delaughter *et al.*, 1999). However, this study was confounded by increased gut, liver and spleen weights as a result of persistent transgene expression (Fiorotto *et al.*, 2003), even though there was no reported increase in serum IGF1 levels (Delaughter *et al.*, 1999). In another transgenic mouse model, cardiac-specific over-expression of IGF1 resulted in cardiac hypertrophy characterised by normal cardiac function (Reiss *et al.*, 1996). However, interpretation of this study was confounded by increased IGF1 secretion from cardiac myocytes of transgenic mice, resulting in increased plasma IGF1 levels and increased organ weights.

To examine IGF1 signalling without the effects of secreted IGF1 on other tissues, transgenic mice over-expressing the insulin-like growth factor 1 receptor (IGF-1R) were generated (McMullen *et al.*, 2004). Cardiac-specific over-expression of IGF-1R induced cardiac hypertrophy without evident histopathology and enhanced systolic function at 3 months of age as well as 12-16 months of age (McMullen *et al.*, 2004). In support of the hypothesis that IGF1 signalling is critical for physiological cardiac hypertrophy, cardiac-specific ablation of the IGF-1R gene in mice reduced the hypertrophic response to swim training compared with Ntg mice (Kim *et al.*, 2008). Over-expression of IGF1 or IGF1-R has been shown to be beneficial in settings of

dilated cardiomyopathy, myocardial infarction and pressure overload (Huynh *et al.*, 2010; Kajstura *et al.*, 2001; Li *et al.*, 1997b; McMullen *et al.*, 2004; Welch *et al.*, 2002).

1.5.1.2. PI3Ks

PI3Ks act downstream of IGF1 (see Figure 6) and are able to induce signals by phosphorylating the hydroxyl group at position 3 of the phosphoinositides (Toker and Cantley, 1997; Vanhaesebroeck *et al.*, 1997; Whitman *et al.*, 1988). They are involved in membrane trafficking, adhesion, actin re-arrangement, cell growth and cell survival (Toker and Cantley, 1997). PI3Ks are divided into three major classes (Class I, II, and III), defined based on their structure, regulation and their specificity for binding to substrates (Fruman *et al.*, 1998; Vanhaesebroeck *et al.*, 1997). These classes are further divided into the various isoforms of PI3K, of which p110 α (Class IA) is of particular significance in regulating physiological heart growth (Luo *et al.*, 2005; McMullen *et al.*, 2003; Shioi *et al.*, 2000). Activation of the p110 α isoform is coupled to receptor tyrosine kinases (such as IGF-1R).

Cardiac-specific transgenic mice expressing a constitutively active PI3K (p110 α) mutant (caPI3K) have increased PI3K (p110 α) activity and larger hearts, while cardiac-specific transgenic mice with a truncated mutant (lacking the kinase domain) of p110 α have depressed PI3K (p110 α) activity [also known as dominant negative PI3K (p110 α) mice (dnPI3K)] have smaller hearts (Figure 8) compared with non-transgenic (Ntg) mice (Shioi *et al.*, 2000). These mice show no signs of cardiomyopathy (such as apoptosis, necrosis, or interstitial fibrosis; Figure 8) and under basal conditions have normal cardiac function and life span compared with Ntg (Shioi *et al.*, 2000).

To assess whether PI3K (p110 α) was critical for the development of physiological or pathological cardiac growth in the adult heart, dnPI3K and Ntg mice were subjected to pressure overload and chronic exercise training (McMullen *et al.*, 2003). dnPI3K transgenic mice displayed a blunted hypertrophic response to exercise (swimming) but not to pressure overload (ascending aortic banding) [Figure 9, (McMullen *et al.*, 2003)]. The contribution of PI3K in regulating an IGF-1R-induced increase in heart size was determined by genetically crossing dnPI3K with IGF-1R

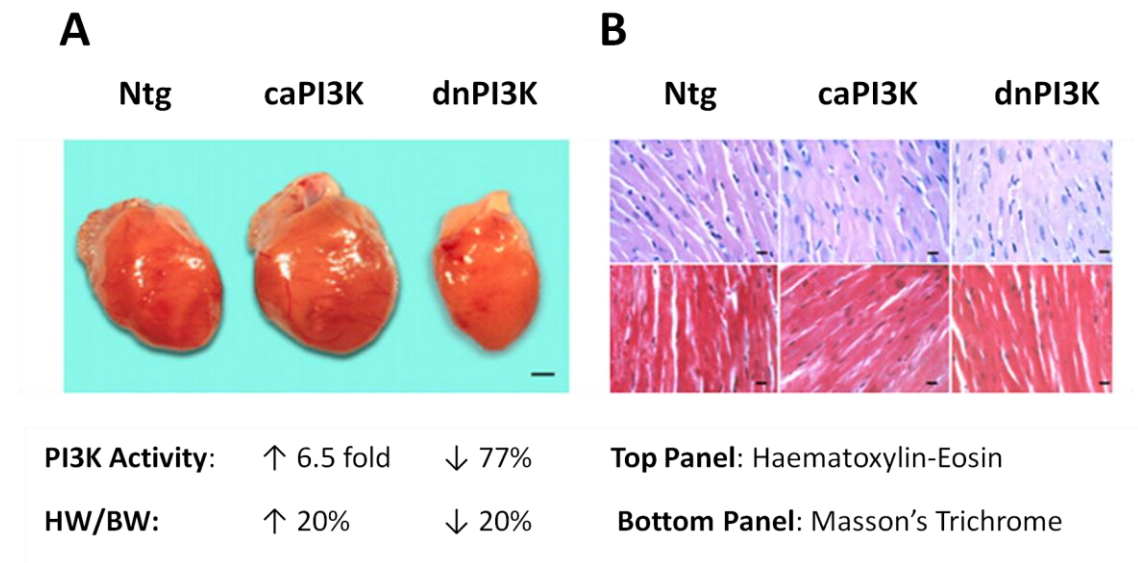


Figure 8. PI3K (p110 α) is necessary and sufficient for physiological postnatal heart growth.

A: Differences in heart size and PI3K activity of constitutively active PI3K (p110 α) (caPI3K) and dominant negative PI3K (p110 α) (dnPI3K) mice, compared with Ntg mice. Increased PI3K (p110 α) activity increases heart size by 20% (caPI3K), while depressed PI3K (p110 α) activity decreases heart size by 20% (dnPI3K). HW/BW indicates heart weight to body weight ratio. Bars represent 1mm. **B:** No sign of histopathology (myocyte disarray or fibrosis) in either caPI3K or dnPI3K mice compared with Ntg mice, as shown by both haematoxylin-eosin staining and Masson's Trichrome staining. Bars represent 10 μ m. Figure adapted from Shioi, T., et al., (2000). *The conserved phosphoinositide 3-kinase pathway determines heart size in mice. EMBO Journal* 19, 2537-2548.

Used with permission of John Wiley and Sons. Copyright © 2000 European Molecular Biology Organization

transgenic mice. The dnPI3K mutant was able to completely inhibit the IGF-1R-induced growth, suggesting that IGF-1R promoted physiological cardiac hypertrophy in a PI3K (p110 α)-dependent manner (McMullen *et al.*, 2004).

PI3K is also important for maintaining cardiac function in response to a pathological stimulus. In response to aortic banding for 1 week, dnPI3K mice displayed depressed systolic function, whereas the Ntg mice did not (McMullen *et al.*, 2003). More recent studies have utilised knockout mice to investigate the role of class IA PI3K in regulating hypertrophy. Mice lacking the regulatory subunits of class IA PI3K or cardiac-specific knockout of p110 α displayed a phenotype of decreased heart size under basal conditions (Lu *et al.*, 2009; Luo *et al.*, 2005). Mice lacking the PI3K regulatory subunits also displayed blunted hypertrophic growth in response to exercise (Luo *et al.*, 2005). Taken together, the above studies support the hypothesis that PI3K (p110 α) is critical for inducing physiological cardiac hypertrophy (Table 4). In settings of pressure overload and dilated cardiomyopathy, increased PI3K (p110 α) activity (using the caPI3K mice) attenuated cardiac dysfunction, blunted pathological cardiac hypertrophy and reduced fibrosis (McMullen *et al.*, 2007). Similarly, caPI3K mice had improved cardiac function and lifespan following myocardial infarction (Lin *et al.*, 2010).

1.5.1.3. Akt

PI3K (p110 α) mediates physiological cardiac hypertrophy, at least in part, through the downstream-activated protein serine/threonine kinase Akt (see Figure 6) (Burgering and Coffey, 1995; Cantley, 2002; Klippel *et al.*, 1997). Akt consists of three isoforms – Akt1, Akt2 and Akt3, but only Akt1 and Akt2 are highly expressed in the heart (Matsui and Rosenzweig, 2005). Initial studies of Akt transgenic mice led to confounding results, as phenotypes ranged from absence of hypertrophy with protection following ischaemia/reperfusion to significant pathological phenotypes and premature death (Condorelli *et al.*, 2002; Matsui *et al.*, 2002; Shioi *et al.*, 2002; Shiraishi *et al.*, 2004). These varying phenotypes may be due to the degree of Akt activation and intracellular

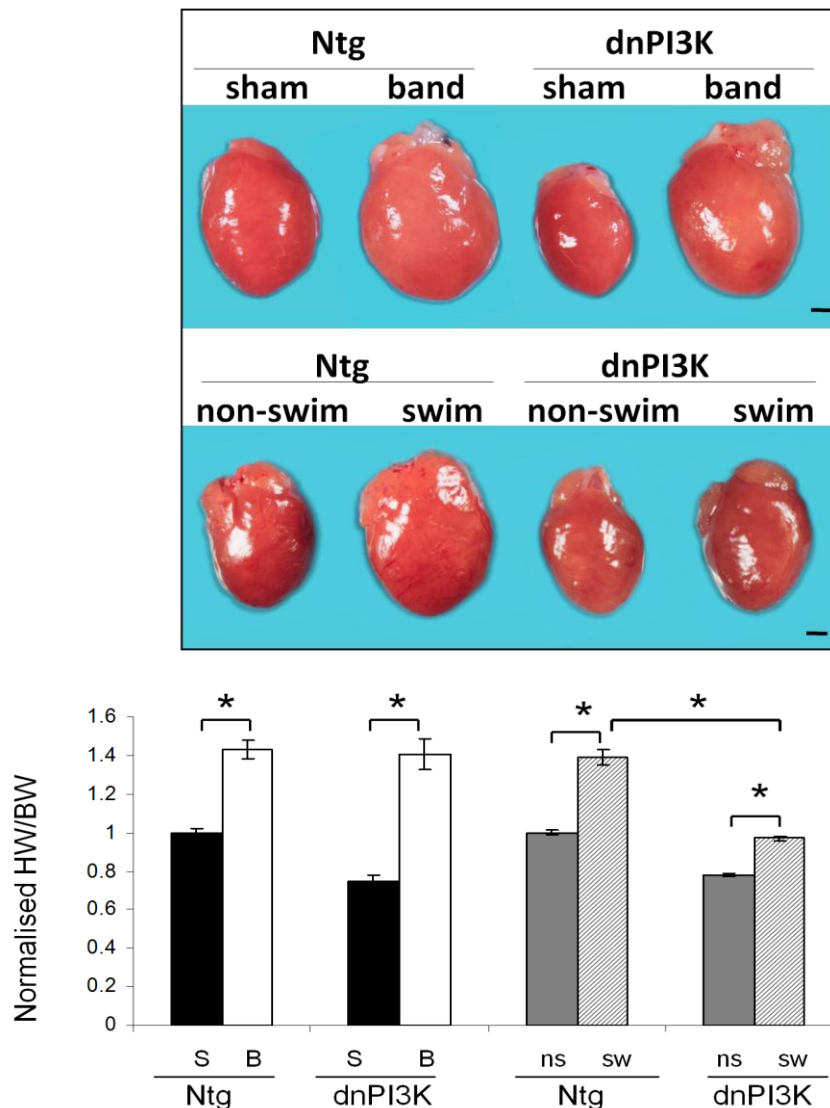


Figure 9. PI3K (p110 α) is critical for physiological exercise-induced cardiac hypertrophy.

Reduction of PI3K (p110 α) activity blunted the cardiac hypertrophic response following swim training, but had no effect on heart size following aortic banding (ascending aortic constriction). Top panel: Hearts from Ntg and dnPI3K mice that were subjected to aortic banding (band) for 1 week compared with hearts from mice that underwent a sham operation. Hearts from Ntg and dnPI3K mice that underwent swim-training (4 weeks) compared with sedentary littermates (non-swim). Bars represent 1mm. Bottom panel: Quantitative analysis of heart weight/body weight ratio (HW/BW) showing that banded (B, white bars) Ntg and dnPI3K mice have similar increases in HW/BW compared with sham mice (S, black bars). Ntg mice that underwent swim training (sw, dashed bars) have increased HW/BW compared with non-swim littermates (ns, grey bars). In contrast, dnPI3K mice that underwent swim training have a blunted cardiac hypertrophic response. * $p < 0.05$. Figure adapted from McMullen, J.R., et al., (2003). Phosphoinositide 3-kinase(p110 α) plays a critical role for the induction of physiological, but not pathological, cardiac hypertrophy. *PNAS* 100, 12355-12360.

Table 4. Animal studies showing that the IGF1R-PI3K (p110 α)-Akt pathway is critical for physiological cardiac hypertrophy.

Mouse model	Basal phenotype (compared with non-transgenic or wild-type)	Response to physiological hypertrophic stimuli
Cardiac-specific insulin-like growth factor 1 receptor knockout mice (Kim <i>et al.</i> , 2008)	- Normal cardiac development - No change in heart size (Kim <i>et al.</i> , 2008)	- Blunted physiological hypertrophy following swim training - Normal cardiac function (Kim <i>et al.</i> , 2008)
Cardiac-specific dominant negative PI3K (p110 α) transgenic mice (Shioi <i>et al.</i> , 2000)	- 20% decrease in heart size - Normal cardiac function - Normal lifespan - No histopathology (Shioi <i>et al.</i> , 2000)	- Blunted physiological hypertrophy following swim training - Normal cardiac function - No histopathology (McMullen <i>et al.</i> , 2003)
Class IA PI3K knockout mice (knockout of p85 α , p55 α , p50 α and p85 β) (Luo <i>et al.</i> , 2005)	- 20% decrease in heart size (Luo <i>et al.</i> , 2005)	- Blunted physiological hypertrophy following swim training - Normal cardiac function - No histopathology (Luo <i>et al.</i> , 2005)
Cardiac-specific knockout of p110 α (Lu <i>et al.</i> , 2009)	- 15% decrease in heart size - Normal cardiac function - No difference in apoptosis (Lu <i>et al.</i> , 2009)	Not examined
Akt1 knockout mice (Cho <i>et al.</i> , 2001)	- Normal lifespan - Normal heart size and cardiac function (DeBosch <i>et al.</i> , 2006b)	- Blunted physiological hypertrophy following swim training - Slight decrease in cardiac function following swim training (DeBosch <i>et al.</i> , 2006b)

localisation. It is now generally accepted that Akt1 mediates cardiac growth (DeBosch *et al.*, 2006b), while Akt2 is important for cardiac metabolism and cell survival (DeBosch *et al.*, 2006a).

It is also important to note, as shown in Figure 6, that Akt can be activated by both receptor tyrosine kinases (such as IGF-1R) and GPCRs, though studies from Akt1 knockout mice suggest that Akt1 is activated in response to physiological stimuli whereas Akt2 is activated in response to pathological stimuli (e.g. ET-1) (DeBosch *et al.*, 2006a; DeBosch *et al.*, 2006b). Akt1 knockout mice had normal cardiac function and lifespan under basal conditions and showed a blunted response to exercise (DeBosch *et al.*, 2006b). In contrast, Akt1 knockout mice developed an exaggerated pathological hypertrophic response to pressure overload (DeBosch *et al.*, 2006b). These studies indicate that Akt1 is critical for the development of physiological cardiac hypertrophy.

Akt is capable of promoting cell growth through regulation of glycogen synthase kinase 3 (GSK-3) and the mammalian target of rapamycin (mTOR) (Figure 6). To date, neither GSK-3 nor mTOR have specifically been shown to regulate physiological cardiac hypertrophy. Akt mediates cell survival through direct regulation and transcription control of several downstream apoptotic effectors including Bad, Bax, Bcl-2, caspase-9, NF κ B, p53, and JNK (Bertrand *et al.*, 2008; Song *et al.*, 2005; Yaoita and Maruyama, 2008). In support of this, transgenic expression of nuclear Akt was beneficial in a setting of pressure overload (Shiraishi *et al.*, 2004).

1.5.1.4. Benefits of IGF1-PI3K (p110 α)-Akt signalling in cardiac disease

Several studies suggest that activation of the IGF1-PI3K-Akt signalling pathway or exercise are beneficial in a setting of cardiac disease (summarised in Table 5). In contrast, decreasing PI3K (p110 α) activity or Akt1 had an adverse effect in a setting of cardiac stress (Table 5).

1.5.2. G-protein coupled receptor pathways

In response to a pathological insult such as pressure overload, hypertrophic agonists, such as Ang II, are released from myocytes and bind to transmembrane GPCRs, causing

Table 5. Mouse models that highlight the protective effects of the IGF1-PI3K (p110 α)-Akt signalling cascade or exercise in settings of heart disease.

Protective mechanism	Mouse model	Gene expression or activity	Evidence of protective effect in a disease setting
Increased IGF1 signalling	IGF1 transgenic (Reiss <i>et al.</i> , 1996)	Cardiac-specific over-expression of IGF1 was associated with increased circulating IGF1 from cardiac myocytes	<ul style="list-style-type: none"> Decreased left ventricular remodelling and cardiac dysfunction in dilated cardiomyopathy (Welch <i>et al.</i>, 2002) Reduced cardiac dysfunction and cell death in diabetic cardiomyopathy (Kajstura <i>et al.</i>, 2001) Attenuated cardiac myocyte necrosis in eccentric cardiac hypertrophy (Li <i>et al.</i>, 1997b) Reduced ventricular dilation and cell death in myocardial infarction (Li <i>et al.</i>, 1997b)
	IGF-1R transgenic (McMullen <i>et al.</i> , 2004)	Cardiac myocyte specific over-expression of IGF-1R	<ul style="list-style-type: none"> Blunted pathological hypertrophy and fibrosis following pressure overload (McMullen <i>et al.</i>, 2004) Reduced diastolic dysfunction and fibrosis in a mouse model of diabetic cardiomyopathy (Huynh <i>et al.</i>, 2010)
Increased PI3K (p110 α) activity	caPI3K transgenic (Shioi <i>et al.</i> , 2000)	Cardiac myocyte specific expression of caPI3K (p110 α) (increased PI3K activity 6.5 fold)	<ul style="list-style-type: none"> Prevented cardiac dysfunction and blunted pathological hypertrophy and fibrosis following pressure overload (McMullen <i>et al.</i>, 2007) Prolonged lifespan in a setting of dilated cardiomyopathy (McMullen <i>et al.</i>, 2007) Blunted cardiac dysfunction in a setting of myocardial infarction (Lin <i>et al.</i>, 2010)
Decreased PI3K (p110 α) activity	dnPI3K transgenic (Shioi <i>et al.</i> , 2000)	Cardiac myocyte specific reduction (77%) in PI3K (p110 α) activity	<ul style="list-style-type: none"> Exacerbated fibrosis and cardiac dysfunction following pressure overload (McMullen <i>et al.</i>, 2003; McMullen <i>et al.</i>, 2007) Reduced lifespan in a setting of dilated cardiomyopathy (McMullen <i>et al.</i>, 2007) Accelerated heart failure progression after myocardial infarction (Lin <i>et al.</i>, 2010)
Increased Akt activity	Akt-nuclear (Shiraishi <i>et al.</i> , 2004)	Increased content and activity of Akt in the nuclei of cardiac myocytes	<ul style="list-style-type: none"> Reduced left ventricular remodelling and cardiac dysfunction, and improved survival following pressure overload (Shiraishi <i>et al.</i>, 2004)
Decreased Akt activity	Akt1 null mice (Akt1 ^{-/-}) (Cho <i>et al.</i> , 2001)	Whole body disruption of Akt1 gene – leads to loss of Akt1 mRNA and protein expression	<ul style="list-style-type: none"> Exacerbated hypertrophy and cardiac dysfunction following pressure overload (DeBosch <i>et al.</i>, 2006b)
Exercise	Voluntary cage wheel running (2-6 months)	Not applicable	<ul style="list-style-type: none"> Reduced fibrosis, prevented apoptosis and reversed the expression of hypertrophic markers in hypertrophic cardiomyopathy (Konhilas <i>et al.</i>, 2006)
	Swim training (10-11 weeks)	Not applicable	<ul style="list-style-type: none"> Prolonged lifespan by 15-20% in dilated cardiomyopathy (McMullen <i>et al.</i>, 2007)

* Table adapted from Bernardo, B.C., Weeks, K.L., Pretorius, L., and McMullen, J.R. (2010). Molecular distinction between physiological and pathological cardiac hypertrophy: experimental findings and therapeutic strategies. *Pharmacology & Therapeutics* 128, 191-227.

Used with permission of Elsevier.

the associated trimeric G_q/G_{11} proteins to dissociate into subunits (e.g. $G_{\alpha q}$, see Figure 6) that stimulate the hydrolysis of the membrane phospholipids to generate two second messengers – diacylglycerol (DAG) and inositol-1,4,5-triphosphate ($\text{Ins}(1,4,5)\text{P}_3$) (Exton, 1996; Neer, 1995; Sugden and Clerk, 1998). Cardiac-specific over-expression of $G_{\alpha q}$ induced pathological hypertrophy and cardiac failure, but did not affect physiological postnatal growth (D'Angelo *et al.*, 1997). Cardiac-specific transgenic mice expressing a G_{qi} inhibitory peptide that specifically inhibits G_q -coupled receptor signalling, and mice lacking the trimeric G proteins $G_{\alpha q}$ and $G_{\alpha 11}$ did not develop cardiac hypertrophy in response to pressure overload (Akhter *et al.*, 1998; Wettschureck *et al.*, 2001). These studies suggest that the G_q/G_{11} pathway mediates pathological cardiac hypertrophy.

DAG production activates PKC and transient receptor potential channels (TRPC, see Figure 6) (Hofmann *et al.*, 1999). The exact role of PKC remains unclear, as some isoforms appear to play a role in adaptive responses, but others appear to have negative consequences. Cardiac-specific over-expression of $\text{PKC}\beta$ resulted in pathological hypertrophy and premature cardiac death (Bowman *et al.*, 1997), while constitutively activated $\text{PKC}\epsilon$ induced no pathological consequences with normal cardiac function (Takeishi *et al.*, 2000).

1.5.3. MAPK and downstream pathways

MAPKs are divided into three subfamilies – ERKs, JNKs, and p38 MAPKs (Johnson *et al.*, 2005; Sugden and Clerk, 1998). It is known that pathological stimuli activate MAPKs and *in vitro* studies suggest that MAPKs play a regulatory role in pathological cardiac hypertrophy (Choukroun *et al.*, 1998; Clerk *et al.*, 1994; Clerk *et al.*, 1998; Komuro *et al.*, 1996; Pearson *et al.*, 2001; Sugden and Clerk, 1998; Takeishi *et al.*, 2001; Wang *et al.*, 1998a). The exact role of MAPKs in cardiac hypertrophy *in vivo* remains unclear, as studies using animal models show conflicting results (Braz *et al.*, 2003; Bueno *et al.*, 2000; Bueno and Molkenin, 2002; Nicol *et al.*, 2001; Zhang *et al.*, 2000).

1.5.3.1. ERK 1/2 pathway

ERK1/2 has been shown to be activated in numerous settings of cardiac hypertrophy and failure downstream of GPCR (Bueno and Molkentin, 2002; Muslin, 2008), including transactivation of EGFR [Figure 6, (Thomas *et al.*, 2002)]. Dominant negative expression of a MAPK kinase (MAPKK) upstream of ERK1/2 blunted pressure overload-induced cardiac hypertrophy (Harris *et al.*, 2004), suggesting ERK1/2 is important for the development of pathological hypertrophy. However, transgenic mice over-expressing MEK1 (directly upstream of ERK1/2 that does not activate other MAPKs) in the heart developed cardiac hypertrophy associated with enhanced cardiac function and no signs of histopathology (Bueno *et al.*, 2000). Using ERK1/2 knockout mice, Purcell and colleagues suggested that ERK1/2 signalling is not required for mediating either physiological or pathological hypertrophy (Purcell *et al.*, 2007).

The molecular mechanism responsible for the hypertrophic effects of ERK1/2 is yet to be resolved, but appears to involve 2 different mechanisms. Activation of the Raf/MEK/ERK pathway has been linked with protein synthesis and a compensatory phenotype as reported in MEK1 transgenic mice (Bueno *et al.*, 2000; Bueno and Molkentin, 2002; Wang *et al.*, 2001). In contrast, autophosphorylation of ERK2 at residue Thr188 promoted nuclear translocation and subsequent phosphorylation of hypertrophic factors (such as c-Myc) that have been linked to pathological hypertrophy (Lorenz *et al.*, 2009).

1.5.3.2. JNKs

Three JNK genes have been identified (JNK 1/2/3), with JNK1 and JNK2 expressed in the heart (Molkentin and Dorn, 2001). JNK isoforms are phosphorylated in response to stress or GPCR activation (Figure 6) (Molkentin and Dorn, 2001), and several studies have shown that JNK1 and JNK2 were elevated in pathological cardiac hypertrophy and myocardial infarction in rats, as well as human heart failure (Choukroun *et al.*, 1999; Cook *et al.*, 1999; Li *et al.*, 1998). JNKs have previously been identified as important in relation to stress responses such as apoptosis (Johnson *et al.*, 1996; Ramirez *et al.*, 1997; Verheij *et al.*, 1996; Xia *et al.*, 1995). Pressure overload in mice has been shown to induce JNK activation at 7 days post-banding (Thorburn *et al.*, 1993). Additionally,

JNK was activated in hearts from HF patients (Cook *et al.*, 1999), and in the myocardium of infarcted rat hearts (Li *et al.*, 1998). *In vitro* studies have shown that JNKs may be important regulators of pathological hypertrophy (Bogoyevitch *et al.*, 1996; Choukroun *et al.*, 1998; Choukroun *et al.*, 1999; Ramirez *et al.*, 1997; Wang *et al.*, 1998b), but *in vivo* data have been more difficult to interpret.

Cardiac-specific JNK activation did not result in hypertrophy but induced premature death associated with congestive HF (Petrich *et al.*, 2003). Dominant negative MEK4 (upstream of JNK, see Figure 6) transgenic mice were able to attenuate pathological cardiac hypertrophy (Choukroun *et al.*, 1999), and knockout of MEKK1 (upstream of MEK4/7, see Figure 6) was essential for $G_{\alpha q}$ -induced pathological cardiac hypertrophy (Minamino *et al.*, 2002), suggesting that JNKs may be important regulators of pathological cardiac hypertrophy. However subsequent studies seem to suggest that individual JNK members are not required for cardiac growth, or that the JNK isoforms are functionally redundant. Transgenic mice expressing a dominant negative mutant of JNK 1/2 in the heart had increased cardiac hypertrophy following pressure overload (Liang *et al.*, 2003), and cardiac-specific deletion of MEK4 did not affect cardiac growth under basal conditions or in response to pressure overload (Liu *et al.*, 2009).

Null MEKK1 mice had similar heart weights compared with wildtype mice but had an enhanced hypertrophic response to pressure overload (Sadoshima *et al.*, 2002). This study suggests that pressure-overload induced hypertrophy occurs in the absence of JNK activation. In support of this, selective deletion of the three JNK isoforms (JNK1/2/3) did not alter the hypertrophic phenotype of mice in response to transverse aortic constriction (Tachibana *et al.*, 2006).

1.5.3.3. p38-MAPKs

The p38 MAPKs (α , β , δ and γ) are important mediators of numerous biological functions, including cell growth, proliferation, cell cycle and cell death, and are considered critical downstream of stress response pathways (Bassi *et al.*, 2008; Wilson *et al.*, 1996). It appears that only the α and β isoforms are expressed in the heart (Clark *et al.*, 2007; Jiang *et al.*, 1997), and p38 α is the predominant isoform in both human

and rodent myocardium (Braz *et al.*, 2003; Lemke *et al.*, 2001). Patients with ischemic heart disease had increased myocardial p38 MAPK activity (Cook *et al.*, 1999), and p38 MAPKs are reported to be involved in the regulation of cardiac gene expression, apoptosis, hypertrophy, remodelling and contractility (Baines and Molkentin, 2005; Liao *et al.*, 2001; Petrich and Wang, 2004; Wang, 2007). The role of p38 α and p38 β has been extensively examined in a variety of animal models. Many studies appear contradictory, and as such the exact role of p38 MAPKs in the heart remains unclear. The discrepancies between the studies described below could be explained by different genetic backgrounds, gender differences (as described earlier, see Section 1.3.7.), as well as distinct roles of p38 α and p38 β that may be differentially regulated by MEK3 and MEK6 (Bernardo *et al.*, 2010; Braz *et al.*, 2003; Liu *et al.*, 2006; Muslin, 2008).

As shown in Figure 6, MEK3 and MEK6 are regulators of p38 MAPK. Dominant negative mutants of both MEK3 and MEK6 developed pathological cardiac hypertrophy with cardiac dysfunction under basal conditions (Braz *et al.*, 2003). In response to pressure overload these transgenic mice displayed an exaggerated hypertrophic response, increased fibrosis and depressed cardiac function (Braz *et al.*, 2003). Activation of p38 MAPKs by MEK3 and MEK6 induced increased expression of the embryonic gene expression profile, loss of contractility and extensive fibrosis under basal conditions (Liao *et al.*, 2001). Results from cardiac-specific dominant negative p38 α mutant mice studies have been contradictory (Braz *et al.*, 2003; Liu *et al.*, 2006; Zhang *et al.*, 2003a). One study reported no basal phenotype with no difference in cardiac hypertrophy following pressure overload and less cardiac fibrosis (Zhang *et al.*, 2003a), while others showed extensive pathological cardiac hypertrophy at baseline (Braz *et al.*, 2003) and exaggerated hypertrophy following pressure overload (Liu *et al.*, 2006).

Additionally, cardiac-specific knockout of p38 α did not alter cardiac structure and function under basal conditions (Nishida *et al.*, 2004). Pressure overload in these mice induced a greater pathological hypertrophic response characterised by significant cardiac dysfunction, fibrosis and apoptosis (Nishida *et al.*, 2004), suggesting that p38 α is critical for cardiac protection in a setting of pressure overload. Cardiac-specific transgenic mice with a dominant negative mutant of p38 β developed no

hypertrophy under basal conditions but had reduced systolic function (Zhang *et al.*, 2003a). These mice displayed a similar degree of cardiac hypertrophy following pressure overload compared with Ntg mice, but developed less fibrosis (Zhang *et al.*, 2003a). Together these studies suggest that p38 MAPKs do not promote hypertrophy but contribute to fibrosis, loss of contractility and promote dilated cardiomyopathy.

1.5.4. Calcium signalling pathway

As previously described, calcium is essential for cardiac contraction (see Section 1.2.4.2.). Calcineurin is one of the best characterised calcium-dependent signalling proteins in the heart and has been implicated in the regulation of cardiac hypertrophy in conjunction with the NFAT family of transcription factors, as shown in Figure 6 (Olson and Williams, 2000). Transgenic mice with cardiac-specific expression of activated forms of calcineurin or NFAT3 developed cardiac hypertrophy and failure, while calcineurin-deficient mice displayed an impaired hypertrophic response to pressure overload (Bueno *et al.*, 2002; Molkenin *et al.*, 1998). Mice expressing a dominant negative mutant of the catalytic subunit of calcineurin (CnA) displayed a blunted hypertrophic response to pressure overload (Zou *et al.*, 2001), and inactivation of the regulatory subunit of calcineurin (CnB) also attenuated the response to pathological stimuli (Bueno *et al.*, 2002).

It has also been shown that calcineurin-NFAT coupling is involved in pathological, but not physiological, cardiac hypertrophy (Wilkins *et al.*, 2004). Pressure overload as well as myocardial infarction induced marked increases in calcineurin-NFAT signalling in NFAT-luciferase reporter transgenic mice, while exercise training failed to upregulate calcineurin-NFAT signalling (Wilkins *et al.*, 2004). Additionally, CnA β null mice have a normal cardiac hypertrophic response to IGF1 infusion (Wilkins *et al.*, 2004). Taken together, these results suggest that calcineurin is important for mediating pathological cardiac hypertrophy.

CAMKII has also been implicated in cardiac hypertrophy and failure. HF patients and animal models of HF showed cardiac up-regulation of CaMKII (Bossuyt *et al.*, 2008; Hoch *et al.*, 1999; Kirchhefer *et al.*, 1999). In the heart, CaMKII δ is the predominant isoform (Tobimatsu and Fujisawa, 1989). Over-expression of the nuclear isoform of CaMKII δ induced dilated cardiomyopathy (Zhang *et al.*, 2002). Similarly,

over-expression of the cytoplasmic isoform of CaMKII δ induced dilated cardiomyopathy and HF associated with mild fibrosis, atrial dilation, lung congestion and oedema (Zhang *et al.*, 2003b). Inhibition of CaMKII prevented pathological cardiac hypertrophy and dysfunction following myocardial infarction (Zhang *et al.*, 2005a). Additionally, CaMKII δ -null mice were protected against pathological hypertrophy and fibrosis in response to pressure overload (Backs *et al.*, 2009; Ling *et al.*, 2009). Recently it was also shown that inhibition of CaMKII δ in patients with HF improved contractility (Sossalla *et al.*, 2010).

1.5.5. Mammalian sterile 20-like kinase 1

Mst1 is a ubiquitously expressed serine/threonine kinase that has been implicated in playing an essential role in mediating cardiac myocyte apoptosis, fibrosis, cardiac dilation and dysfunction (Dan *et al.*, 2001; Odashima *et al.*, 2007; Ura *et al.*, 2001). Numerous studies have shown that ischaemia/reperfusion injury causes apoptosis of cardiac myocytes (Freude *et al.*, 2000; Kang *et al.*, 2000; Saraste *et al.*, 1997) and this has been linked to the activation of Mst1, which can activate p38 MAPK (Figure 10) (Yamamoto *et al.*, 2003). Cardiac-specific transgenic mice that over-express Mst1 developed a dilated cardiomyopathy phenotype (Figure 10), associated with apoptosis, fibrosis and pulmonary congestion (Yamamoto *et al.*, 2003).

1.5.6. Crosstalk between PI3K and GPCR regulated signalling pathways in the heart

It is now recognised that there is significant crosstalk between the IGF1-PI3K (p110 α)-Akt signalling pathway and other signalling cascades, including GPCR signalling pathways (see Figure 6). Such crosstalk may explain some of the benefits of activating this pathway in a setting of disease. Increased PI3K (p110 α) activity in the caPI3K mice inhibited ERK1/2 activation, while decreased PI3K (p110 α) activity in the dnPI3K mice showed up-regulation of ERK1/2 activation and an exaggerated pathological hypertrophic response to pressure overload (McMullen *et al.*, 2004; McMullen *et al.*, 2007). Similarly, Akt1^{-/-} mice displayed an exaggerated response to pressure overload, and the authors suggested that this may be due to hyperactivation of the MAPKs (DeBosch *et al.*, 2006b). It has also been proposed that PI3K (p110 α) signalling acts as

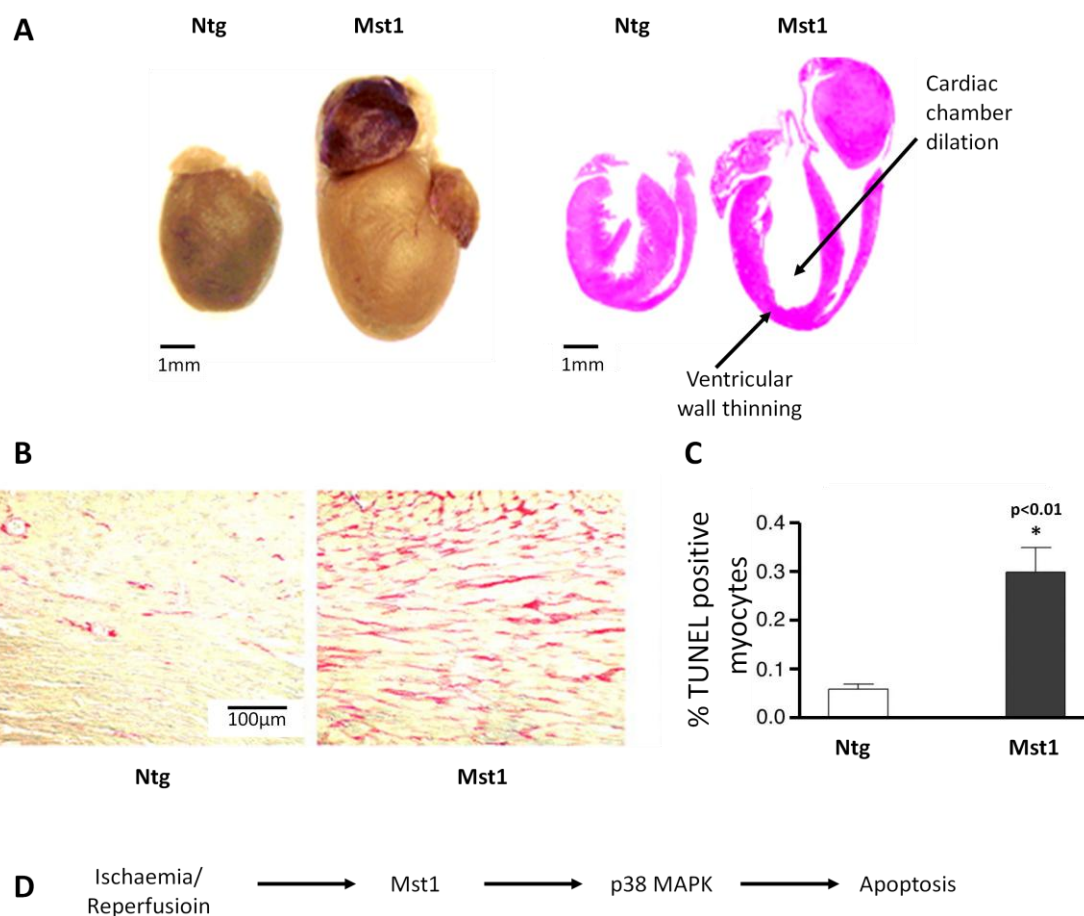


Figure 10. Transgenic mice with cardiac-specific over-expression of Mst1 develop dilated cardiomyopathy characterised by chamber dilation, wall thinning, fibrosis and apoptosis.

A: Gross appearance and transverse section of cardiac-specific mice over-expressing mammalian sterile 20-like kinase 1 (Mst1), showing dilated cardiomyopathy at three months of age compared with non-transgenic (Ntg) mice. Systolic function was 42% lower in the transgenic Mst1 mice compared to Ntg mice. **B:** Mst1 transgenic mice show marked fibrosis (shown in red using Sirius Red stain). **C:** Quantitative analysis of apoptosis [using terminal deoxynucleotidyl transferase nick end labelling (TUNEL) staining] showing increased apoptosis in Mst1 transgenic mice. **D:** Ischaemia/reperfusion activates Mst1 and p38 mitogen-activated protein kinases (MAPK) leading to apoptosis of cardiac myocytes. Figure adapted from Yamamoto, S., et al., (2003). Activation of Mst1 causes dilated cardiomyopathy by stimulating apoptosis without compensatory ventricular myocyte hypertrophy. *Journal of Clinical Investigation* 111, 1463-1474.

Used with permission of American Society for Clinical Investigation, from Activation of Mst1 causes dilated cardiomyopathy by stimulating apoptosis without compensatory ventricular myocyte hypertrophy, Yamamoto S., et al., 2003; permission conveyed through Copyright Clearance Center, Inc.

an upstream modulator of PKC β . Transgenic expression of caPI3K improved cardiac function in a mouse model of pathological hypertrophy and heart failure due to transgenic expression of PKC β (Rigor *et al.*, 2009). Increased PI3K (p110 α) activity in caPI3K hearts also downregulated expression of PKC β (Rigor *et al.*, 2009). In summary, a beneficial effect of activating PI3K (p110 α) in the heart is the ability to inhibit signalling proteins downstream of GPCR.

1.5.7. Signalling mechanisms that mediate gender differences

The underlying signalling cascades responsible for gender differences in the heart are complex and not completely understood. The steroid hormones (estrogen, progesterone and testosterone) and their respective receptors (estrogen receptors [ERs], progesterone receptor [PR], and androgen receptor [AR] respectively) are considered to play an important role (Babiker *et al.*, 2002; Du *et al.*, 2006; Konhilas and Leinwand, 2007; Mendelsohn and Karas, 2005). The steroid hormones activate their respective receptors, induce a conformational change, dimerize and bind to specific response elements to induce transcriptional activity (Edwards, 2005; Mangelsdorf *et al.*, 1995; Mendelsohn and Karas, 1999; Tsai and O'Malley, 1994). These receptors interact with a broad array of coactivator and corepressor proteins, and post-translational modification enables tissue specific regulation of transcription (Edwards, 2005; Kumar and Thompson, 2003; McKenna and O'Malley, 2002; Tsai and O'Malley, 1994).

The apparent cardioprotection seen in females has often been attributed to the actions of estrogen (Babiker *et al.*, 2002; Mikkola and Clarkson, 2002; Sullivan, 2003). Experimental trials of estrogen therapy however, have been controversial (Grady *et al.*, 2002; Hulley *et al.*, 1998; Manson *et al.*, 2003; Patten and Karas, 2006; Rossouw *et al.*, 2002; Shlipak *et al.*, 2001). In fact, hormone replacement therapy trials have provided evidence for increased cardiovascular risk, particularly within the first year following the beginning of therapy (Rossouw *et al.*, 2002). Subsequent evaluation of these clinical trials suggests that a number of factors contribute to the impact of hormone replacement therapy on cardiovascular risk in postmenopausal women. Combination estrogen and progesterone replacement appears to increase

cardiovascular risk (Hulley *et al.*, 1998; Manson *et al.*, 2003; Rossouw *et al.*, 2002; Santen *et al.*, 2010), but dermal (rather than oral) delivery of estrogen replacement therapy alone was associated with cardiac benefit (Santen *et al.*, 2010). Initiation of hormone replacement close to the time of menopause tended to decrease cardiovascular risk, while hormone replacement more distant from menopause did not (Rossouw *et al.*, 2007; Santen *et al.*, 2010). Additionally, pre-existing cardiovascular disease may have an impact on subsequent outcome (Santen *et al.*, 2010). It is therefore clear that the molecular mechanisms underlying gender dimorphism are complex, and that a better understanding of these molecular mechanisms is essential.

Estrogen and its receptors have been relatively well characterised in the heart. The long term effects of estrogen are mediated by ER α and ER β , both of which have been identified in the heart (Grohe *et al.*, 1998; Konhilas and Leinwand, 2007; Taylor and Al-Azzawi, 2000). Both men and women produce estrogen, but circulating levels of estrogen are 10-20 fold lower in men (Luczak and Leinwand, 2009). While expression of ER α is similar in both genders, ER β expression is significantly higher in males (Mahmoodzadeh *et al.*, 2006). Differential up- and down-regulation of ER α and ER β has been implicated in various cardiovascular phenotypes, including dilated cardiomyopathy (Mahmoodzadeh *et al.*, 2006), aortic stenosis (Nordmeyer *et al.*, 2004), ischemia/reperfusion injury (Gabel *et al.*, 2005; Zhai *et al.*, 2000), pressure overload (Skavdahl *et al.*, 2005) and the progression to HF following myocardial infarction (Pelzer *et al.*, 2005). Studies have implicated ER β , rather than ER α , in the gender differences associated with the development of pathological cardiac hypertrophy induced by pressure overload or cardioprotection following ischaemia/reperfusion (Gabel *et al.*, 2005; Pelzer *et al.*, 2005; Skavdahl *et al.*, 2005). However, these studies have been questioned and this requires further investigation.

Estrogen can initiate both rapid non-genomic signalling pathways, as well as genomic responses (de Jager *et al.*, 2001; Deroo and Korach, 2006; Du *et al.*, 2006; Konhilas *et al.*, 2004). Most notably members of the MAPK family have been shown to be important targets of estrogenic action (Kato *et al.*, 1995; Kim *et al.*, 2006; Levin, 2001; Liu *et al.*, 2010; Pelzer *et al.*, 1996). Other signalling pathways targeted by estrogen include GPCR pathways [particularly G_{i/o} and G protein coupled receptor-30 (also known as G protein coupled estrogen receptor, GPER)] (Chung *et al.*, 2004;

Deschamps and Murphy, 2009; Filice *et al.*, 2009; Prossnitz *et al.*, 2008; Revankar *et al.*, 2005), PKC signalling, and alterations of Ca²⁺ and K⁺ channels (Chung *et al.*, 2004; Hall *et al.*, 2001; Hisamoto and Bender, 2005; Jiang *et al.*, 1992; Kravtsov *et al.*, 2007; Levin, 2001; Sak and Everaus, 2004).

Estrogen has been shown to initiate anti-hypertrophic actions, by increasing ANP and BNP expression (Jankowski *et al.*, 2005; van Eickels *et al.*, 2001) and increasing calcineurin degradation (Donaldson *et al.*, 2009). Activation of cell survival pathways (including Akt) by estrogen has also been shown, and this occurs through a direct, non-nuclear pathway involving the regulatory subunit of PI3K (Simoncini *et al.*, 2000). Additionally, estrogen has anti-apoptotic actions through differential regulation of p38 MAPK isoforms (Kim *et al.*, 2006; Liu *et al.*, 2010). Finally, estrogen is also able to regulate energy metabolism, particularly via interaction with peroxisome proliferator-activated receptors (PPARs) and PPAR α -activated γ coactivator-1 (PGC1), as well as up-regulation of lipid utilization and down-regulation of glucose oxidation (Bourdoncle *et al.*, 2005; Du *et al.*, 2006; Kamei *et al.*, 2003; Keller *et al.*, 1995; Ma *et al.*, 1998; Nunez *et al.*, 1997; Schreiber *et al.*, 2003; Schreiber *et al.*, 2004; Tcherepanova *et al.*, 2000). A summary of the signalling cascades involved in estrogen-mediated cardiac hypertrophic responses are shown in Figure 11.

Progesterone signalling has been widely studied in reproductive tissues (Gellersen *et al.*, 2009; Mahesh *et al.*, 1996), however the actions of progesterone in cardiac tissues have not been examined in detail. This is likely due to previous studies showing that the impact of progesterone on the overall beneficial effects of hormone replacement therapy is insignificant (Du *et al.*, 2006; Grodstein *et al.*, 2000).

The importance of the male hormone testosterone and its receptor AR have been characterized in cardiac tissues (Li *et al.*, 2004b; Li *et al.*, 2004c; Marsh *et al.*, 1998). Testosterone treatment in male rats induced cardiac hypertrophy under basal conditions with no change in ANP expression, but significantly higher IGF1 expression (Nahrendorf *et al.*, 2003). This heart growth is reminiscent of physiological hypertrophy. Additionally, testosterone treatment in the rats reduced wall stress and left ventricular end diastolic pressure following coronary artery ligation (Nahrendorf *et al.*, 2003). It is thought that AR is necessary for postnatal cardiac growth, and is

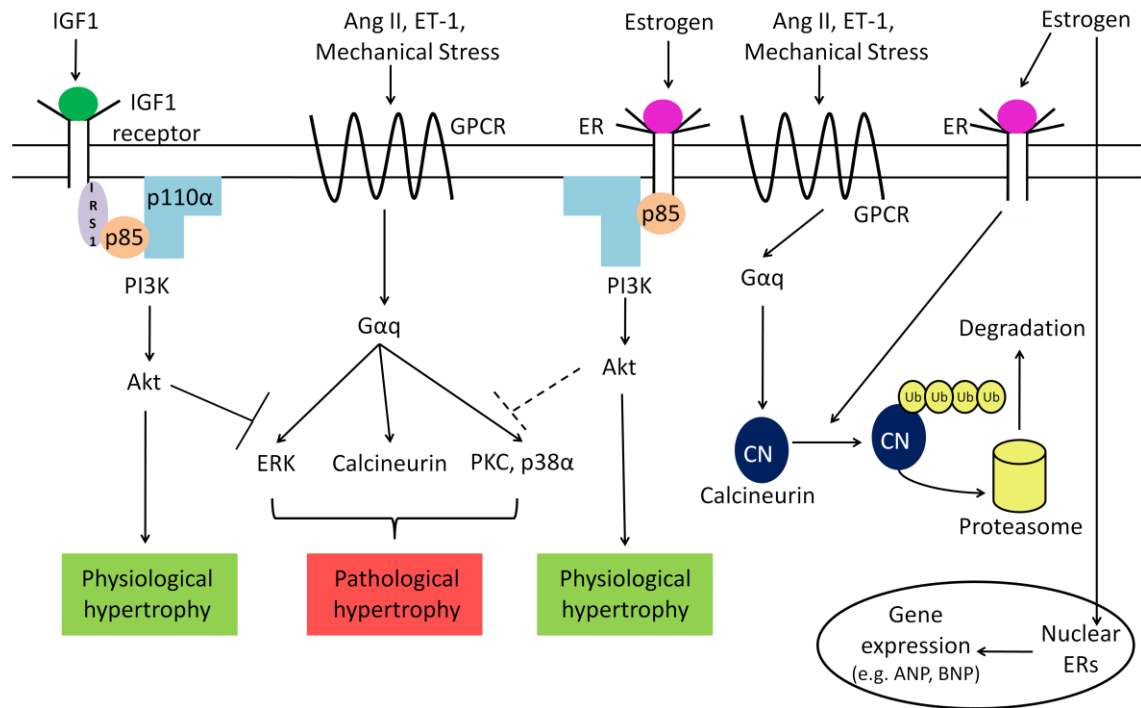


Figure 11. Proposed signalling cascades involved in estrogen-mediated effects in the heart.

Estrogen acts via the estrogen receptor which interacts with the p85 regulatory subunit of PI3K to induce physiological hypertrophy and attenuate pathological signalling cascades. Nuclear estrogen receptors alter gene expression to regulate cardiac hypertrophic responses. Estrogen is also able to induce ubiquitination of calcineurin, which leads to degradation of calcineurin by the proteasome. Ang II: angiotensin II, ANP: Atrial natriuretic peptide, BNP: B-type natriuretic peptide, CN: calcineurin, ER: estrogen receptor, ERK: extracellular regulated kinase, ET-1: endothelin-1, GPCR: G protein-coupled receptor, IGF1: insulin-like growth factor 1, IRS1: insulin receptor substrate 1, PI3K: phosphoinositide 3-kinase, PKC: protein kinase C, Ub: Ubiquitin. Figure reproduced from Bernardo, B.C., Weeks, K.L., Pretorius, L., and McMullen, J.R. (2010). Molecular distinction between physiological and pathological cardiac hypertrophy: experimental findings and therapeutic strategies. *Pharmacology & Therapeutics* 128, 191-227.

Used with permission of Elsevier.

anti-fibrotic (Du *et al.*, 2006; Ikeda *et al.*, 2005). Knockout of AR in mice reduced cardiac hypertrophy following Ang II stimulation (Ikeda *et al.*, 2005), but exacerbated cardiac fibrosis and oxidative stress (Ikeda *et al.*, 2005; Ikeda *et al.*, 2009). Recently, it was also shown that AR can reduce cardiotoxicity induced by doxorubicin (Ikeda *et al.*, 2010). Doxorubicin is a potent anti-cancer agent against a variety of malignant tumours, but induces cardiomyopathy due to increased apoptosis (Singal and Iliskovic, 1998). AR knockout mice displayed significantly worse survival and cardiac function compared with wildtype animals following doxorubicin treatment, with markedly increased apoptosis and severely impaired cardiac Akt phosphorylation (Ikeda *et al.*, 2010). Thus it has been suggested that the androgen-AR system may protect cardiomyocytes from doxorubicin-induced apoptosis through activation of the PI3K (p110 α)-Akt pathway (Ikeda *et al.*, 2010).

1.5.7.1. Gender differences in genetic mouse models

Genetic mouse models in which hypertrophic regulators have been manipulated also show gender dimorphism. In mice lacking AT₁ receptors myocardial infarction lead to similar left ventricular remodelling and dysfunction between males and females, but only male AT₁ knockout mice developed increased cardiac hypertrophy (Bridgman *et al.*, 2005). Similarly, cardiac-specific over-expression of the β 2-adrenergic receptor resulted in decreased survival, increased left ventricular dilation, increased myocyte hypertrophy and fibrosis, and reduced contractile function in males (Gao *et al.*, 2003a). Females however, were able to significantly blunt all these pathological features (Gao *et al.*, 2003a). Mice null for both $\alpha_{1A/C}$ and α_{1B} adrenergic receptors, or mice over-expressing myostatin (a regulator of muscle growth), showed reduced cardiac size only in males (O'Connell *et al.*, 2003; Reisz-Porszasz *et al.*, 2003), suggesting a reduction in adaptive capability in response to cardiac stress in the male animals. Disruption of the FKBP12.6 gene or loss of CD38 (a regulator of calcium homeostasis) only induced hypertrophy in male mice (Takahashi *et al.*, 2003; Xin *et al.*, 2002). Interestingly, female dominant negative p38 α mice displayed greater hypertrophy than males under both basal and pressure overload conditions (Liu *et al.*, 2006). Over-expression of tumour necrosis factor (TNF) α in the mouse heart induced ventricular hypertrophy in

both genders but only males developed ventricular dilation (Kubota *et al.*, 1997). Male mice null for the relaxin gene (an insulin-like growth factor peptide hormone) showed impaired diastolic function and increased atrial dilation, whereas females did not (Du *et al.*, 2003).

1.5.7.2. Crosstalk between PI3K and estrogen-receptor mediated signalling

As previously described, females have been shown to have increased cardiovascular disease risk in settings of diabetes or hypertension (Regitz-Zagrosek, 2006). Diabetes and hypertension have been associated with depressed or defective PI3K (p110 α) signalling (Chen *et al.*, 2005; Hansen *et al.*, 2001; Kim *et al.*, 1999; Mauvais-Jarvis *et al.*, 2002; Ohanian and Heagerty, 1992). It has also been shown that estrogen can activate Akt in neonatal rat cardiac myocytes through mechanisms involving PI3K (Patten and Karas, 2006), and female rodent and human hearts have increased levels of Akt compared with males (Camper-Kirby *et al.*, 2001). Taken together, these results suggest the possibility that cardioprotection in females is mediated, at least in part, through an interaction between estrogen and PI3K (p110 α). This will be assessed in my project (see Chapter 5).

1.5.8. Signalling and atrial fibrillation

As previously described, pathological cardiac hypertrophy and HF can be associated with complications including AF (see Section 1.1.3. and Section 1.3.). AF is the most common sustained arrhythmia presenting at cardiology departments worldwide, and is characterised by disorganised atrial depolarisation without atrial contraction (Zipes *et al.*, 2005), with a rapid atrial rate that prevents detection of discrete p-waves on an ECG (Lilly, 2007). Consequently, AF can be recognised on ECG traces as absent p-waves during periods of irregular heart rhythm (R-R interval). AF is associated with substantially increased mortality and morbidity from HF, stroke and thromboembolism (Fuster *et al.*, 2001; Fuster *et al.*, 2006; Zannad *et al.*, 2009). The incidence of AF increases with age, with prevalence nearly 20% over the age of 85 (Heeringa *et al.*, 2006; Nattel *et al.*, 2008). Data from the Framingham Heart Study indicated that 2.2 million Americans had AF (with a mean age of 75), and that it occurred more

commonly in men (Feinberg *et al.*, 1995). With a growing aging population, AF is adding considerably to health care costs (Benjamin *et al.*, 1998; Fuster *et al.*, 2001; Fuster *et al.*, 2006; Lip and Tse, 2007; Thrall *et al.*, 2006). AF is commonly associated with right or left atrial enlargement, and is potentially dangerous for two reasons. Firstly, the rapid ventricular rates and loss of atrial contribution to ventricular filling compromise cardiac output leading to pulmonary congestion as well as hypotension (Lilly, 2007). Secondly, the disorganized atrial contraction leads to blood stasis in the atria, increasing the risk of thrombus formation (left atria), and therefore increasing the risk of stroke due to an embolism (Lilly, 2007).

The physiological and molecular mechanisms associated with the development of AF are complex (summarised in Figure 12) and difficult to elucidate as AF also perpetuates further AF (Lu *et al.*, 2008; Rostock *et al.*, 2008; Wijffels *et al.*, 1995). Despite these complexities several mechanisms that mediate structural remodelling associated with AF development have been investigated [reviewed extensively by (Corradi *et al.*, 2008; Nattel *et al.*, 2008; Nishida *et al.*, 2010)].

It is clear that atrial remodelling (any change in atrial structure or function) contributes to the initiation and maintenance of AF (Corradi *et al.*, 2008; Nattel *et al.*, 2008; Nishida *et al.*, 2010). Dilatation results in unequal stretch of the atrial myocytes and is associated with delayed signal conduction, consequently promoting the creation of re-entry circuits (Corradi *et al.*, 2008; Nishida *et al.*, 2010; Satoh and Zipes, 1996; Solti *et al.*, 1989). Additionally, the larger atrial size can accommodate more re-entry circuits (Nattel *et al.*, 2008). Animal models of HF or mitral valve disease were characterised by ionic remodelling of the L-type Ca^{2+} current and the slow potassium current, but this was not associated with reduced action potentials in the myocytes (Li *et al.*, 1999; Nattel, 2002; Tavi *et al.*, 1998). The Na^+ - Ca^{2+} exchange current was increased in HF, leading to delayed depolarisation and the generation of ectopic beats [see Figure 12, (Corradi *et al.*, 2008; Nattel, 2002)]. Mechanical stretching can also induce hyperpolarisation of fibroblasts by reducing Na^+ entry, thereby transducing altered electrical conduction signals (Kamkin *et al.*, 2005).

Atrial ischaemia, inflammation, oxidative stress, fibrosis and apoptosis, as well as atrial dilatation make the atria more vulnerable to the development of AF. The

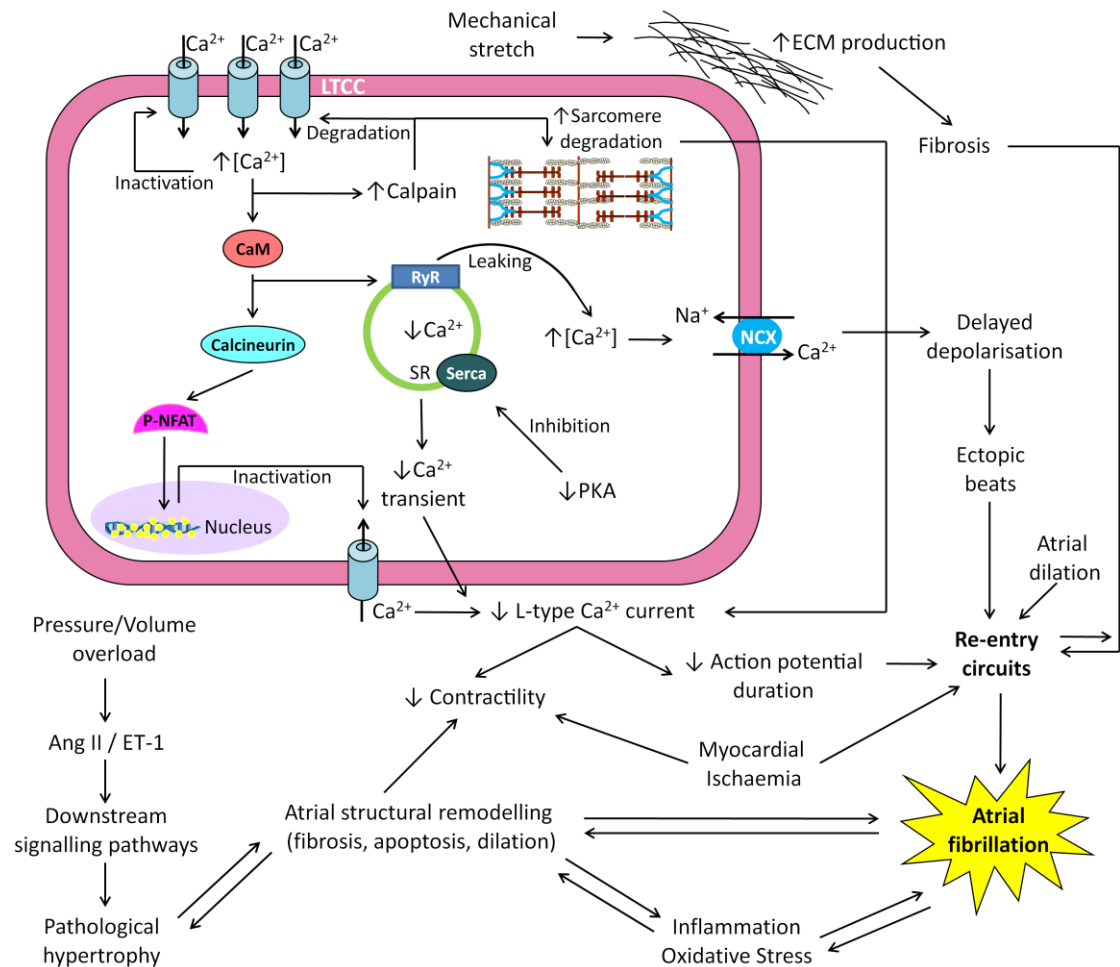


Figure 12. Mechanisms involved in the development and maintenance of atrial fibrillation.

Mechanisms involved in the development and maintenance of atrial fibrillation (AF) include tachycardia, impaired Ca²⁺ handling within the myocyte, pressure or volume overload, atrial dilation, myocardial ischaemia, inflammation and oxidative stress, fibrosis and apoptosis. These mechanisms induce re-entry circuits and remodelling of the atria which further perpetuates AF. AF itself also perpetuates further AF by increasing the number of re-entry circuits, inducing inflammation and further mediating the structural remodelling of atria. Ang II: Angiotensin II; CaM: calmodulin; ECM: extracellular matrix; ET-1: Endothelin 1; LTCC: L-type Ca²⁺ channel; NCX: Na⁺/Ca²⁺ exchanger; PKA: protein kinase A; P-NFAT: phosphorylated nuclear factor of activated T cells; RyR: ryanodine receptor; SR: sarcoplasmic reticulum; and Serca: sarcoplasmic reticulum Ca²⁺ ATPase 2a.

role of inflammation and oxidative stress in the development of AF has been extensively investigated (Abdelhadi *et al.*, 2004; Chung *et al.*, 2001; Dernellis and Panaretou, 2001; Dernellis and Panaretou, 2005; Kallergis *et al.*, 2008; Korantzopoulos *et al.*, 2007; Liu *et al.*, 2007; Mihm *et al.*, 2001; Savelieva and Camm, 2008; Shiroshita-Takeshita *et al.*, 2004). Inflammation is considered both a cause and consequence of arrhythmia (Liu *et al.*, 2007; Savelieva and Camm, 2008), and can alter atrial conduction principally by creating unstable short-duration re-entry circuits (Kumagai *et al.*, 1997). Chronic inflammatory infiltrates were detected in two-thirds of patients with lone AF (Frustaci *et al.*, 1997). Levels of C-reactive protein were increased in AF, and was proportionally increased as AF duration increased (Chung *et al.*, 2001; Dernellis and Panaretou, 2001; Kallergis *et al.*, 2008). Additional studies are required to determine whether oxidative stress is a primary cause of AF, or merely a consequence of arrhythmia (Corradi *et al.*, 2008; Korantzopoulos *et al.*, 2007).

Interstitial fibrosis is a hallmark of HF-induced AF, impeding normal cardiac conduction, and thereby promoting alternative propagation pathways and re-entry circuits [see Figure 12, (Assayag *et al.*, 1997)]. Interstitial fibrosis can be a result of increased repair due to myocyte necrosis or up-regulation of profibrotic signalling pathways (Burstein and Nattel, 2008; Olivetti *et al.*, 1997). MMPs were up-regulated and TIMPs were downregulated in patients with AF (Xu *et al.*, 2004), promoting deposition of collagen. A major profibrotic downstream mediator of Ang II is TGF- β 1. Atrial cells were particularly susceptible to TGF- β 1-mediated fibrosis (Nakajima *et al.*, 2000). Mechanical stretch itself can also induce Ang II and TGF- β 1 in fibroblasts (Schotten *et al.*, 2003) and can up-regulate ECM production through ET-1, TNF α and Ang II [see Figure 12, (MacKenna *et al.*, 2000)].

Cardiac gap junctions are composed of four trans-membrane proteins that belong to the connexin family, with three isoforms of connexins present in the atrium – connexin 40, connexin 43, and connexin 45 (Duffy and Wit, 2008). Additionally, connexin 46 has been identified in the SA node of mice and other mammals (Bruzzone *et al.*, 1996; Coppen *et al.*, 1999; van der Velden *et al.*, 2000a; Verheijck *et al.*, 2001). Gap junction composition and distribution can be altered in AF patients (Kanagaratnam *et al.*, 2002), and switches in connexin isoforms have also been observed (Dupont *et al.*, 2001a; Dupont *et al.*, 2001b; Kostin *et al.*, 2002; Nao *et al.*,

2003), but the functional significance of these changes is still unknown. It is also still unclear whether the remodelling of connexins in the myocardium is an adaptive response to or a consequence of AF. It is possible that in the initial stages of AF pre-existing characteristics of the gap junctions may predispose the atria and initiate arrhythmia, while connexin remodelling in chronic AF could be a part of the structural remodelling associated with AF, thereby maintaining an arrhythmic environment within the atria (Corradi *et al.*, 2008; Severs *et al.*, 2008).

Ectopic beats are generated by abnormal electrical firing in regions other than the sino-atrial node, leading to uncoordinated contraction, or due to early or delayed after-depolarisation within the atria (Nishida *et al.*, 2010). Early after-depolarisation involves re-activation of the L-type Ca^{2+} channels as a result of a prolonged repolarisation phase (Nishida *et al.*, 2010). In contrast, delayed after-depolarisation results from the release of Ca^{2+} during diastole which activates the sodium-calcium exchanger (Nishida *et al.*, 2010). Any change in the membrane potential that reaches the threshold level triggers ectopic firing, which in turn initiates the formation of re-entrant circuits within the atria due to irregular conduction through the atrial substrate (Nishida *et al.*, 2010). Re-entry also reduces the refractory period within the atria, further perpetuating re-entry and AF (Nishida *et al.*, 2010). Studies have also shown that rapidly firing ectopic beats in and around the pulmonary veins initiate and further promote re-entry circuits (Chen *et al.*, 1999; Haissaguerre *et al.*, 1998; Wellens, 2000).

Tachycardia is a potent stimulus for structural remodelling inducing AF, and AF is also associated with the development of further AF (Corradi *et al.*, 2008; Nishida *et al.*, 2010). Rapid atrial pacing in a goat model induced the gradual loss of cardiac myocytes (Ausma *et al.*, 1997). Increased atrial rate in AF animal models was shown to increase the intracellular Ca^{2+} load and activate the calmodulin-calcineurin-NFAT signalling cascade [see Figure 12, (Qi *et al.*, 2008; Sun *et al.*, 2001)]. L-type Ca^{2+} channels were inactivated in atrial tachycardia and AF, and subsequently the Ca^{2+} current density was reduced (Brundel *et al.*, 1999; Dinanian *et al.*, 2008; Lai *et al.*, 1999; Nattel, 1999; van der Velden *et al.*, 2000b; Van Wagoner *et al.*, 1999; Yue *et al.*, 1999). Reduction of the L-type Ca^{2+} channels resulted in reduced action potential duration and atrial refractoriness, predisposing the atria to the development of re-

entry circuits and consequently perpetuating AF [see Figure 12, (Fareh *et al.*, 1998; Gaspo *et al.*, 1997; Haissaguerre *et al.*, 1998; Klein *et al.*, 2003; Mandapati *et al.*, 2000; Nattel and Li, 2000; Wijffels *et al.*, 1995)]. Tachycardia also activated proteases such as calpain, mediating sarcomere loss and L-type Ca²⁺ channel degradation [see Figure 12, (Brundel *et al.*, 2002; Corradi *et al.*, 2008; Ke *et al.*, 2008; Nishida *et al.*, 2010; Suzuki *et al.*, 1987)], and inhibition of calpain prevented myocyte remodelling (Brundel *et al.*, 2004). A rapid atrial rate also altered calcium handling proteins (such as SERCA-2a and the ryanodine receptor) and reduced the transient outward potassium current, further contributing to decreased action potential duration (Bosch *et al.*, 1999; Greiser *et al.*, 2009; Nishida *et al.*, 2010; Ohkusa *et al.*, 1999).

Despite its clinical significance, there is a very limited understanding of the molecular mechanisms responsible for the development of AF, and this has greatly hindered the development of treatment strategies. Experimental studies have been restricted by a lack of small animal models, particularly rodents. To date, most of the described AF models involve large animals such as dogs and sheep with paced atria or ventricles, or with induced mitral valve regurgitation (Cardin *et al.*, 2007; Morton *et al.*, 2002). The advantages of these models include that the heart size, as well as the cellular electrophysiology, is not too dissimilar from humans. However, these models are limited by high costs (Pu *et al.*, 2005), and identification of molecular mechanisms can be difficult as there is a lack of genetic models and a limited availability of protein sequences and antibodies.

Murine AF models are more cost effective and in combination with genetic manipulation provide greater scope for elucidating the molecular mechanisms of AF (Olgin and Verheule, 2002). However finding clinically relevant AF mouse models has been difficult, as mice have very small atria and very fast heart rates, which may be a disadvantage for the maintenance of re-entry based arrhythmias. However, despite this difficulty there have been several genetically modified mouse models that are susceptible to AF (Table 6). It is also important to note that in murine models, AF usually presents in short episodes (paroxysmal AF). The models described in Table 6 all developed atrial-ventricular conduction blockade (Table 6). Additionally, atrial dilation, fibrosis, reduced electrophysiological amplitudes and premature death were present in

Table 6. Electrophysiological and histopathological changes seen in AF mouse models (paroxysmal or induced AF).

Mouse model	Atrial dilation	Atrial fibrosis	DCM	AVB	Reduced R-amplitude	Reduced P-amplitude	Paroxysmal AF	Induced AF	Premature death
Cx40 deficient mice (Hagendorff <i>et al.</i> , 1999; Kirchoff <i>et al.</i> , 1998)	No	No	No	✓	No	No	No	✓	No
KCNE1 knockout mice (Temple <i>et al.</i> , 2005)	No	No	No	✓	No	No	✓	✓	No
NUP155 knockout mice (Zhang <i>et al.</i> , 2008)	No	No	No	✓	✓	✓	✓	N/A	N/A
Mutation of the ryanodine receptor RyR2 (Chelu <i>et al.</i> , 2009)	No	No	No	✓	No	No	No	✓	No
Potassium channel IK1 over-expression (Li <i>et al.</i> , 2004a)	✓	N/A	✓	✓	No	No	✓	N/A	✓
α -1D LTCC knockout mice (Mancarella <i>et al.</i> , 2008; Platzer <i>et al.</i> , 2000)	No	No	N/A	✓	No	✓	✓	✓	N/A
CaV1.3 knockout mice (Zhang <i>et al.</i> , 2005b)	N/A	N/A	N/A	✓	N/A	N/A	No	✓	N/A
RhoA over-expression (Sah <i>et al.</i> , 1999)	✓	✓	✓	✓	✓	✓	✓	N/A	✓
JDP over-expressoin (Kehat <i>et al.</i> , 2006)	✓	N/A	No	✓	✓	✓	✓	N/A	✓
ACE over-expression (Xiao <i>et al.</i> , 2004)	✓	✓	No	✓	✓	✓	✓	N/A	✓
TGF β 1 over-expression (Verheule <i>et al.</i> , 2004)	No	✓	No	✓	No	✓	No	✓	No
Junctin over-expression (Hong <i>et al.</i> , 2002)	✓	✓	✓	✓	✓	✓	✓	✓	N/A
Junctate-1 over-expression (Hong <i>et al.</i> , 2008)	✓	✓	✓	✓	✓	✓	✓	N/A	✓
Cre modulator over-expression (Muller <i>et al.</i> , 2005)	✓	No	✓	✓	No	✓	✓	N/A	✓
HopX over-expression (Liu <i>et al.</i> , 2008)	✓	✓	✓	✓	✓	✓	No	✓	N/A
TNF α over-expression (Saba <i>et al.</i> , 2005)	✓	N/A	No	✓	✓	✓	✓	✓	✓
Rac1 over-expression (Adam <i>et al.</i> , 2007)	✓	✓	✓	✓	No	No	✓	N/A	No
MURC over-expression (Ogata <i>et al.</i> , 2008)	✓	✓	No	✓	✓	✓	✓	N/A	No

* N/A: Not assessed. ACE: angiotensin converting enzyme; AF: atrial fibrillation; AVB: atrial-ventricular conduction blockade; Cre: cAMP response element; Cx: connexin; DCM: dilated cardiomyopathy; HopX: homeodomain only protein of histone deacetylase; JDP: Jun dimerization protein; KCNE1: potassium voltage-gated channel subfamily E member 1; LTCC: L-type calcium channel; MURC: muscle restricted coiled-coil protein; NUP155: nuclear pore complex protein (also known as nucleoporin); Rac1: Ras-related C3 botulinum toxin substrate 1; RhoA: Ras homolog gene family, member A; TGF: transforming growth factor; and TNF: tumour necrosis factor.

some of the models (Table 6). However, the animal models previously described did not develop most of the key clinical features of AF and often died at a young age, making delineation of the molecular mechanisms responsible for AF development difficult. Therefore there is a clear need for an animal model that simulates the important characteristics of clinical AF and has a longer lifespan in order to further examine the molecular mechanisms responsible for AF. This will be examined in my project (see Chapter 4).

1.6. Outline of PhD project

My PhD project is comprised of 3 major components:

- 1) Examination of the benefits of PI3K (p110 α) signalling in a model of dilated cardiomyopathy,
- 2) Investigation of a link between PI3K (p110 α) and AF in the stressed heart, and
- 3) Examination of the role of PI3K (p110 α) in estrogen-mediated cardioprotection

1.6.1. Project rationale

1.6.1.1. Benefits of PI3K (p110 α) signalling in a model of dilated cardiomyopathy

In a previous study, McMullen and colleagues crossed the caPI3K and dnPI3K mice with a cardiac-specific Cre model of dilated cardiomyopathy and were able to show that increased PI3K (p110 α) improved lifespan while decreased PI3K (p110 α) accelerated HF (McMullen *et al.*, 2007). However, due to the severe disease progression in these mice (lifespan of only 40 days) cardiac function and the molecular mechanisms responsible for the protective properties of PI3K (p110 α) could not be assessed. Furthermore, a disadvantage of the Cre model was that dilated cardiomyopathy was induced by a non-specific mechanism due to high-level cardiac expression of Cre recombinase (Buerger *et al.*, 2006). Transgenic mouse lines that express Cre recombinase at low levels are healthy and have proven a powerful tool for deleting genes *in vivo* from mice carrying a floxed allele (lox P). The studies described in this thesis have investigated the cardioprotective properties of PI3K (p110 α) in a more

clinically relevant mouse model of dilated cardiomyopathy [due to over-expression of Mst1 (Yamamoto *et al.*, 2003), see Section 1.5.5.]. Over-expression of Mst1 is considered more relevant because Mst1 is activated by pathological insults such as ischaemia/reperfusion and induced dilated cardiomyopathy via activation of caspases leading to increased apoptosis (Yamamoto *et al.*, 2003). Mst1 was also increased in a mouse model of cardiomyopathy due to over-expression of the β 1-adrenergic receptor (Peter *et al.*, 2007). Finally, Mst1 mice also have a lifespan of approximately 8 months that allows for the examination of cardiac function and molecular mechanisms.

1.6.1.2. PI3K (p110 α) and atrial fibrillation

There is clear evidence that pathological cardiac hypertrophy and HF are risk factors for the development of cardiac conduction abnormalities and AF (see Section 1.1.3.), and it has been suggested that AF and HF may share common mechanisms and treatment strategies (Heist and Ruskin, 2006). Several studies have suggested a potential link between AF and PI3K (p110 α) activity.

- Aging, obesity and diabetes are all considered risk factors for the development of AF (Benjamin *et al.*, 1994; Feinberg *et al.*, 1995; Lip and Varughese, 2005; Wang *et al.*, 2004; Zipes *et al.*, 2005), and are all associated with insulin resistance that leads to depressed or defective PI3K (p110 α) signalling (Fink *et al.*, 1983; Kahn and Flier, 2000; Tsang *et al.*, 2005).
- Pilot studies from our laboratory have shown that dnPI3K mice have altered expression of ion channels in ventricular tissue and as previously discussed, AF is associated with ion channel remodelling (see Figure 12).
- Cardiotoxic drugs acting via adrenergic stimulation induce AF in patients (van der Hooft *et al.*, 2004) and PI3K (p110 α) can inhibit signalling cascades downstream of the GPCR signalling pathway (McMullen *et al.*, 2007), suggesting that reduced PI3K (p110 α) activity may increase the likelihood of cardiotoxicity and therefore AF.
- Increased expression of heat shock protein 70 [Hsp70, a cardioprotective protein with increased expression in settings of cardiac stress such as diabetes (Soti *et al.*, 2005)] has been shown to reduce the incidence of post-

operative AF, while reduced Hsp70 activity (due to an M439T substitution) increased the risk of post-operative AF (Afzal *et al.*, 2008; Kampinga *et al.*, 2007; Mandal *et al.*, 2005; St Rammos *et al.*, 2002). Studies from our laboratory have shown caPI3K mice have increased Hsp70 expression, while dnPI3K mice have decreased Hsp70 expression (McMullen *et al.*, 2004).

To my knowledge, the studies described in this thesis are the first to examine whether reduction of the cardioprotective kinase PI3K (p110 α) increases the heart's susceptibility to AF.

1.6.1.3. The role of PI3K (p110 α) in estrogen-mediated cardioprotection

Females are typically more protected against cardiac disease compared with males, and this has long been attributed to the actions of estrogen (Babiker *et al.*, 2002; Mikkola and Clarkson, 2002; Sullivan, 2003). However, the impact of hormone replacement on cardiovascular disease has remained controversial (Grady *et al.*, 2002; Hulley *et al.*, 1998; Manson *et al.*, 2003; Patten and Karas, 2006; Rossouw *et al.*, 2002; Shlipak *et al.*, 2001). Previous studies have suggested a link between PI3K (p110 α) and estrogen.

- It has been shown that estrogen interacts with the regulatory subunit of PI3K (p110 α) *in vitro* (Simoncini *et al.*, 2000).
- Hearts from pre-menopausal women contain higher levels of Akt [downstream of PI3K (p110 α)] compared with either aged-matched men or post-menopausal women (Camper-Kirby *et al.*, 2001). Expression of Akt is also higher in female mouse hearts compared with male hearts.
- Estrogen activates Akt in neonatal cardiac myocytes (Camper-Kirby *et al.*, 2001).

Collectively these studies suggest that there may be an important interaction between PI3K (p110 α) and estrogen in the heart. To my knowledge, this will be the first study to examine the association and functional significance of an interaction between PI3K (p110 α) and estrogen in the adult heart *in vivo*.

1.6.2. Aims of PhD project

1. To investigate the protective effects of PI3K (p110 α) in an *in vivo* mouse model of dilated cardiomyopathy and to elucidate the mechanisms responsible.
2. To assess whether reduced activation of PI3K (p110 α) makes the compromised heart more susceptible to cardiac conduction abnormalities and AF.
3. To examine the contribution of PI3K (p110 α) in mediating cardioprotection induced by estrogen in the adult heart.

1.6.3. Hypotheses of PhD project

1. PI3K (p110 α) will be critical for maintaining cardiac structure and function in a setting of HF
 - Increased PI3K (p110 α) expression is expected to confer protection in a setting of HF through differential up- and down-regulation of protein and gene expression, as well as reduction of fibrosis and apoptosis in the heart.
 - Decreased PI3K (p110 α) expression is expected to be detrimental to cardiac function and lifespan in a setting of HF, and to induce increased fibrosis and apoptosis in the heart.
2. A reduction in PI3K (p110 α) activity will make the stressed heart more susceptible to AF.
3. There is an association between PI3K (p110 α) and estrogen in the heart, and that this association is important in mediating the cardioprotective actions of estrogen.

Chapter 2 – Materials and methods

2.1. Ethics approval for animal and human care and experimentation

2.1.1. Ethics approval and animal care for mouse studies

All aspects of animal care and experimentation conducted in this project were approved by the Alfred Medical Research and Education Precinct Animal Ethics Committee and conformed to the National Health and Medical Research Council of Australia guidelines. All animals were housed in the Precinct Animal Centre at the Alfred Medical Research and Education Precinct, where animals were monitored daily by the Precinct Animal Centre staff. All animals had access to water and food *ad libitum*.

2.1.2. Ethics approval for human studies

All aspects of the studies conducted on human atrial tissue were approved by the Alfred Hospital Human Ethics Committee and conformed to the National Health and Medical Research Council of Australia guidelines. Informed consent was obtained from all participants.

2.2. Generation of cardiac-specific transgenic mouse models

The α -MHC promoter is active in the ventricles mainly after birth (Franke *et al.*, 1997; Hu *et al.*, 1995; Martin *et al.*, 1996). This feature allows it to drive transgenes exclusively in cardiac myocytes following the perinatal period (Kadambi and Kranias, 1998; Shioi *et al.*, 2000; Wakasaki *et al.*, 1997), thus ensuring cardiac-specific transgene expression.

2.2.1. Constitutively active PI3K transgenic mice

Activation of PI3K (p110 α) requires the interaction of the regulatory unit of p85 with the amino terminal of p110 via the inter SRC homology 2 (iSH2) domain (Shioi *et al.*, 2000). To generate a constitutively active PI3K (p110 α) transgene the iSH2 of p85 was fused to the N-terminus of bovine p110 α (iSH2p110) by a flexible glycine linker (Franke *et al.*, 1997; Shioi *et al.*, 2000). This construct has been shown to function as a

constitutively active molecule both *in vitro* and *in vivo* (Hu *et al.*, 1995; Martin *et al.*, 1996). Heterozygous caPI3K transgenic mice (FVB/N background) were generated by cloning the iSH2p110 mutant into the α -MHC promoter along with the Myc epitope tag, producing a constitutively activated form of PI3K with a 6.5 fold increase in cardiac PI3K activity compared with Ntg (Shioi *et al.*, 2000).

2.2.2. Dominant negative PI3K transgenic mice

Heterozygous dnPI3K transgenic mice (FVB/N background) were generated by cloning a truncated p110 mutant lacking its kinase domain into the α -MHC promoter along with the FLAG epitope tag (Shioi *et al.*, 2000). The resulting catalytically inactive p110 molecule competes with endogenous p110 for interaction with the p85 subunit, thus inhibiting the function of the endogenous p110 molecule *in vivo*, and producing a 77% decrease in cardiac PI3K activity compared with Ntg (Shioi *et al.*, 2000).

2.2.3. Mst1 transgenic mice

Heterozygous Mst1 transgenic mice (line number 28, C57BL/6 background) were generated by cloning a cDNA of human Mst1 into the α -MHC promoter along with the Myc epitope tag, which increased Mst1 activity 7.5 fold compared to Ntg (Yamamoto *et al.*, 2003).

2.2.4. Kinase dead Akt transgenic mice

Kinase dead Akt (kdAkt) transgenic mice (FVB/N background) were generated by cloning a cDNA for mouse Akt1 (Akt1K179M) in which the critical ATP binding site was mutated into the α -MHC promoter (Shioi *et al.*, 2002). The resulting kdAkt transgene competes with endogenous Akt, resulting in a 55% reduction in baseline Akt activity and a 65% decrease in Akt activation following IGF1 stimulation (Shioi *et al.*, 2002).

2.2.5. Double-transgenic mice

To explore the role of increasing or decreasing PI3K (p110 α) activity in the Mst1 transgenic model, double transgenic mice were generated by crossing the PI3K and

Mst1 transgenic mouse models described above. Heterozygous female PI3K mice (Shioi *et al.*, 2000) and heterozygous male Mst1 mice (Yamamoto *et al.*, 2003) were crossed to produce the following genotypes: Ntg, caPI3K, dnPI3K, Mst1, caPI3K-Mst1, and dnPI3K-Mst1 (Table 7), all on a mixed C57BL6/FVB/N background. Only male Mst1 transgenic mice were used for mating, as it has been shown that female mice with the Mst1 transgene die during pregnancy (experimental observation – Dr. Julie McMullen).

Table 7. Genotypes generated by crossing PI3K and Mst1 transgenic mice.

	caPI3K (-)	caPI3K (+)
Mst1 (-)	caPI3K (-) Mst1 (-) [Ntg]	caPI3K (+) Mst1 (-) [caPI3K]
Mst1 (+)	caPI3K (-) Mst1 (+) [Mst1]	caPI3K (+) Mst1 (+) [caPI3K-Mst]

	dnPI3K (-)	dnPI3K (+)
Mst1 (-)	dnPI3K (-) Mst1 (-) [Ntg]	dnPI3K (+) Mst1 (-) [dnPI3K]
Mst1 (+)	dnPI3K (-) Mst1 (+) [Mst1]	dnPI3K (+) Mst1 (+) [dnPI3K-Mst]

2.2.6. Triple-transgenic mice

To assess the role of Akt in caPI3K-Mst1 transgenic mice, triple transgenic mice were generated by crossing heterozygous male caPI3K-Mst1 mice with heterozygous female kdAkt mice to produce the following genotypes: Ntg, caPI3K, Mst1, kdAkt, caPI3K-Mst1, caPI3K-kdAkt; Mst1-kdAkt, and caPI3K-Mst1-kdAkt (Table 8).

Table 8. Genotypes generated by crossing caPI3K-Mst1 and kdAkt mice.

	kdAkt (+)	kdAkt (-)
caPI3K (+) Mst1 (+)	caPI3K (+) Mst1 (+) kdAkt (+) [caPI3K-Mst1-kdAkt]	caPI3K (+) Mst1 (+) kdAkt (-) [caPI3K-Mst1]
caPI3K (+) Mst1 (-)	caPI3K (+) Mst1 (-) kdAkt (+) [caPI3K-kdAkt]	caPI3K (+) Mst1 (-) kdAkt (-) [caPI3K]
caPI3K (-) Mst1 (+)	caPI3K (-) Mst1 (+) kdAkt (+) [Mst1-kdAkt]	caPI3K (-) Mst1 (+) kdAkt (-) [Mst1]
caPI3K (-) Mst1 (-)	caPI3K (-) Mst1 (-) kdAkt (+) [kdAkt]	caPI3K (-) Mst1 (-) kdAkt (-) [Ntg]

2.3. Genotyping

Genotyping of mice was conducted at 3-4 weeks of age. The Precinct Animal Centre staff collected a tail clipping from each mouse after weaning. Tail clippings were digested, DNA extracted and analysed for gene expression using polymerase chain reaction (PCR).

2.3.1. Mouse tail DNA digestion and extraction

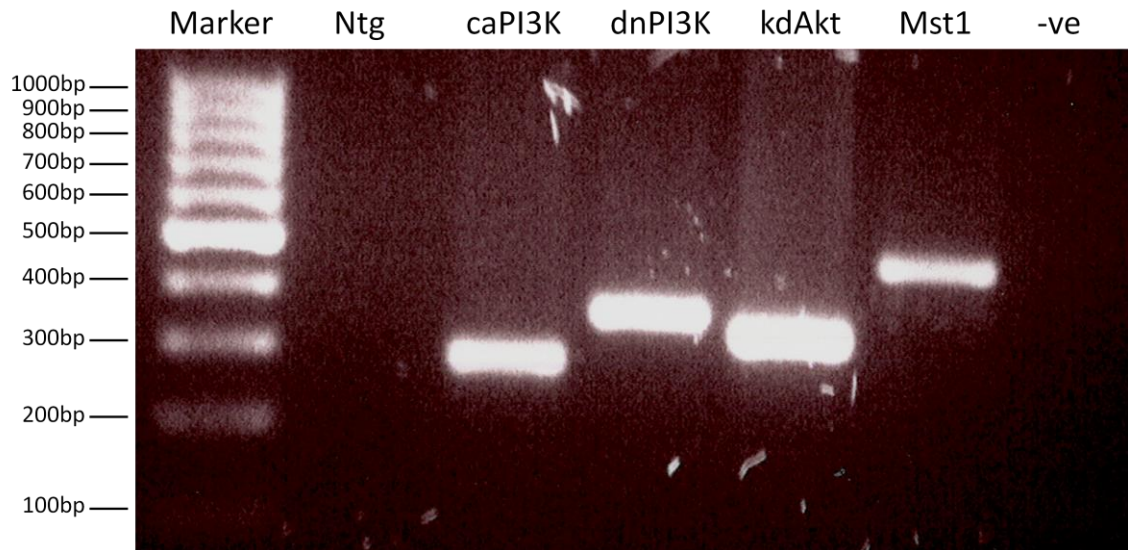
Mice tail clippings were placed in a solution containing 0.5ml Tail Lysis Buffer (83% Milli Q water [MqH₂O], 10% 1M Tris-HCl pH 8.5, 1% 0.5M EDTA, 4% 5M NaCl, 2% of SDS [10%]) and 5µl proteinase K (10mg/mL) (Fermentas, Catalogue Number E00419) and digested overnight at 55°C. The following day the tubes containing the digested tails were mixed by inversion 20-30 times and centrifuged at room temperature (RT) for 10 minutes at 14,000 rpm. In order to precipitate the DNA from the solution, 0.5ml of isopropanol was added to each tube and the tubes were inverted 20-30 times and centrifuged at RT for 2 minutes at 14,000 rpm. The supernatant was discarded, after which the remaining DNA pellet was washed with 70% ethanol, and re-suspended in 200µl of MqH₂O. The tubes were left at RT overnight and vortexed briefly at medium speed the next morning to ensure that the pellet was completely dissolved.

2.3.2. PCR

The PCR master mix was prepared on ice by adding 12.9µl MqH₂O, 4µl 5 X Promega GoTaq FLEXI colourless buffer (catalogue number M8291, part number M890A), 1.2µl MgCl₂ (25mM), 0.4µl Promega dNTPs (10mM, catalogue number U1511), 0.2µl forward primer, 0.2µl reverse primer, and 0.1µl Promega GoTaq DNA Polymerase (catalogue number M8291, part number M829A) for each PCR sample. The primers and sizes for each gene are shown in Table 9 and Figure 13. Nineteen µl of the appropriate master mix was added to each PCR tube on ice, followed by 1µl of tail DNA. A negative control of 1µl of MqH₂O was used for all genotypes to ensure that the samples were not contaminated. An appropriate positive DNA control (a sample that previously tested

Table 9. Primer sequences for genotyping using PCR.

Genotype	Forward/ Reverse	Primer Name	Primer Sequence (5' - 3')	Size
caPI3K	Forward	p110-1	AGA CCC TAG CTT TAG ATA AA	250 bp
caPI3K	Reverse	α MHC-2R	TGG TGG GCA CTG GAG TGG CA	
dnPI3K	Forward	α MHC-4	GGC ACT TTA CAT GGA GTC CT	350 bp
dnPI3K	Reverse	p110-2R	TGG CCT CTC TGA ACA GTT CAT	
Mst1	Forward	1-S	GGC ACT CTT AGC AAA CCT CA	420 bp
Mst1	Reverse	2-AS	GAT TCC ACA GGA ACT TGC TT	
kdAkt	Forward	α MHC-4	GGC ACT TTA CAT GGA GTC CT	300 bp
kdAkt	Reverse	AKT-2R	AGC CAA TAA AGG TGC CAT CGT	

**Figure 13. PCR of Ntg, caPI3K, dnPI3K, kdAkt and Mst1 mice, showing respective base pair sizes.**

positive) was used for all genotypes. The DNA samples were amplified in the PCR machine using the following protocol:

- DNA samples were pre-incubated at 94°C for 2 minutes,
- DNA samples underwent 33 cycles of amplification,
 - DNA samples were denatured at 94°C for 45 seconds,
 - DNA samples were annealed at 55°C for 45 seconds,
 - DNA samples were elongated at 72°C for 1 minute,
- Following incubation at 72°C for a further 10 minutes, the amplified DNA samples were stored at 4°C until required for electrophoresis.

Two µl of gel loading buffer (5% of 1% Bromophenol blue, 5% of 1% xylene cyanol, 50% glycerol, and 40% MqH₂O) was added to each DNA sample. In order to visualise the PCR products under UV light, samples were run on an ethidium bromide (1mg/ml) stained 2% agarose gel in 1 X TAE buffer (4.84g/L Tris-Base, 10% 0.5M EDTA [pH 8.0], 5.71% glacial acetic acid, and 90% MqH₂O) for 45 minutes at 100V. To determine the size of any positive bands, 5µl of the GeneRuler 100 base pair ladder (Fermentas, catalogue number SM0241) was run alongside the PCR products. The DNA fragments were visualised under 305nm UV light. Double- and triple-transgenic mice have positive bands for both, or all three, genes respectively (see Figure 14).

2.4. Measurement of cardiac function and electrophysiology

Cardiac function and electrophysiology was assessed non-invasively (using echocardiography and electrocardiography), and invasively (using catheterisation and telemetry recordings) at various age-points, as described below.

2.4.1. Echocardiography

Visualisation of the heart chambers can be accomplished non-invasively through echocardiography, which provides a graphic outline of the movement of cardiac structures through ultrasonography (Harris *et al.*, 2006). It is also useful for the exami-

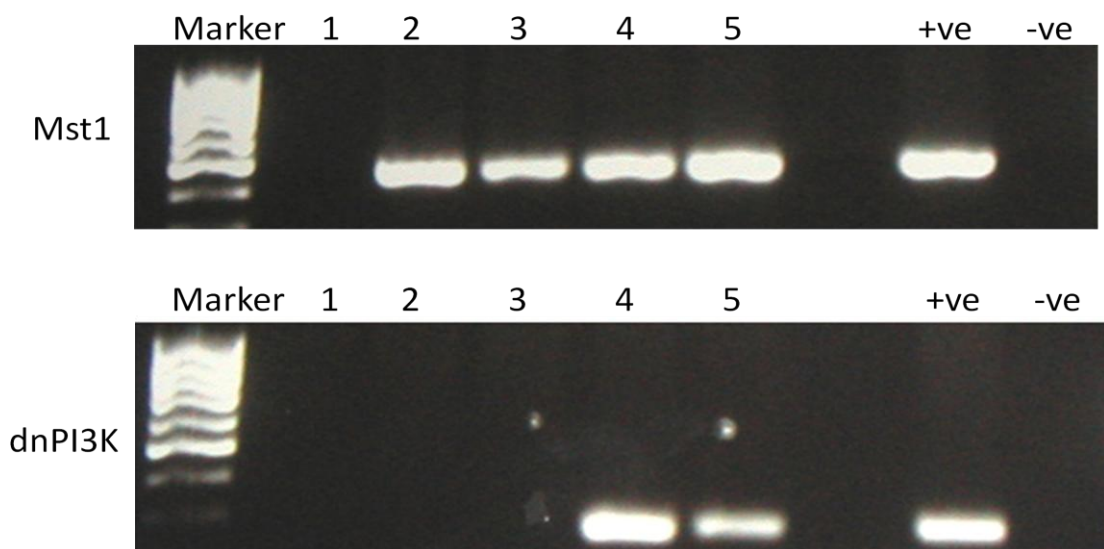


Figure 14. PCR of double-transgenic mice, showing positive bands for both the *Mst1* and *dnPI3K* genes.

Top panel: *Mst1* transgene expression, (samples 2, 3, 4 and 5 are positive). **Bottom panel:** *dnPI3K* transgene expression (samples 4 and 5 are positive). Therefore, samples 4 and 5 are double-transgenic.

nation of cardiac function at different time points (i.e. the same mouse can be examined at different ages). Mice were anaesthetised with an intraperitoneal injection of 2,2,2-tribromoethanol (240 mg/kg) as it has been shown to have only modest effects on cardiac function and output, compared to pentobarbitone and ketamine-xylazine anaesthesia (Kiatchoosakun *et al.*, 2001). The chest of the mouse was shaven and the mouse placed on a heating pad (constant temperature of 37°C) in a supine position for the duration of the procedure. Ultrasound transmission gel (Aquasonic 100, Parker Laboratories) was applied and transthoracic echocardiography was performed using a Hewlett Packard Sonos 5500 ultrasound machine with a 15 MHz linear transducer array or the Philips IE33 echocardiography system.

A 2-D guided M-mode trace crossing the anterior and posterior wall of the left ventricle was recorded at the level of the papillary muscles, as previously described (Gao *et al.*, 2000). Left ventricular end-systolic dimension (LVESD), left ventricular end-diastolic dimension (LVEDD), and ventricular wall thicknesses [interventricular septal width (IVS), and left ventricular posterior wall thickness (LVPW)] were measured from the M-mode images (see Figure 15) and averaged from three cardiac cycles. Additionally, systolic cardiac function was determined by calculating left ventricular fractional shortening, according to the following equation:

$$\% \text{ Fractional Shortening} = [(LVEDD - LVESD) / LVEDD] \times 100\%$$

2.4.2. Catheterisation

Cardiac catheterisation was performed to measure cardiac function and ventricular pressures, as previously described (Du *et al.*, 2000a). Mice were anaesthetised with an intraperitoneal injection of Ketamine/Xylazine/Atropine (KXA; 100/10/1.2 mg/kg) and placed on a heating pad (constant temperature of 37°C) in a supine position. The right main carotid artery was dissected and a microtipped transducer catheter (1.4FR, Millar Instruments) was inserted into the carotid artery and progressed into the left ventricle. Aortic blood pressure, left ventricular systolic and diastolic pressures (LVSP and LVEDP, respectively), and maximal rate of rise and fall of left ventricular pressures (dP/dt_{Max} and dP/dt_{Min} , respectively) were recorded using the Powerlab system (ADInstruments). A representative blood pressure trace is shown in Figure 16.

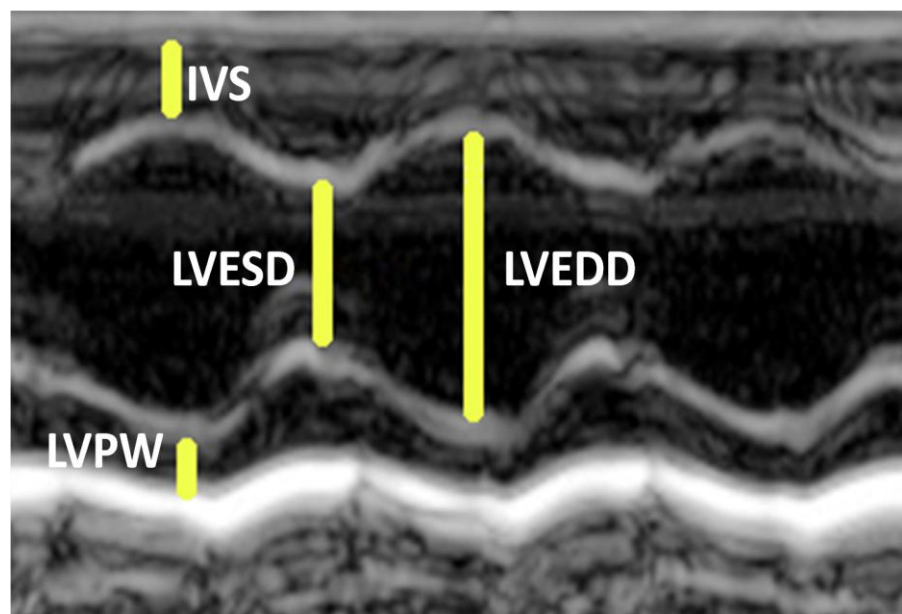


Figure 15. M-mode echocardiographic trace of a mouse heart, showing the measurement of chamber dimensions and wall thicknesses.

LVESD: Left ventricular end-systolic dimension; LVEDD: Left ventricular end-diastolic dimension;

IVS: Interventricular septal width; and LVPW: Left ventricular posterior wall thickness

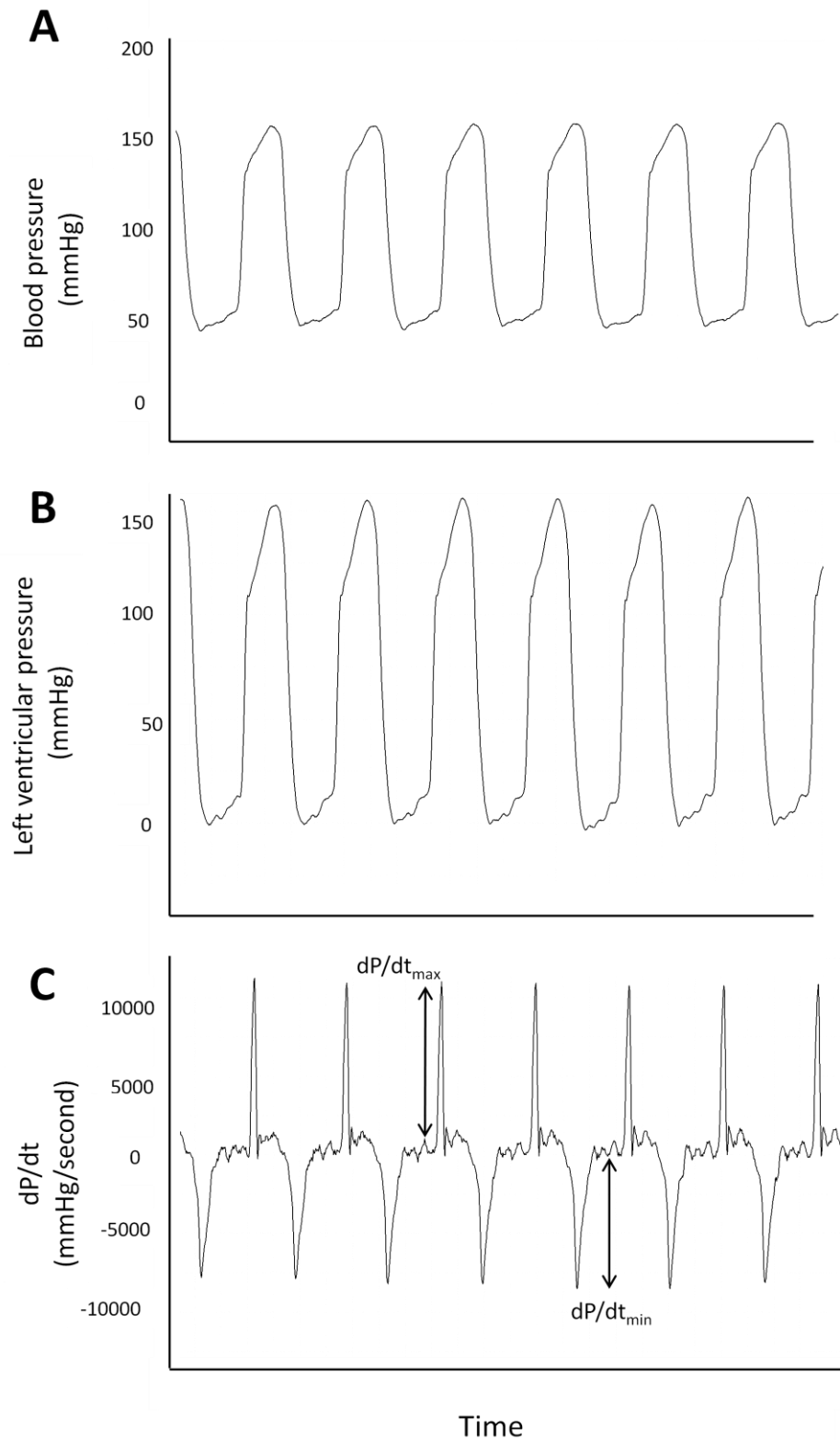


Figure 16. Catheterisation of the mouse heart.

A: Trace of cardiac blood pressure. **B:** Left ventricular pressure. **C:** Maximum rise (dP/dt_{max}) and fall (dP/dt_{min}) of left ventricular pressure.

Cardiac catheterisation is a terminal procedure. During catheterisation, blood was collected by cardiac puncture and placed in primed heparinised tubes (heparin concentration 100 units/ml). Plasma was obtained from blood samples as described in Section 2.9. Following catheterisation mice were dissected and tissues collected, as described in Section 2.6.

2.4.3. Electrocardiography

Mice were subjected to non-invasive ECG to examine the electrical conduction and any associated cardiac abnormalities, including arrhythmias. Mice were anaesthetised with an intraperitoneal injection of 2,2,2-tribromoethanol (240 mg/kg), and were placed on a heating pad at 37°C for the duration of recording and recovery. To minimize the impact of electrical interference, a water-based heating pad was used instead of an electrical heating pad, and all ECG recordings were conducted in a radio-frequency shielded room.

Two pairs of 27-gauge needle electrodes were placed subcutaneously on the right arm and chest to obtain recordings for the chest lead (equivalent to V5 of human ECG leads) and on the right arm and left leg to obtain recordings for lead II. All signals were sampled at 1kHz for a period of 5 to 10 minutes using the Powerlab system (ADInstruments). Analysis of ECG recordings was performed using the Chart5 ECG Analysis module (ADInstruments), with the signal averaging method (averaging 4 beats for each measurement). The following parameters were measured: P-R, R-R interval, QRS interval, R-amplitude, and P-amplitude, as shown in Figure 17. AF was classified as absent P-waves during periods of overtly irregular R-R intervals. Heart rate was also calculated from the ECG recordings, according to the following equation:

$$\text{Heart rate (beats per minute [bpm])} = [1 \text{ second/R-R interval (seconds)}] \times 60$$

2.4.4. Intracardiac electrocardiography catheterisation

A small subset of mice was subjected to intracardiac ECG catheterisation to measure the action potential of the bundle of His. Mice were anaesthetised with an intraperitoneal injection of KXA (100/10/1.2 mg/kg) and placed on a water-based heating pad (constant temperature of 37°C) in a supine position. An electrophysiology

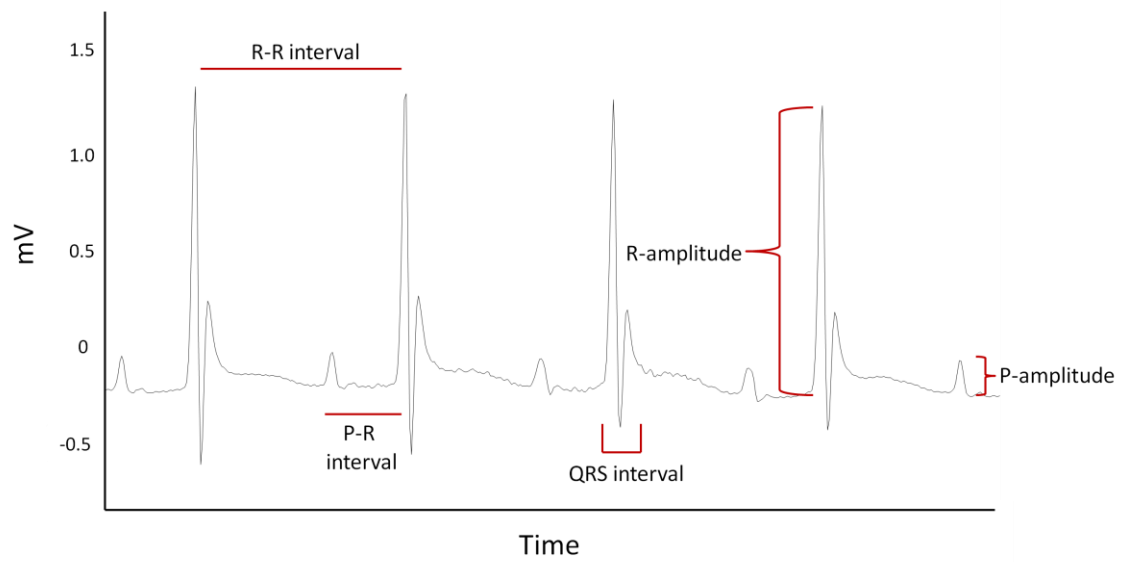


Figure 17. Parameters measured by ECG in the mouse heart.

catheter with 8 ECG sensors, each 0.25mm long and separated by 1 mm, (Figure 18 A, Ultra-Miniature Electrophysiology Catheter, 1.1F, Catalogue Number: EPR-800, Millar Instruments) was inserted into the jugular vein for placement inside the right atrium and right ventricle. Intracardiac ECG measurements were recorded for a period of 5 to 10 minutes using the Powerlab system (ADInstruments) (as shown in Figure 18 B), and surface ECG recordings (lead II position) were measured simultaneously.

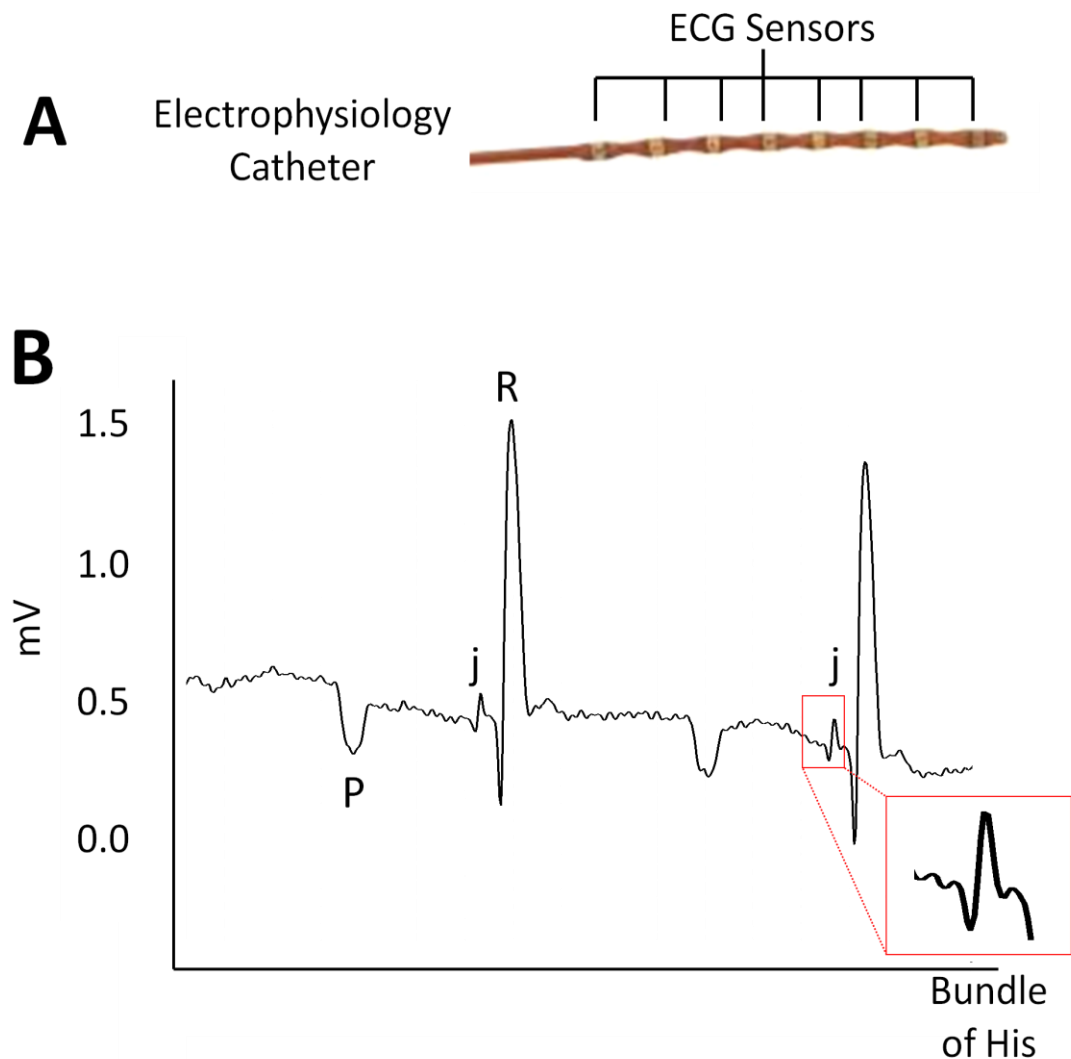


Figure 18. Intracardiac ECG catheter recordings of the mouse heart.

A: Electrophysiology catheter with 8 ECG sensors to detect intracardiac potentials. **B:** Intracardiac ECG recording showing the Bundle of His peak (*j*) that occurs after atrial depolarisation (*P*) but before ventricular depolarisation (*R*).

2.4.5. Telemetry

To confirm the anaesthetised ECG findings, ambulatory ECGs were recorded in conscious unrestrained mice after implantation of telemeters (TA10EA-F20, Data Sciences International). Mice were anaesthetised with an intraperitoneal injection of KXA (100/20/1.2 mg/kg) and placed on a heating pad (37°C). The telemeter (3.9g in weight, 1.9ml in volume) was inserted into the peritoneal cavity and the leads were connected to the right foreleg and left side of the chest (a similar position to the surface leads, V5). The telemeter was sutured to the abdominal wall to keep it in position, and the abdominal wall was closed with stitches. Carprofen (2mg/kg, Pfizer Incorporated) was administered for pain relief.

Mice were allowed 1 week to recover from surgery. After recovery, the telemeters were turned on non-invasively using a magnet. Continuous ambulatory data recordings were made non-invasively for 1 week while mice were in their cages under normal conditions. After 1 week, ECG recordings were taken (as previously described, see page 73) simultaneously with the ECG recordings from the telemetry transmitter (Figure 19). Files were recorded using Data Sciences International Dataquest A.R.T. acquisition, and analysed using the Chart5 Powerlab software (ADInstruments).

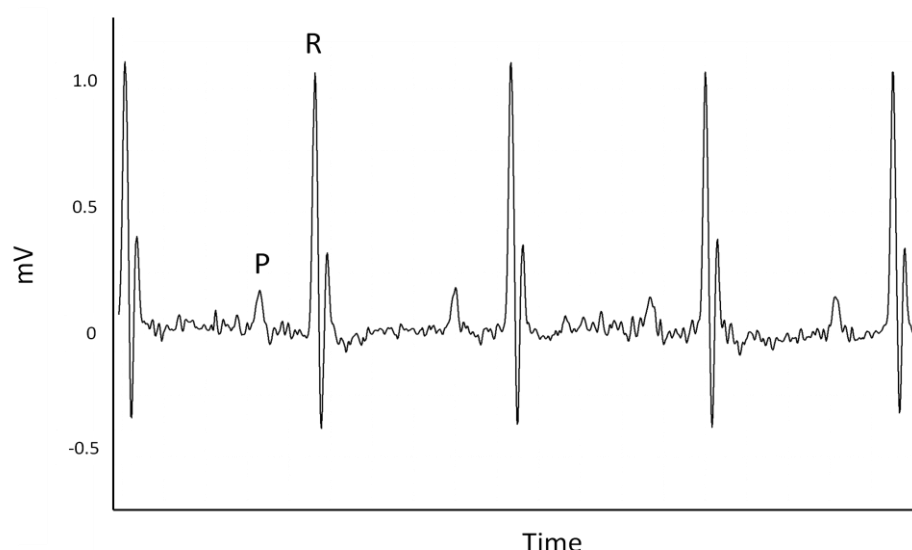


Figure 19. ECG of the mouse heart recorded by telemetry.

ECG of a mouse heart recorded by ambulatory telemetry showing atrial depolarisation (P) and ventricular depolarisation (R).

2.5. Ovariectomy and hormone replacement therapy

To investigate the effects of hormonal deficiency in adult female mice, female mice were randomly subjected to bilateral ovariectomy or sham ovariectomy at 23-27 days of age, as puberty occurs at approximately 4 weeks in mice (Silverman *et al.*, 1989). Mice were anaesthetized with an intraperitoneal injection of KXA (100/10/1.2 mg/kg). Mice were placed in a prone position under a dissection microscope and ovariectomy or sham operation performed (Figure 20). Small incisions were made on both sides at the approximate level of the last rib, approximately 1.5cm off the midline. A small incision on the abdominal wall was made through the opening to expose the ovaries. The fallopian tubes were located with blunt forceps and ligated (using 6-0 monofilament prolene surgical suture, Ethicon Incorporated), after which the ovaries were removed. Mice in the sham ovariectomy group underwent a similar procedure, but ovaries were left intact. To investigate the effect of estrogen replacement therapy, a subgroup of ovariectomised mice received subcutaneously implanted 90-day release pellets of 17 β -estradiol [2.5mg equivalent to 27.8 μ g/day; Innovative Research of America, based on a therapeutic dose from previous studies (Cavasin *et al.*, 2003; Lekgabe *et al.*, 2006)] or placebo (2.5mg; Innovative Research of America) at the same time as ovariectomy surgery.

Following suturing of the wound, mice were placed on a heating pad (constant temperature of 37°C) to recover. Betadine antiseptic ointment (10% w/w Povidone-Iodine; equivalent to 1% w/w available Iodine, Mayne Consumer Products) was applied to wounds to prevent infection. All mice were administered a subcutaneous injection of anti-sedan (0.2mg/kg, Novartis Pty. Ltd.) to assist with recovery from the anaesthetic, as well as carprofen (2mg/kg, Pfizer Incorporated) for pain relief. Following recovery, mice were monitored daily to ensure stitches remained secure and no adverse reactions to the surgery were observed. The mice were monitored until 4.5 months of age. Animals that underwent ovariectomy or sham surgery were fed a soy-free diet (Speciality Feeds, SF06-053) to prevent the influence of phytoestrogens from food (Albertazzi and Purdie, 2002; Mitchell *et al.*, 2001; Setchell, 1998), while all other animals were fed a control rodent diet (Irradiated Rat and Mouse Diet, Speciality Feeds). These two diets provided similar levels of digestible energy (Table 10).

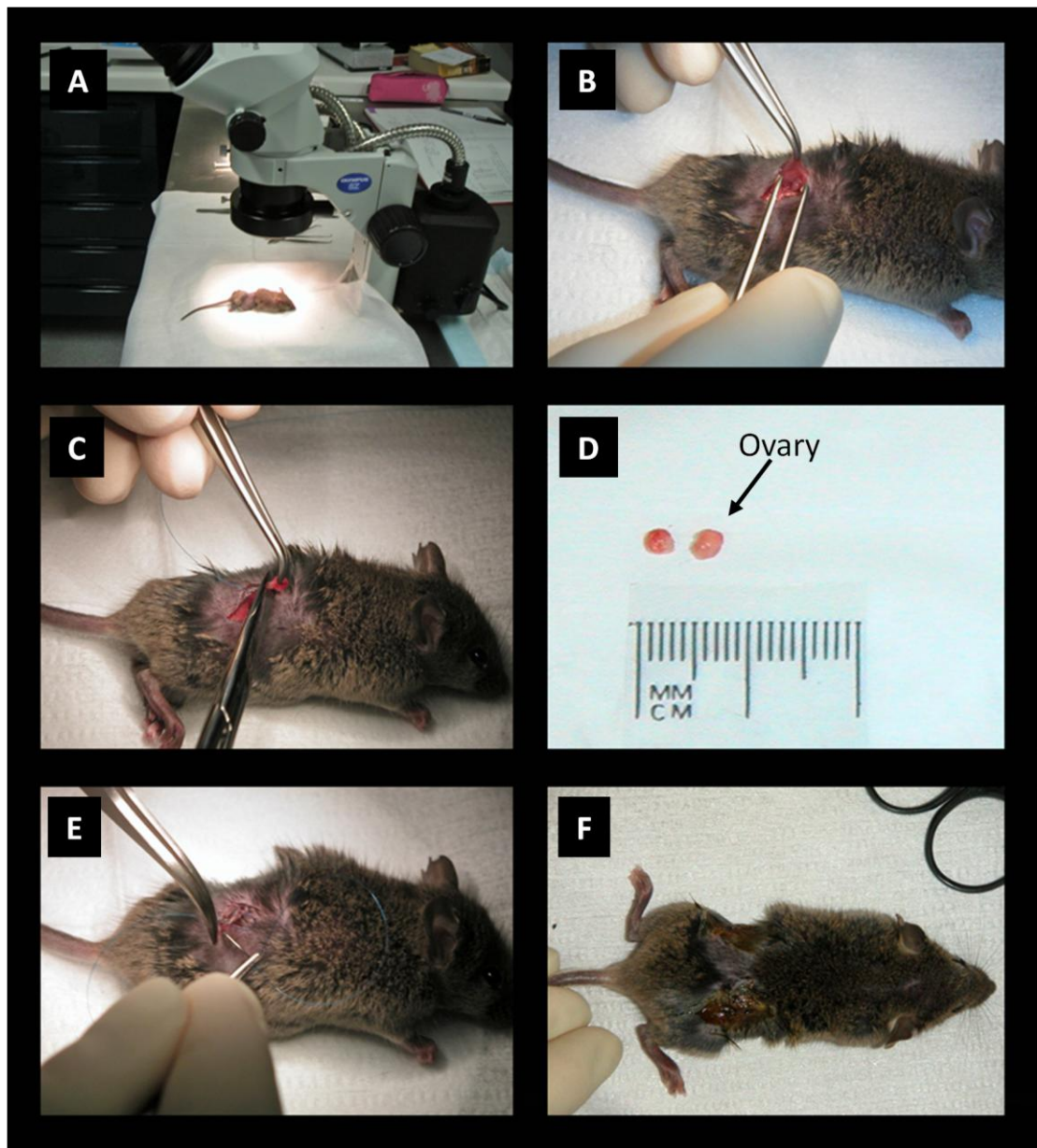


Figure 20. Ovariectomy surgery in mice.

A: Mouse is placed in a prone position under a dissection microscope. **B:** A transverse incision is made at the approximate level of the last rib, and another incision is made through the opening to expose the ovaries. **C & D:** The fallopian tubes are located and ligated, after which the ovaries are removed. **E & F:** The wound is sutured closed and antiseptic ointment applied to prevent infection.

Table 10. Comparison of the nutritional content of the soy-free and control diets.

	Soy-free diet	Control diet
Protein	18.5%	19.4%
Total Fat	5.9%	4.8%
Crude Fibre	3.4%	5.1%
Digestible Energy	14.3 MJ/Kg	14.0 MJ/KG

2.6. Tissue harvesting and tibia length measurement

Mice were anaesthetised with an intra-peritoneal injection of Lethabarb (sodium pentobarbitone; 80mg/kg) and then killed by cervical dislocation. The heart, atria, and lungs were dissected and weighed, after which the apexes of the hearts were snap frozen in liquid nitrogen for RNA or protein analyses. Atria were also snap frozen in liquid nitrogen, except when required for histological sectioning when they were fixed in 4% paraformaldehyde (PFA, Sigma-Aldrich, catalogue number P6148500G). The basal portion of the ventricles and the lungs were also fixed in 4% PFA for histological analysis. A small piece of tail and a single hind limb (containing the tibia) were collected for DNA analysis and tibia length measurement, respectively. For ovariectomy studies, uterine weights (in females) were also recorded.

Tibia lengths were measured to standardise organ weights, in addition to body weights which can differ between mice and between genders. The hind leg collected during tissue harvesting was placed in 3ml of 1M NaOH and incubated in a 37°C oven overnight to digest the skin, muscle, and fat. The next morning, the tibia was removed from the tube and measured using a vernier caliper (Figure 21).

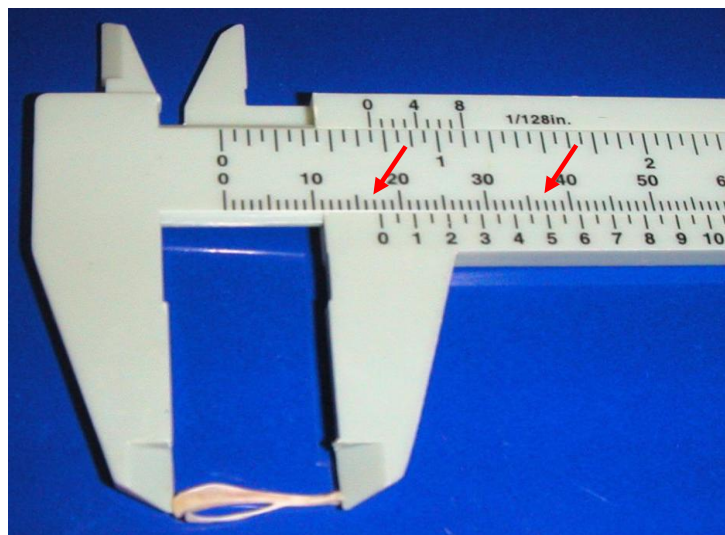


Figure 21. Measurement of tibia length using a vernier caliper.

Tibia length is measured by placing the tibia between the caliper notches and aligning the upper and lower calibration lines – in this example the tibia length is 17.5mm.

2.7. Protein expression analysis

2.7.1. Heart homogenisation

Hearts were homogenised using the homogeniser PRO 200[®] (Harvard Apparatus, catalogue number 72-1297) with a cutting saw-tooth probe (7mm x 95mm generator, Pro Scientific, part number 02-07095). Heart lysis buffer (HLB) was prepared [20% glycerol, 137mM NaCl (2.74% of total volume), 20mM Tris-HCl (pH 7.4; 2% of total volume), 4µg/ml of both the aprotinin and leupeptin inhibitors (0.08% each of total volume), 1mM PMSF (2% of total volume), 4µg/ml pepstatin (0.4% of total volume), 10mM EDTA (2% of total volume), 1mM EGTA (2.5% of total volume), 20mM NaF (4% of total volume), 1mM Na-pyrophosphate (1% of total volume), 1mM sodium vanadates (1% of total volume), and 53.2% MqH₂O; the additional 10% of the total volume was made up by adding the detergent IGE-PAL CA-630 (final concentration 1%; Sigma Aldrich, catalogue number I2031) later, see Section 2.7.2], and 400µl of the HLB was added to 5ml homogeniser tubes (Labserv, product number LBS450). Hearts (approximately 35mg, one quarter of a heart) were added to the HLB and the tube kept in an ice and water slush to ensure that the sample remained cold. The hearts were homogenised using the two lowest possible settings (5,000-6,000 rpm) in brief spurts (less than 10 seconds) to minimise any increase in temperature of the sample, and the probe was cleaned following each sample to prevent contamination between samples.

2.7.2. Protein extraction

Following homogenisation, the heart homogenate was transferred into an eppendorf tube and the detergent IGE-PAL CA-630 (10% of total volume of homogenate; final concentration 1%) was added to break the cytoplasmic membranes. The sample was vortexed to ensure that the solutions were sufficiently mixed and then incubated for 15 minutes on ice. Following incubation, the samples were centrifuged at 13,200 rpm for 15 minutes at 4°C and the supernatant (heart homogenate) collected. Samples were stored at -80°C until required for analysis.

2.7.3. Measurement of protein concentration – Bradford assay

The concentrations of the protein samples were determined using the Bradford assay (Bradford, 1976). Protein standards were prepared using bovine serum albumin (BSA, Sigma-Aldrich, catalogue number A9418) and MqH_2O to give final concentrations of 0, 0.2, 0.4, 0.6, 0.8, and 1.0 mg/ml. Eighteen μl of MqH_2O and 2 μl of heart lysate was added to each experimental tube, followed by 1ml of 1 X Bradford reagent (1 in 5 dilution of Bio-rad Protein Assay Dye Reagent Concentrate, catalogue number 500-0006). Samples were vortexed to ensure mixing of the solution, and the tubes were incubated at RT for 15 minutes.

Standards were placed in a Beckman Coulter DU640[®] spectrophotometer under visible light to produce a standard curve of absorbencies at known protein concentrations (using the standard BSA samples). The samples were placed in the spectrophotometer and their absorbencies determined. Using the previously obtained standard curve and correcting for any dilution factors, the protein concentrations of the samples were calculated. All sample measurements were repeated to ensure accuracy. These protein concentrations were used to standardise the different protein samples for use in Western Blotting (described below).

2.7.4. Western blotting

Western blotting (Burnette, 1981) is a standard laboratory technique used to detect individual proteins from a complex mixture of proteins by separating them according to their molecular mass (Sambrook and Russel, 2001). Protein samples can be dissociated into their individual polypeptide units by using the strongly anionic detergent sodium dodecyl sulfate (SDS) in combination with a reducing agent. The polypeptides bind to the SDS and become negatively charged. The amount of SDS bound to the polypeptide is proportional to its size and consequently the samples can be separated in a polyacrylamide gel according to their size and identified using a marker of known molecular weight. Following the separation of the proteins on a gel, the proteins can be transferred onto a membrane and then specifically detected and identified using a specific antibody. A summary of the western blotting protocol is shown in Figure 22.

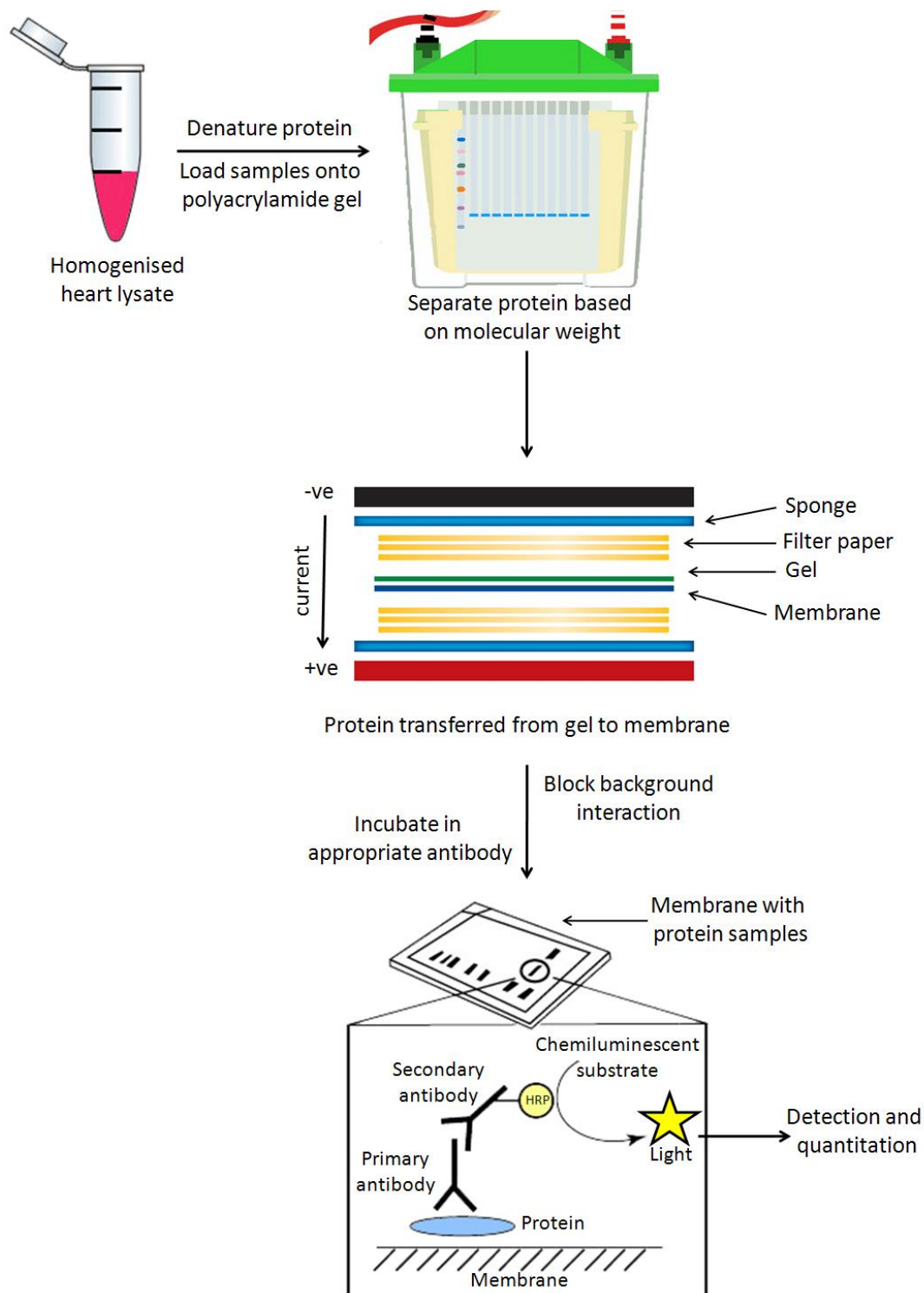


Figure 22. Western blotting to examine protein expression in tissue.

Homogenised tissue is denatured and loaded onto a polyacrylamide gel. Running the samples through the gel allows for the separation of protein based on size. The samples on the gel are then transferred to a nitrocellulose membrane using electric current. The resulting membrane is probed for protein expression by placing it in primary antibody, and then a secondary antibody. The secondary antibody is conjugated to horse radish peroxidase, which can be detected by a chemiluminescent substrate. The resulting light signal can then be detected using X-ray film.

A 10% separating gel [5ml 30% Acrylamide/Bis, 3.75ml 4 X Tris/SDS pH 8.8, 6.25ml MqH₂O, 50µl 10% ammonium persulfate (APS) and 10µl Tetramethylethylenediamine (TEMED)] was prepared and covered with a layer of MqH₂O (approximately 1.5cm) to prevent dehydration. The gel was left to polymerise for 30 to 60 minutes at RT. Following polymerisation, the MqH₂O was removed and the stacking gel (650µl 30% Acrylamide/Bis, 1.25ml 4 X Tris/SDS pH 6.8, 3.05ml MqH₂O, 25µl 10% APS and 5µl TEMED) was placed on top of the separating gel. The well comb was inserted and the gel left to polymerise for 30 to 45 minutes at RT.

Using the previously determined protein concentrations (using the Bradford Assay), 100µg of each protein sample was measured and 5µl of 6 X SDS Sample Buffer (70% 4 X Tris/SDS pH 6.8, 30% Glycerol, 0.1g/ml SDS, 0.093g/ml Dithiothreitol (DTT, Sigma Aldrich, catalogue number D0632-5G), 1% Bromophenol blue) was added to each sample. The gel was pre-run at 150V for 15 minutes. Protein samples (with 6 X SDS sample buffer) were vortexed, heat denatured at 95°C for 5 minutes and briefly centrifuged for 5 seconds. Protein samples were loaded onto the gel using gel loading tips. To enable the identification of the different protein sizes, 20µl Kaleidoscope marker (Bio-rad, catalogue number 161-0324) was run along with the protein samples. The samples were run at 150V for 60 minutes.

A 6 x 9 cm membrane (Immobilon P^{5Q} 0.2µm Membrane, Millipore, catalogue number IPVH00010) was prepared for protein transfer by soaking it in 100% methanol for 15 seconds, MqH₂O for 1 minute, and in transfer buffer (25mM Tris-base, 192mM Glycine, in 90% MqH₂O, and 10% of 100% methanol) for 15-30 minutes with gentle shaking. Proteins were transferred onto the membrane for 90 minutes at 36V or overnight at 9V at 4°C on a stirring platform, using a Mini-PROTEAN 3 cell transfer apparatus according to the manufacturer's instructions (BIO-RAD, catalogue number 165-3301). Following transfer, the protein was baked onto the membrane between Whatman filter paper for 10 minutes at 65°C. The membrane was rehydrated by placing it in 100% methanol for 1 minute, in MqH₂O for 2 minutes and in TBST (3% 5M NaCl, 1% 1M Tris.HCl pH 8.0, 0.25% of 20% Tween 20, and 95.75% MqH₂O) for 5 minutes with gentle shaking. Following rehydration, the membrane was placed in 5% non-fat milk/TBST with gentle shaking for 60 minutes, in order to block non-specific background interactions. The membrane was removed from the 5% non-fat milk/TBST

and incubated at 4°C overnight with gentle rocking in the appropriate primary antibody (see Table 11) diluted in either 5% non-fat milk/TBST or 5% BSA/TBST as per the manufacturer's instructions.

Table 11. Antibodies used for western blotting.

Primary antibody	Concentration	Manufacturer	Secondary antibody	Molecular weight (kDa)
Phospho-Akt	1:500	Cell Signaling Technologies; catalogue number: #9271	Anti-rabbit; 1:2500	60
Akt	1:500	Cell Signaling Technologies; catalogue number: #9272	Anti-rabbit; 1:2500	60
phospho-p44/p42 MAPK	1:200	Santa Cruz Biotechnology; catalogue number: sc-7383	Anti-mouse; 1:2500	44 & 42
p44/p42 MAPK	1:1000	Cell Signaling Technologies; catalogue number: #9102	Anti-rabbit; 1:2500	44 & 42
phospho-p38 MAPK	1:500	Cell Signaling Technologies; catalogue number: #9215	Anti-rabbit; 1:2500	43
p38 MAPK	1:2500	Santa Cruz Biotechnology; catalogue number: sc-535	Anti-rabbit; 1:2500	38
GAPDH	1:500	Santa Cruz Biotechnology; catalogue number: sc-32233	Anti-mouse; 1:5000	37
PI3K p85	1:5000	Upstate; catalogue number: #06-195	Anti-rabbit; 1:5000	85
ERα	1:500	Stressgen; catalogue number: #SRA-1010	Anti-mouse; 1:2500	66

The following day the membrane was rocked an additional 90 minutes at RT. The membrane was washed four times for 5 minutes in TBST and incubated with the appropriate secondary antibody (Australian Laboratory Services Pty Ltd., catalogue numbers: anti-mouse HRP #715-035-150; and anti-rabbit HRP #711-035-152,

concentration 1:2500) diluted in 5% non-fat milk/TBST for 90 minutes at RT with gentle rocking.

Following the antibody incubation, the membrane was washed with TBST four times for 5 minutes. One ml of each of the Pierce SuperSignal® West Pico Chemiluminescent Substrate solutions (SuperSignal® West Pico Stable Peroxide Solution and SuperSignal® West Pico Luminol/Enhancer Solution, product number 34090) was mixed and the membrane was incubated for 2-5 minutes at RT. The membrane was wrapped in plastic wrap and exposed to Amersham Hyperfilm ECL (GE Healthcare, catalogue number 28906837). Samples were quantified using ImageJ (version 1.42q) software (National Institutes of Health, USA) by measuring the signal density relative to either the non-phosphorylated form of the antibody or a house-keeping protein.

In order to probe the nitrocellulose membranes with various antibodies, the membranes were stripped by placing them in 10ml of Western Blot Stripping Buffer (0.78% 2-mercaptoethanol, 20% of 10% SDS, 12.5% 0.5M Tris pH 8.0, and 66.72% MqH_2O) and incubating at 65°C for 30 minutes in a rotating hybridisation oven. Following stripping, membranes were washed in TBST for 5 minutes twice, and stored in fresh TBST at 4°C until required for further immunodetection.

2.7.5. Immunoprecipitation

In order to identify whether there is an interaction between PI3K (p110 α) and ER α , samples were immunoprecipitated with a PI3K p85 antibody using Protein A Sepharose beads (GE Healthcare, product code 17-5280-04) and probed for ER α (see Table 11). To allow for the removal of non-specific binding to the Protein A beads, 700 μ l of HLB (as described earlier) and 500 μ g of heart lysate were incubated with 50 μ l Protein A beads at 4°C for an hour. The tubes were centrifuged for 1 minute at 9,000 rpm, and the supernatant used for the remainder of the experiment. The PI3K p85 antibody (0.5 μ l) was added to each tube, excluding the “no-antibody” control and rocked overnight at 4°C. A 10% acrylamide SDS-PAGE gel was prepared as described earlier. The following day, 50 μ l of Protein A Sepharose was added to each tube and incubated for 1 hour at 4°C, to allow the antibody-protein complex of interest to bind to the Protein A beads.

The beads were washed 3 times, by centrifuging for 9,000 rpm (at 4°C), removing the supernatant, adding 700µl fresh HLB, and incubating for another 10 minutes. Following the washes, the beads were centrifuged at 9,000 rpm for 1 minute, and all the supernatant aspirated using a 30 gauge needle.

Thirty µl of 2 X SDS Sample Buffer (1:3 dilution of 6 X SDS Sample Buffer, page 82) was added to the remaining bead complex in each tube, and the tubes were incubated at 95°C for 5 minutes to induce the breakage of the antibody-lysate-protein A-complex. Twenty µl of Kaleidoscope marker, followed by 25µl of each sample in subsequent lanes, was loaded onto the SDS-PAGE gel, and the gel run at 150V for 45 minutes. Following running of the gel, the protocol for immunoblotting and immunodetection for Western Blotting was used to detect protein interactions (see Section 2.7.4.).

2.7.6. PI3K activity assay

2.7.6.1. Mouse ventricular tissue

To measure PI3K activity in mouse ventricular heart samples, 500µg of lysate was immunoprecipitated with a PI3K p85 antibody (see Table 11) using Protein A, as previously described (see Section 2.7.5.). The following day, the Protein A beads were washed twice in HLB, as well as twice in 4-(2-hydroxyethyl)-1-piperazineethanesulfonic acid (HEPES) buffer [10mM HEPES (pH 7.4, 1% of total volume; Sigma Aldrich, catalogue number H4034-100G), 0.1mM EGTA (0.25% of total volume; MP Biomedicals, catalogue number 195174), 0.015% IGE-PAL, 1mM DTT (0.01% of total volume), and 98.725% MqH₂O] by centrifuging at 10,000 rpm for 1 minute, removing the supernatant, and adding 700µl of new HEPES buffer.

Three hundred µl of the bead-lysate suspension was aliquoted into a new tube and centrifuged at 10,000 rpm for 1 minute and the supernatant removed. Twenty five µl of 2 X SB was added to each sample and the samples denatured at 100°C for 5 minutes. Fifteen µl of each sample was loaded onto a 7% acrylamide gel and run according to the western blotting protocol described previously (see Section 2.7.4.). The remaining 400µl of the bead-lysate suspension was centrifuged at 10,000 rpm for 1 minute and the supernatant removed. The beads were resuspended in 30µl

HEPES buffer and stored on ice until required for the kinase assay. A 20 x 20cm thin-layer chromatography (TLC) plate (Merck, catalogue number 1.05553.0001) was baked at 100°C for 1 hour. Lipid solution was prepared by adding 0.6µl phosphatidyl inositol in chloroform [CHCl₃] (10mg/ml, Sigma Aldrich, catalogue number P2517) and 0.6µl phosphatidyl serine in CHCl₃ (10mg/ml, Sigma Aldrich, catalogue number P6641) for each sample to be blotted, and the CHCl₃ removed using a speed vacuum at -97°C for 5 minutes with a vacuum pressure of 0.1. The lipid solution was resuspended in 100µl HEPES buffer, sonicated for 40 seconds using a microtip probe sonicator, and stored at RT until use.

The extraction solution (1:1 dilution of CHCl₃ and methanol) and 5 X ATP mix [50mM HEPES (pH 7.4), 25mM MgCl₂, 100µM ATP, 36.25% MqH₂O, and 5% radioactively labelled 32-phosphorous ATP (γ -³²P-dATP)] were prepared. Ten µl of lipid and 10µl of 5 X ATP mix was added to each sample, and the sample mixed in a thermomixer (Eppendorf) at 25°C, 1,400 rpm for 10 minutes. The reaction was stopped by placing the samples on ice and adding 60µl of 2M HCl and 160µl of the extraction solution. Tubes were vortexed for 1 minute, and centrifuged at 14,000 rpm for 1 minute to separate the aqueous and organic phases.

The aqueous phase was removed, as it contained the free ATP that can result in high background readings. Sixty µl of the organic phase was spotted onto the TLC plate drop by drop, allowing each drop to dry before adding the next. The TLC plate was placed in a TLC tank containing tank buffer (65% propenol, 35% 2M acetic acid). The solvent front was allowed to rise by capillary action overnight, to separate the components of the samples. The next day, the TLC plate was removed from the TLC tank and allowed to dry for 10 minutes. The plate was exposed to Amersham Hyperfilm MP (GE Healthcare, 28906845) at -80°C.

2.7.6.2. Human atrial tissue

PI3K activity was also assessed in atrial tissue samples from patients undergoing CABG surgery (right appendage only) who did or did not develop acute AF, as well as patients undergoing mitral valve surgery (left appendages) with chronic AF. Medications (statins, beta-blockers and ACE inhibitors) were evenly distributed

between groups and stopped the night before surgery. Patients with diabetes were not included in the study. PI3K activity was assessed as previously described, using 1mg of human atrial tissue lysate.

2.7.7. Gelatin Zymography

Gelatin zymography was performed by Dr. Yi-Dan Su (Experimental Cardiology Laboratory, BakerIDI Heart & Diabetes Institute). MMP-2 (gelatinase A) and MMP-9 (gelatinase B) expression and activity were measured in heart tissue as previously described (Lekgabe *et al.*, 2005). Briefly, cardiac tissue was homogenised in 0.25% Triton X-100 (Sigma Aldrich, catalogue number X100) containing 10mM CaCl₂. The homogenate was centrifuged at 6,000 rpm for 30 minutes at 4°C and the pellet (containing 80-90% of the MMPs) was resuspended in 0.1M CaCl₂. MMPs were extracted by placing the suspension in a shaking water bath for 4 minutes at 60°C. The samples were then chilled on ice for 2 minutes, before being centrifuged again at 13,000 rpm for 30 minutes at 4°C. The supernatant was then transferred to centricon concentrator tubes (Millipore) with a 10kDa molecular weight cut off and concentrated 20 times by centrifugation at 6,500 rpm. Aliquots of tissue extracts containing the MMPs were then mixed with sample buffer (62.5mM Tris/HCL, pH 6.8, 2% SDS, 10% glycerol, and 0.0025% bromophenol blue) at a ratio of 3 parts enzyme sample and 1 part sample buffer for 60 minutes at RT. Samples were loaded on a 7.5% acrylamide gel containing 0.05mg/ml gelatin and 3.5% stacking gel, and electrophoresed at 100V (through the stacking gel) and 200V (through the separating gel) at 4°C until the bromophenol blue marker dye reached the bottom of the gel.

Following electrophoresis, the SDS was removed by washing the gel for 15 minutes in Triton X-100 (0.25%) twice. The MMPs were allowed to renature and digest the surrounding gelatin overnight at 37°C in incubation buffer (50mM Tris/HCL, pH 7.5, 10mM CaCl₂, 1µM ZnCl₂, 1% Triton X-100 and 0.02% NaN₃, in MqH₂O) (Woessner, 1995). Following incubation, the gels were stained with 0.1% Coomassie brilliant blue (containing 40% isopropanol) for a minimum period of 1 hour at RT. The gels were de-stained with 20% methanol containing 7% acetic acid until clear bands were visible (2-4 hours). The gels were dried, scanned and densitometry levels were determined.

2.8. Gene expression analysis

2.8.1. RNA extraction

RNA was extracted from heart samples, using Trizol (Invitrogen, catalogue number 15596-018). Heart samples were placed in 14ml sterile tubes with either 2.0ml Trizol (for ventricular samples) or 1.0ml Trizol (for atrial samples), and homogenised at RT. Following homogenisation of each sample, the probe was cleaned using diethyl-pyrocabonate (DEPC) water to prevent any cross-contamination between samples. The samples were incubated at RT for 5 minutes and centrifuged at 4°C for 10 minutes at 3,100 rpm. The supernatant (containing the RNA) was collected into two new tubes (approximately 1ml of solution in each tube), and the pellet (containing the extracellular membranes, polysaccharides and high molecular weight DNA) was discarded.

To precipitate the RNA, 0.2ml of chloroform was added to each tube and shaken vigorously. The tubes were incubated at RT for 3 minutes and centrifuged at 4°C for 10 minutes at 10,000 rpm. The supernatant was discarded and 1ml of 75% DEPC treated ethanol was added to each sample to wash the RNA pellet. The ethanol was discarded and the tubes left to dry at RT for 2-3 minutes. The RNA pellet was washed again using 1ml of 75% DEPC treated ethanol, after which the samples were centrifuged at 4°C for 5 minutes at 9000 rpm. The ethanol discarded and the tubes left to air dry on paper towel for 5-10 minutes at RT in order to evaporate any residual ethanol. 100µl of MQH₂O was added to each tube to dissolve the RNA pellet. RNA samples were stored at -80°C until required for analysis.

2.8.2. Measurement of RNA concentration and quality

RNA concentration was determined by recording the absorbance of RNA samples (2µl of RNA in 98µl of DEPC water) under UV light (wavelengths 260 and 280nm) in a Beckman Coulter DU640[®] spectrophotometer. RNA concentration was determined using the following equation: RNA concentration (ug/ml) = Abs (260nm) X 50 (dilution factor) X 40 (optical density for RNA is 40µg/ml). Purity of the RNA samples was determined by assessing the RNA ratio (absorbance at 260nm/absorbance at 280nm),

in addition to visualisation of 28S and 18S band on the Northern gel (Figure 23).

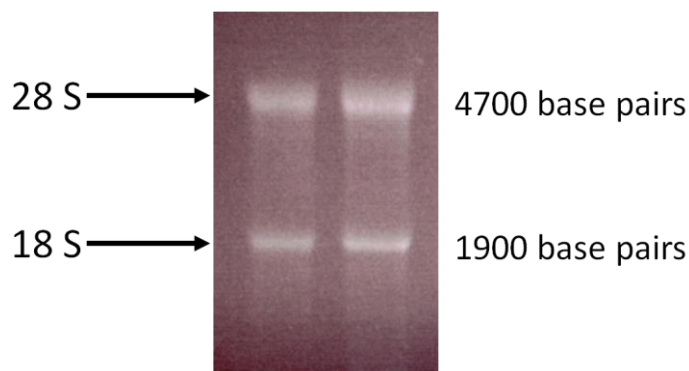


Figure 23. Examination of 28S and 18S bands to determine RNA quality.

The 28S band represents 4700 base pairs in size, and the 18S band represents 1900 base pairs in size.

2.8.3. Northern gel preparation and transfer

First described in 1977 (Alwine *et al.*, 1977), Northern blotting is still considered a gold standard method for gene expression analysis as it allows for the direct comparison of the messenger RNA abundance between samples on a single membrane (Streit *et al.*, 2009). Following RNA extraction, samples are prepared and run on a denaturing formaldehyde agarose gel to separate the samples based on size. The samples are transferred from the gel to a positively charged membrane and this membrane is used for further probing.

Using the concentrations obtained from spectrophotometry, 10 μ g of the samples were made up to 100 μ l with DEPC-treated water. The RNA was precipitated out of solution by adding 250 μ l of cold 100% ethanol, and 10 μ l of 3M sodium acetate (pH 6.0) and incubating the tubes at -80°C overnight. The gel apparatus was decontaminated by soaking it in 5% hydrogen peroxide overnight to prevent the degradation of the RNA by ribonucleases (Sambrook and Russel, 2001). The following day a 1.3% agarose gel was prepared (0.013g/ml agarose, 10% 10 X MOPS, 90% DEPC-treated water). Formaldehyde (8ml, saturated solution: 37% by mass in water) was added to ensure the RNA remained denatured, thus limiting the formation of secondary structures (Streit *et al.*, 2009). Thirty μ l ethidium bromide (1mg/ml) was

also added to allow visualisation under UV light, thus enabling the examination of the quality and quantity of RNA prior to blotting. The gel was left for an hour to set.

The RNA samples were removed from -80°C and centrifuged at 13,200 rpm at 4°C for 15 minutes. The supernatant was discarded and $200\mu\text{l}$ of cold 70% DEPC-treated ethanol added to wash the RNA pellet. Following gentle agitation of the pellet, the samples were centrifuged for an additional 2 minutes at 13,200rpm at 4°C . The ethanol was discarded and $20\mu\text{l}$ of RNA loading buffer [22% DEPC-treated water, 10% 10 X MOPS, 18% formaldehyde (saturated solution, 37%), and 50% formamide] added to each sample. The samples were incubated at 65°C for 15 minutes to denature the RNA and placed directly on ice. Four μl of 10 X Northern dye (50% glycerol, 2% 0.5M EDTA pH 8.0, 0.25% bromophenol blue, and 47.75% of DEPC-treated water) was added to each sample and the samples were loaded onto the Northern gel. The gel was run for approximately 2 hours in 1 X MOPS and then visualised under UV light to examine the presence of the 18S and 28S bands [a measure of RNA quality, as previously described (see Figure 23) with smearing indicative of RNA degradation].

A Northern transfer apparatus was prepared using a large baking dish with a glass plate on top and 600ml of 20 X SSC in the dish. A 570 x 150 mm piece of Whatman filter paper was wrapped around the glass plate and allowed to remain in contact with the 20 X SSC, allowing it to soak up the solution and facilitate upward capillary transfer (Sambrook and Russel, 2001). The gel was placed upside down on the Whatman filter paper, and the 150 x 100mm membrane (soaked in water and in 20 X SSC, Hybond-N membrane, Amersham Biosciences, product code: RPN303N) placed on top of the gel. A 150 x 100mm piece of Whatman filter paper soaked in 20 X SSC was placed on top of the membrane to keep it moist and paper towel was placed on top of the filter paper. A glass plate with a bottle containing approximately 500ml of solution on top was placed on the paper towel as a weight. This apparatus allows the RNA to transfer from the gel to the membrane through upward capillary action overnight (Sambrook and Russel, 2001) (Figure 24).

The following day, the gel and membrane were removed from the apparatus and the wells marked using a ball point pen. Another UV image was taken to ensure complete RNA transfer and the membrane was cross-linked twice with a UV

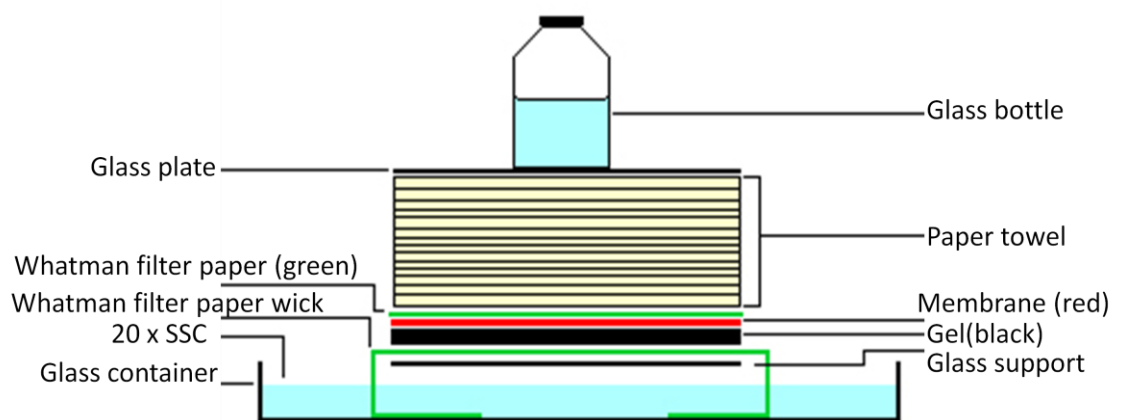


Figure 24. Northern gel transfer apparatus enabling upward capillary transfer of RNA from northern gel to Hybond-N membrane.

cross-linker, using the auto crosslink setting (Stratagen, catalogue number 400072). Following approximately 30 minutes of air drying, the membrane was ready for probing with a 32-phosphorous CTP (^{32}P -dCTP) labelled probe.

2.8.4. Northern blotting

Prehybridisation solution [25% 20 X SSC, 10% 50 X filtered Denharts solution (10mg/ml BSA, 10mg/ml Ficoll 400, 10mg/ml polycinalpyrrolidone (Sigma Aldrich, catalogue number P5288), in MqH_2O), 5% of 10% SDS, 10% DEPC water, 50% formamide] was warmed in a 42°C water bath. The membrane was placed into a hybridisation bottle with 10ml of prehybridisation solution and 100 μl of denatured salmon sperm DNA (10mg/ml; Sigma-Aldrich, catalogue number D1626-250MG). Salmon sperm DNA acts as a blocking agent in Northern Blotting protocols by preferentially binding to background nucleotides thereby preventing non-specific absorption of the radioactive probe (Sambrook and Russel, 2001). The membrane was incubated in a rotating hybridisation oven at 42°C for at least an hour before addition of the radio-labelled probe. Probes for mouse α -skeletal actin, α -MHC, ANP, β -MHC, BNP, SERCA-2a, and Glyceraldehyde 3-phosphate dehydrogenase (GAPDH) were generated as previously described (McMullen *et al.*, 2003; Shioi *et al.*, 2000; Tanaka *et al.*, 1999). Northern probe band sizes are shown in Table 12.

Fifty ng of the probe DNA (in a total volume of 10 μl with MqH_2O) was placed at 100°C for 5 minutes to separate the DNA and immediately placed on ice to prevent the DNA strands from re-annealing. The radio-labelled probe was prepared using the Promega Prime-a-gene® labelling kit [catalogue number U1100, 18 μl MqH_2O , 10 μl 5 X buffer, 2 μl BSA (10mg/ml), 2 μl dTTP (1.5mM), 2 μl dGTP (1.5mM), and 2 μl dATP (1.5mM)]. Ten μl of the probe DNA, 5 μl of α - ^{32}P -dCTP (50 μCi) and 1.5 μl of Klenow enzyme was added and the mixture was vortexed and centrifuged for 10 seconds. Klenow allows the synthesis of a complementary strand of DNA in which α - ^{32}P -dCTP is incorporated. The probe was incubated at RT for at least one hour.

The unincorporated nucleotides were removed using a MicroSpin S-300 HR column (GE Healthcare, catalogue number 27-05130-01) by adding the probe to the column and centrifuging at 3,000 rpm for 2 minutes. One μl of the probe was used to

Table 12. Northern probe band sizes.

Probe	Size (base pair)
α-skeletal actin	1433
α-myosin heavy chain (α-MHC)	3578
Atrial natriuretic peptide (ANP)	865
β-myosin heavy chain (β-MHC)	6163
B-type natriuretic peptide (BNP)	781
Sarcoplasmic reticulum Ca²⁺ ATPase 2a (SERCA-2a)	5763
GAPDH	1420

* Note 28S represents 4700 base pairs, and 18S represents 1900 base pairs.

measure the incorporation of the α - ^{32}P -dCTP in the probe using a Beckman-Coulter LS6000TA scintillation counter. The optimal concentration of the probe in hybridisation solution is approximately 2×10^6 cpm/ml. The volume of the probe required was calculated using the following equation:

$$\text{Hybridisation solution (ml)} = \text{Radioactivity count (cpm)} \times 60\mu\text{l} / 2,000,000 \text{ (cpm/ml)}$$

$$\text{Volume of probe needed } (\mu\text{l}) = 60 / (\text{hybridisation solution required (ml)} / 10\text{ml})$$

The radioactive probe DNA was incubated at 100°C for 5 minutes to separate the DNA and immediately placed directly on ice again to prevent the DNA strands from re-annealing. The prehybridisation solution in the hybridisation bottle with the membrane was discarded and 10ml of new hybridisation solution was added. The DNA radio-labelled probe was removed from ice and centrifuged for 10 seconds and added to the solution in the hybridisation bottle. The membrane was incubated with the probe in a rotating hybridisation oven overnight at 42°C . The following day, the membrane was washed in pre-warmed (42°C) 2 X SSC twice, in pre-warmed (42°C) 2 X SSC/1% SDS at 42°C for 5 minutes twice, and in pre-warmed (42°C) 0.1 X SSC at 42°C for 30 minutes twice. The membrane was wrapped in glad wrap, placed in a Kodak film cassette and exposed to Amersham Hyperfilm MP with an intensifying screen. Samples were quantified using ImageJ (version 1.42q) software (National Institutes of Health, USA). To probe the same Northern membrane with subsequent probes, the membrane was stripped according to the following protocol. Eight hundred ml of MqH_2O was heated to 95°C and 8ml of 10% SDS was added. The membrane was placed in the solution and not removed until the solution had cooled to approximately 40°C . The membrane was washed in 2 X SSC for 5 minutes, twice. The membrane was stored in fresh 2 X SSC until required for further probing.

2.8.5. Microarray gene expression analysis

The microarray gene expression analysis was performed by Dr. Ruby C.Y. Lin (Ramaciotti Centre for Gene Function Analysis, University of New South Wales, Australia). The use of distinct DNA arrays for expression profiling was first described to

identify genes modulated by interferon (Kulesh *et al.*, 1987), and the first reported use of microarrays was in 1995 (Schena *et al.*, 1995). Microarray technology is now commonly used to analyse whole genome wide gene expression. Gene expression profiling was performed on atrial samples of 32 male mice using Affymetrix GeneChip® Mouse Gene 1.0 ST arrays. RNA was extracted using Trizol, after which sense DNA targets were generated from 100ng of total RNA according to the manufacturer's protocol (Affymetrix), and hybridisation, wash and scan were performed.

Array data was processed using robust multiple-array average normalisation (Partek v6.4, Partek Inc.). Principle component analysis was used to identify batch and technical variations and these were removed for subsequent analysis. Differences across genotypes were compared using an ANOVA, and an unpaired t-test was used to look for differences between specific genotypes. Since left and right atria from the same mouse were processed, a “matched-paired-organ” analysis was carried out using the ratio of left/right atria of the same mouse. An ANOVA was then carried out to look for differential gene expression between genotypes.

Following the generation of gene lists, the data was adjusted to control the false discovery rate, at a q value of 0.01. Hierarchical clustering and functional annotation were carried out. The experimental design, RNA extraction and microarray experiment in this study are all MIAME (minimum information about a microarray experiment)-compliant. The complete raw and normalised array data are available through the Gene Expression Omnibus of the National Centre for Biotechnology Information (<http://www.ncbi.nlm.nih.gov/geo/>, accession number GSE12420).

2.9. Plasminogen assays

To assess fibrinolytic activity in mouse plasma, plasminogen assays were performed by the laboratory of Associate Professor Robert Medcalf (Australian Center for Blood Diseases, Monash University), as previously described (Granelli-Piperno and Reich, 1978; Liberatore *et al.*, 2003). Plasma samples were obtained from blood samples collected from mice that underwent catheterisation (described in Section 2.4.2). Blood samples were centrifuged at 13,000 rpm for 10 minutes at 4°C. Approximately 1ml of

plasma was aliquoted into a new eppendorf tube and stored at -80°C until required for analysis. Five µl of the undiluted plasma samples were run on 10% acrylamide gels, followed by fibrin zymography (Granelli-Piperno and Reich, 1978; Liberatore *et al.*, 2003), using recombinant human tissue plasminogen protein as a standard. Gels were incubated at 37°C in a humidified chamber until regions of proteolysis appeared.

2.10. Histology and fibrosis examination

Mouse ventricles, atria and lungs were fixed in 4% PFA overnight, placed in pathology cassettes and taken to the Alfred Hospital Pathology department for embedding, processing and staining. Heart sections were obtained for assessment of fibrosis. In brief, the ventricles and atria were embedded in paraffin and three 6µm sections were cut from each heart. Sections were stained using Masson's trichrome staining (Gomori, 1950; Masson, 1929; Wheatley, 1951) to enable the identification of collagen deposits (fibrosis) in the cardiac tissue. Sections were post-fixed in Bouins at 60°C, rinsed and stained with Weigerts haematoxylin (first in 1% haematoxylin in absolute ethanol, and then in 4% ferric chloride (30%), 95% distilled water, and 1% concentrated HCl). Samples were rinsed and differentiated using acid alcohol if required. Rinsed samples were then stained with brilliant crocein/acid fuchsin (0.01g/ml brilliant crocein, 0.01g/ml phosphotungstic acid, 10% of 1% acid fuchsin, and 90% distilled water). The stain was washed off using 1% phosphotungstic acid and stained in 2% light green in 1% acetic acid. The stain was washed off using 1% acetic acid, dehydrated in absolute ethanol, and cleared in xylene. Sections were placed under a coverslip for further analysis. Lung sections were obtained for assessment of pulmonary congestion. The lungs were embedded in paraffin and three 3µm sections were cut from each lung. Sections were stained using haematoxylin and eosin as described previously (Yamamoto *et al.*, 2003).

Light microscope images (approximately 12-15 images per section) of the Masson Trichrome-stained heart ventricles and atria were captured using a JVC digital camera (4 X or 10 X objective; eye piece 10 X) (see Figure 25). The percentage area of fibrosis relative to the total area of the left ventricle was determined for each sample using the software program Olympus Image Pro Plus 6 (Media Cybergenetics). Representative images of the lung sections were also taken (4 X objective).

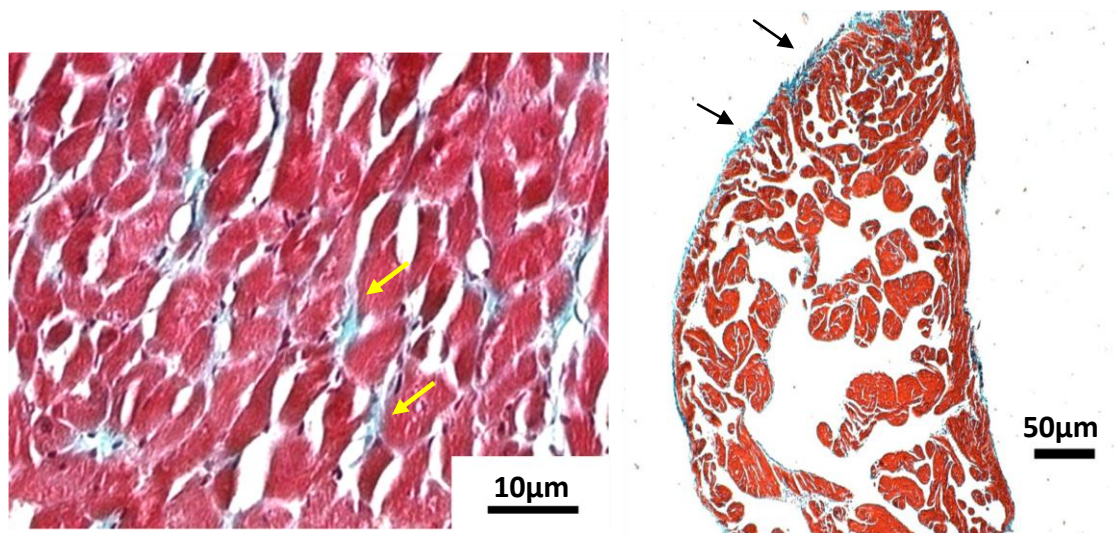


Figure 25. Masson's Trichrome stained cardiac tissue sections.

Left panel: Masson's Trichrome stained ventricular tissue section (100 X magnification). **Right panel:** Masson's Trichrome stained atrial tissue section (40 X magnification). Fibrosis is shown in blue, and indicated by arrows.

2.11. TUNEL staining for apoptosis

Apoptosis can be examined using a variety of methods. While the gold standard for apoptosis detection is electron microscopy which can demonstrate a variety of apoptotic markers such as cell shrinkage, chromatin condensation, and apoptotic bodies, it requires specialised equipment, is labour intensive and expensive. A much more cost-effective and widely accepted method for examining apoptosis involves detection of DNA fragmentation using terminal deoxynucleotidyl transferase nick end labelling (TUNEL) staining. First described in 1992 (Gavrieli *et al.*, 1992), TUNEL staining preferentially labels DNA strand breaks generated during apoptosis, enabling discrimination of apoptosis from necrosis, as well as from primary DNA strand breaks induced by, for example, irradiation. It is important to note that TUNEL staining does have inherent limitations. False positive results can occur, as TUNEL staining labels all fragmented DNA, not just apoptotic nuclei (Kano *et al.*, 1999; Ohno *et al.*, 1998). Quantification of apoptosis also requires a large sampling area, as the distribution of apoptotic nuclei is variable in different areas of a sample.

PFA-fixed heart sections were dewaxed twice in xylene for 5 minutes, and then hydrated by placing them in decreasing ethanol concentrations (100%, 90%, 70%) twice for 3 minutes. Sections were placed in distilled water for 3 minutes, and then washed in 1 X PBS for 3 minutes, twice. A Dako pen (Dako, catalogue number S2002) was used to draw a water-repelling barrier around the tissue sections in order to contain staining solutions around the section of interest. Nonspecific binding of the anti-fluorescein antibody to the tissue was blocked by adding 50µl of proteinase K (14µg/ml in 10mM Tris/HCl pH 7.4) to each section, and incubating the sections for 15 minutes at 37°C. Fifty µl of 0.1% H₂O₂ in methanol was added to each section and incubated for 5 minutes at RT (to block any background reactivity). Slides were washed for 3 minutes in 1 X PBS, three times and 50µl of 0.1M Tris-HCl, 3% BSA (pH 7.5) solution (0.013g/ml Tris-HCl, 0.03g/ml BSA, in MqH₂O) added to each section. Slides were incubated for 30 minutes at RT and washed in 1 X PBS for 3 minutes, three times.

TUNEL staining was performed using the commercially available kit from Roche Applied Sciences (*In Situ* Cell Detection Kit, POD, catalogue number 1 684 817) with some modifications, as outlined below. The enzyme and label solutions were defrosted on ice, vortexed, and centrifuged at 12,000 rpm for 1 minute. The solutions

were diluted to a ratio of 1:10 of enzyme solution: label solution. This solution was serially diluted to a concentration of 1:20 (TUNEL reaction mixture) using a TUNEL dilution buffer [30mM tris (hydroxymethyl) methane, 140mM sodium cacodylate, 1mM cobalt chloride, in 1 X PBS]. Fifty μ l of the TUNEL reaction mixture was added to each section and the sections incubated for 60 minutes at 37°C in a humidified atmosphere.

Slides were washed in 1 X PBS for 3 minutes, three times and 50 μ l of 0.1M Tris-HCl, 3% BSA [pH 7.5] solution added to each section (to block background reactivity). Slides were incubated for 30 minutes at RT and washed in 1 X PBS for 5 minutes, two times. The converter POD solution (the anti-fluorescein antibody, Fab fragment conjugated with peroxidase) was diluted 1:2 with 1 X PBS, and 50 μ l was added to each section. Sections were incubated for 30 minutes at 37°C in a humidified atmosphere, and washed in 1 X PBS for 5 minutes, three times. H₂O₂ was added to 3,3'-diamino-benzidine (DAB) solution to make the DAB reagent [1 DAB tablet (Sigma Aldrich, catalogue number D5905), 1-2mg of Imidazole (C₃H₄N₂), 7.5 μ l 30% H₂O₂ and 20ml 1 X PBS] and 50 μ l DAB reagent added to each section. Sections were incubated for 5 minutes at RT and the excess DAB reagent removed. Slides were washed in 1 X PBS for 5 minutes, three times and placed in Myer's Haematoxylin for 30 seconds. The Myer's Haematoxylin was rinsed off and sections placed in Scott's tap water for 2 minutes.

Sections were dehydrated by placing them in increasing concentrations of ethanol (70% for 2 minutes, 90% for 2 minutes, 100% for 2 minutes three times) and in xylene for 5 minutes twice. Slides were mounted under a coverslip using Depex and examined under light microscopy. Nuclei that were stained brown (Figure 26, indicated by arrow) were classified as positive. Positive-stained nuclei were manually counted and quantified relative to total number of nuclei present in the tissue section (40 X magnification, 100 microscope fields per section).

2.12. Sample Analysis and Statistics

Data obtained were analysed using computer statistical programs StatView (Version 5.0.1, SAS Institute Inc.) and Microsoft® Office Excel® 2007 (Version 12.0.6545.5000, SP

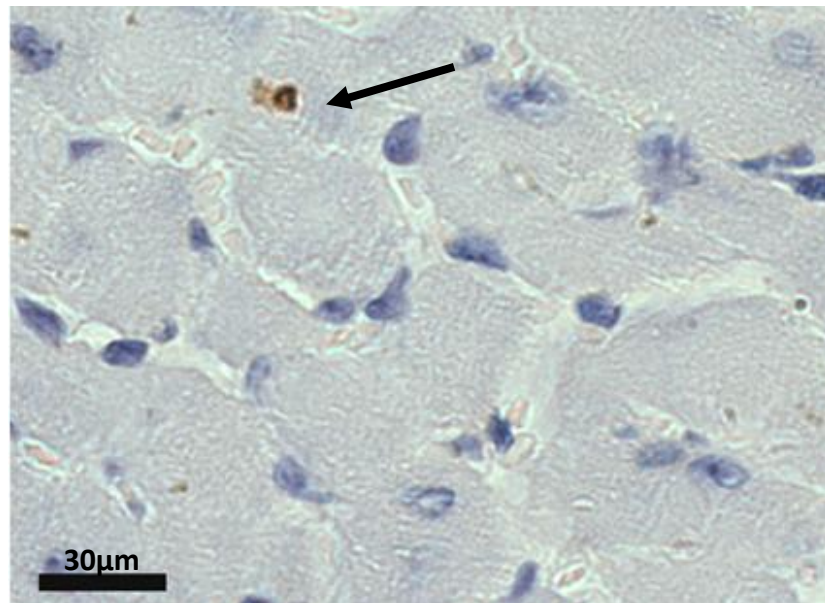


Figure 26. TUNEL staining of a cardiac tissue section.

TUNEL staining of a cardiac tissue section (400 X magnification), showing a nucleus that is apoptotic (brown colour, indicated by arrow), compared with normal nuclei (blue colour).

MSO 12.0.6435.5002, Microsoft Corporation). Kaplan-Meier survival curves were generated using GraphPad Prism (Version 4.01, GraphPad Software Incorporated). Western and Northern blots, as well as PI3K assays were scanned and analysed using ImageJ (Version 1.42q, National Institutes of Health, USA). Blinded analyses of cardiac function, fibrosis and apoptosis were performed with the analyst unaware of the genotype of the sample being investigated. Percentage fibrosis-stained tissue was determined relative to total tissue section, using Olympus Image Pro Plus (Media Cybergenetics).

Results are presented as mean \pm standard error, and a statistically significant p-value of $p < 0.05$ was considered significant. Differences between groups were identified using one-way ANOVA for overall significance, followed by Tukey and Fischer's multiple comparison post-hoc tests. Significant differences in survival (Kaplan-Meier survival curves) were determined using the log rank test.

Chapter 3 – The role of PI3K (p110 α) in a mouse model of dilated cardiomyopathy

3.1. Introduction

As described in the introduction to this thesis (see Chapter 1), the IGF1-PI3K (p110 α) pathway is a critical regulator of physiological hypertrophy (e.g. exercise-induced heart growth) (McMullen *et al.*, 2003). Physiological cardiac hypertrophy is considered beneficial, and is associated with preserved or even enhanced cardiac function (McMullen and Jennings, 2007; Pretorius *et al.*, 2008). In contrast, pathological cardiac hypertrophy is typically mediated by activation of signalling proteins downstream of GPCRs (Akhter *et al.*, 1998; Sakata *et al.*, 1998; Wettschureck *et al.*, 2001), and occurs in response to chronic pressure or volume overload in a setting of disease. It was recently shown that PI3K (p110 α) may also have the ability to partially inhibit pathological cardiac hypertrophy through negative regulation of ERK1/2 (McMullen *et al.*, 2007).

The first aim of this thesis was to examine the protective effects of PI3K (p110 α) in an *in vivo* mouse model of HF [dilated cardiomyopathy due to over-expression of Mst1 (Yamamoto *et al.*, 2003)], and determine the molecular mechanisms responsible for any protective properties. In order to address this question, the effects of either increasing PI3K (p110 α) activity or decreasing PI3K (p110 α) activity in a setting of HF was examined by crossing caPI3K and dnPI3K mice with Mst1 mice and examining the resulting phenotypes. Increased PI3K (p110 α) activity was expected to confer protection in a setting of HF through differential up- and down-regulation of protein and gene expression, as well as reduction of fibrosis and apoptosis in the heart. Conversely, decreased PI3K (p110 α) activity was expected to be detrimental to cardiac function and lifespan in a setting of HF, and to induce increased fibrosis and apoptosis in the heart.

3.2. Methods

3.2.1. Techniques used in this chapter

The following techniques were used for the studies described in this chapter:

- Transgenic mouse model generation (as described in Chapter 2, page 63)
- Transgenic mouse model genotyping (as described in Chapter 2, pages 66-68)
- Echocardiography (as described in Chapter 2, page 68)
- Tissue harvesting and tibia length measurement (as described in Chapter 2, page 80)
- Protein extraction, measurement of protein concentration, and Western blotting (as described in Chapter 2, pages 81-86)
- RNA extraction, calculation of RNA concentration and quality, and Northern blotting (as described in Chapter 2, pages 90-96)
- Tissue fibrosis examination (as described in Chapter 2, page 98)
- Tissue apoptosis examination (TUNEL staining as described in Chapter 2, page 100)

3.2.2. Animals

This chapter describes the characterisation of female and male Ntg, caPI3K, dnPI3K, Mst1, caPI3K-Mst1, and dnPI3K-Mst1 mice at approximately 4.5 months of age. All the transgenic mice were heterozygous for the transgene (as previously described in Chapter 2, pages 62-64). To examine whether increased PI3K (p110 α) activity would be beneficial in aged mice, the phenotypes of female and male Ntg, caPI3K, Mst1, and caPI3K-Mst1 mice were also characterised at 8 months of age. To examine the molecular mechanisms responsible for the effects of increased PI3K (p110 α) activity in Mst1 mice, caPI3K-Mst1 mice were also crossed with kdAkt mice and the phenotype of the resulting triple-transgenic (caPI3K-Mst1-kdAkt) mice characterised. Akt is a well characterised downstream target of PI3K (p110 α) [see Figure 6 (page 29), (Burgering and Coffey, 1995; Cantley, 2002; DeBosch *et al.*, 2006b; Klippel *et al.*, 1997)].

3.2.2.1. Inheritance pattern of transgenic mice

Genetic inheritance based on Mendelian principles predicts that the genetic crossing of two unlinked genes will result in a 25% likelihood of obtaining a specific genotype (Campbell and Reece, 2002). Inheritance frequencies were examined in the transgenic

mouse models. Relative Mendelian inheritance proportions were observed in both the heterozygous caPI3K crossed with heterozygous Mst1 mice [caPI3K-Mst1 mice comprised 24% of the population (Table 13)], and the heterozygous dnPI3K crossed with heterozygous Mst1 mice [dnPI3K-Mst1 mice comprised 26% of the population (Table 14)].

Table 13. Inheritance pattern of caPI3K mice crossed with Mst1 mice.

Genotype	Frequency	Percentage
Ntg	83	28%
caPI3K	76	25%
Mst1	68	23%
caPI3K-Mst1	72	24%
Total	299	100%

Table 14. Inheritance pattern of dnPI3K mice crossed with Mst1 mice.

Genotype	Frequency	Percentage
Ntg	75	27%
dnPI3K	71	25%
Mst1	62	22%
dnPI3K-Mst1	74	26%
Total	282	100%

Inheritance frequencies were also examined in the heterozygous caPI3K mice crossed with both heterozygous Mst1 and heterozygous kdAkt (see Table 15). According to Mendelian inheritance principles, the likelihood of obtaining a specific genotype when three unlinked genes are crossed is 12.5% (Campbell and Reece, 2002). Relative Mendelian inheritance proportions were also observed in this transgenic line, with triple-transgenic mice (caPI3K-Mst1-kdAkt) comprising 17% of the population (Table 15).

Table 15. Inheritance pattern of triple-transgenic mice.

Genotype	Frequency	Percentage
Ntg	9	10%
caPI3K	9	10%
Mst1	12	14%
kdAkt	9	10%
caPI3K-Mst1	10	12%
caPI3K-kdAkt	10	12%
Mst1-kdAkt	13	15%
caPI3K-Mst1-kdAkt	15	17%
Total	87	100%

3.3. Results

3.3.1. Lifespan of double-transgenic mice

Ntg mice have a lifespan of approximately 2 years. It has previously been shown that caPI3K and dnPI3K mice have a normal lifespan under basal conditions (Shioi *et al.*, 2000) and experimental observations have indicated that the Mst1 transgenic mice have a lifespan of approximately 8 months (Dr. Junichi Sadoshima, personal communication). It was therefore important to examine whether manipulating cardiac PI3K (p110 α) activity had an impact on lifespan in Mst1 mice.

Ntg, caPI3K and dnPI3K mice showed a normal lifespan of at least 18 months, as previously reported (Shioi *et al.*, 2000). Mst1 mice had a lifespan of 7.9 ± 0.4 months (Figure 27). caPI3K-Mst1 mice displayed a 70% improvement in lifespan ($p < 0.0001$) compared with Mst1 mice alone, with a mean survival of 13.4 ± 0.9 months (Figure 27). In contrast, dnPI3K-Mst1 mice displayed a 43% decrease in lifespan ($p < 0.0001$) compared with Mst1 mice alone, with a mean survival of 4.5 ± 0.3 months (Figure 27). As a result of the lifespan data, subsequent studies were performed at two time-points. Mice were examined at 4.5 months old to examine the dnPI3K-Mst1 mice compared with all other genotypes, as well as at 8 months old to examine the Mst1 mice compared with the caPI3K-Mst1 mice.

Lifespan was not different between female and male Mst1 or caPI3K-Mst1 mice (Figure 28), but female dnPI3K-Mst1 mice had a significantly shorter lifespan compared with male dnPI3K-Mst1 mice (Figure 28).

The premature mortality seen in the dnPI3K-Mst1 mice was further examined in a small subset of mice through daily animal monitoring ($n=4$). Progressive signs of congestive HF (laboured breathing and inactivity) were not a common feature of the dnPI3K-Mst1 mice. One of the 4 mice assessed showed signs of HF and was euthanised. The other three mice all died suddenly, after having been active the previous day. This suggests that the majority of dnPI3K-Mst1 mice may die due to an arrhythmia-related event. This was further examined in Chapter 4.

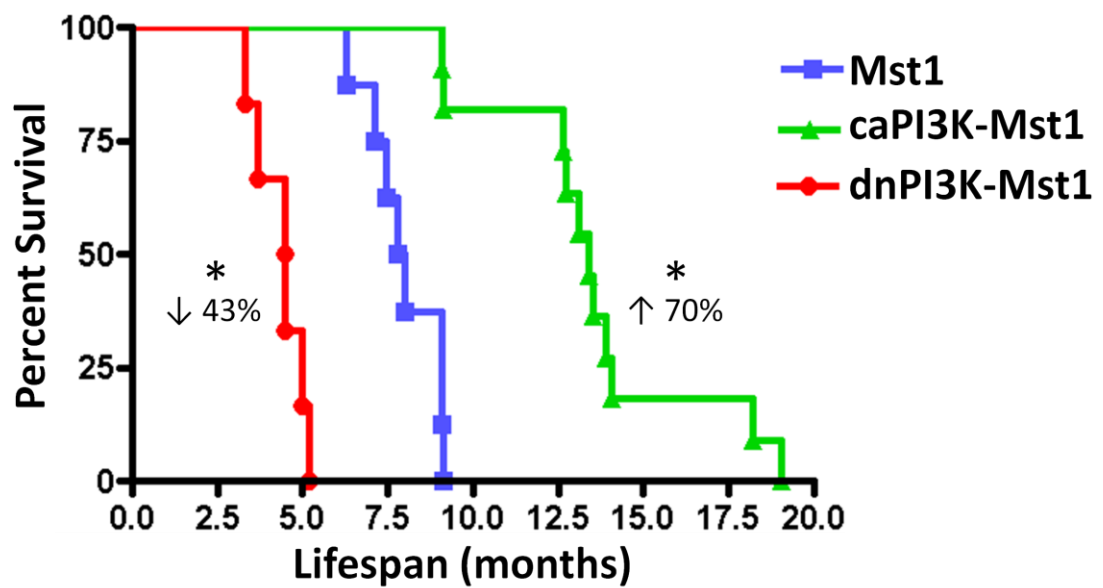


Figure 27. Survival of caPI3K-Mst1 and dnPI3K-Mst1 mice compared with Mst1 mice. Kaplan-Meier survival curve, showing percent survival of Mst1 (n=7, blue), caPI3K-Mst1 (n=11, green) and dnPI3K-Mst1 (n=6, red) mice. Mst1 mice displayed a lifespan of 7.9 ± 0.4 months. caPI3K transgene expression in the Mst1 mice significantly improved mean survival to 13.4 ± 0.9 months, while dnPI3K transgene expression in the Mst1 mice markedly reduced lifespan to 4.5 ± 0.3 months. * $p < 0.0001$ compared with Mst1.

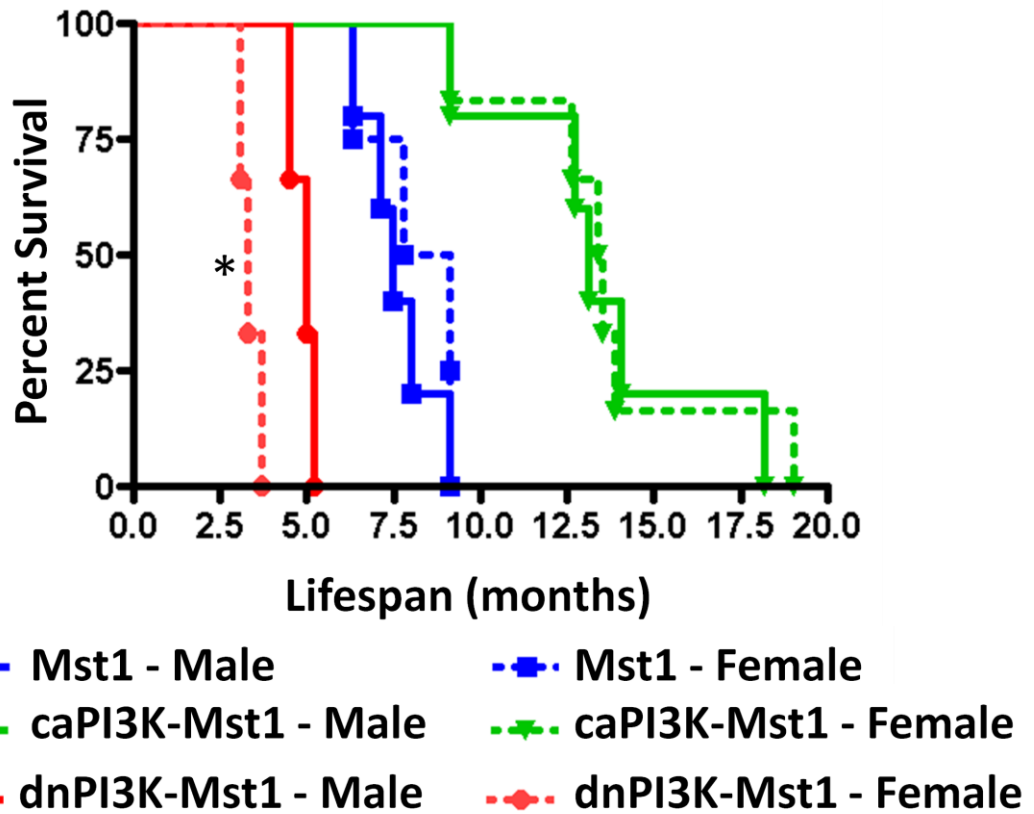


Figure 28. Female dnPI3K-Mst1 mice have a significantly shorter lifespan compared with their male counterparts.

Kaplan-Meier survival curve, showing percent survival of female (dashed lines) and male (solid lines) mice. Mst1 (blue) and caPI3K-Mst1 mice (green) showed no difference in lifespan between genders. dnPI3K-Mst1 mice (red) showed a marked gender difference, with female mice having a significantly shorter lifespan compared with male mice. n=3-6 in each group.

* $p < 0.0001$ compared with male dnPI3K-Mst1.

3.3.2. Characterisation of the cardiac phenotype of the transgenic mice

3.3.2.1. Cardiac dimensions

Cardiac dimensions were determined using echocardiography, as previously described (see Section 2.4.1.). There was no difference in tibia length between any of the groups at 4.5 months or 8 months of age indicating the mice were of similar size (Table 16, Table 17). Heart rates were similar between Ntg, caPI3K, and dnPI3K mice at 4.5 months of age (Table 16). On average, the Mst1 groups showed a small but significant decrease in heart rate (approximately 60 beats per minute) under anaesthetised conditions compared to Ntg, caPI3K, and dnPI3K mice (Table 16). Importantly, there were no differences in heart rate between the Mst1, caPI3K-Mst1, and dnPI3K-Mst1 groups, allowing for comparison of cardiac chamber dimensions and wall thicknesses between the Mst1 groups (Table 16).

At 4.5 months of age, there was a significant increase or trend for an increase in chamber dimensions and wall thicknesses in caPI3K mice, consistent with these mice developing physiological hypertrophy (Table 16). In contrast, there was a significant decrease or trend for a decrease in chamber dimensions and wall thicknesses in dnPI3K mice, consistent with these mice having a small heart phenotype (Table 16). Mst1 mice showed larger LVESD and LVEDD compared with Ntg, caPI3K, and dnPI3K mice (Table 16). Mst1 mice also had thinner ventricular walls compared with Ntg and caPI3K mice (Table 16, LVPW and IVS). Collectively this demonstrates that Mst1 mice developed dilated cardiomyopathy. caPI3K-Mst1 mice had smaller LVESD and greater LVPW compared with Mst1 mice alone (Table 16). Thus, expression of the caPI3K transgene in Mst1 mice (i.e. caPI3K-Mst1) was in part able to protect the heart. In contrast, dnPI3K-Mst1 mice displayed more severe dilated cardiomyopathy with significantly larger LVESD and LVEDD and thinner ventricular walls (IVS and LVPW) compared with all groups (Table 16). At 8 months of age, Mst1 mice also had dilated chambers (LVESD and LVEDD) compared with Ntg and caPI3K mice (Table 17). caPI3K-Mst1 mice displayed reduced LVESD and LVEDD compared with Mst1 mice alone (Table 17).

Table 16. Left ventricular wall thicknesses and chamber dimensions in transgenic mice at 4.5 months of age.

LVESD: left ventricular end-systolic dimension, LVEDD: left ventricular end-diastolic dimension, LVPW: left ventricular posterior wall thickness, and IVS: interventricular septal width. * $p < 0.05$ compared with Ntg; † $p < 0.05$ compared with caPI3K; ^ $p < 0.05$ compared with dnPI3K; # $p < 0.05$ compared with Mst1; and † $p < 0.05$ compared with caPI3K-Mst1.

	N	Tibia Length (mm)	Heart Rate (beats per minute)	LVESD (mm)	LVEDD (mm)	LVPW (mm)	IVS (mm)	Fractional Shortening (%)
Ntg	20	17.5±0.2 (n=15)	526±12	1.97±0.04	3.87±0.04	0.90±0.05	0.88±0.04	49±1
caPI3K	19	17.5±0.2 (n=18)	495±16	2.11±0.07	4.12±0.08 *	0.93±0.03	1.12±0.06 *	49±1
dnPI3K	17	17.4±0.1	511±10	1.84±0.05 †	3.75±0.09 †	0.52±0.02 *†	0.62±0.03 *†	51±1
Mst1	17	17.4±0.2 (n=16)	464±10 *^	2.99±0.06 *†^	4.58±0.05 *†^	0.74±0.02 *†^	0.76±0.01 *†^	35±1 *†^
caPI3K-Mst1	16	17.7±0.2 (n=13)	450±12 *†^	2.59±0.10 *†^#	4.38±0.11 *†^	0.86±0.05 ^#	0.79±0.05 *†^	41±1 *†^#
dnPI3K-Mst1	15	17.7±0.1 (n=13)	451±15 *†^	3.69±0.17 *†^#†	5.01±0.09 *†^#†	0.39±0.03 *†^#†	0.40±0.05 *†^#†	27±2 *†^#†

Table 17. Left ventricular wall thicknesses and chamber dimensions in transgenic mice at 8 months of age.

LVEDS: left ventricular end-systolic dimension, LVEDD: left ventricular end-diastolic dimension, LVPW: left ventricular posterior wall thickness, and IVS: interventricular septal width. * $p < 0.05$ compared with Ntg; † $p < 0.05$ compared with caPI3K; and # $p < 0.05$ compared with Mst1.

	N	Tibia Length (mm)	Heart Rate (beats per minute)	LVEDS (mm)	LVEDD (mm)	LVPW (mm)	IVS (mm)	Fractional Shortening (%)
Ntg	11	17.2 ± 0.1 (n=10)	458 ± 25	2.55 ± 0.09	4.79 ± 0.13	0.96 ± 0.06	1.08 ± 0.04	47 ± 1
caPI3K	11	17.4 ± 0.2 (n=10)	492 ± 16	2.32 ± 0.06	4.36 ± 0.07 *	1.09 ± 0.03	1.26 ± 0.04 *	47 ± 1
Mst1	19	17.5 ± 0.1 (n=17)	492 ± 13	3.35 ± 0.10 *†	5.00 ± 0.12 †	0.94 ± 0.04 †	1.04 ± 0.03 †	33 ± 1 *†
caPI3K-Mst1	14	17.2 ± 0.1 (n=13)	428 ± 19 †#	2.98 ± 0.09 *†#	4.85 ± 0.09 †	0.89 ± 0.04 †	1.03 ± 0.05 †	39 ± 1 *†#

3.3.2.2. Systolic function

Systolic function was assessed at 4.5 months and 8 months of age by determining fractional shortening from echocardiographic M-mode images (see Section 2.4.1.). There was no difference in fractional shortening between the Ntg, caPI3K and dnPI3K mice at 4.5 months of age (Table 16; Figure 29) or between Ntg and caPI3K mice at 8 months of age (Table 17; Figure 30). At 4.5 months of age, Mst1 mice showed an approximate 30% decrease in fractional shortening compared with Ntg mice alone (Table 16; Figure 29). There was an approximate 17% improvement in fractional shortening in the caPI3K-Mst1 mice compared with the Mst1 mice alone (Table 16; Figure 29). The dnPI3K-Mst1 mice showed a further approximate 20% reduction in fractional shortening compared with Mst1 mice alone (Table 16; Figure 29). At 8 months of age, Mst1 mice also displayed depressed systolic function compared with Ntg (an approximate 30% decrease in fractional shortening; Table 17, Figure 30). Expression of the caPI3K transgene in caPI3K-Mst1 improved fractional shortening by approximately 18% compared with Mst1 alone (Table 17, Figure 30).

3.3.2.3. Gender differences in cardiac dimensions and systolic function

As previously described, heart rates were generally lower in the Mst1 transgenic groups, independent of gender (Table 18). Significant differences in chamber dimensions, wall thicknesses, and systolic function previously discussed in the different transgenic mice (see Section 3.3.2. and Table 17) were also apparent when males and females were analysed separately (Table 18). The most distinct gender differences were observed in the dnPI3K-Mst1 mice. Female dnPI3K-Mst1 mice had larger LVESD and LVEDD compared with males (Table 18).

No difference in fractional shortening was seen between male and female Ntg, caPI3K, dnPI3K, Mst1, or caPI3K-Mst1 mice at 4.5 months (Table 18; Figure 31). In contrast, fractional shortening was significantly lower in female dnPI3K-Mst1 mice (21%) versus male dnPI3K-Mst1 mice (34%) (Table 18; Figure 31). At 8 months of age there were no distinct gender differences within the Ntg, caPI3K, Mst1 and caPI3K-Mst1 groups (Table 19).

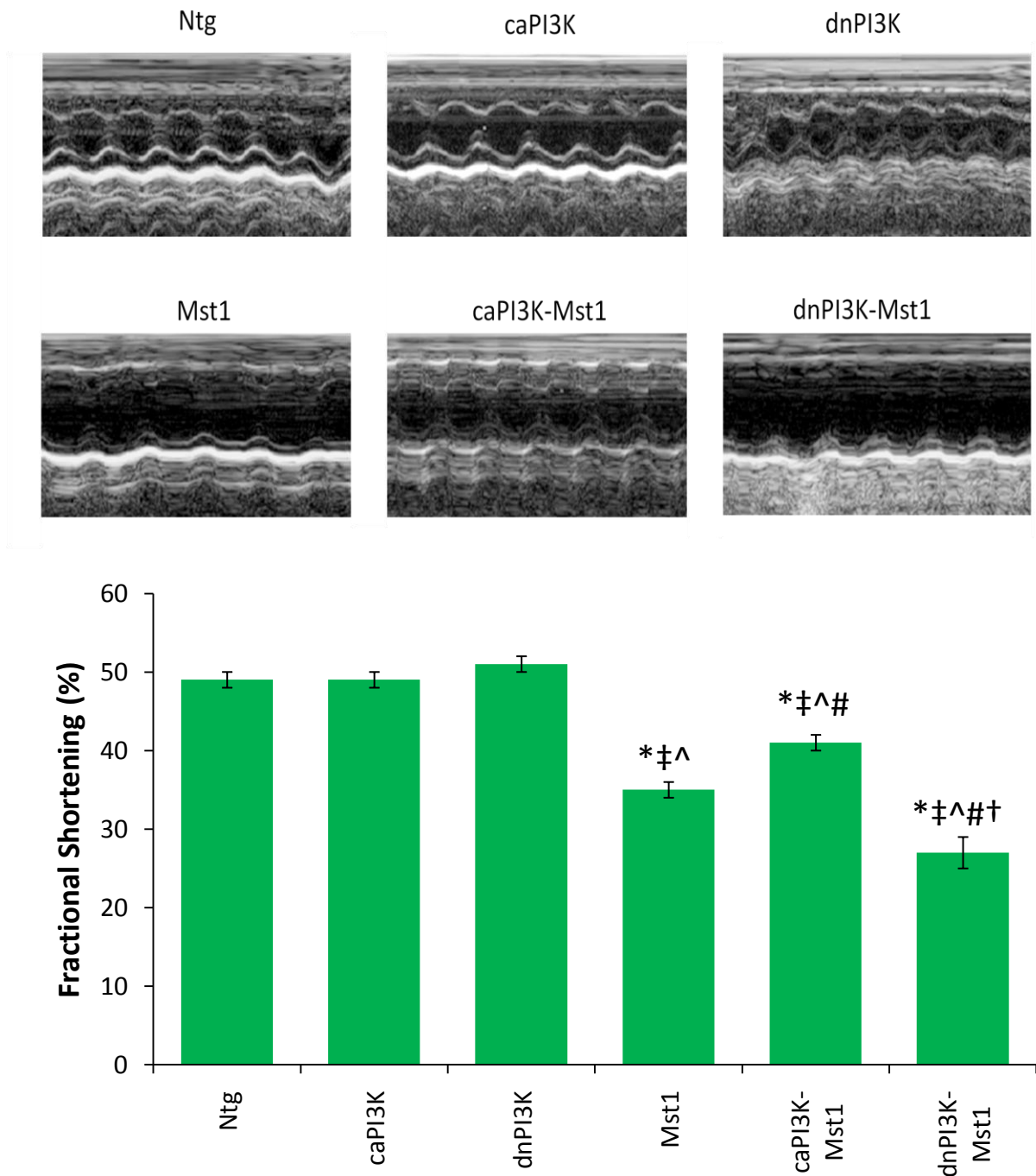


Figure 29. Systolic function of transgenic mice at 4.5 months of age

Top panel: Representative M-mode echocardiography images from transgenic mice. **Bottom panel:** Quantitative analysis of fractional shortening. * $p < 0.05$ compared with Ntg; † $p < 0.05$ compared with caPI3K; ^ $p < 0.05$ compared with dnPI3K; # $p < 0.05$ compared with Mst1; and † $p < 0.05$ compared with caPI3K-Mst1, $n = 15-20$ in each group.

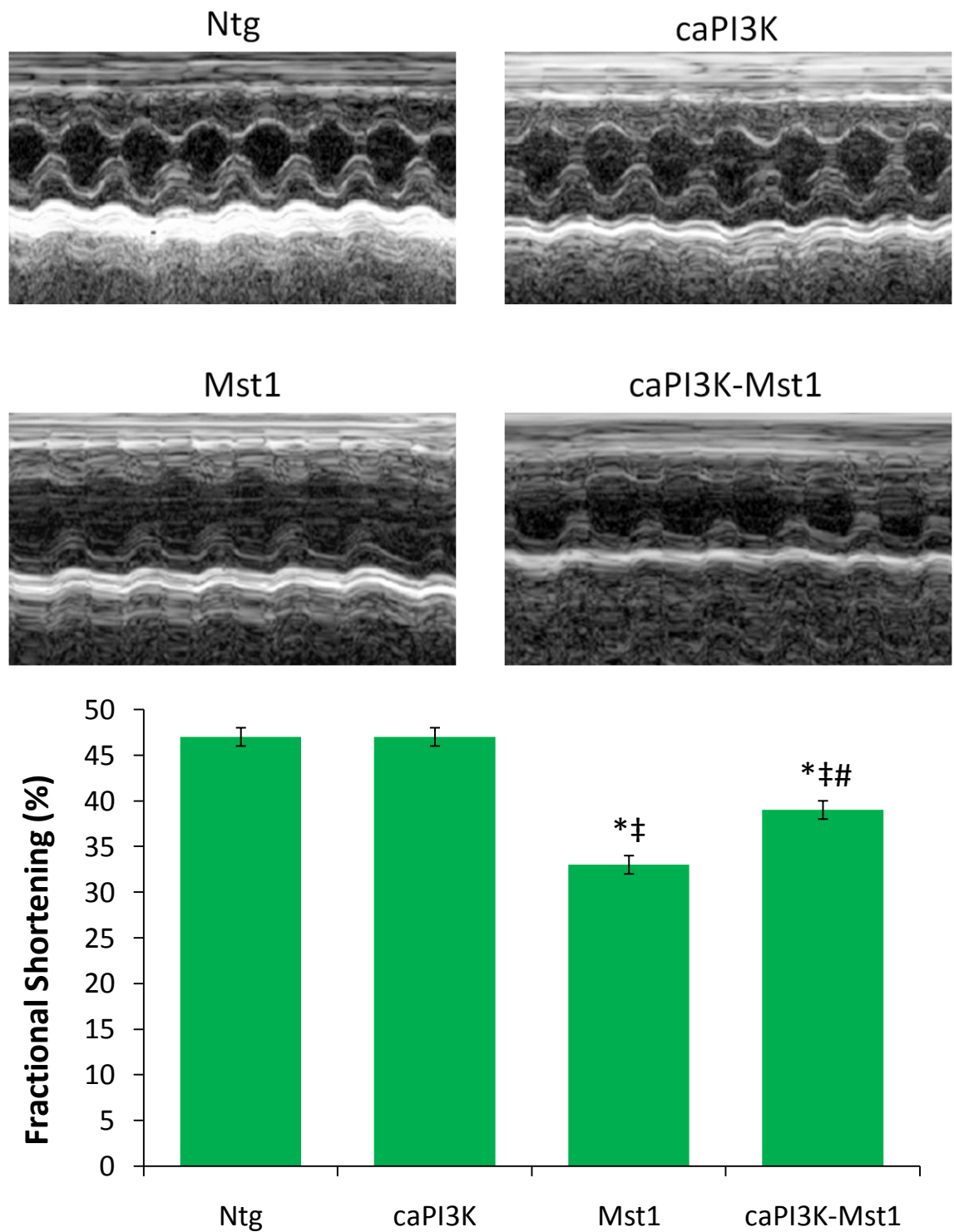


Figure 30. Systolic function of transgenic mice at 8 months of age.

Top panel: Representative M-mode echocardiography images from transgenic mice. **Bottom panel:** Quantitative analysis of fractional shortening. * $p < 0.05$ compared with Ntg; ‡ $p < 0.05$ compared with caPI3K; # $p < 0.05$ compared with Mst1, $n = 8-17$ in each group.

Table 18. Gender differences in left ventricular chamber dimensions and wall thicknesses in transgenic mice at 4.5 months of age.

LVESD: left ventricular end-systolic dimension, LVEDD: left ventricular end-diastolic dimension, LVPW: left ventricular posterior wall thickness, and IVS: interventricular septal width. ~ $p < 0.05$ compared with female of the same genotype; * $p < 0.05$ compared with Ntg of the same gender; ‡ $p < 0.05$ compared with caPI3K of the same gender; ^ $p < 0.05$ compared with dnPI3K of the same gender; # $p < 0.05$ compared with Mst1 of the same gender; and † $p < 0.05$ compared with caPI3K-Mst1 of the same gender.

	Gender	Ntg	caPI3K	dnPI3K	Mst1	caPI3K-Mst1	dnPI3K-Mst1
N	Female	11	8	8	9	8	8
	Male	9	11	9	8	8	7
Tibia Length (mm)	Female	17.7±0.3 (n=6)	17.7±0.3	17.4±0.1	17.7±0.3 (n=8)	17.7±0.4 (n=5)	17.8±0.2 (n=7)
	Male	17.3±0.2	17.3±0.2 (n=10)	17.4±0.1	17.9±0.2	17.7±0.2	17.6±0.2 (n=6)
Heart Rate (beats per minute)	Female	506±17	461±15	502±11	476±14	436±20 *^	436±15 *^
	Male	551±11	520±24 ~	520±16	450±14 *‡^	464±15 *‡^	469±27 *‡
LVESD (mm)	Female	2.07±0.04	2.09±0.11	1.89±0.09	3.00±0.05 *‡^	2.59±0.12 *‡^#	4.18±0.14 *‡^#†
	Male	1.85±0.04	2.12±0.10 *	1.79±0.06 ‡	2.98±0.12 *‡^	2.59±0.17 *‡^#	3.13±0.12 ~*‡^†
LVEDD (mm)	Female	3.93±0.06	3.95±0.09	3.71±0.12	4.53±0.05 *‡^	4.27±0.14 *‡^	5.25±0.07 *‡^#†
	Male	3.79±0.05	4.23±0.10 ~*	3.79±0.13 ‡	4.62±0.10 *‡^	4.50±0.16 *‡^	4.74±0.10 ~*‡^†
LVPW (mm)	Female	0.83±0.06	0.86±0.04	0.54±0.03 *‡	0.77±0.02 ^	0.92±0.06 ^#	0.39±0.05 *‡^#†
	Male	0.98±0.07 ~	0.97±0.03	0.50±0.02 *‡	0.70±0.03 *‡^	0.80±0.08 ^#	0.39±0.04 *‡^#†
IVS (mm)	Female	0.80±0.03	1.02±0.07 *	0.70±0.05 ‡	0.78±0.02 ‡	0.85±0.06 ‡^#	0.41±0.09 *‡^#†
	Male	0.98±0.08 ~	1.19±0.07 ~*	0.55±0.03 *‡	0.73±0.02 *‡^	0.73±0.07 *‡^#	0.38±0.04 *‡^#†
Fractional Shortening (%)	Female	47±1	47±2	49±2	34±1 *‡^	39±2 *‡^#	21±2 *‡^#†
	Male	51±1	50±1	53±1	36±2 *‡^	43±2 *‡^#	34±3 ~*‡^†

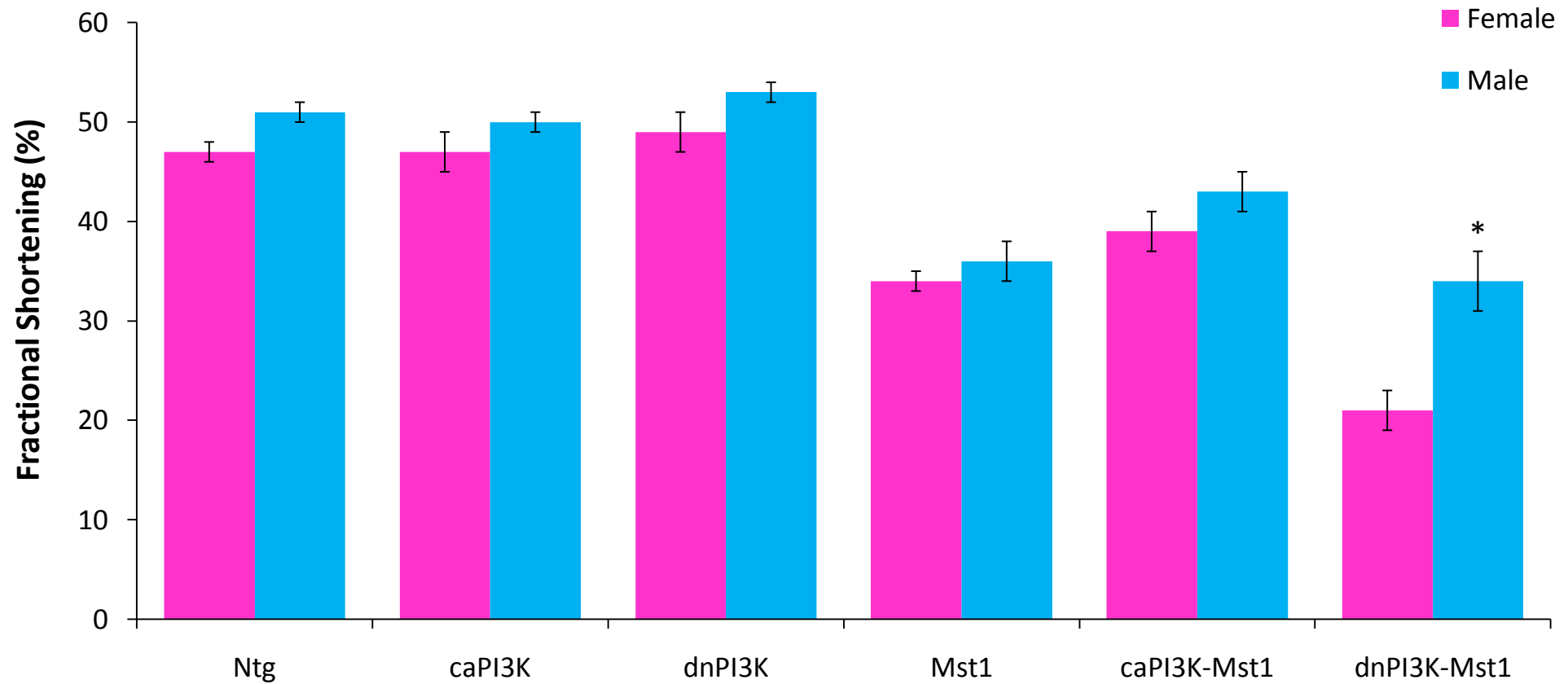


Figure 31. Gender-associated differences in systolic function in the transgenic mice at 4.5 months of age.

* $p < 0.05$ compared with female counterpart; $n = 7-11$ in each group. Only statistics related to gender differences are presented on this graph for simplicity. Statistics related to differences in genotype are presented in Table 18.

Table 19. Gender differences in left ventricular chamber dimensions and wall thicknesses in transgenic mice at 8 months of age.

LVEDS: left ventricular end-systolic dimension, LVEDD: left ventricular end-diastolic dimension, LVPW: left ventricular posterior wall thickness, and IVS: interventricular septal width. ~ $p < 0.05$ compared with female of the same genotype; * $p < 0.05$ compared with Ntg of same gender; † $p < 0.05$ compared with caPI3K of same gender; and # $p < 0.05$ compared with Mst1 of same gender.

	Gender	Ntg	caPI3K	Mst1	caPI3K-Mst1
N	Female	6	5	9	6
	Male	5	6	10	8
Tibia Length (mm)	Female	17.1 ± 0.1 (n=5)	17.4 ± 0.2	17.4 ± 0.1 (n=9)	17.1 ± 0.2
	Male	17.3 ± 0.2	17.4 ± 0.3 (n=5)	17.6 ± 0.2 (n=8)	17.3 ± 0.2 (n=7)
Heart Rate (beats per minute)	Female	400 ± 15	489 ± 27 *	496 ± 19 *	378 ± 9 †#
	Male	529 ± 30 ~	495 ± 21	489 ± 18	466 ± 19 ~
LVEDS (mm)	Female	2.69 ± 0.12	2.23 ± 0.08 *	3.35 ± 0.14 *†	3.05 ± 0.17 †
	Male	2.39 ± 0.11	2.40 ± 0.08	3.34 ± 0.14 *†	2.93 ± 0.10 *†#
LVEDD (mm)	Female	4.98 ± 0.15	4.28 ± 0.12 *	4.93 ± 0.12 †	4.88 ± 0.18 †
	Male	4.57 ± 0.17	4.43 ± 0.08	5.07 ± 0.21 *†	4.83 ± 0.09
LVPW (mm)	Female	0.87 ± 0.08	1.11 ± 0.04 *	0.90 ± 0.06 †	0.85 ± 0.04 †
	Male	1.06 ± 0.07	1.07 ± 0.05	1.00 ± 0.06	0.92 ± 0.07
IVS (mm)	Female	1.00 ± 0.04	1.27 ± 0.06 *	1.01 ± 0.06 †	0.97 ± 0.07 †
	Male	1.17 ± 0.04~	1.24 ± 0.05	1.06 ± 0.03 †	1.08 ± 0.07 †
Fractional Shortening (%)	Female	46 ± 1	48 ± 1	32 ± 2 *†	38 ± 2 *†#
	Male	48 ± 2	46 ± 2	34 ± 1 *†	39 ± 2 *†#

3.3.3. Morphology

3.3.3.1. Organ weights

Organ weights at autopsy (at 4.5 months and 8 months) were assessed and are presented in Table 20 and Table 21. At 4.5 months of age, there was a small but statistically significant decrease in tibia length in the caPI3K mice compared with all other groups (Table 20). However, this difference was less than 2%, and as such was not considered to be of biological significance. There were no significant differences in body weights between groups (Table 20). All organ weight measurements are shown as a ratio to tibia length to account for any differences in mouse weight [heart weight to tibia length ratio (HW/TL), atrial weight to tibia length ratio (AW/TL) and lung weight to tibia length ratio (LW/TL)].

At 4.5 months of age, caPI3K mice displayed an increased HW/TL compared with Ntg, while dnPI3K mice had a reduced HW/TL (Table 20), as previously shown (Shioi et al., 2000). Mst1 mice developed dilated cardiomyopathy as previously reported (Yamamoto et al., 2003), which was associated with an increased HW/TL compared with Ntg and dnPI3K mice (Table 20). There was no difference in HW/TL between Mst1, caPI3K-Mst1, and dnPI3K-Mst1 mice, but all were significantly increased compared with Ntg and dnPI3K mice alone (Table 20). dnPI3K mice had significantly smaller AW/TL compared with Ntg mice alone (Table 20). This is likely attributable to the smaller heart phenotype of dnPI3K mice (Shioi *et al.*, 2000). AW/TL was increased in the Mst1 and caPI3K-Mst1 mice compared with Ntg, caPI3K, and dnPI3K mice (Table 20). dnPI3K-Mst1 mice showed an even more pronounced increase in AW/TL compared with all other genotypes (Table 20). There was no difference in LW/TL between Ntg, caPI3K and dnPI3K mice at 4.5 months of age (Table 20). LW/TL was significantly increased in the Mst1 and caPI3K-Mst1 mice compared with Ntg, caPI3K, and dnPI3K mice (Table 20). The increased LW/TL in the Mst1 mice is consistent with previously published data (Yamamoto et al., 2003). dnPI3K-Mst1 mice had a more pronounced increase in LW/TL compared with all other genotypes (Table 20). LW/TL was significantly lower in caPI3K-Mst1 mice compared with dnPI3K-Mst1 mice alone (Table 20).

Table 20. Organ weights of transgenic mice at 4.5 months of age.

HW/TL refers to the heart weight / tibia length ratio; AW/TL refers to atrial weight / tibia length ratio; and LW/TL refers to the lung weight / tibia length ratio.

* $p < 0.05$ compared with Ntg; ‡ $p < 0.05$ compared with caPI3K; ^ $p < 0.05$ compared with dnPI3K; # $p < 0.05$ compared with Mst1; and † $p < 0.05$ compared with caPI3K-Mst1.

	Ntg	caPI3K	dnPI3K	Mst1	caPI3K-Mst1	dnPI3K-Mst1
N	25	19	23	29	16	28
Body weight (g)	34.4 ± 1.6	34.5 ± 1.8	35.0 ± 1.9	33.6 ± 1.5	30.7 ± 1.3	33.3 ± 1.0
Tibia length (mm)	17.3 ± 0.0	17.0 ± 0.1 *	17.2 ± 0.1 ‡	17.4 ± 0.1 ‡	17.2 ± 0.1 ‡	17.3 ± 0.1 ‡
Heart weight (mg)	139.2 ± 4.6	164.2 ± 5.2 *	105.1 ± 3.6 *‡	151.5 ± 3.6 *‡^	150.0 ± 2.7 *‡^	150.4 ± 5.0 *‡^
HW/TL (mg/mm)	8.05 ± 0.27	9.66 ± 0.29 *	6.09 ± 0.19 *‡	8.72 ± 0.19 *‡^	8.71 ± 0.18 *‡^	8.70 ± 0.27 *‡^
Atrial weight (mg)	8.2 ± 0.4	9.1 ± 0.6	5.4 ± 0.3 ‡	14.5 ± 0.5 *‡^	14.5 ± 0.6 *‡^	18.4 ± 2.1 *‡^#†
AW/TL (mg/mm)	0.47 ± 0.03	0.54 ± 0.04	0.32 ± 0.02 ‡	0.83 ± 0.03 *‡^	0.84 ± 0.03 *‡^	1.06 ± 0.11 *‡^#†
Lung weight (mg)	153.2 ± 2.0	162.2 ± 4.1	151.7 ± 2.3	179.7 ± 3.4 *‡^	170.7 ± 4.8 *‡^	201.1 ± 7.6 *‡^#†
LW/TL (mg/mm)	8.86 ± 0.11	9.55 ± 0.22	8.80 ± 0.11	10.36 ± 0.19 *‡^	9.92 ± 0.29 *‡^	11.62 ± 0.42 *‡^#†

Table 21. Organ weights of transgenic mice at 8 months of age.

HW/TL refers to the heart weight / tibia length ratio; AW/TL refers to atrial weight / tibia length ratio; and LW/TL refers to the lung weight / tibia length ratio.

* $p < 0.05$ compared with Ntg; § $p = 0.051$ compared with Ntg; and ‡ $p < 0.05$ compared with caPI3K.

	Ntg	caPI3K	Mst1	caPI3K-Mst1
N	18	14	22	21
Body weight (g)	39.5 ± 2.2	38.1 ± 2.3	39.3 ± 1.8	40.0 ± 2.0
Tibia length (mm)	17.6 ± 0.1	17.4 ± 0.2	17.7 ± 0.1	17.6 ± 0.1
Heart weight (mg)	154.6 ± 5.9	172.3 ± 8.1	167.2 ± 6.4	170.1 ± 5.3
HW/TL (mg/mm)	8.77 ± 0.31	9.87 ± 0.43 *	9.40 ± 0.31	9.67 ± 0.28 §
Atrial weight (mg)	11.0 ± 1.3	8.7 ± 0.8	18.8 ± 1.4 *‡	17.9 ± 1.2 *‡
AW/TL (mg/mm)	0.62 ± 0.07	0.50 ± 0.05	1.05 ± 0.07 *‡	1.01 ± 0.06 *‡
Lung weight (mg)	172.9 ± 4.5	169.7 ± 4.1	211.9 ± 8.1 *‡	204.3 ± 8.8 *‡
LW/TL (mg/mm)	9.82 ± 0.25	9.74 ± 0.23	11.91 ± 0.40 *‡	11.63 ± 0.49 *‡

At 8 months of age HW/TL was significantly increased in caPI3K mice compared with Ntg mice, and tended to increase in caPI3K-Mst1 mice ($p=0.051$; Table 21). There were no differences in morphology between Mst1 and caPI3K-Mst1 mice at 8 months of age.

3.3.3.2. Gender differences in organ weights

Since significant differences in cardiac dimensions and systolic function were observed in the dnPI3K-Mst1 mice (see Section 3.3.2.3.), morphological data from males and females were also analysed separately (Table 22). As found in the functional parameters, the most significant gender differences were identified in the dnPI3K-Mst1 mice. Consistent with female dnPI3K-Mst1 mice having reduced fractional shortening versus male dnPI3K-Mst1 mice (see Figure 31), normalised HW/TL, AW/TL, and LW/TL were all greater in female dnPI3K-Mst1 compared with male dnPI3K-Mst1 mice (Table 22, Figure 32, Figure 33). Collectively, this demonstrates that female dnPI3K-Mst1 mice develop a more severe dilated cardiomyopathy phenotype than males. Interestingly, female Mst1 and caPI3K-Mst1 mice also had greater normalised HW/TL than male counterparts, but this was not associated with significant differences in function (Figure 31), AW/TL or LW/TL (Table 22).

At 8 months of age there were significant increases or trends for an increase in AW/TL and LW/TL in males from each of the 4 groups (Ntg, caPI3K, Mst1, or caPI3K-Mst1; Table 23). Interestingly, differences tended to be less pronounced in the caPI3K and caPI3K-Mst1 groups. However, these gender differences were not associated with significant differences in systolic function (Figure 31).

3.3.3.3. Bulging of eyes associated with severe cardiac dysfunction

A very distinct phenotype of the dnPI3K-Mst1 mice apparent as early as 4 weeks of age was bulging eyes. This phenotype was very prominent at 4.5 months of age (Figure 34). This phenotype was not observed in the other groups of mice at 4.5 months of age. Bulging of eyes was observed in some older Mst1 mice (greater than 6 months of age).

Table 22. Gender-associated differences in organ weights of transgenic mice at 4.5 months of age.

HW/TL refers to the heart weight / tibia length ratio; normalised HW/TL refers to Ntg HW/TL of each gender normalised to 1.0 and each genotype expressed relative to this; AW/TL refers to atrial weight / tibia length ratio; and LW/TL refers to the lung weight / tibia length ratio. ~ $p < 0.05$ compared with female of same genotype; * $p < 0.05$ compared with Ntg of same gender; † $p < 0.05$ compared with caPI3K of same gender; ^ $p < 0.05$ compared with dnPI3K of same gender; # $p < 0.05$ compared with Mst1 of same gender; and † $p < 0.05$ compared with caPI3K-Mst1 of same gender.

	Gender	N	Body weight (g)	Tibia length (mm)	Heart weight (mg)	HW/TL (mg/mm)	Normalised HW/TL (fold change)	Atrial weight (mg)	AW/TL (mg/mm)	Lung weight (mg)	LW/TL (mg/mm)
Ntg	Female	10	25.8±0.5	17.2±0.1	114.0±2.7	6.61±0.17	1.00±0.03	6.4±0.2	0.37±0.02	149.6±1.9	8.68±0.11
	Male	15	40.2±0.9~	17.3±0.1	156.1±2.9~	9.02±0.17~	1.00±0.02	9.3±0.5~	0.54±0.03~	155.6±3.0	8.99±0.17
caPI3K	Female	8	26.1±0.8	16.9±0.1	145.0±4.2*	8.57±0.22*	1.30±0.03*	7.6±0.9	0.45±0.05	156.7±4.2	9.26±0.24
	Male	11	40.6±1.0~	17.0±0.1*	178.2±5.4~*	10.46±0.29~*	1.16±0.03~*	10.2±0.8~	0.60±0.05~	166.2±6.2	9.75±0.34
dnPI3K	Female	10	25.2±0.3	17.0±0.1	88.6±1.2*†	5.21±0.06*†	0.79±0.01*†	4.3±0.2	0.25±0.01	143.1±1.7	8.42±0.12
	Male	13	42.5±1.1~	17.4±0.1†	117.8±3.1~*†	6.76±0.17~*†	0.75±0.02*†	6.4±0.3~*†	0.37±0.02~*†	158.3±2.6~	9.08±0.12~
Mst1	Female	15	26.1±0.4	17.3±0.1†	137.9±3.7*^	7.94±0.17*^	1.20±0.03*^	13.7±0.7*^†	0.79±0.04*^†	179.3±5.3*^†	10.34±0.29*^†
	Male	14	41.5±0.9~	17.4±0.1†	166.1±3.4~*^†	9.56±0.17~*^†	1.06±0.02~†	15.3±0.7*^†	0.88±0.04*^†	180.1±4.3*^†	10.38±0.26*^†
caPI3K-Mst1	Female	9	26.4±0.5	17.5±0.1*^†	145.9±4.0*^	8.33±0.23*^	1.26±0.03*^	14.3±0.9*^†	0.82±0.06*^†	170.4±8.1*^†	9.73±0.45*^†
	Male	7	36.2±0.8~*^†#	16.9±0.2*^#	154.9±2.5~†	9.19±0.14~†	1.02±0.02~†	14.7±0.5*^†	0.88±0.03*^†	171.0±4.5*^†	10.16±0.32*^†
dnPI3K-Mst1	Female	11	27.5±0.5*^#	17.4±0.1†	156.6±10.3*^#	8.98±0.55*^#	1.36±0.08*^#	25.0±4.8*^#†	1.43±0.26*^#†	218.2±8.9*^#†	12.52±0.46*^#†
	Male	17	37.1±0.2~*^#	17.2±0.1†	146.4±4.8*^#	8.52±0.28*^#†	0.94±0.03~†	14.5±0.9~*^†	0.84±0.05~*^†	189.6±10.4~*^†	11.38±0.59~*^†

Table 23. Gender-associated differences in organ weights of transgenic mice at 8 months of age.

HW/TL refers to the heart weight / tibia length ratio; normalised HW/TL refers to Ntg HW/TL of each gender normalised to 1.0 and each genotype expressed relative to this; AW/TL refers to atrial weight / tibia length ratio; and LW/TL refers to the lung weight / tibia length ratio. ~ $p < 0.05$ compared with female of same genotype; § $p = 0.07$ compared with female of the same genotype; * $p < 0.05$ compared with Ntg of same gender; ‡ $p < 0.05$ compared with caPI3K of same gender.

	Gender	N	Body weight (g)	Tibia length (mm)	Heart weight (mg)	HW/TL (mg/mm)	Normalised HW/TL (fold change)	Atrial weight (mg)	AW/TL (mg/mm)	Lung weight (mg)	LW/TL (mg/mm)
Ntg	Female	10	34.1±2.5	17.6±0.2	137.8±5.3	7.80±0.23	1.00±0.03	7.8±1.1	0.44±0.06	161.4±1.7	9.17±0.10
	Male	8	46.4±1.9~	17.6±0.2	175.7±5.7~	9.97±0.28~	1.00±0.03	15.1±1.7~	0.85±0.09~	187.3±7.3~	10.63±0.38~
caPI3K	Female	7	31.4±2.0	17.5±0.2	150.2±8.7	8.57±0.42	1.10±0.05	6.3±0.7	0.36±0.03	160.9±2.1	9.21±0.17
	Male	7	44.9±1.7~	17.4±0.2	194.5±6.6~	11.17±0.27~	1.12±0.03	11.1±0.8~	0.64±0.04~	178.6±7.3~	10.27±0.33~
Mst1	Female	12	32.9±1.0	17.8±0.2	153.7±7.1	8.59±0.31*	1.10±0.04	16.6±1.2*‡	0.92±0.06*‡	202.1±9.5*‡	11.31±0.45*‡
	Male	10	46.9±1.8~	17.7±0.2	183.5±9.1~	10.36±0.42~*	1.04±0.04	21.4±2.6~*‡	1.20±0.13~*‡	223.7±13.2~*‡	12.63±0.65~*‡
caPI3K-Mst1	Female	9	31.2±1.4	17.6±0.1	155.6±7.1	8.86±0.37*	1.14±0.05	16.3±1.8*‡	0.93±0.10*‡	191.0±7.8*‡	10.89±0.44*‡
	Male	12	46.5±1.6~	17.6±0.2	181.0±6.1~	10.28±0.30~*	1.03±0.03	19.0±1.5~*‡	1.08±0.08*‡	214.4±13.9*‡	12.18±0.77§*‡

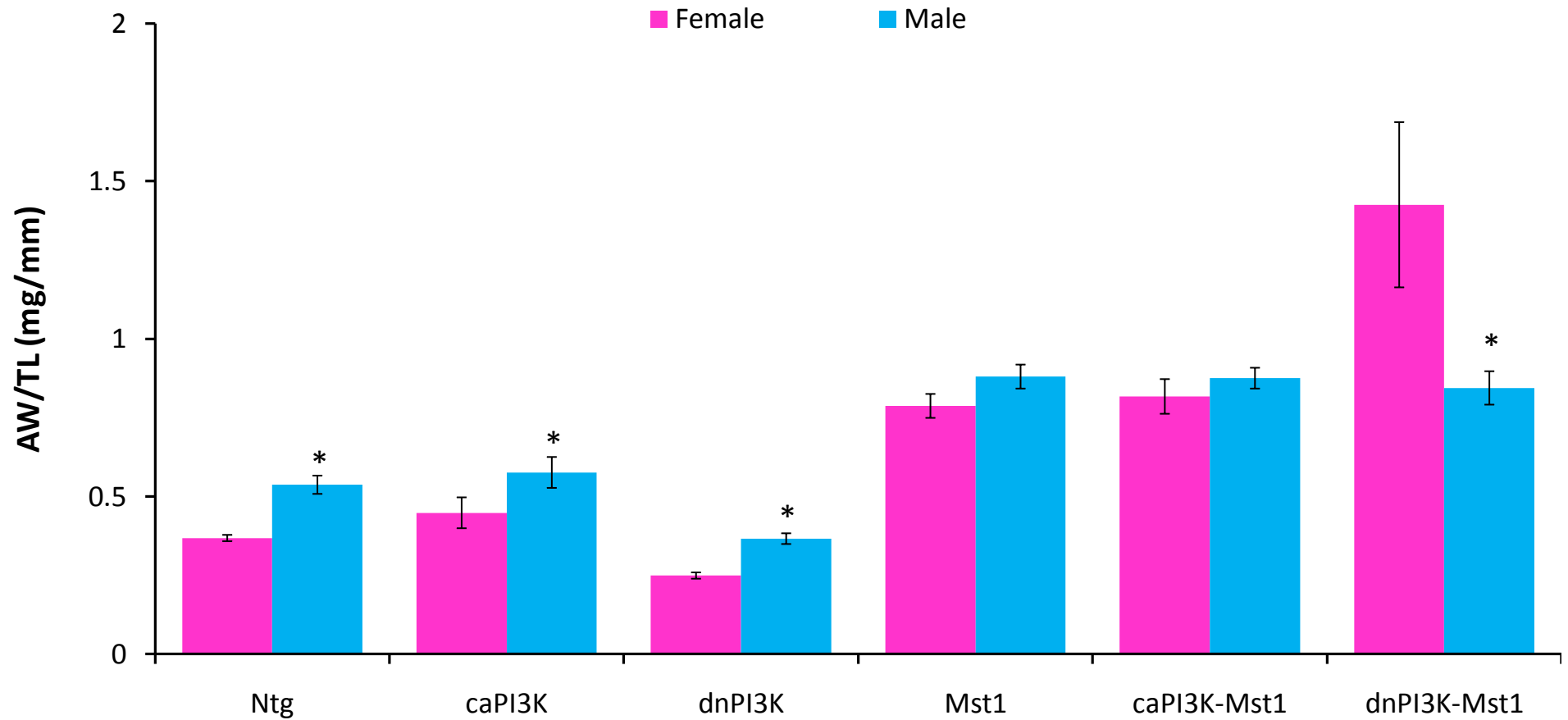


Figure 32. Atrial weight measurements of female and male mice at 4.5 months of age.

* $p < 0.05$ compared with female counterpart; $n = 7-17$ in each group. Only statistics related to gender differences are presented on this graph for simplicity.

Statistics related to differences in genotype are presented in Table 22.

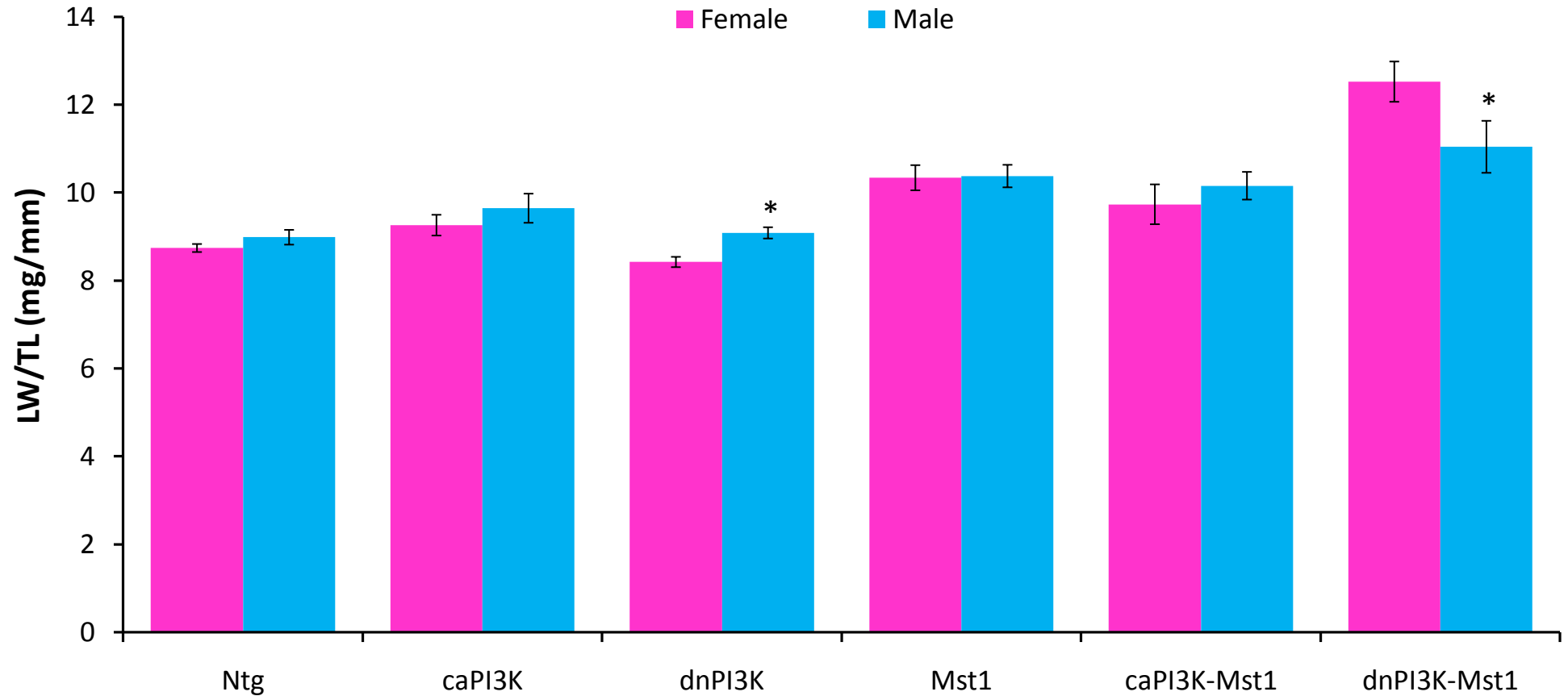


Figure 33. Lung weight measurements of female and male mice at 4.5 months of age.

* $p < 0.05$ compared with female counterpart; $n = 7-17$ in each group. Only statistics related to gender differences are presented on this graph for simplicity. Statistics related to differences in genotype are presented in Table 22.



Figure 34. Bulging of the eyes in a dnPI3K-Mst1 mouse compared with a Ntg mouse.
The dnPI3K-Mst1 mouse (right) develops bulgy eyes (indicated by arrow) compared with the Ntg mouse (left).

The development of bulging eyes is often a sign of thyroid dysfunction (Jayatileke and Rockman, 2005), but as the transgene expression in the mice is cardiac-specific, it is highly unlikely that thyroiditis would develop. In this case the bulging of the eyes is most likely caused by severe increases in venous pressure due to congestive HF (Earnest and Hurst, 1970). An increase in venous pressure would cause an increase in intraocular pressure, which would become visible as bulging of the eyes (Earnest and Hurst, 1970).

3.3.4. Histopathology

3.3.4.1. Measurement of cardiac chamber dilation and fibrosis

Tissue sections from the hearts of transgenic mice were obtained as previously described (see Section 2.10.). Atria from Mst1 mice were dilated compared with Ntg mice, and dnPI3K-Mst1 mice showed an even more pronounced dilation compared with Mst1 (Figure 35). Examination of the ventricular tissue showed dilation of the ventricular chambers of the dnPI3K-Mst1 mice compared with both Ntg and Mst1 mice (Figure 36). This chamber dilation was also associated with marked ventricular wall thinning (Figure 36).

Masson's Trichrome stained tissue sections were quantitated as described (see Section 2.10.). There was no difference in atrial fibrosis between Ntg, caPI3K, and dnPI3K mice (Figure 37). Fibrosis was increased approximately 3-fold in the Mst1 mice compared with Ntg mice alone (Figure 37). caPI3K-Mst1 mice had significantly less fibrosis compared with Mst1 mice, and this was not significantly different from Ntg mice (Figure 37). dnPI3K-Mst1 mice showed more pronounced atrial fibrosis compared with Mst1 mice (2-fold greater than Mst1 mice alone), and this was approximately 6-fold greater than in Ntg mice alone (Figure 37).

Analysis of ventricular fibrosis showed no difference between Ntg, caPI3K and dnPI3K mice (Figure 38). Mst1 mice showed a 2.7-fold increase in fibrosis compared with Ntg mice, which was attenuated in the caPI3K-Mst1 mice (Figure 38). dnPI3K-Mst1 had more pronounced ventricular fibrosis compared with Mst1 mice alone (Figure 38).



Figure 35. Increased atrial dilation and fibrosis in dnPI3K-Mst1 mice.

The dnPI3K-Mst1 mouse (right) had markedly dilated atrial chambers, which were associated with increased fibrosis (stained blue with Masson's Trichrome) compared with Mst1 (middle) and Ntg (left) mice at 4.5 months of age. 1 X magnification.



Figure 36. Ventricular chamber dilation and wall thinning in the dnPI3K-Mst1 mice compared with both Ntg and Mst1 mice at 4.5 months of age.

LV refers to the left ventricle; RV refers to the right ventricle. 1 X magnification.

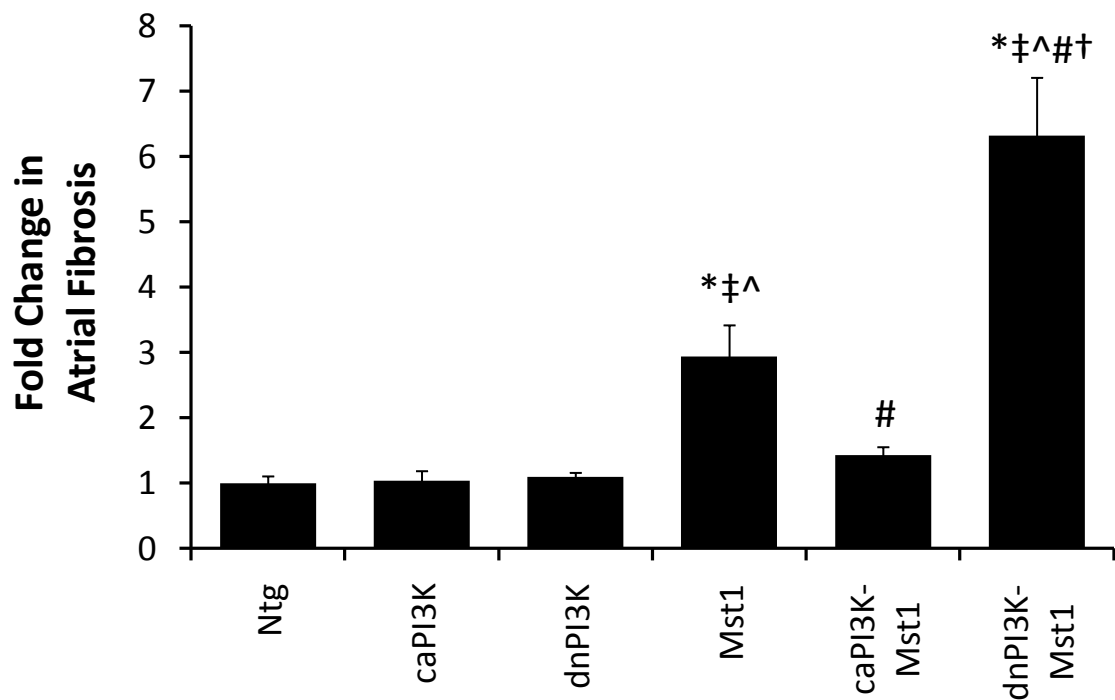


Figure 37. Atrial fibrosis in transgenic mice at 4.5 months of age.

Fold change in total atrial fibrosis in transgenic mice at 4.5 months of age (Ntg normalised to 1; $n=3-5$ in each group). * $p<0.05$ compared with Ntg; ‡ $p<0.05$ compared with caPI3K; ^ $p<0.05$ compared with dnPI3K; # $p<0.05$ compared with Mst1; and † $p<0.05$ compared with caPI3K-Mst1.

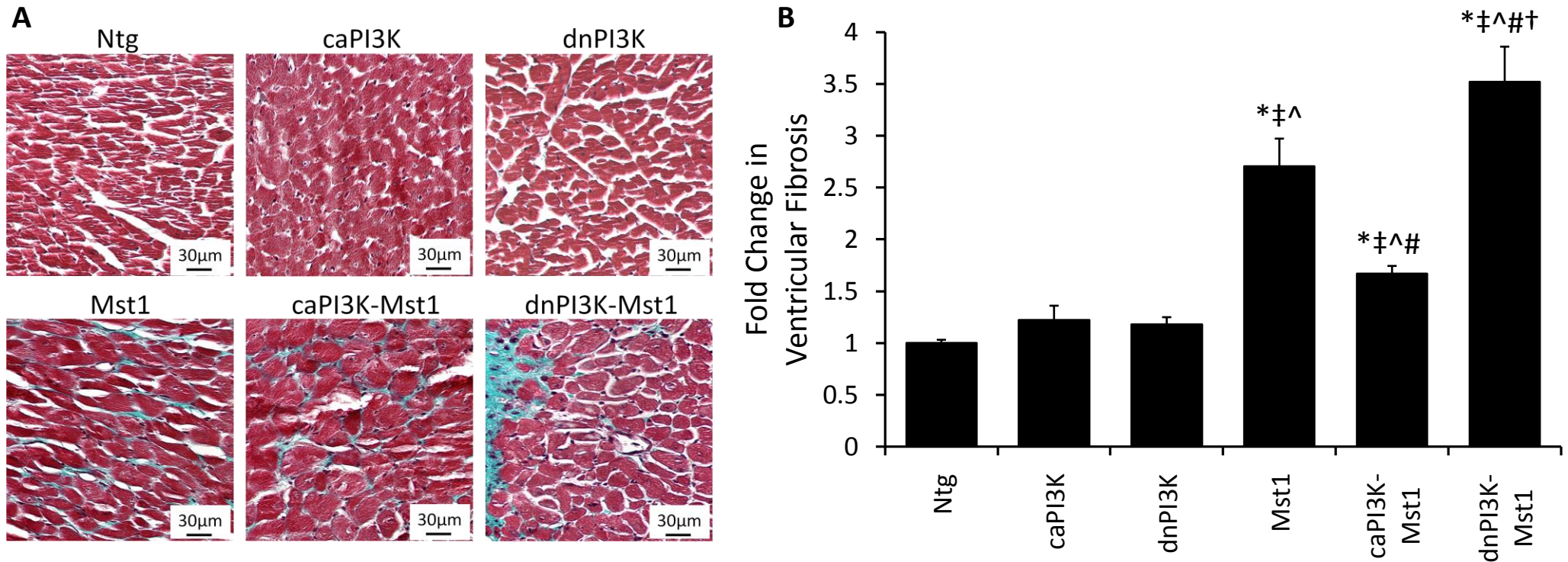


Figure 38. Ventricular fibrosis in transgenic mice at 4.5 months of age.

A: Representative ventricle sections from transgenic mice showing fibrosis (stained in blue using Masson's Trichrome stain, 200 X magnification). **B:** Fold change in ventricular fibrosis in transgenic mice at 4.5 months of age (Ntg normalised to 1; n=3-6 in all groups). * $p < 0.05$ compared with Ntg; ‡ $p < 0.05$ compared with caPI3K; ^ $p < 0.05$ compared with dnPI3K; # $p < 0.05$ compared with Mst1; and † $p < 0.05$ compared with caPI3K-Mst1.

3.3.4.2. Examination of lung congestion in transgenic mice

Lung congestion is a common complication of congestive HF in humans (Gehlbach and Geppert, 2004) and has previously been reported in the Mst1 mice (Yamamoto *et al.*, 2003). As previously shown, Mst1 mice showed an increase in LW/TL compared with Ntg (Table 20), consistent with published data (Yamamoto *et al.*, 2003). As previously noted, dnPI3K-Mst1 mice had a further increase in LW/TL compared with Mst1 mice (Table 20), and this was clearly visible in tissue sections (Figure 39). While LW/TL was not significantly different between caPI3K-Mst1 and Mst1 mice (Table 20) it tended to be reduced, and lung congestion appeared reduced in the caPI3K-Mst1 mice compared with the Mst1 mice alone on histological analysis (Figure 39).

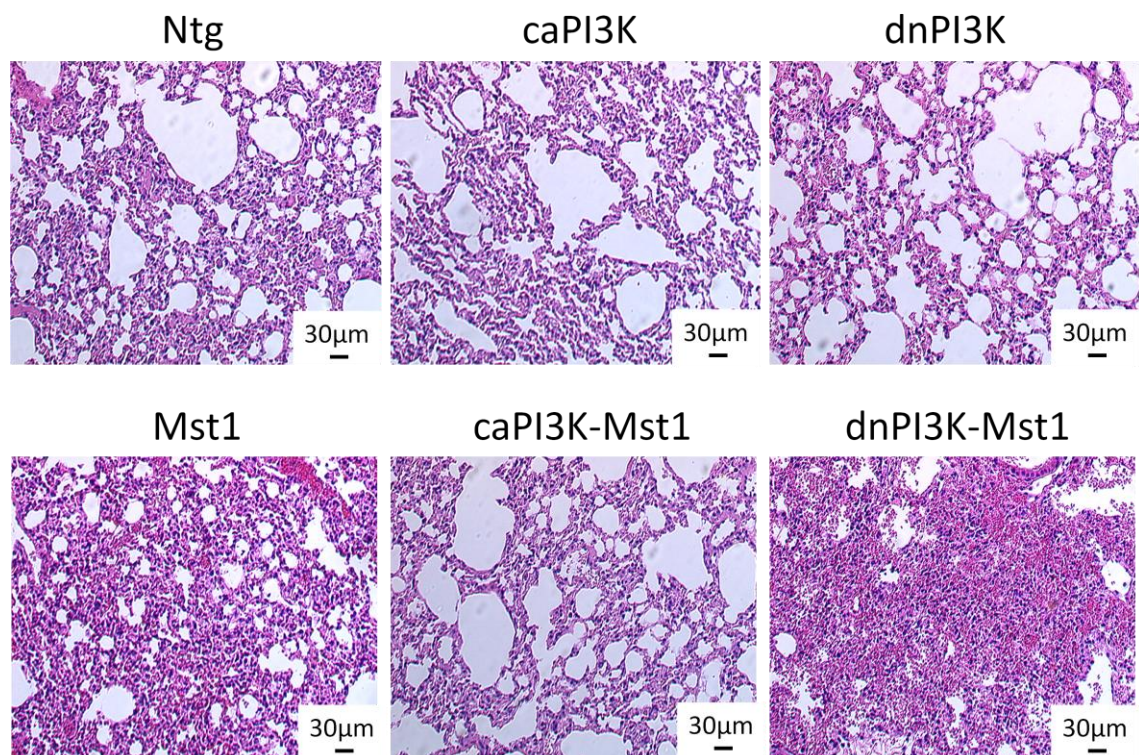


Figure 39. Examination of lung congestion in transgenic mice at 4.5 months of age.

Lung tissue of transgenic mice at 4.5 months of age stained with haematoxylin and eosin (40 X magnification), showing increased lung congestion in Mst1 compared with Ntg, and in the dnPI3K-Mst1 mice compared with all other groups.

3.3.4.3. Measurement of apoptosis in transgenic mice

Increased apoptosis was previously reported in the Mst1 mice (Yamamoto *et al.*, 2003). As such, apoptosis levels were examined in the transgenic mice using TUNEL staining (Figure 40), as previously described (see Section 2.11.). There was no difference in apoptosis levels between Ntg, caPI3K, or dnPI3K mice (Figure 40). Mst1 mice showed an approximate 5-fold increase in apoptosis (Figure 40), as previously described (Yamamoto *et al.*, 2003). caPI3K-Mst1 mice showed a 36% decrease in TUNEL-positive staining compared with Mst1 mice alone (Figure 40). Apoptosis was increased by approximately 48% in the dnPI3K-Mst1 mice compared with the Mst1 mice alone (7.5-fold increased compared with Ntg, Figure 40).

3.3.5. Gene expression in transgenic heart tissue

3.3.5.1. Gene expression in Mst1 mice at 8 months of age

The initial characterisation of the Mst1 mice did not examine embryonic gene expression (Yamamoto *et al.*, 2003). Thus, initially gene expression in ventricular tissue from 8-month old Mst1 mice was examined by Northern blotting as previously described (see Section 2.8.4.). α -skeletal actin, ANP and BNP were elevated in hearts of Mst1 mice compared with Ntg mice (Figure 41), consistent with a heart failure gene signature. SERCA-2a and α -MHC gene expression were decreased in hearts of Mst1 mice (Figure 41).

3.3.5.2. Gene expression in transgenic mice at 4.5 months of age

As previously shown (McMullen *et al.*, 2003), ANP and BNP were elevated in hearts of dnPI3K mice compared with Ntg (Figure 42). Expression of α -skeletal actin, ANP, BNP, and β -MHC were increased in hearts of Mst1 mice compared with Ntg (Figure 42). The caPI3K transgene had no significant effect on gene expression in Mst1 mice (see caPI3K-Mst1, Figure 42). dnPI3K-Mst1 mice had significantly higher ANP expression compared with all genotypes, as well as significant down-regulation of SERCA-2a (Figure 42). Expression of β -MHC, BNP and α -skeletal actin was not significantly different between Mst1, caPI3K-Mst1, and dnPI3K-Mst1 mice (Figure 42).

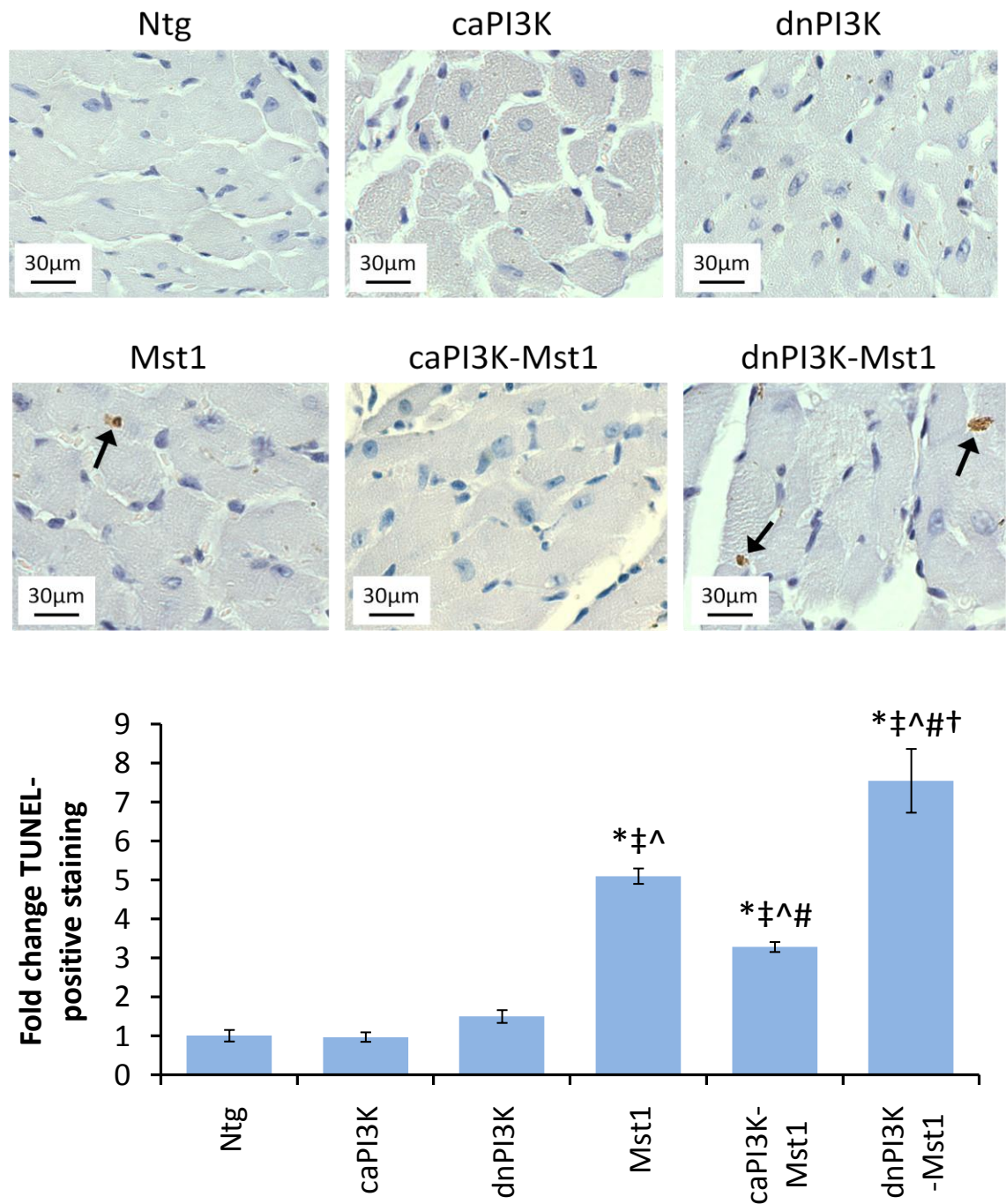


Figure 40. Apoptosis in hearts of transgenic mice measured by TUNEL staining.

A: Representative ventricle sections from transgenic mice showing apoptosis (indicated by arrows, 400 X magnification). **B:** Fold change in terminal deoxynucleotidyl transferase nick end labelling (TUNEL)-positive staining in transgenic mice at 4.5 months of age (Ntg normalised to 1; n=3 in all groups). * $p < 0.05$ compared with Ntg; ‡ $p < 0.05$ compared with caPI3K; ^ $p < 0.05$ compared with dnPI3K; # $p < 0.05$ compared with Mst1; and † $p < 0.05$ compared with caPI3K-Mst1.

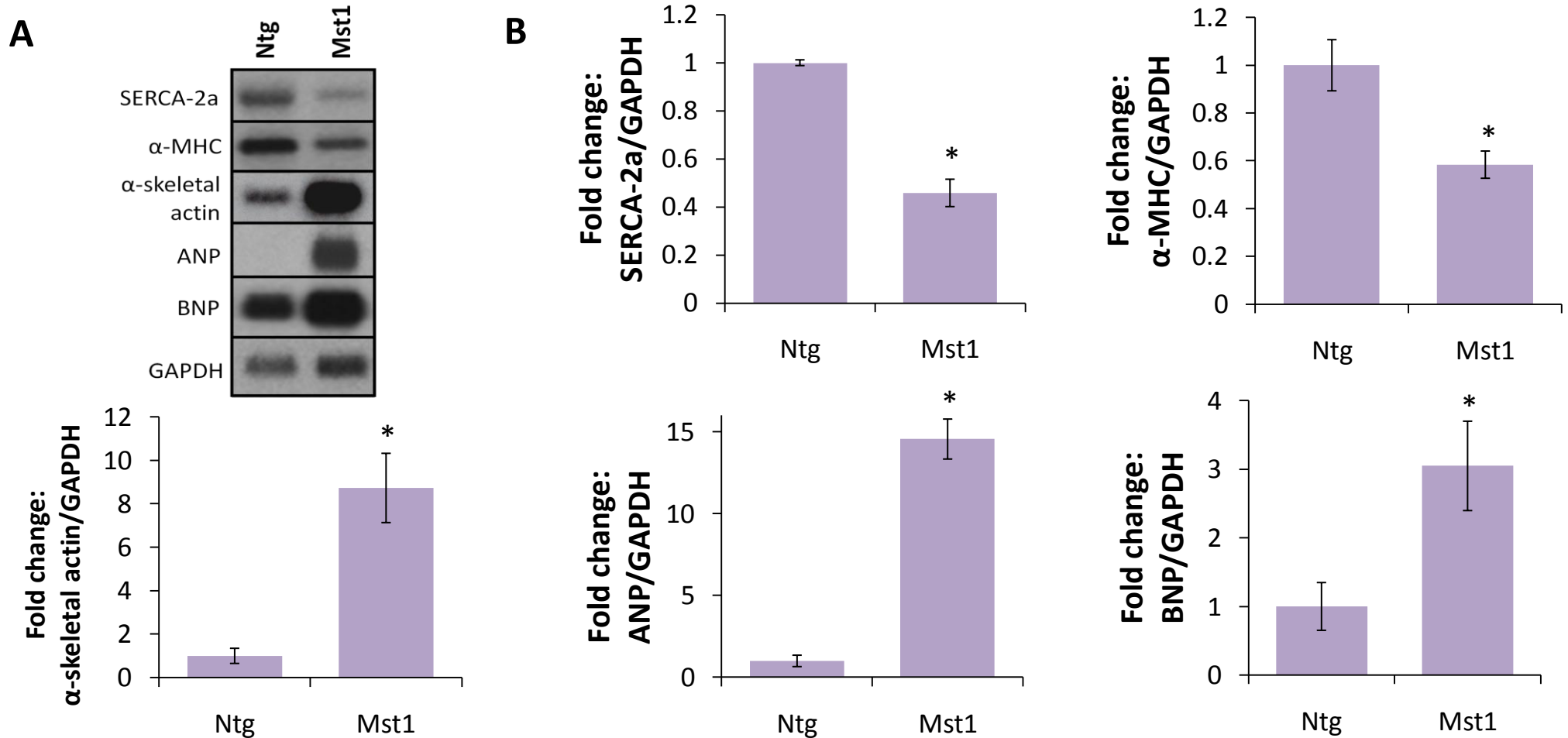


Figure 41. Gene expression of embryonic genes and genes associated with calcium handling in the hearts of Mst1 mice at 8 months of age.

Representative Northern blot images (A) and quantitative analyses (B) of embryonic and calcium handling gene expression in 8-month old Ntg and Mst1 mice, Ntg normalised to 1 ($n=3$ in each group). SERCA-2a: Sarcoplasmic reticulum Ca^{2+} ATPase 2a; MHC: myosin heavy chain; ANP: atrial natriuretic peptide; and BNP: B-type natriuretic peptide. Genes expressed relative to GAPDH. The same Northern blot was stripped and re-probed. * $p < 0.05$ compared with Ntg.

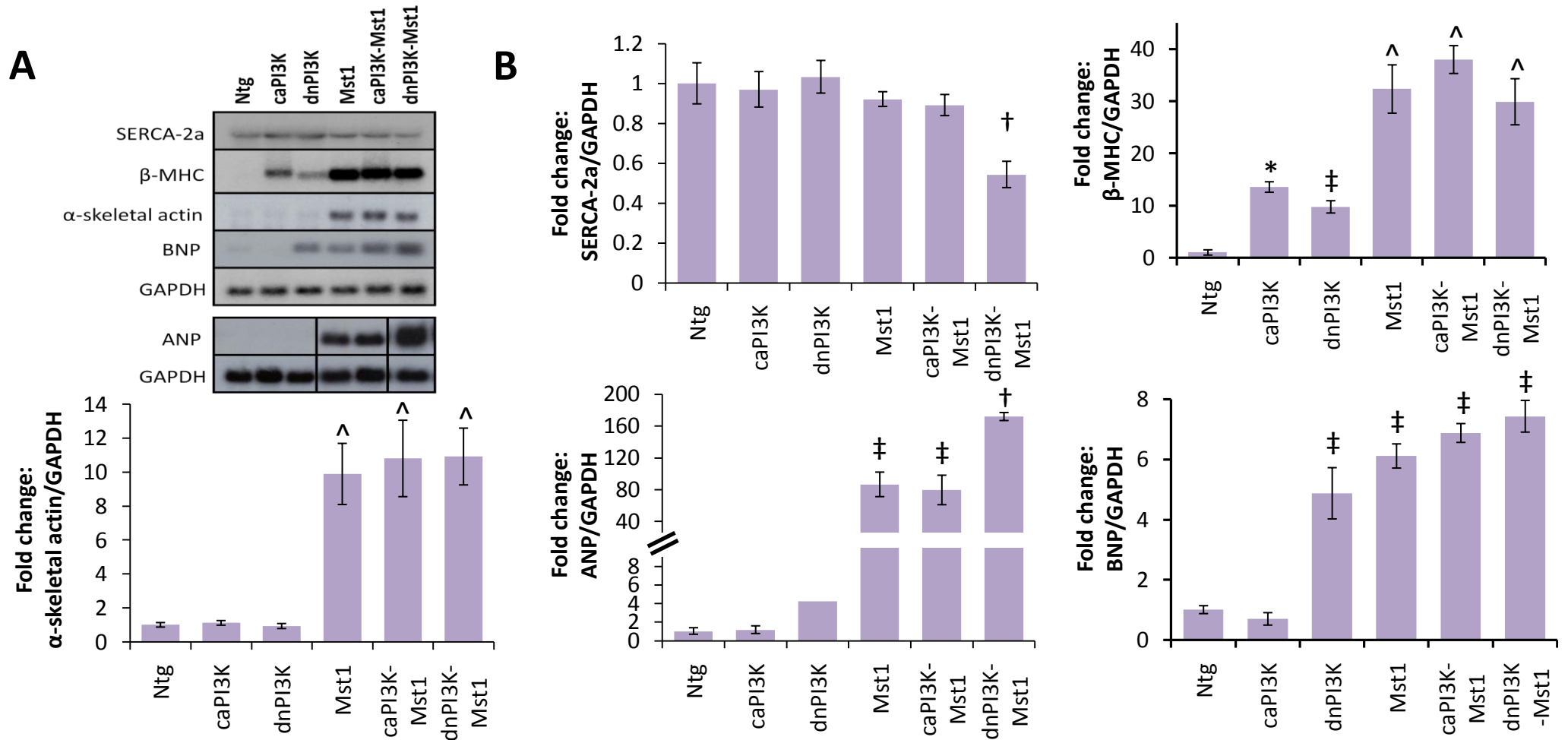


Figure 42. Gene expression of embryonic genes and genes associated with calcium handling in the hearts of transgenic mice at 4.5 months of age. Representative Northern blot images (A) and quantitative analyses (B) of embryonic gene expression in 4.5-month old transgenic mice ($n=5-8$ in each group for SERCA-2a/GAPDH, α -skeletal actin/GAPDH, and BNP/GAPDH; $n=3$ in each group for β -MHC/GAPDH, and $n=3$ for Ntg, caPI3K, Mst1, caPI3K-Mst1, and dnPI3K-Mst1 ANP/GAPDH, $n=2$ for dnPI3K ANP/GAPDH), Ntg normalised to 1. SERCA-2a: Sarcoplasmic reticulum Ca^{2+} ATPase 2a; MHC: myosin heavy chain; ANP: atrial natriuretic peptide; and BNP: B-type natriuretic peptide. The same Northern blot was stripped and re-probed (SERCA-2a, β -MHC, α -skeletal actin, BNP, and GAPDH). A different Northern blot was stripped and re-probed for ANP and GAPDH. * $p<0.05$ compared with Ntg; † $p<0.05$ compared with Ntg and caPI3K; ^ $p<0.05$ compared with Ntg, caPI3K, and dnPI3K; and ‡ $p<0.05$ compared with all genotypes.

3.3.6. Protein expression in transgenic heart tissue

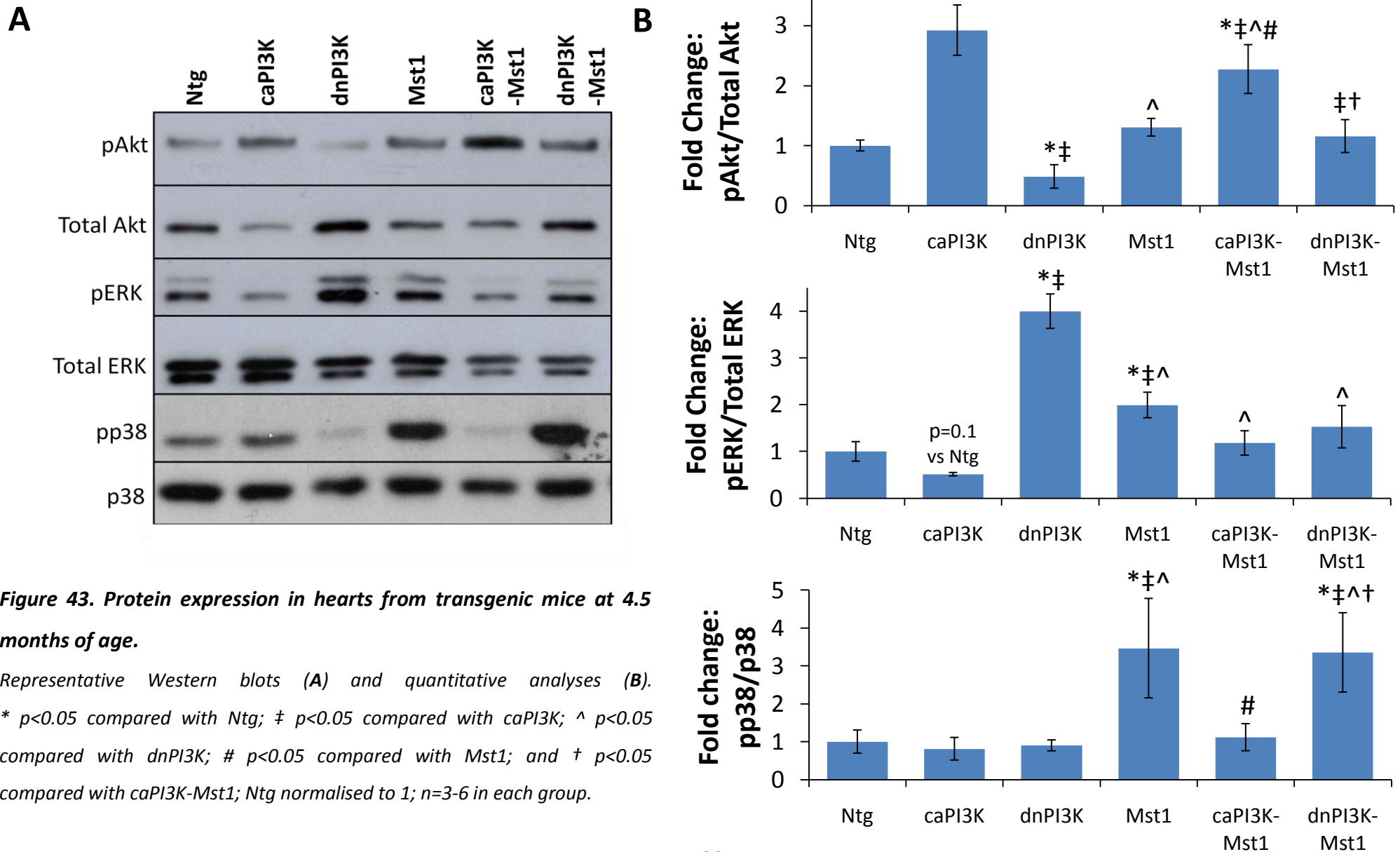
Heart tissue from the transgenic mice were examined for Akt expression [downstream target of PI3K (p110 α)], ERK expression (downstream of GPCR), and p38 expression [downstream of GPCR, and associated with Mst1], as previously described (see Section 2.7.). As previously shown (Shioi *et al.*, 2000), the phosphorylation of Akt (pAkt) relative to total Akt was decreased in hearts of dnPI3K mice and increased in hearts of caPI3K mice compared with Ntg mice alone (Figure 43). Increased pAkt/total Akt was also seen in caPI3K-Mst1 mice, but not in any of the other groups (Figure 43), suggesting that the protective effects of over-expressing PI3K (p110 α) may be mediated, at least in part, via the phosphorylation of Akt.

The phosphorylation of ERK (pERK) relative to total ERK was up-regulated in the hearts of dnPI3K mice compared with Ntg (Figure 43), as previously shown (McMullen *et al.*, 2007). While not significant, there was a trend for decreased pERK/total ERK in the caPI3K mice compared with Ntg mice alone (p=0.1, Figure 43), consistent with previously published data (McMullen *et al.*, 2007). There was increased pERK/total ERK in Mst1 compared with Ntg (Figure 43). However, pERK/total ERK was comparable in both double-transgenics (i.e. caPI3K-Mst1 and dnPI3K-Mst1; Figure 43), suggesting that the protection in the caPI3K-Mst1 mice was not attributable to changes in pERK.

The phosphorylation of p38 (pp38) relative to p38 was not different between Ntg, caPI3K, dnPI3K, and caPI3K-Mst1 (Figure 43). pp38/p38 was increased in hearts of Mst1 and dnPI3K-Mst1 mice (Figure 43).

3.3.7. Akt contributes to the cardioprotective properties of PI3K (p110 α)

To examine whether Akt was responsible for mediating cardiac protection in caPI3K-Mst1 mice compared with Mst1 mice, caPI3K-Mst1 mice were crossed with kdAkt mice as previously described (see Section 2.2.6.). This allowed for the generation and phenotype comparison of caPI3K-Mst1-kdAkt (triple-transgenic) mice with caPI3K-Mst1 and Mst1 mice alone. It was hypothesised that if Akt was critical for mediating protection in caPI3K-Mst1 mice, the triple transgenic mice would have depressed



function in comparison to caPI3K-Mst1 and a cardiac phenotype more similar to the Mst1 mice.

3.3.7.1. Cardiac dimensions and systolic function of triple-transgenic mice

Body weight, tibia length, and heart rate were similar in all groups studied (Table 24). There were no differences in chamber dimensions, wall thicknesses, or fractional shortening between Ntg, and kdAkt mice (Table 24; Figure 44). This is consistent with previously published data (Shioi *et al.*, 2002). Mst1 mice showed increased LVESD and reduced fractional shortening compared with Ntg, caPI3K and kdAkt mice (Table 24; Figure 44). caPI3K-Mst1 mice had smaller LVESD and improved systolic function compared with Mst1 mice (Table 24; Figure 44). The cardiac phenotype of the caPI3K-kdAkt mice was not significantly different from Ntg mice (Table 24). Mst1-kdAkt mice displayed a phenotype not significantly different from Mst1 mice alone (Table 24). Triple-transgenic mice had depressed cardiac function compared with caPI3K-Mst1 but improved function compared with Mst1 mice alone (Table 24; Figure 44). These data suggest that Akt only in part mediates the protective effects of caPI3K in the Mst1 model.

3.3.7.2. Morphology of triple-transgenic mice

From a cohort of 71 transgenic mice, there were only 2 triple-transgenic males (i.e. caPI3K-Mst1-kdAkt). Thus, morphology data has only been presented for female mice. Organ weights at autopsy (4.5 months of age) were assessed and are shown in Table 25. Body weight and tibia length were similar between groups (Table 25). No difference in organ weights were seen between Ntg and kdAkt mice (Table 25), as previously reported (Shioi *et al.*, 2002). HW/TL was significantly increased in caPI3K, Mst1, caPI3K-Mst1, caPI3K-kdAkt, Mst1-kdAkt, and triple-transgenic mice compared with Ntg (Table 25). As previously shown (Shioi *et al.*, 2002), HW/TL tended to be lower ($p=0.14$) in caPI3K-kdAkt mice compared with caPI3K, reflecting the role of the Akt pathway mediating PI3K (p110 α)-induced heart growth. This difference probably didn't reach statistical significance because of the low numbers in the caPI3K group ($n=3$).

Table 24. Left ventricular wall thicknesses and chamber dimensions in triple-transgenic mice at 4.5 months of age.

LVESD: left ventricular end-systolic dimension, LVEDD: left ventricular end-diastolic dimension, LVPW: left ventricular posterior wall thickness, and IVS: interventricular septal width. * $p < 0.05$ compared with Ntg; † $p < 0.05$ compared with caPI3K; # $p < 0.05$ compared with Mst1; † $p < 0.05$ compared with kdAkt; ~ $p < 0.05$ compared with caPI3K-Mst1; ^ $p < 0.05$ compared with caPI3K-kdAkt; and § $p < 0.05$ compared with Mst1-kdAkt.

	N	Body Weight (g)	Tibia Length (mm)	Heart Rate (beats per minute)	LVESD (mm)	LVEDD (mm)	LVPW (mm)	IVS (mm)	Fractional Shortening (%)
Ntg	5	33.5±2.2	17.1 ± 0.1	441 ± 17	1.95 ± 0.11	3.98 ± 0.23	1.12 ± 0.20	1.19 ± 0.10	52 ± 0
caPI3K	5	29.1±2.7	16.6 ± 0.1	451 ± 18	1.84 ± 0.12	4.11 ± 0.25	1.32 ± 0.13	1.30 ± 0.06	55 ± 0
Mst1	9	30.3±1.7	16.8 ± 0.2	389 ± 19	3.28 ± 0.29 *†	4.80 ± 0.27	1.02 ± 0.08	1.05 ± 0.16	33 ± 2 *†
kdAkt	3	26.5±1.7	16.9 ± 0.2	425 ± 4	2.09 ± 0.05 #	4.33 ± 0.12	0.96 ± 0.03	0.92 ± 0.03	52 ± 0 #
caPI3K-Mst1	4	26.5±2.4	16.5 ± 0.3	398 ± 9	2.31 ± 0.16 #	4.29 ± 0.23	1.21 ± 0.21	0.86 ± 0.23	46 ± 2 †#
caPI3K-kdAkt	6	28.6±2.3	16.9 ± 0.2	420 ± 20	2.00 ± 0.17 #	3.92 ± 0.23	1.08 ± 0.14	1.29 ± 0.08	49 ± 1 †#
Mst1-kdAkt	8	26.0±2.5	16.5 ± 0.1	389 ± 17	3.14 ± 0.15 *†~^	4.41 ± 0.24	1.28 ± 0.09	1.00 ± 0.07	29 ± 1 *†~^
caPI3K-Mst1-kdAkt	6	26.1±1.1	16.7 ± 0.1	375 ± 19	2.67 ± 0.40 †	4.29 ± 0.46	1.29 ± 0.16	0.97 ± 0.09	39 ± 2 *†#~^§

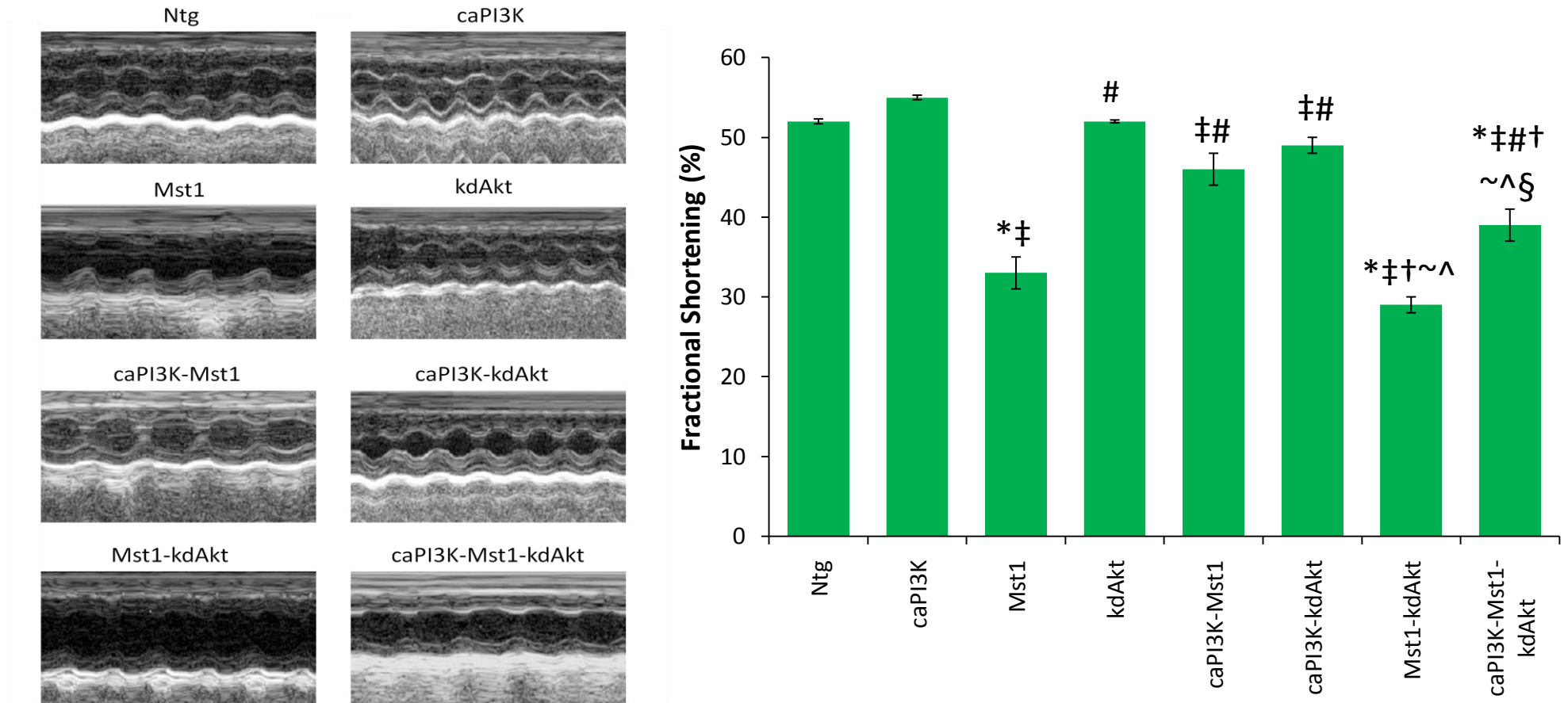


Figure 44. Fractional shortening in triple transgenic mice at 4.5 months of age.

Left panel: Representative M-mode echocardiography images from transgenic mice. **Right panel:** Quantitative analysis of fractional shortening. * $p < 0.05$ compared with Ntg; † $p < 0.05$ compared with caPI3K; # $p < 0.05$ compared with Mst1; ‡ $p < 0.05$ compared with kdAkt; ~ $p < 0.05$ compared with caPI3K-Mst1; ^ $p < 0.05$ compared with caPI3K-kdAkt; and § $p < 0.05$ compared with Mst1-kdAkt.

Table 25. Organ weights of female triple-transgenic mice at 4.5 months of age.

HW/TL refers to the heart weight / tibia length ratio; AW/TL refers to atrial weight / tibia length ratio; and LW/TL refers to the lung weight / tibia length ratio.

* $p < 0.05$ compared with Ntg; ‡ $p < 0.05$ compared with caPI3K; # $p < 0.05$ compared with Mst1; † $p < 0.05$ compared with kdAkt; ~ $p < 0.05$ compared with caPI3K-Mst1; and

^ $p < 0.05$ compared with caPI3K-kdAkt.

	Ntg	caPI3K	Mst1	kdAkt	caPI3K-Mst1	caPI3K-kdAkt	Mst1-kdAkt	caPI3K-Mst1-kdAkt
N	3	3	7	4	6	5	6	8
Body weight (g)	23.0±1.1	26.6±2.0	26.8±1.4	23.2±1.4	25.7±1.0	26.4±1.2	25.9±0.7	24.6±1.0
Tibia length (mm)	16.7±0.1	16.8±0.1	16.8±0.1	16.4±0.3	16.6±0.2	16.9±0.2	16.7±0.1	16.7±0.1
Heart weight (mg)	98.3±3.1	145.6±17.4*	127.5±6.6*	92.7±4.9‡#	129.3±2.8*†	130.3±7.0*†	124.0±4.0*†	125.9±7.2*†
HW/TL (mg/mm)	5.89±0.15	8.64±0.98*	7.57±0.34*	5.65±0.23‡#	7.80±0.15*†	7.70±0.38*†	7.41±0.22*††	7.54±0.38*†
Atrial weight (mg)	5.5±0.6	6.4±0.8	15.0±1.9*‡	5.8±0.5#	14.5±1.0*††	6.7±0.3#~	14.8±0.9*††^	14.6±1.4*††^
AW/TL (mg/mm)	0.33±0.03	0.38±0.04	0.89±0.10*‡	0.35±0.03#	0.88±0.07*††	0.40±0.01#~	0.88±0.06*††^	0.87±0.08*††^
Lung weight (mg)	134.7±3.7	143.5±3.3	192.8±13.8*‡	129.2±8.8#	185.1±9.4*††	137.3±7.1#~	165.9±7.0*††^	170.7±8.8*††^
LW/TL (mg/mm)	8.08±0.16	8.52±0.16	11.45±0.75*‡	7.88±0.44#	11.17±0.59*††	8.13±0.45#~	9.91±0.44#†^	10.23±0.47*^

Despite significant differences in fractional shortening (Table 24), there were no differences in HW/TL between caPI3K-Mst1, Mst1 and triple-transgenic mice (Table 25).

3.4. Discussion

3.4.1. Summary of major findings

The studies described in this chapter were designed to examine whether PI3K (p110 α) is protective in a mouse model of dilated cardiomyopathy and to determine the molecular mechanisms responsible for any protective properties. Increased PI3K (p110 α) activity in a setting of dilated cardiomyopathy improved survival and cardiac function, while decreased PI3K (p110 α) induced a more severe HF phenotype associated with a significantly reduced lifespan, depressed cardiac function, increased cardiac fibrosis and apoptosis. Protein expression analyses suggested that PI3K (p110 α) may exert its beneficial effects via its downstream kinase Akt. Using kdAkt transgenic mice it was demonstrated that Akt, in part, explains the protection mediated via PI3K (p110 α).

The increased fibrosis, apoptosis, cardiac dysfunction, and mortality associated with decreased PI3K (p110 α) activity in a setting of disease suggested a potential impairment of cardiac conduction in dnPI3K-Mst1 mice. This was further examined in Chapter 4 of this thesis (see pages 151-183). Another interesting finding from these studies was that female mice with reduced PI3K (p110 α) activity in a setting of HF developed a more severe disease phenotype compared with their male counterparts, with reduced lifespan and cardiac function, as well as increased atrial size and lung congestion. This was further examined in Chapter 5 of this thesis (see pages 184-205).

3.4.2. Impact of manipulating PI3K (p110 α) in the stressed heart: PI3K (p110 α) is critical for cardiac function and survival, and protects the heart against heart failure

As previously reported, Mst1 mice displayed depressed cardiac function compared with Ntg mice (Yamamoto *et al.*, 2003). There was no difference in cardiac function

between Ntg, caPI3K and dnPI3K mice. Increasing PI3K activity in the Mst1 mice (caPI3K-Mst1) significantly improved cardiac function and improved lifespan (increased by 70%) compared with Mst1 mice alone. Decreasing PI3K activity in the Mst1 mice (dnPI3K-Mst1) was associated with deterioration in cardiac function and significantly reduced lifespan (reduced by 43%) compared with Mst1 mice. Ventricular wall thicknesses were decreased in the dnPI3K-Mst1 mice compared with Ntg and Mst1, and there was significant dilation of the ventricular chambers. The caPI3K-Mst1 mice showed less chamber dilation and ventricular wall thinning compared with Mst1 mice.

As described in the general introduction of this thesis, PI3K (p110 α) is an important regulator of heart size in mice. HW/TL data showed that dnPI3K mice had smaller hearts compared with Ntg mice, while the caPI3K mice had enlarged hearts, similar to previous reports (McMullen *et al.*, 2003; Shioi *et al.*, 2000). Morphological examination at 4.5 months of age showed increased HW/LT, AW/TL, and LW/TL in the Mst1 mice compared with Ntg mice. The dnPI3K mutant was unable to blunt the cardiac hypertrophic response induced by expression of Mst1, consistent with the idea that the dnPI3K mutant can inhibit physiological but not pathological heart growth (McMullen *et al.*, 2003). caPI3K-Mst1 mice showed similar HW/TL compared with Mst1 mice, but this could be attributed to physiological cardiac hypertrophy, as caPI3K-Mst1 mice did not have reduced cardiac function.

Increases in atrial weight and lung weight were more dramatic in the dnPI3K-Mst1 mice compared with Mst1 mice. Atria commonly enlarge when the heart has depressed function (Kumar *et al.*, 2005), supporting the hypothesis that dnPI3K-Mst1 mice have more depressed function than the Mst1 mice alone. Lung congestion is characteristic of the Mst1 phenotype (Yamamoto *et al.*, 2003) and is a common complication of congestive HF in humans (Gehlbach and Geppert, 2004). dnPI3K-Mst1 mice had increased LW/TL as well as lung congestion under histological examination. On histological assessment, lung congestion appeared reduced in caPI3K-Mst1, most likely through the improvement of contractile function.

Histological analysis of the atria and ventricles from the transgenic mice showed increased fibrosis in the Mst1 mice compared with Ntg mice, and decreased fibrosis in the caPI3K-Mst1 mice compared with Mst1 mice (reduced by 51% and 38%, respectively). This suggests that the increased cardiac expression of PI3K (p110 α) in the

caPI3K-Mst1 mice had a protective effect in part by inhibition of atrial and ventricular fibrosis. There was significantly more fibrosis in the atria and ventricles of the dnPI3K-Mst1 mice compared with Mst1 mice (increased by 115% and 30%, respectively). Examination of apoptosis showed increased apoptosis in the ventricles of Mst1 mice, as previously described (Yamamoto *et al.*, 2003). caPI3K-Mst1 mice had significantly less apoptosis compared with Mst1 mice alone (reduced by 36%), while dnPI3K-Mst1 mice had greater apoptosis (increased by 48%). Taken together these results show that PI3K (p110 α) can partly inhibit the pathological consequences of HF.

Collectively these results suggest that PI3K (p110 α) is protective in a setting of dilated cardiomyopathy. PI3K (p110 α) has previously been shown to play a critical role in the maintenance of cardiac function in a pressure overload model (McMullen *et al.*, 2003), a transgenic dilated cardiomyopathy model (McMullen *et al.*, 2007), and after myocardial infarction (Lin *et al.*, 2010). These studies also suggest that expression of PI3K (p110 α) improves cardiac function through physiological hypertrophy, while also inhibiting the pathological consequences of HF such as chamber dilation and wall thinning. The dilated cardiomyopathy model used in the studies described in this chapter has advantages over the model previously used by McMullen and colleagues (McMullen *et al.*, 2007), because it has a significantly longer lifespan (approximately 4.5 months compared with approximately 40 days). This allowed for the examination of the molecular mechanisms responsible for the protective actions of PI3K (p110 α) in a setting of dilated cardiomyopathy. Additionally, it also allowed for a comprehensive examination of the actions of PI3K (p110 α) on cardiac function (echocardiography and catheter studies), and cardiac pathology (fibrosis and apoptosis) in a setting of dilated cardiomyopathy, which was not previously possible.

3.4.3. Molecular mechanisms responsible for the cardioprotective properties induced by caPI3K

Akt, a down-stream target of PI3K, is important for cell growth and survival (Burgering and Coffey, 1995; Cantley, 2002; Datta *et al.*, 1997; Klippel *et al.*, 1997). Results from protein expression analysis by western blotting showed that the phosphorylation of Akt was up-regulated in hearts of caPI3K mice and tended to decrease in dnPI3K, as

previously described (McMullen *et al.*, 2003). caPI3K-Mst1 mice also showed an up-regulation of the phosphorylation of Akt, suggesting that Akt may be the downstream effector of PI3K (p110 α) through which its protective effects are mediated. To assess the role of Akt in the caPI3K-Mst1 model, kdAkt mice were crossed with caPI3K-Mst1 mice. Triple-transgenic mice (caPI3K-Mst1-kdAkt) had worse cardiac function compared with caPI3K-Mst1 mice, but cardiac function was improved compared with Mst1 mice alone. Morphological examination showed no difference in HW/TL, AW/TL, or LW/TL between the Mst1 and triple-transgenic mice. Taken together, these results show that PI3K (p110 α) improves cardiac function in part via its downstream effector Akt. The studies with the kdAkt transgenic mice highlight that future studies should address the question of what Akt-independent mechanisms are also important in mediating PI3K (p110 α)-induced cardiac protection. Pilot studies from our laboratory suggest that a potential negative feedback mechanism increases expression of IGF-1R in a setting of low Akt expression (i.e. kdAkt mice). Further elucidation of this negative feedback mechanism would be of interest.

In this chapter it was also demonstrated that decreased PI3K (p110 α) activity in the Mst1 mice induced greater apoptosis compared with Mst1 mice alone, while increased PI3K (p110 α) activity in the Mst1 mice reduced apoptosis levels. It would be interesting to examine the molecular mechanism responsible for this differential regulation of apoptosis. After my project had commenced, it was shown that there is a link between the PI3K (p110 α) and Mst1 signalling pathways that can influence signalling through the transcription factor Forkhead Box O (FoxO) in HEK293 cells (Jang *et al.*, 2007). In previous studies, FoxO was shown to mediate cell death by regulating apoptotic genes (Brunet *et al.*, 1999; Jang *et al.*, 2007; Kops and Burgering, 1999; Van Der Heide *et al.*, 2004), and it was known that Mst1 can directly phosphorylate FoxO (Lehtinen *et al.*, 2006). PI3K (p110 α) and Mst1 signalling pathways had not previously been shown to interact with each other. It has subsequently been shown that Akt can directly phosphorylate Mst1, which blocks the nuclear translocation and subsequent apoptotic action of FoxO3 (Jang *et al.*, 2007), providing a potential molecular mechanism responsible for the reduced apoptosis seen in the caPI3K-Mst1 mice. Additionally, Lehtinen and colleagues showed that Mst1 directly phosphorylates FoxO proteins, promoting nuclear translocation and subsequent

apoptosis in neurons (Lehtinen *et al.*, 2006). From these studies it seems possible that the dnPI3K-Mst1 mice may have aberrant FoxO signalling in the heart which may be partly responsible for the increased apoptosis observed in these mice hearts, as decreased PI3K (p110 α) activity would lead to decreased Mst1 phosphorylation and consequently increased FoxO activity. Future studies will need to focus on whether this interesting interaction between PI3K (p110 α), Mst1 and FoxO (summarised in Figure 45) is responsible for the anti-apoptotic actions of PI3K (p110 α) in the stressed heart.

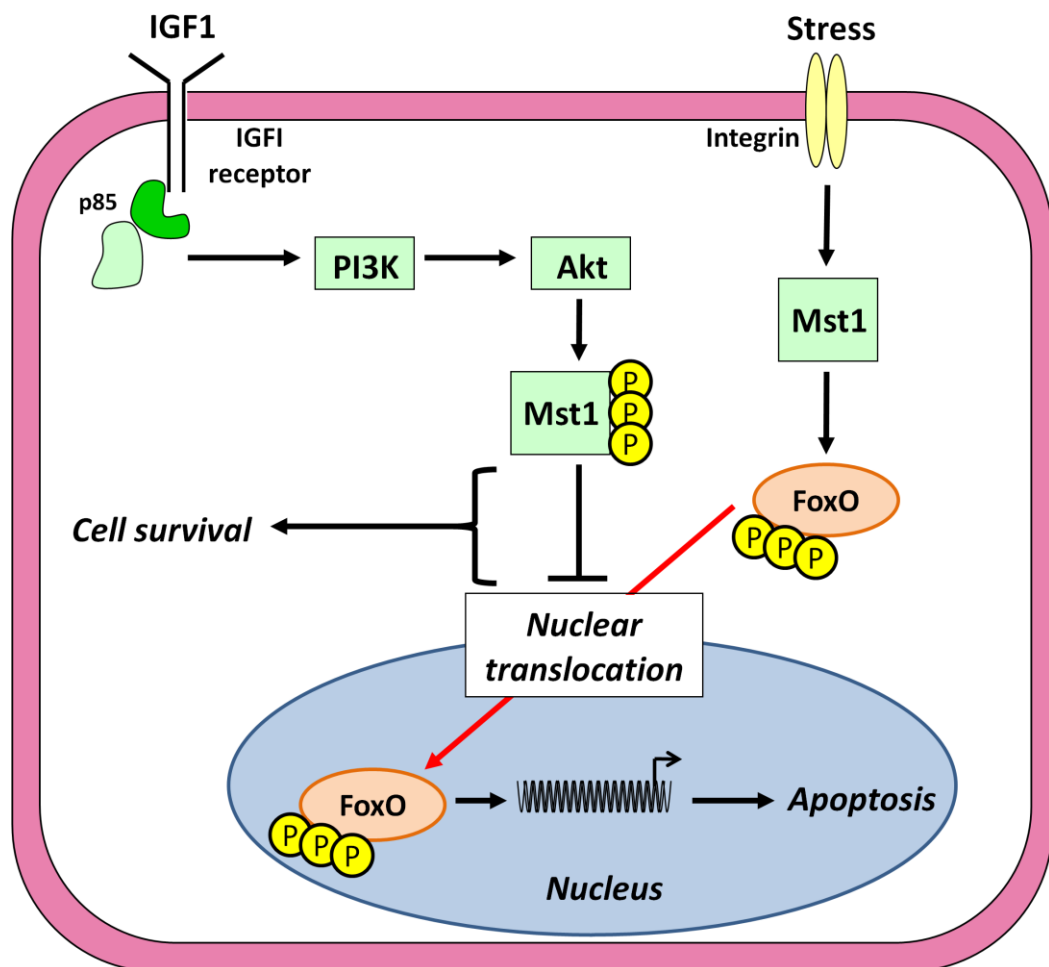


Figure 45. Proposed molecular mechanism responsible for the anti-apoptotic action of PI3K (p110 α) in the Mst1 mice.

Mammalian sterile 20-like kinase 1 (Mst1) can induce apoptosis through phosphorylation of forkhead box O (FoxO). The phosphorylation of FoxO by Mst1 leads to nuclear translocation of the transcription factor, promoting apoptosis (Daitoku and Fukamizu, 2007; Lehtinen *et al.*, 2006). Signalling through the insulin-like growth factor 1 (IGF1) receptor-phosphoinositide 3-kinase p110 α (PI3K)-Akt signalling pathway directly phosphorylates Mst1, leading to inhibition of the nuclear translocation machinery, thereby reducing apoptosis (Jang *et al.*, 2007).

3.4.4. Decreased PI3K (p110 α) activity in a setting of cardiac stress induces more severe disease in females

Gender differences were apparent in cardiac structure and function in the transgenic mice, with the most distinct gender differences observed in the dnPI3K-Mst1 mice. Female dnPI3K-Mst1 mice had a shorter lifespan, increased chamber dilation, and reduced systolic function compared with their male counterparts. Morphological studies also showed increased AW/TL and LW/TL in the female dnPI3K-Mst1 mice compared with their male counterparts. This suggests that PI3K (p110 α) signalling may be particularly important for cardioprotection in females. This interesting finding was further examined in Chapter 5 of this thesis (see pages 184-205). Interestingly, female Mst1 and caPI3K-Mst1 mice also had greater normalised HW/TL than their male counterparts, but this was not associated with significant differences in function, AW/TL or LW/TL.

3.4.5. Future directions

In addition to the future studies discussed in Section 3.4.3., it would also be of interest to investigate the effect of increasing PI3K (p110 α) activity in setting of established cardiac disease. The studies described in this chapter represent a scenario in which PI3K (p110 α) activity is increased from just after birth due to transgene expression using the α -MHC promoter {Gulick, 1991 #7779}. It would therefore be of interest to examine whether increasing PI3K (p110 α) activity can reverse cardiac pathology once cardiac disease is already manifested. Another PhD student in our laboratory is addressing this question utilising an adeno-associated viral approach. The PI3K (p110 α) transgene has been inserted into recombinant adeno-associated virus pseudotype 6. It has previously been shown that systemic delivery of adeno-associated virus 6 transduces gene expression in striated muscle (cardiac and skeletal muscle) (Gregorevic *et al.*, 2004). Using this system, it is hypothesised that it would be possible to deliver the PI3K (p110 α) transgene specifically to the heart, and that this would improve the phenotype of the Mst1 mice following established disease.

3.5. Conclusion

The studies described in this chapter show that elevated PI3K (p110 α) is beneficial in a setting of HF. Expression of caPI3K in a setting of dilated cardiomyopathy increased lifespan and cardiac function, and significantly decreased lung congestion, fibrosis and apoptosis. It was also shown that PI3K (p110 α) is critical for the maintenance of cardiac function in a setting of HF. Inhibition of PI3K (p110 α) in a setting of dilated cardiomyopathy significantly reduced lifespan and cardiac function, and increased lung congestion, fibrosis and apoptosis. Protein analyses and genetic mouse studies suggest that PI3K (p110 α) exerts its beneficial effects in part through the phosphorylation of Akt. A summary of the novel findings from this chapter are presented in Figure 46.

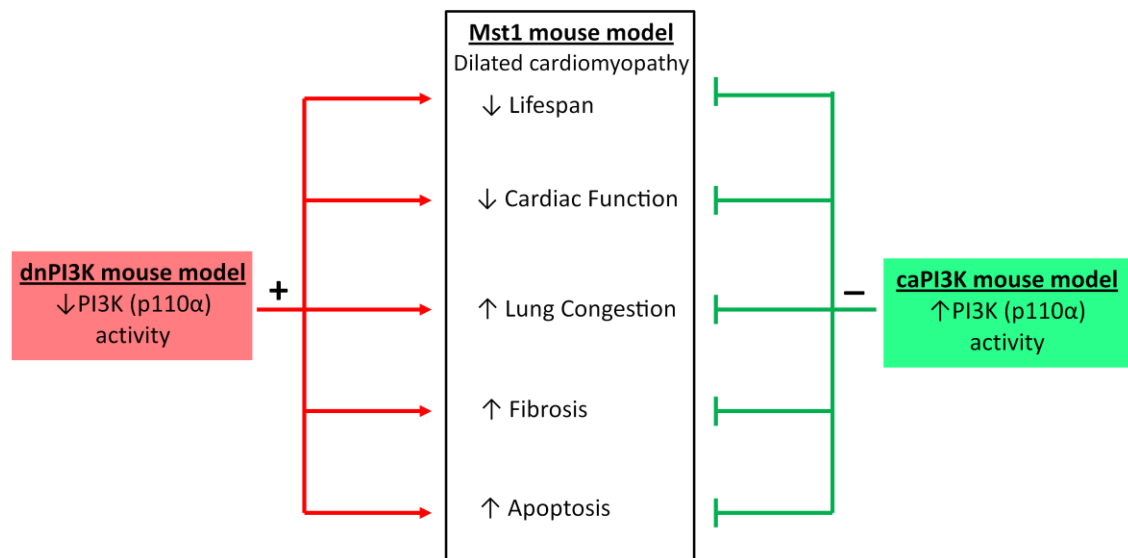


Figure 46. Role of PI3K (p110 α) in a setting of dilated cardiomyopathy.

Mice over-expressing mammalian sterile 20-like kinase 1 [Mst1, (Yamamoto et al., 2003)] develop dilated cardiomyopathy with reduced lifespan and cardiac function, as well as increased lung congestion, fibrosis, and apoptosis. Increasing PI3K (p110 α) activity in the Mst1 mice [using the constitutive active PI3K (p110 α) (caPI3K) transgenic mice (Shioi et al., 2000)] improves lifespan and cardiac function, and reduces lung congestion, fibrosis, and apoptosis. In contrast, reducing PI3K (p110 α) activity in the Mst1 mice [using the dominant negative PI3K (p110 α) (dnPI3K) transgenic mice (Shioi et al., 2000)] further reduces lifespan and cardiac function, and increases lung congestion, fibrosis, and apoptosis.

Findings from the following chapter were published in Pretorius, L., Du, X.J., Woodcock, E.A., Kiriazis, H., Lin, R.C., Marasco, S., Medcalf, R.L., Ming, Z., Head, G.A., Tan, J.W., Cemerlang, N., Sadoshima, J., Shioi, T., Izumo, S., Lukoshkova, E.V., Dart, A.M., Jennings, G.L., and McMullen, J.R. (2009). Reduced phosphoinositide 3-kinase (p110alpha) activation increases the susceptibility to atrial fibrillation. *American Journal of Pathology* 175, 998-1009.

<https://doi.org/10.2353/ajpath.2009.090126>

Used with permission.

Chapter 4 – Reduced PI3K (p110 α) activity increases the heart's susceptibility to atrial fibrillation

4.1. Introduction

This chapter examines a potential link between AF and PI3K (p110 α) activity. Previous data from my laboratory and the literature have suggested that such a link may exist. First, reduced PI3K activation (in the dnPI3K mice) alters gene expression of ion channels in ventricular tissue (McMullen *et al.*, 2004). Second, adrenergic stimulation and cardiotoxicity induced by several classes of drugs induce AF in patients (van der Hooft *et al.*, 2004), and PI3K (p110 α) has been shown to inhibit pathological signalling cascades downstream of GPCR (McMullen *et al.*, 2007). Thus, reduced PI3K (p110 α) would be expected to increase the likelihood of cardiotoxicity and activation of signalling downstream of GPCR. Third, it has been shown that increased PI3K (p110 α) activation induces increased expression of Hsp70, while decreased PI3K (p110 α) activation reduces expression of Hsp70 (McMullen *et al.*, 2004). Previous studies have shown that patients with high expression levels of Hsp70 have a lower incidence of postoperative AF, while an M439T substitution in Hsp70 increased the risk of postoperative AF (Afzal *et al.*, 2008; Kampinga *et al.*, 2007; Mandal *et al.*, 2005; St Rammos *et al.*, 2002). Finally, age, obesity and diabetes are risk factors for the development of AF (Benjamin *et al.*, 1994; Lip and Varughese, 2005; Wang *et al.*, 2004). These factors are typically associated with reduced physical activity and insulin resistance. PI3K (p110 α) is activated in response to exercise as a critical molecular signal for insulin, and PI3K (p110 α) activation is reduced in the hearts of obese, diabetic and aged patients (Goodyear *et al.*, 1995; Kajantie *et al.*, 2003; Kim *et al.*, 1999; Rondinone *et al.*, 1997; Sancho *et al.*, 2007; Vasan *et al.*, 2003). It was therefore of interest to examine whether reduced PI3K (p110 α) activity increases the risk for the development of AF.

AF often occurs in combination with HF, and it has been suggested that AF and HF may share common mechanisms and treatment strategies (Heist and Ruskin, 2006). However, the factors that precipitate the onset of AF in patients with pre-existing heart disease remain unclear (Heist and Ruskin, 2006; Nattel, 2002). In this chapter I assessed whether mice with an underlying cardiomyopathy and reduced PI3K

(p110 α) activity developed AF. In Chapter 3 it was shown that the dnPI3K-Mst1 mice had depressed cardiac function and this was associated with premature mortality compared with Mst1 mice alone (see Sections 3.3.1. and 3.3.2.). These mice also showed increased fibrosis in both the atria and ventricles (see Section 3.3.4.1.), suggesting that cardiac conduction may be impaired. Collectively, these data led to the hypothesis that reduced PI3K (p110 α) activity may cause severe cardiac conduction abnormalities in the stressed heart.

4.2. Methods

4.2.1 Techniques used in this study

The following techniques were used for the studies described in this chapter:

- Transgenic mouse model generation (as described in Chapter 2, page 63)
- Transgenic mouse model genotyping (as described in Chapter 2, pages 66-68)
- Echocardiography (as described in Chapter 2, page 68)
- Cardiac catheterisation (as described in Chapter 2, page 70)
- ECG and intracardiac catheterisation (as described in Chapter 2, pages 70-75)
- Telemetry recordings (as described in Chapter 2, page 76)
- Tissue harvesting and tibia length measurement (as described in Chapter 2, page 80)
- Tissue fibrosis examination (as described in Chapter 2, page 98)
- Protein extraction, measurement of protein concentration, and Western blotting (as described in Chapter 2, pages 81-86)
- Microarray gene expression analysis (as described in Chapter 2, page 96)
- Plasminogen assay (as described in Chapter 2, page 97)
- Gelatin zymography (as described in Chapter 2, page 89)
- PI3K activity assay (as described in Chapter 2, page 87-89)

4.2.2. Animals

All animals used in the studies described in this chapter are female Ntg, dnPI3K, Mst1 and dnPI3K-Mst1 mice. The majority of mice described are between 4.2 and 4.9

months of age, as dnPI3K-Mst1 mice have a lifespan of approximately 4.5 ± 0.3 months (see Section 3.3.1.). Aged Mst1 mice (15.0 ± 1.3 months) were also examined in this study.

4.3. Results

4.3.1. PI3K (p110 α) activity in dnPI3K-Mst1 mice

To confirm depressed PI3K (p110 α) activity in the dnPI3K-Mst1 mice, PI3K activity assays were performed, as previously described (see Section 2.7.6.1.). PI3K (p110 α) activity, as well as the phosphorylation of a downstream target, Akt, were significantly depressed in ventricular tissue from dnPI3K mice (Figure 47, A & B). There was no difference in PI3K (p110 α) activity between Ntg and Mst1 mice (Figure 47 A). PI3K (p110 α) activity was significantly depressed in the dnPI3K-Mst1 mice compared with Ntg and Mst1 mice alone (Figure 47 A). While not significant, there was a trend for a decrease in phosphorylation of Akt in the hearts of dnPI3K-Mst1 mice compared with Ntg and Mst1 mice (Figure 47 B).

4.3.2. Extended characterisation of the cardiac phenotype of the dnPI3K-Mst1 mice

4.3.2.1. Haemodynamic characteristics of the dnPI3K-Mst1 mice

As described in Chapter 3, dnPI3K-Mst1 mice have depressed cardiac function characterised by dilated cardiac chambers and thin ventricular walls (see Section 3.3.2.1. and Section 3.3.4.1.). The cardiac phenotype was further characterised using cardiac catheterisation as previously described (see Section 2.4.2.). Heart rates were similar between groups (Table 26). Systolic blood pressure was decreased in the dnPI3K mice compared with the Ntg mice (Table 26). Systolic blood pressure was further depressed in Mst1 and dnPI3K-Mst1 mice compared with Ntg and dnPI3K mice (Table 26). Diastolic blood pressure was similar in Ntg and dnPI3K mice (Table 26). Mst1 and dnPI3K-Mst1 mice displayed depressed diastolic blood pressure compared with both Ntg and dnPI3K mice (Table 26). LVSP, LVEDP, dP/dt_{max} , and dP/dt_{min} were not significantly different between Ntg and dnPI3K mice (Table 26). Mst1 and dnPI3K-

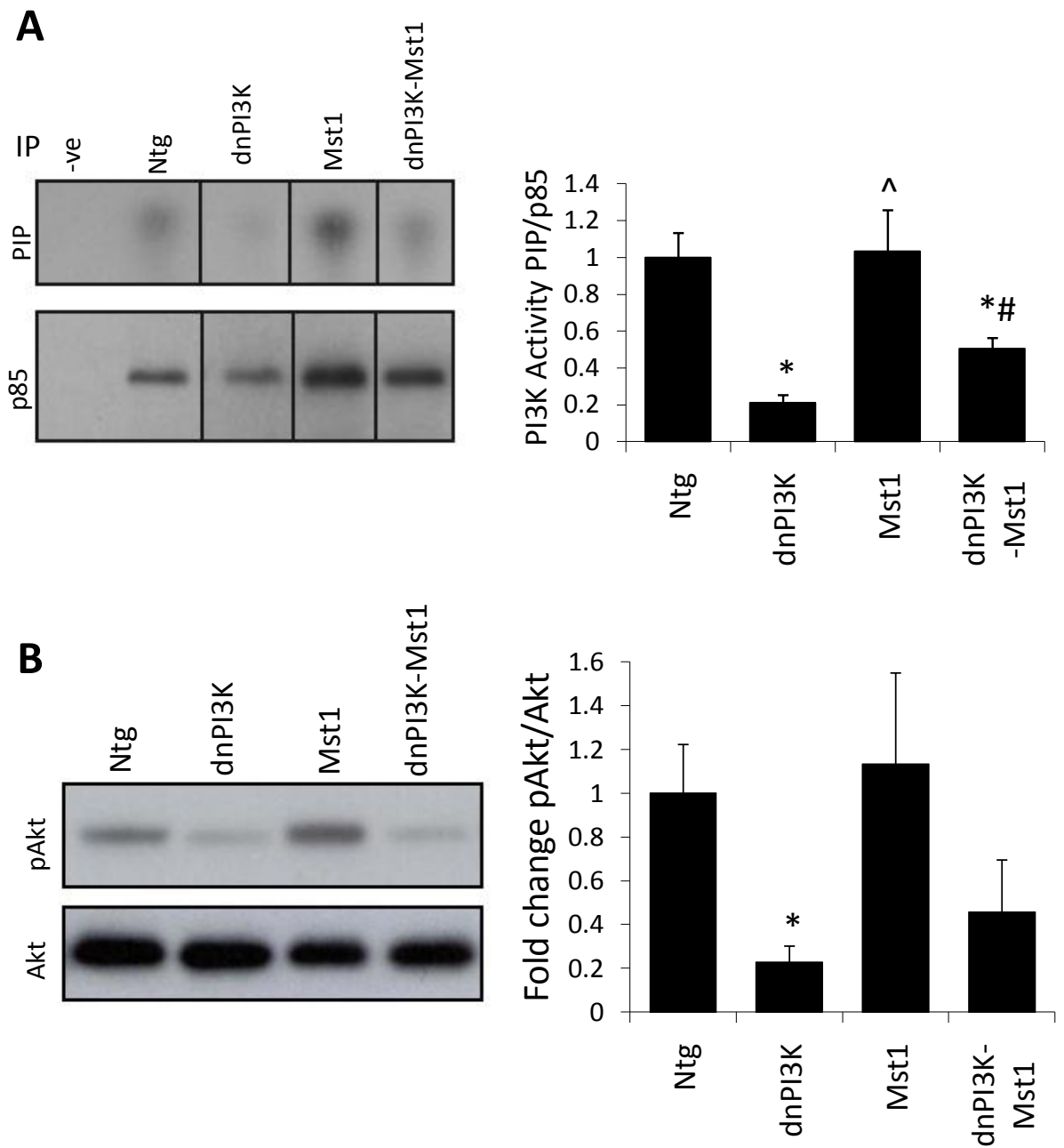


Figure 47. PI3K activity and phosphorylation of Akt in mouse ventricular samples.

A: PI3K (p110 α) activity (**left panel**) and quantitative analysis (**right panel**), $n=6-8$ in each group. IP: immunoprecipitate; -ve: negative control (sample without antibody); PIP: phosphatidylinositol 3-phosphate. A portion of the immunoprecipitated antibody was subjected to Western blotting and probed with an anti-p85 antibody. **B:** Representative Western blot showing pAkt and total Akt (**left panel**) and quantitative analysis (**right panel**), $n=3$ in each group. * $p<0.05$ compared with Ntg, [^] $p<0.05$ compared with dnPI3K; and # $p<0.05$ compared with Mst1. Ntg was normalised to 1.0.

Table 26. Haemodynamic analyses from transgenic mice at 4.2-4.9 months of age.

LVSP: Left ventricular systolic pressure; LVEDP: Left ventricular end-diastolic pressure; dP/dt_{max} and dP/dt_{min} : maximum rise and fall of left ventricular pressures. * $p < 0.05$ compared with Ntg; ^ $p < 0.05$ compared with dnPI3K; and # $p < 0.05$ compared with Mst1.

	Ntg	dnPI3K	Mst1	dnPI3K-Mst1
N	5	3	4	4
Body Weight (g)	29.3 \pm 2.7	28.5 \pm 2.2	29.2 \pm 2.7	27.1 \pm 0.8
Heart Rate (beats/minute)	352 \pm 19	360 \pm 52	382 \pm 18	379 \pm 18
Systolic Blood Pressure (mmHg)	117 \pm 5	100 \pm 3 *	84 \pm 4 *^	76 \pm 5 *^
Diastolic Blood Pressure (mmHg)	80 \pm 3	75 \pm 4	61 \pm 3 *^	57 \pm 2 *^
LVSP (mmHg)	110 \pm 4	101 \pm 3	81 \pm 2 *^	74 \pm 3 *^
LVEDP (mmHg)	6 \pm 1	6 \pm 0	11 \pm 1 *^	15 \pm 0 *^#
dP/dt_{max} (mmHg/s)	7427 \pm 383	7064 \pm 391	6722 \pm 645	4128 \pm 245 *^#
dP/dt_{min} (mmHg/s)	7039 \pm 411	6105 \pm 245	5011 \pm 388 *	3259 \pm 85 *^#

Mst1 mice had significantly decreased LVSP compared with Ntg and dnPI3K mice (Table 26). LVEDP was significantly increased in the Mst1 mice, and this was further increased in the dnPI3K-Mst1 mice (Table 26). Mst1 mice showed no significant difference in dP/dt_{\max} compared with Ntg and dnPI3K mice, but had a reduced dP/dt_{\min} (Table 26). dnPI3K-Mst1 mice had a significantly reduced dP/dt_{\max} and dP/dt_{\min} compared with all other groups (Table 26).

4.3.2.2. Left atrial and ventricular enlargement in dnPI3K-Mst1 mice

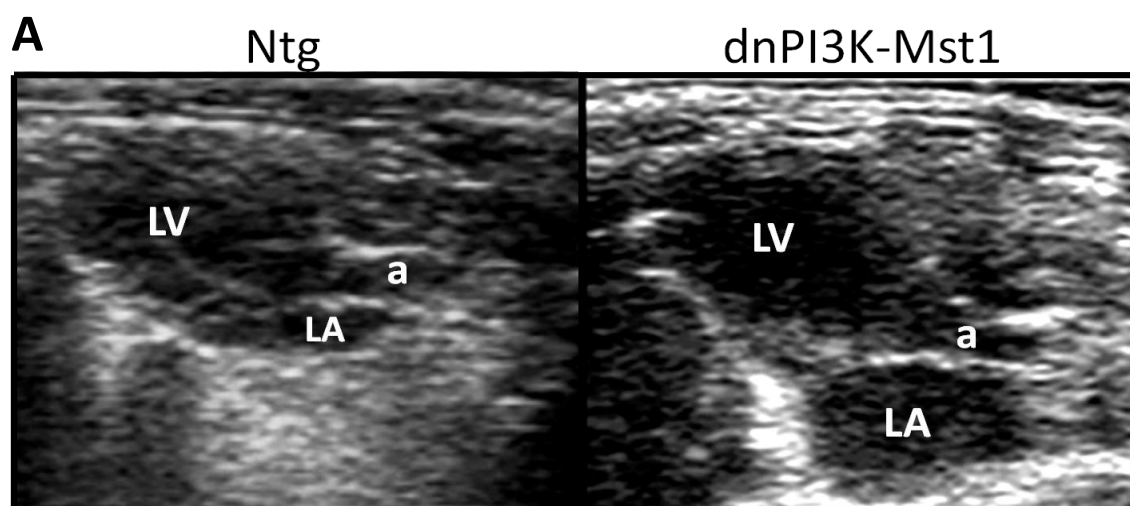
By echocardiography there was clear enlargement of the left atrial and left ventricular chambers in the dnPI3K-Mst1 mice compared with Ntg mice (Figure 48 A). Left atrial chamber size was significantly greater in Mst1 mice compared with Ntg and dnPI3K mice (Figure 48 B), and this enlargement was further exacerbated in the dnPI3K-Mst1 mice (Figure 48 B).

4.3.2.3. Increased fibrosis in left atria of dnPI3K-Mst1 mice

As shown in Chapter 3, dnPI3K-Mst1 mice have increased atrial fibrosis compared with Mst1 mice alone (see Figure 37). Upon detailed examination of the left and right atria separately, it became apparent that the majority of atrial fibrosis was localised in the left atria of the dnPI3K-Mst1 mice (Figure 49). All other genotypes showed similar levels of fibrosis in both atria (Figure 49).

4.3.2.4. Expression of fibrotic genes in atria of dnPI3K-Mst1 mice

Gene expression in the atria of female Ntg, dnPI3K, Mst1 and dnPI3K-Mst1 mice was examined using microarray technology, as previously described (see Section 2.8.5.). Consistent with results from histological examination, gene expression changes in a number of extracellular matrix- and fibrosis-related genes were increased in the atria of Mst1 mice compared with Ntg and dnPI3K mice, and even more significantly increased in the dnPI3K-Mst1 mice compared with all other groups (Figure 50).



B Left atrial size (mm²)

Ntg	dnPI3K	Mst1	dnPI3K-Mst1
4.0 ± 0.3	2.6 ± 0.3	8.1 ± 0.9 *	13.8 ± 1.7 *#

Figure 48. Assessment of cardiac chamber dimensions in transgenic mice.

A: Representative 2D-echocardiographic image (long axis) showing cardiac chamber sizes in the Ntg (left panel) and dnPI3K-Mst1 (right panel) mice. dnPI3K-Mst1 mice show marked enlargement of the left ventricle (LV), and the left atrium (LA) compared with Ntg mice. Ascending aorta (a) as indicated. **B:** Left atrial size of transgenic mice determined from long-axis two-dimensional images at end-systole. n=5-6 in each group. * p<0.05 compared with Ntg and dnPI3K, and # p<0.05 compared with Mst1.

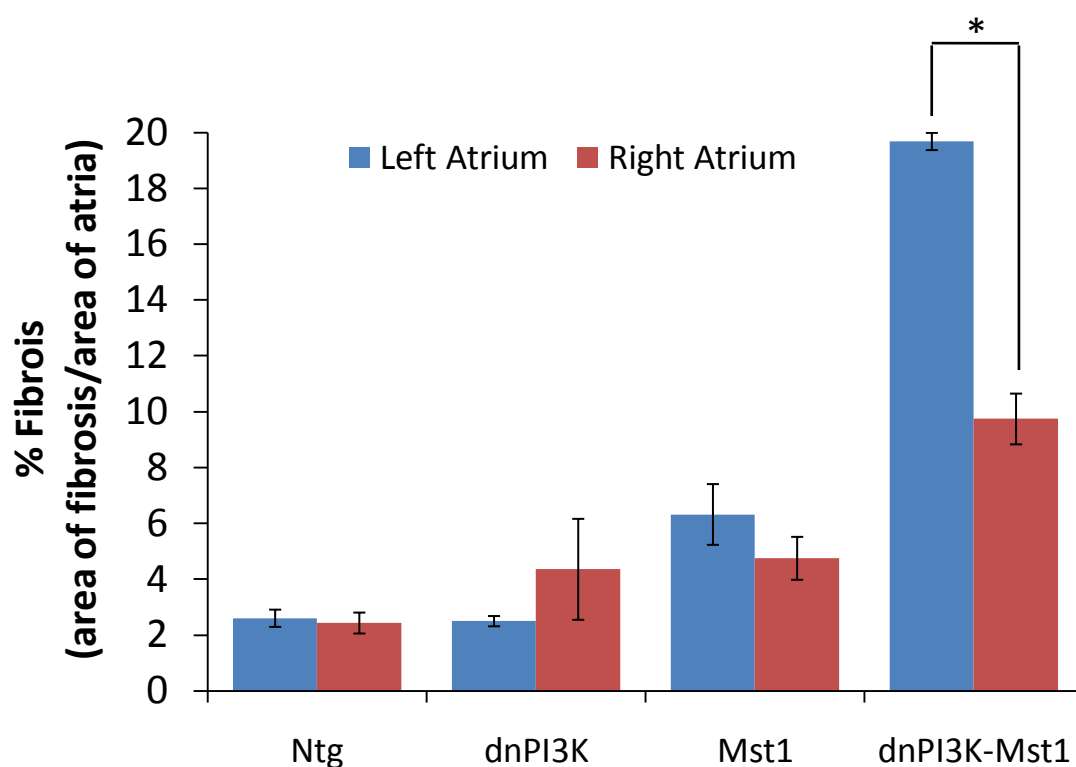


Figure 49. dnPI3K-Mst1 mice have more severe fibrosis in the left atrium compared with the right atrium.

dnPI3K-Mst1 mice developed a 10-fold increase in left atrial fibrosis and a 5-fold increase in right atrial fibrosis compared with Ntg. $n=3-6$ in each group; * $p<0.05$.

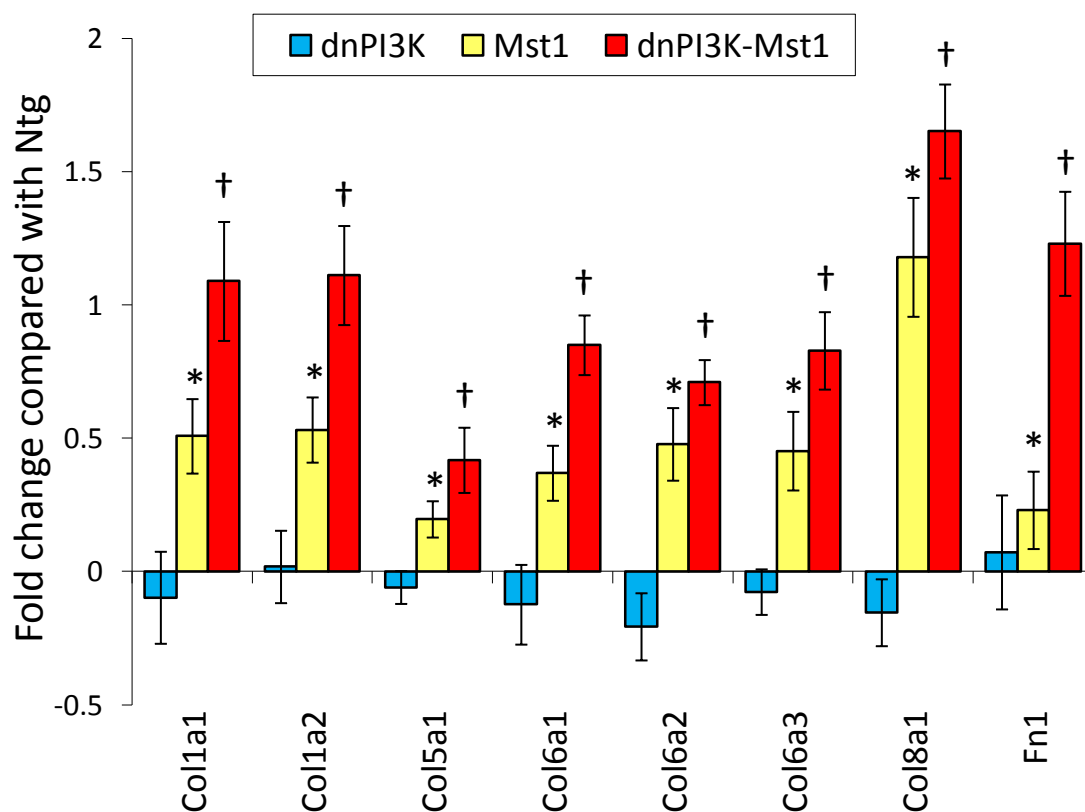


Figure 50. Gene expression changes of extracellular matrix- and fibrosis-related genes in the atria from transgenic mice.

Col, procollagen types; Fn1, fibronectin. * $p < 0.05$ compared with Ntg and dnPI3K; † $p < 0.05$ compared with Ntg, dnPI3K, and Mst1 ($n = 4$ in each group).

4.3.2.5. Atrial thrombi formation in dnPI3K-Mst1 mice

At autopsy, approximately 50% (8 of 17 mice) of the dnPI3K-Mst1 mice developed chronic atrial thrombi in the left atrium (Figure 51). Thrombus formation was not a feature of any other genotypes.

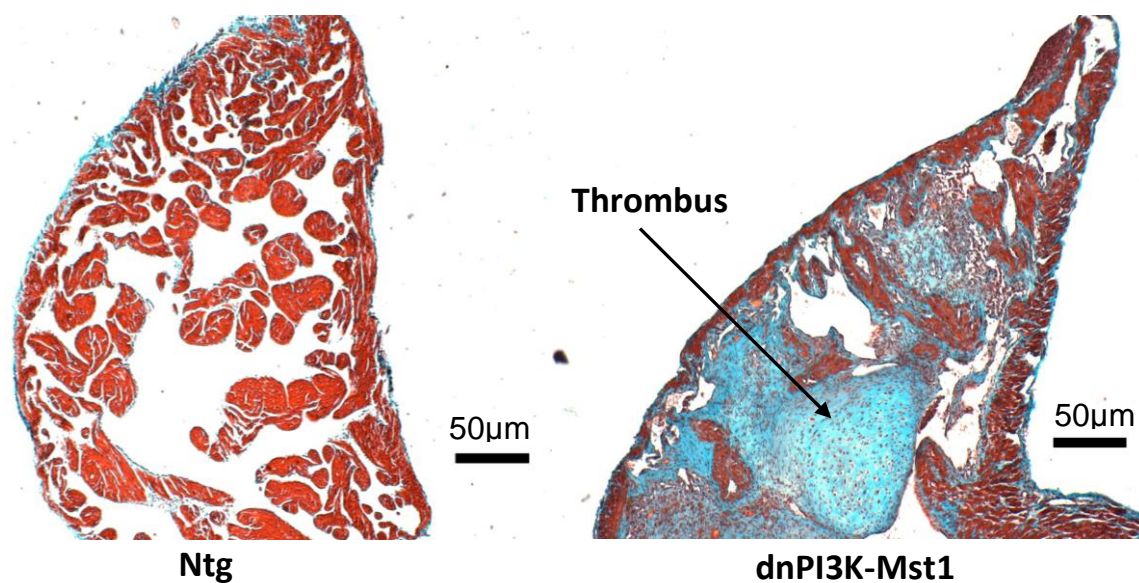


Figure 51. Atrial thrombus formation in dnPI3K-Mst1 mice.

dnPI3K-Mst1 mice (**right panel**) develop chronic atrial thrombi (indicated by arrow) in approximately 50% of cases, with marked atrial fibrosis (blue staining indicates collagen deposition, Masson's trichrome stain). Fibrosis was not visible in the area of Ntg mice (**left panel**). 40 X magnification.

4.3.2.6. Mechanisms responsible for atrial thrombi formation

Atrial thrombus formation is a common complication of HF and a variety of arrhythmic disorders, particularly AF (Agmon *et al.*, 2002; De Caterina, 2009; Freeman and Aguilar, 2008; Tang *et al.*, 2009), and is associated with an increased risk of stroke. Thrombi can result from several underlying pathophysiological changes including anatomical and structural changes, abnormal changes in blood constituents, or blood stasis due to HF (Esmon, 2009). dnPI3K-Mst1 mice have marked structural remodelling due to increased atrial and ventricular fibrosis (see Section 3.3.4.1., Figure 49) as well as

marked cardiac dysfunction (see Section 3.3.2.2.), which could explain the formation of thrombi. However, to explore whether changes in blood constituents contribute to increased blood clotting, global fibrinolytic activity was assessed in plasma from Ntg, dnPI3K, Mst1 and dnPI3K-Mst1 mice. No difference in fibrinolytic activity was seen between any of the genotypes (Figure 52).

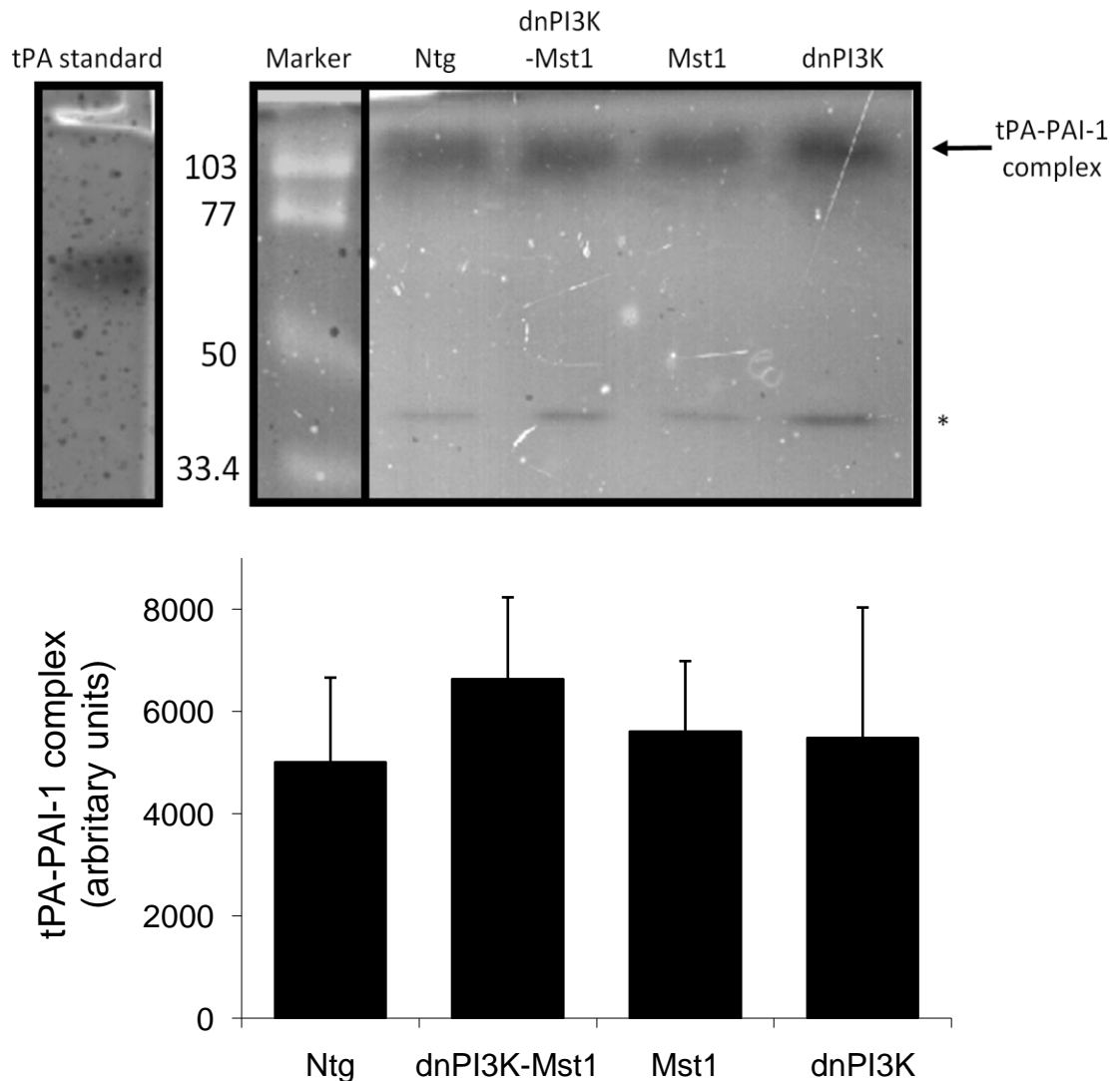


Figure 52. Global fibrinolytic activity in plasma from transgenic mice.

Top panel: Tissue plasminogen (tPA) standard; molecular weight marker [kilodaltons (kd)]; tPa-plasminogen activator inhibitor 1 (PAI-1) complex (indicated by arrow). Bands indicated by asterisk may represent mouse urokinase (u-Pa) which migrates at 45-48 kd. Regardless of its formal identity, no obvious difference was detected between groups. **Bottom panel:** Quantitative analysis of the tPA-PAI-1 complex (n=4 in each group).

To examine whether changes in blood components contribute to atrial and left ventricular structural disarrangement and ECM remodelling through activation of pro-MMPs to MMPs to increase collagen deposition, gelatin zymography was performed as previously described (see Section 2.7.7.). Zymography was performed on ventricular tissue, as there is inadequate tissue available in the atria. MMP-2 and MMP-9 have previously been associated with marked structural abnormalities in the atria in a setting of HF (Boixel *et al.*, 2003; Spinale, 2007). MMP-9 (latent or active form) did not change, but total MMP-2 was increased in both the Mst1 and dnPI3K-Mst1 mice compared with Ntg and dnPI3K mice (Figure 53). No difference was seen between Mst1 and dnPI3K-Mst1 (Figure 53).

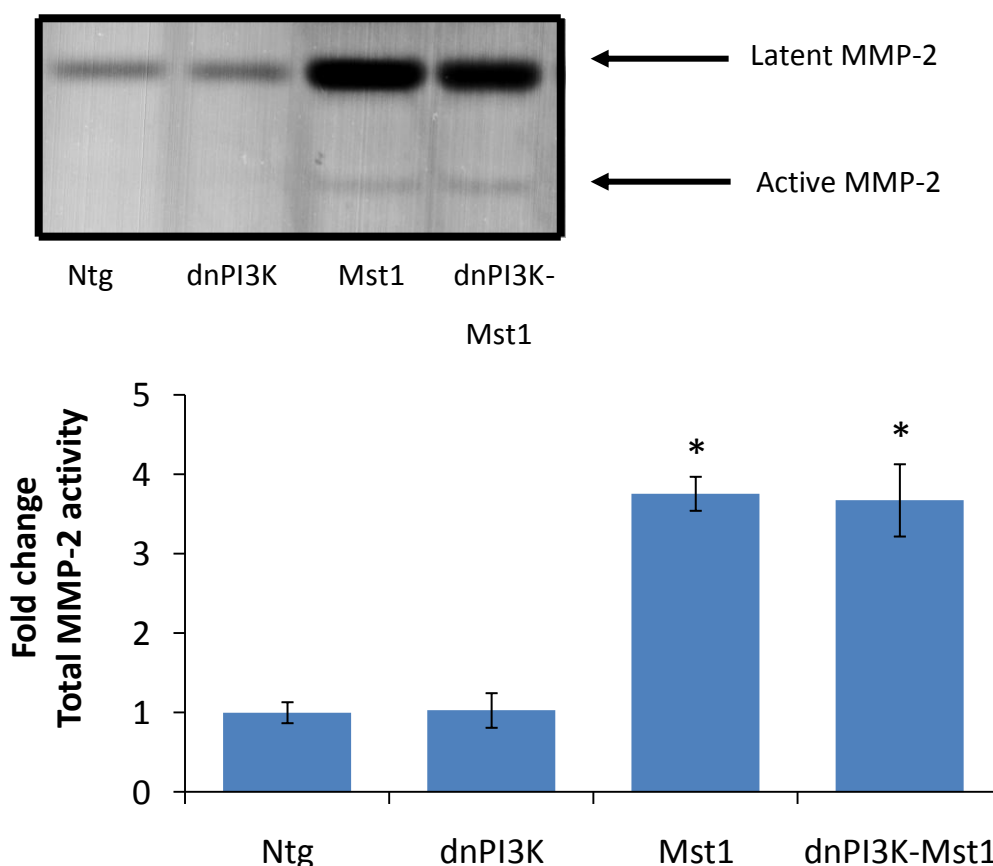


Figure 53. MMP-2 activity in ventricular tissue from transgenic mice.

Top panel: Gelatin zymography of latent and active forms of MMP-2 (as indicated by arrows).

Bottom panel: Quantitative analysis of total MMP-2 activity. Ntg was normalised to 1.0.

* $p < 0.0001$ compared with Ntg and dnPI3K, $n = 3$ in each group.

4.3.3. Changes in cardiac conduction in dnPI3K-Mst1 transgenic mice

The premature death, increased atrial fibrosis, and presence of thrombi in the dnPI3K-Mst1 mice suggested a possible defect in cardiac conduction. As such, cardiac conduction was assessed using ECG, telemetry and catheterisation recordings, as previously described (see Section 2.4.).

4.3.3.1. Electrical conduction abnormalities in dnPI3K-Mst1 mice

ECG analyses were performed on 6-12 Ntg, dnPI3K, Mst1, and dnPI3K-Mst1 mice as previously described (see Section 2.4.3.). Mild to major ECG abnormalities were observed in dnPI3K, Mst1, and dnPI3K-Mst1 mice compared with Ntg (Table 27, Figure 54). There was no difference in heart rate, R-R interval, or QRS interval in any of the groups (Table 27). P-R interval was prolonged approximately 43% in the Mst1 mice compared with both the Ntg and dnPI3K mice, and this was further exacerbated in the dnPI3K-Mst1 mice (an approximate 132% increase compared with Ntg and dnPI3K mice, Table 27). dnPI3K mice had slightly smaller P-amplitudes and R-amplitudes compared with Ntg mice (Table 27), likely due to the smaller size of the heart (see Table 20, page 121). Mst1 mice had reduced R-amplitudes compared with Ntg and dnPI3K (Table 27). dnPI3K-Mst1 mice had significantly depressed P-amplitudes and R-amplitudes compared with Ntg, dnPI3K, and Mst1 (Table 27, Figure 54).

Several P-wave abnormalities were observed in the dnPI3K-Mst1 mice, including double peaks (Figure 55 A). All dnPI3K-Mst1 mice examined displayed varying degrees of atrial-ventricular conduction blockade (AVB), including first degree AVB (Figure 55 A), second degree AVB (Figure 55 B), and third degree block AVB (Figure 55 C). To investigate whether β -adrenergic stimulation could improve conduction, isoproterenol (3ng i.v.) was administered to the dnPI3K-Mst1 mice and ECG recorded for a further 5 minutes. There was no change in P-R interval (Figure 55 D).

Table 27. ECG analyses from transgenic mice at 4.5 months of age.

* $p < 0.05$ compared with Ntg; ^ $p < 0.05$ compared with dnPI3K; and # $p < 0.05$ compared with Mst1.

	Ntg	dnPI3K	Mst1	dnPI3K-Mst1
N	12	8	6	8
Heart Rate (beats/minute)	477 \pm 7	475 \pm 11	472 \pm 20	514 \pm 18
R-R interval (ms)	126 \pm 2	127 \pm 3	128 \pm 5	118 \pm 4
P-R interval (ms)	37 \pm 1	39 \pm 1	53 \pm 2 *^	86 \pm 9 *^#
QRS interval (ms)	9.0 \pm 0.2	9.0 \pm 0.4	8.0 \pm 0.2	8.0 \pm 0.3
P-amplitude (mV)	0.14 \pm 0.01	0.08 \pm 0.01 *	0.09 \pm 0.01 *	0.05 \pm 0.01 *^#
R-amplitude (mV)	1.55 \pm 0.08	1.31 \pm 0.09 *	0.93 \pm 0.09 *^	0.40 \pm 0.08 *^#

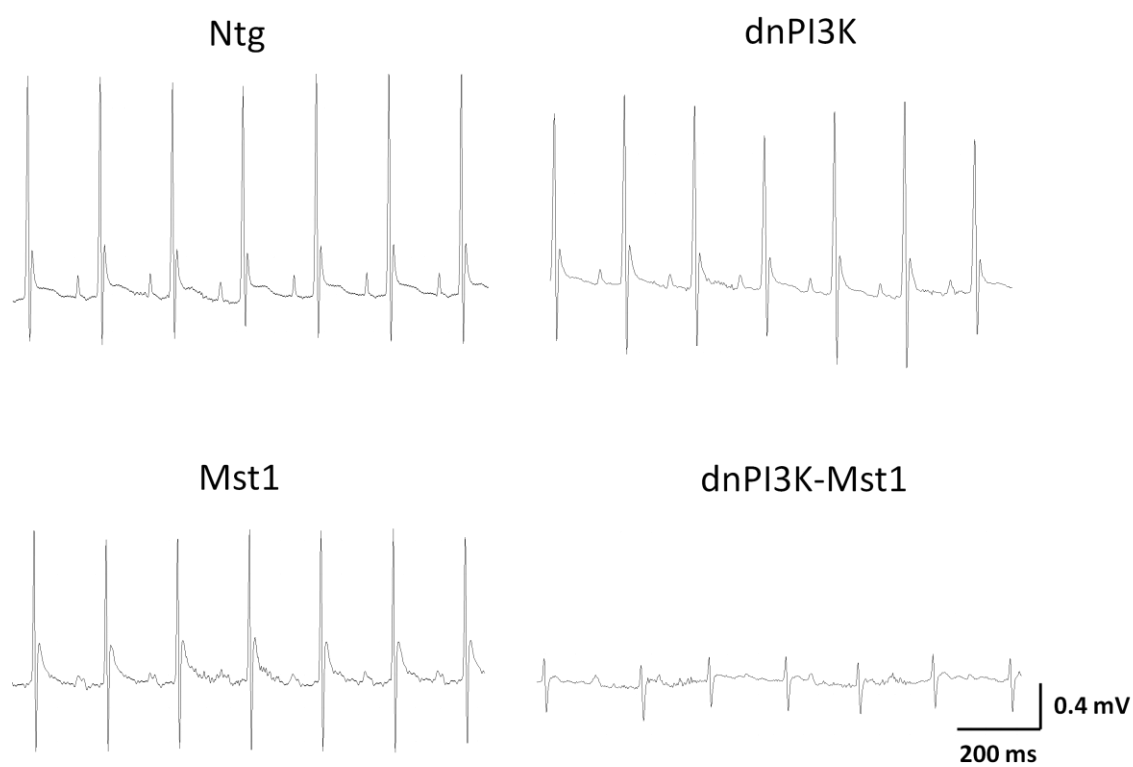


Figure 54. Representative surface ECG traces from *Ntg*, *dnPI3K*, *Mst1*, and *dnPI3K-Mst1* mice.

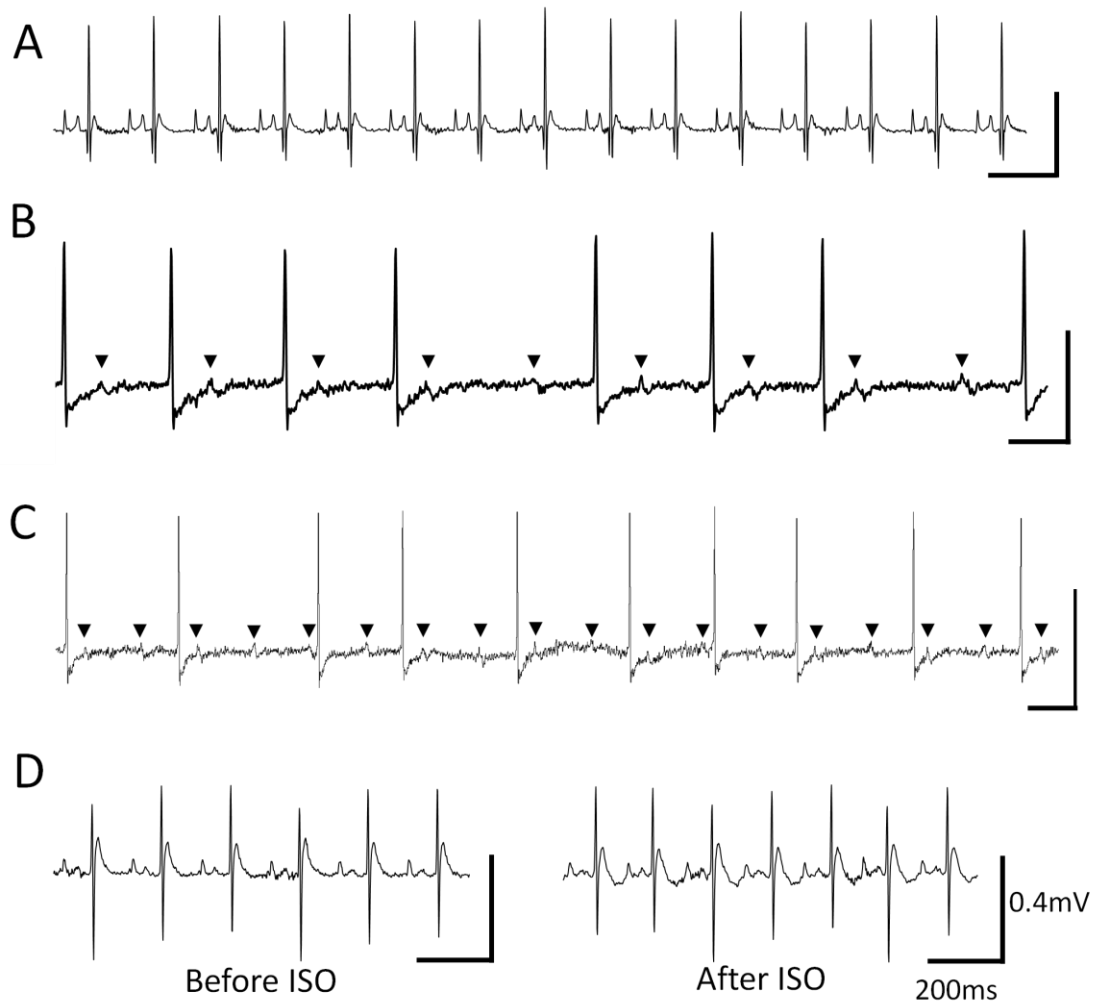
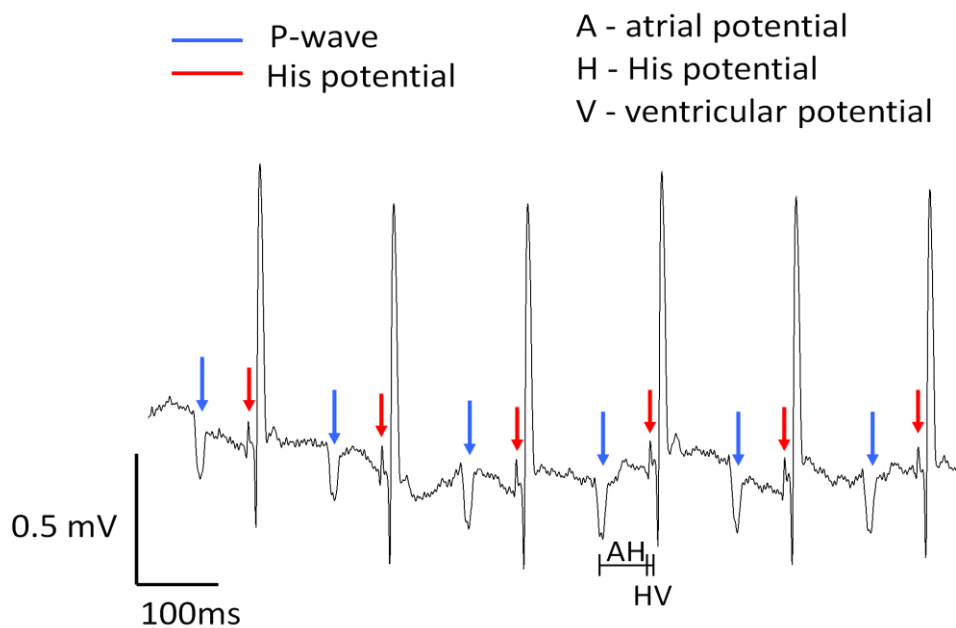


Figure 55. Atrial-ventricular conduction blockade in dnPI3K-Mst1 mice.

A: First-degree AVB (constant prolonged PR interval and double p-waves), **B:** Mobitz type 1 second-degree AVB (gradual prolongation of the P-R interval before complete block), solid triangles indicate p-waves, **C:** Third-degree AVB (no relationship between P-waves and QRS complexes). **D:** No difference in P-R interval following isoproterenol (ISO) stimulation.

4.3.3.2. Location of the conduction blockade in dnPI3K-Mst1 mice

To determine the location of the conduction blockade in the dnPI3K-Mst1 mice, intracardiac ECG catheter recordings were recorded in Ntg and dnPI3K-Mst1 mice as previously described (see Section 2.4.4.). dnPI3K-Mst1 mice had a prolonged interval between the atrial (A) to His (H) potential (Figure 56). There was no difference between Ntg and dnPI3K-Mst1 mice in the His to ventricular potential (Figure 56), indicating the conduction blockade occurred prior to the His bundle.



	Ntg	dnPI3K-Mst1
N	3	3
Heart Rate (beats/minute)	416 ± 27	460 ± 20
Atrial – His potential (ms)	23 ± 0	49 ± 1 *
His – Ventricular potential (ms)	11 ± 1	10 ± 1

Figure 56. ECG trace and measurements obtained from an intracardiac electrophysiology catheter located in the right ventricle.

A: atrial potential, H: his potential, V: ventricular potential. * $p < 0.05$ compared with Ntg.

4.3.3.3. *dnPI3K-Mst1* mice are more susceptible to atrial fibrillation

Paroxysmal AF (absent P-waves during overtly irregular R-R intervals) was detected in approximately 40% of *dnPI3K-Mst1* mice (6 of 16 animals) during short periods of surface ECG recordings (5-10 minutes) under anaesthesia (Figure 57). The absence of the P-waves was confirmed by intracardiac catheter recordings (Figure 57; lower 2 panels). AF was not present in Ntg, *dnPI3K* or *Mst1* mice ($n=6-12$ in each group). In order to confirm anaesthetised findings, ambulatory ECG telemetry studies were performed. Telemetry recordings suggest that the incidence of AF is higher than 40% when the *dnPI3K-Mst1* mice are monitored for 24 hours. Short as well as prolonged periods of AF were detected in 100% (6 of 6 animals) of the *dnPI3K-Mst1* mice when monitored for 24 hours (Figure 58). Atrial tachycardia was also detected in the *dnPI3K-Mst1* mice (Figure 58).

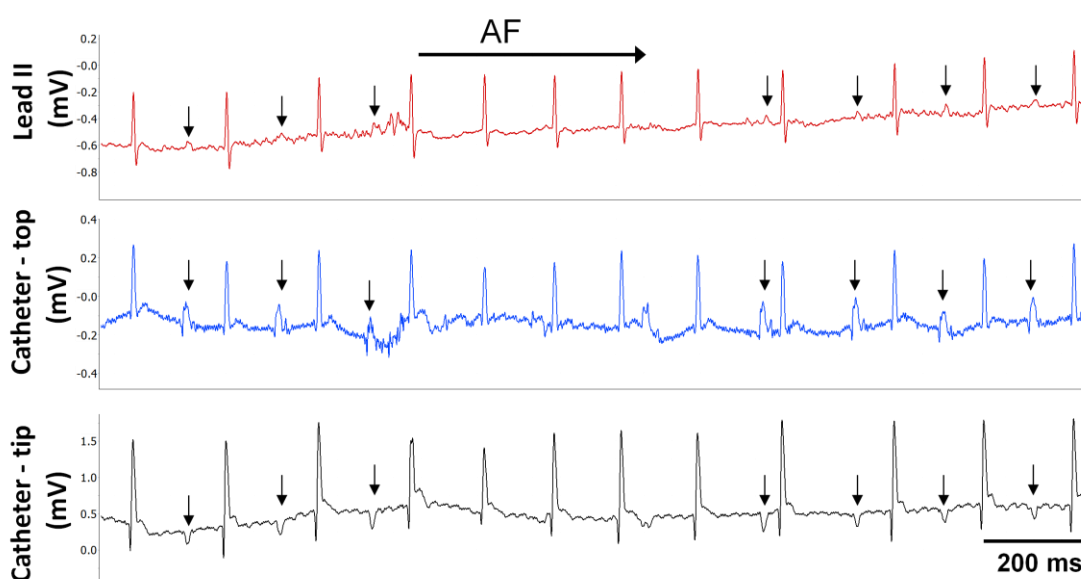


Figure 57. ECG from *dnPI3K-Mst1* showing episodes of atrial fibrillation.

Short period of AF recorded simultaneously from Lead II (upper panel) and an intracardiac electrophysiology catheter (lower two panels). P-waves are indicated by arrows.

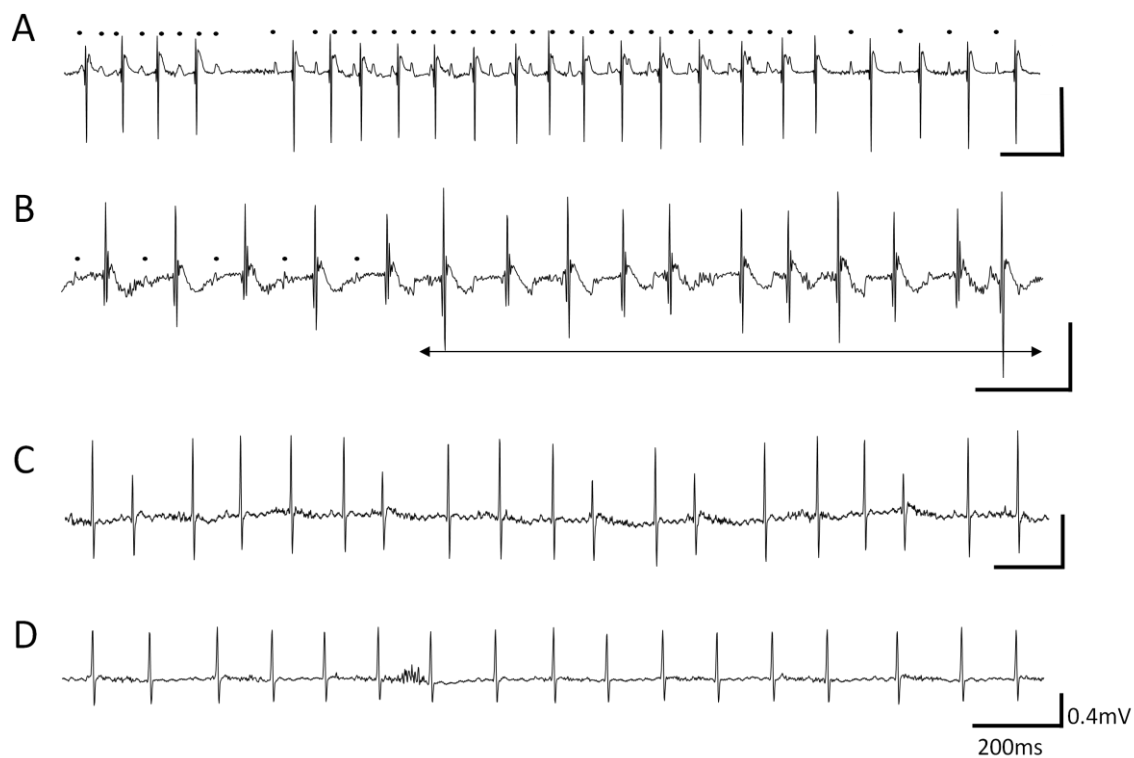


Figure 58. ECG telemetry traces from *dnPI3K-Mst1* mice showing episodes of atrial tachycardia and atrial fibrillation.

A: Atrial tachycardia (dots indicate P-waves), atrial rate approximately 1000 beats/min. **B:** Short episode of AF (indicated by horizontal arrow). **C & D:** Prolonged episodes of AF, demonstrated by the absence of P-waves during overtly irregular R-R intervals.

4.3.3.4. ECG characteristics of aged dnPI3K and Mst1 mice

To assess whether AF in the dnPI3K-Mst1 mice was simply a result of a more severe dilated cardiomyopathy phenotype compared with the Mst1 mice alone, cardiac conduction was assessed in aged Mst1 (15.0 ± 1.3 months, $n=6$) mice. While Mst1 mice have an average lifespan of approximately 8 months (see Figure 27, page 109), a small percentage of mice live considerably longer. Aged Mst1 mice displayed a similar HF phenotype to that of dnPI3K-Mst1 mice at 4.5 months of age [similar atrial weights (Mst1: 33.8 ± 3.9 mg; dnPI3K-Mst1: 32.8 ± 8.2 mg) and lung weights (Mst1: 285.5 ± 47.3 mg; dnPI3K-Mst1: 226.7 ± 11.5 mg)]. Cardiac conduction was also assessed in a group of aged dnPI3K (16.1 ± 1.6 months, $n=6$).

Despite having a similar HF phenotype, ECG abnormalities were still more severe in the dnPI3K-Mst1 mice at 4.5 months (see Table 27, page 164) compared with aged Mst1 (Table 28). There was a fall in R-amplitude in aged Mst1 mice and an increase in P-R interval compared with younger Mst1 mice (Table 27 compared with Table 28) but these changes were significantly smaller than those observed in dnPI3K-Mst1 mice at 4.5 months (see Table 27 and Table 28; R-amplitude approximately 0.5mV in aged Mst1, approximately 0.4mV in 4.5 month dnPI3K-Mst1; P-R interval approximately 63ms in aged Mst1, approximately 86ms in 4.5 month dnPI3K-Mst1). There was also no evidence of AF in aged Mst1 mice. Interestingly, in aged dnPI3K mice there was also a fall in R-amplitude and a small but significant increase in P-R interval compared with younger dnPI3K and aged Ntg mice (see Table 27, Table 28, and Figure 59). Aged dnPI3K mice also displayed periods with irregular R-R intervals (Figure 59).

4.3.4. Gene expression profiles in mouse atrial samples

Gene expression was analysed in mouse atria using microarray, as previously described (see Section 2.8.5.) to determine whether the observed AF in the dnPI3K-Mst1 mice was associated with changes in gene expression that have been reported in humans or large animal models of AF (including fibrogenic genes, connexin proteins, potassium channels, and metabolic genes). As shown previously, genes associated with fibrosis or the ECM were up-regulated in Mst1 mice, and this was further exacerbated in the dnPI3K-Mst1 mice (see Figure 50, page 159).

Table 28. Parameters derived from ECG of aged transgenic mice.

* $p < 0.05$ compared with Ntg; ^ $p < 0.05$ compared with dnPI3K.

	Ntg	dnPI3K	Mst1
N	6	5	6
Age (months)	13.5 \pm 2.7	16.1 \pm 1.6	15.0 \pm 1.3
Heart Rate (beats/minute)	491 \pm 21	485 \pm 16	430 \pm 53
R-R interval (ms)	124 \pm 6	124 \pm 4	159 \pm 33
P-R interval (ms)	37 \pm 1	44 \pm 2*	63 \pm 7*^
QRS interval (ms)	10.0 \pm 0.0	11.0 \pm 0.1	11.0 \pm 0.1
P-amplitude (mV)	0.18 \pm 0.02	0.09 \pm 0.01*	0.09 \pm 0.02*
R-amplitude (mV)	1.48 \pm 0.07	1.01 \pm 0.18 *	0.52 \pm 0.06 *^

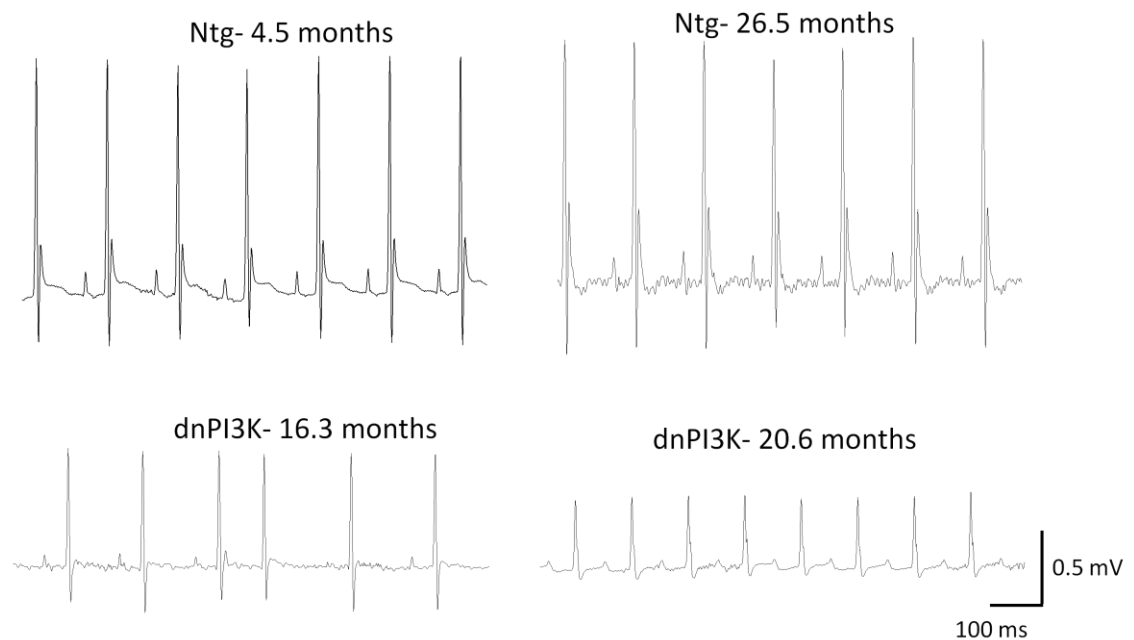


Figure 59. Surface ECG recordings of aged dnPI3K compared with aged Ntg mice.

Aged dnPI3K mice have blunted R-amplitudes, prolonged P-R intervals, and periods with irregular R-R intervals.

Connexin proteins are important for inter-cellular signalling, and form gap junctions within cells (Bruzzone *et al.*, 1996; van der Velden *et al.*, 2000a). In the mammalian heart, connexins 37, 40, 43, 45, and 46 have been identified (Bruzzone *et al.*, 1996; Haefliger *et al.*, 1992; Kanter *et al.*, 1992; Reed *et al.*, 1993). In the present study, differential regulation of connexin 37 and connexin 46 was observed in the transgenic mice (Figure 60). Connexin 37 was down-regulated while connexin 46 was up-regulated as disease worsened (Figure 60). Connexin 37 has been shown to be expressed in endothelial and endocardial cells (Reed *et al.*, 1993; Verheule *et al.*, 1997). Of particular interest, connexin 46 is expressed in the pacemaker cells of the SA node of mice and other mammals (Bruzzone *et al.*, 1996; Coppen *et al.*, 1999; van der Velden *et al.*, 2000a; Verheijck *et al.*, 2001).

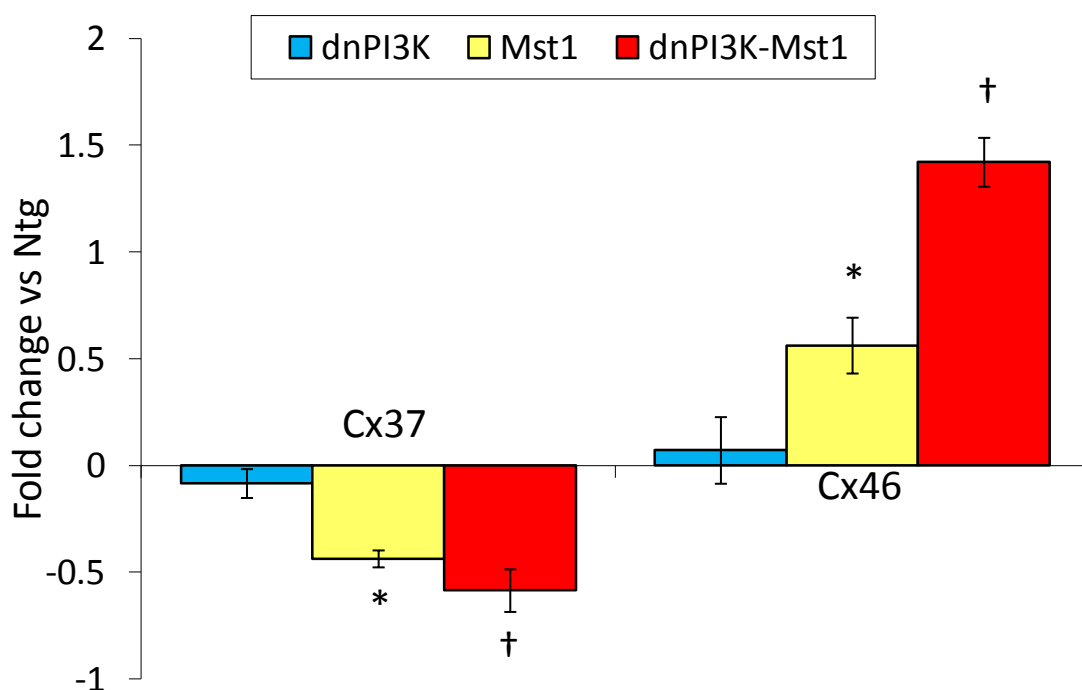


Figure 60. Changes in gene expression of connexin proteins in the atria from transgenic mice.

Cx: connexin subtypes. * $p < 0.05$ compared with Ntg and dnPI3K; † $p < 0.05$ compared with Ntg, dnPI3K, and Mst1 ($n = 4$ in each group).

Changes in potassium channel gene expression have previously been linked with AF in animal models and humans (Tsai *et al.*, 2008). In particular, the potassium ion channel Kv4.3 [encoded by potassium voltage-gated channel Shal-related family member 3 (Kcnd3)] has previously been associated with AF in humans and dogs (Borlak and Thum, 2003; Brundel *et al.*, 2001; Grammer *et al.*, 2000; Yue *et al.*, 1999). In the present study, differential regulation was observed in potassium channel subfamily V member 2 (Kcnv2), potassium channel subfamily T member 2 (Kcnt2), Kcnd3, and potassium inwardly rectifying channel subfamily J member 2 (Kcnj2) (Figure 61). As disease progressed Kcnt2 was up-regulated, while Kcnv2, Kcnd3, and Kcnj2 were down-regulated (Figure 61).

Changes in genes encoding metabolic pathways have also been associated with the development of AF in both animal models and humans (Ausma *et al.*, 2000; Mihm *et al.*, 2001). Several genes important in metabolic pathways (particularly in the electron transport chain, amino acid metabolism and the tricarboxylic acid cycle) were significantly altered in the atria from transgenic mice (Figure 61).

4.3.5. Reduced PI3K (p110 α) activity in atrial appendages of patients with atrial fibrillation

The studies described earlier in this chapter suggest that reduced PI3K (p110 α) signalling accelerates HF progression, and makes the heart more susceptible to develop AF. To determine whether reduced PI3K (p110 α) activity may also be a contributing factor to the development of AF in humans, PI3K (p110 α) activity was assessed in atrial appendages from patients with acute or chronic AF.

PI3K (p110 α) activity was measured in atrial appendages from patients who underwent CABG surgery and either did (66 ± 3 years, $n=4$) or did not (64 ± 4 years, $n=6$) develop AF postoperatively. In another group, atrial tissues were obtained from patients who underwent mitral valve surgery with chronic AF (76 ± 3 years, $n=5$). Both acute and chronic AF was associated with a reduction in PI3K (p110 α) activity (Figure 62), compared with patients who did not develop AF (Figure 62).

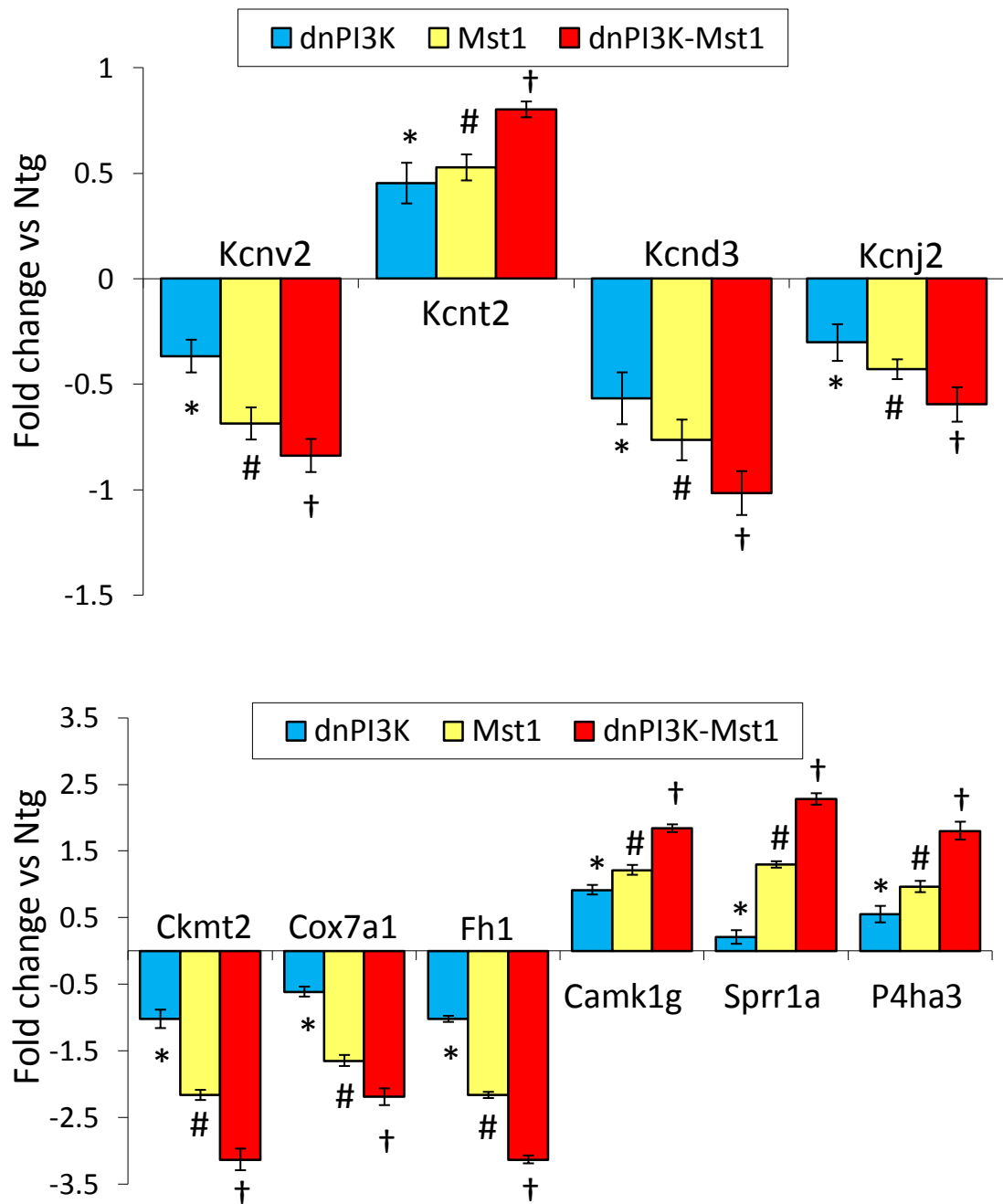


Figure 61. Expression changes of potassium channels and metabolic genes in atria of transgenic mice.

Potassium channels (upper panel): *Kcnv2*: potassium channel, subfamily V, member 2; *Kcnt2*: potassium channel, subfamily T, member 2; *Kcnd3*: potassium voltage-gated channel, *Shal*-related family, member 3; *Kcnj2*: potassium inwardly rectifying channel, subfamily J, member 2. **Metabolism genes (lower panel):** *Ckmt2*: creatine kinase, mitochondrial 2; *Cox7a1*: cytochrome c oxidase, subunit VIIa 1; *Fh1*: fumarate hydratase 1; *Camk1g*: calcium/calmodulin dependent protein kinase I γ ; *Sprr1a*: small proline-rich protein 1A; *P4ha3*: procollagen-proline, 2-oxoglutarate 4-dioxygenase. * $p < 0.05$ compared with Ntg, # $p < 0.05$ compared with Ntg and dnPI3K; † $p < 0.05$ compared with Ntg, dnPI3K, and Mst1 ($n = 4$ in each group).

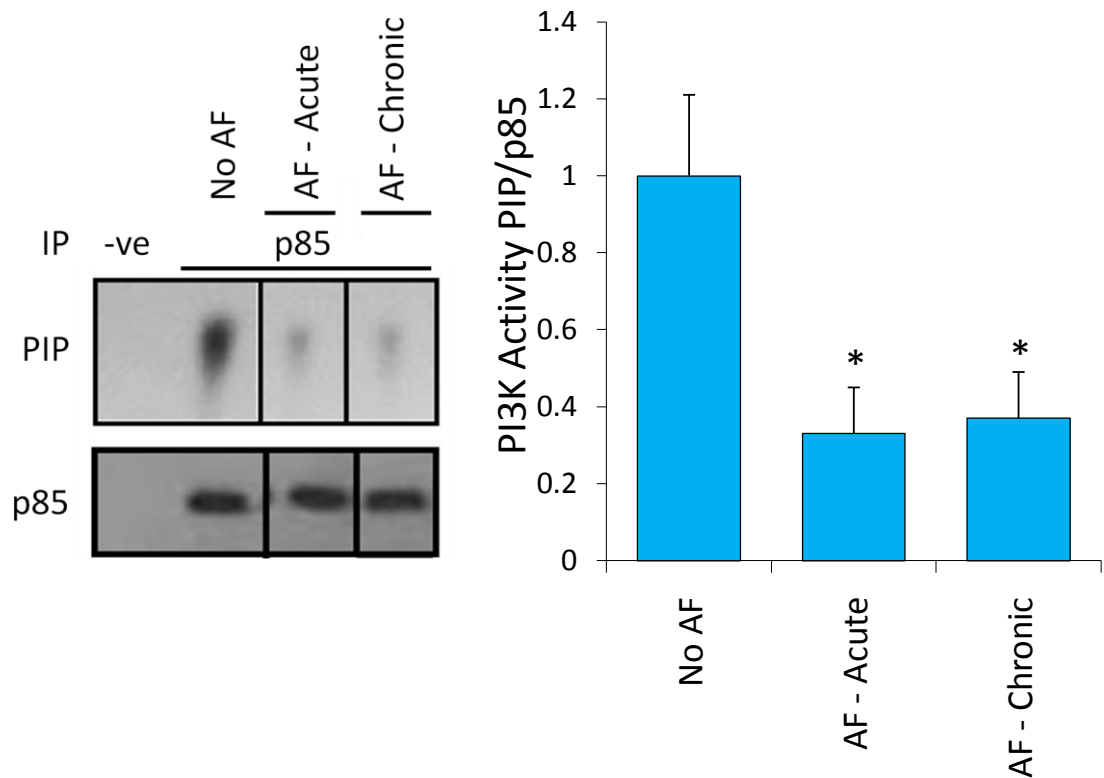


Figure 62. PI3K (p110 α) activity in human atrial samples from patients with either acute or chronic AF compared with patients who did not develop AF post-operatively. PI3K activity (**left, upper panel**) in human atrial samples from patients undergoing CABG surgery who did (AF - Acute, n=4) or did not (No AF, n=6) develop AF postoperatively, and patients with mitral valve disease and chronic AF (AF - Chronic, n=5). IP: immunoprecipitate; -ve: negative control (sample without antibody); PIP: phosphatidylinositol 3-phosphate. A portion of the immunoprecipitated antibody was subjected to Western blotting and probed with an anti-p85 antibody (**left lower panel**). Quantitative analysis (**right panel**). * $p < 0.05$ compared with No AF; No AF was normalized to 1.0.

4.3.6. Increased PI3K (p110 α) activity protects against abnormalities in Mst1 mice

Collectively, the data in this chapter (mouse and human) suggests that reduced PI3K (p110 α) activity increases the heart's susceptibility to AF. Next, I investigated whether increased PI3K (p110 α) activity could reverse some of the conduction related abnormalities associated with the Mst1 phenotype by examining the caPI3K-Mst1 mice (previously characterised in Chapter 3). As Mst1 mice (either at 4.5 or 15 months of age) do not develop AF, it was not possible to assess whether increased PI3K (p110 α) activity reduced the incidence of AF directly. However, to partly address this question, I assessed atrial fibrosis and the P-R interval in the caPI3K-Mst1 mice and compared this to Mst1 mice. Both increased atrial fibrosis and increased P-R interval were associated with the increased susceptibility to AF in the dnPI3K-Mst1 mice. caPI3K-Mst1 mice had reduced atrial fibrosis compared with Mst1 mice (Figure 63) at 4.5 months of age. Additionally, P-R intervals were significantly reduced in the caPI3K-Mst1 mice (45 ± 2 ms; n=5) compared with Mst1 mice (53 ± 2 ms; n=5) at approximately 6.8 months of age (heart rates were similar, caPI3K-Mst1: 504 ± 15 bpm; Mst1: 498 ± 9 bpm).

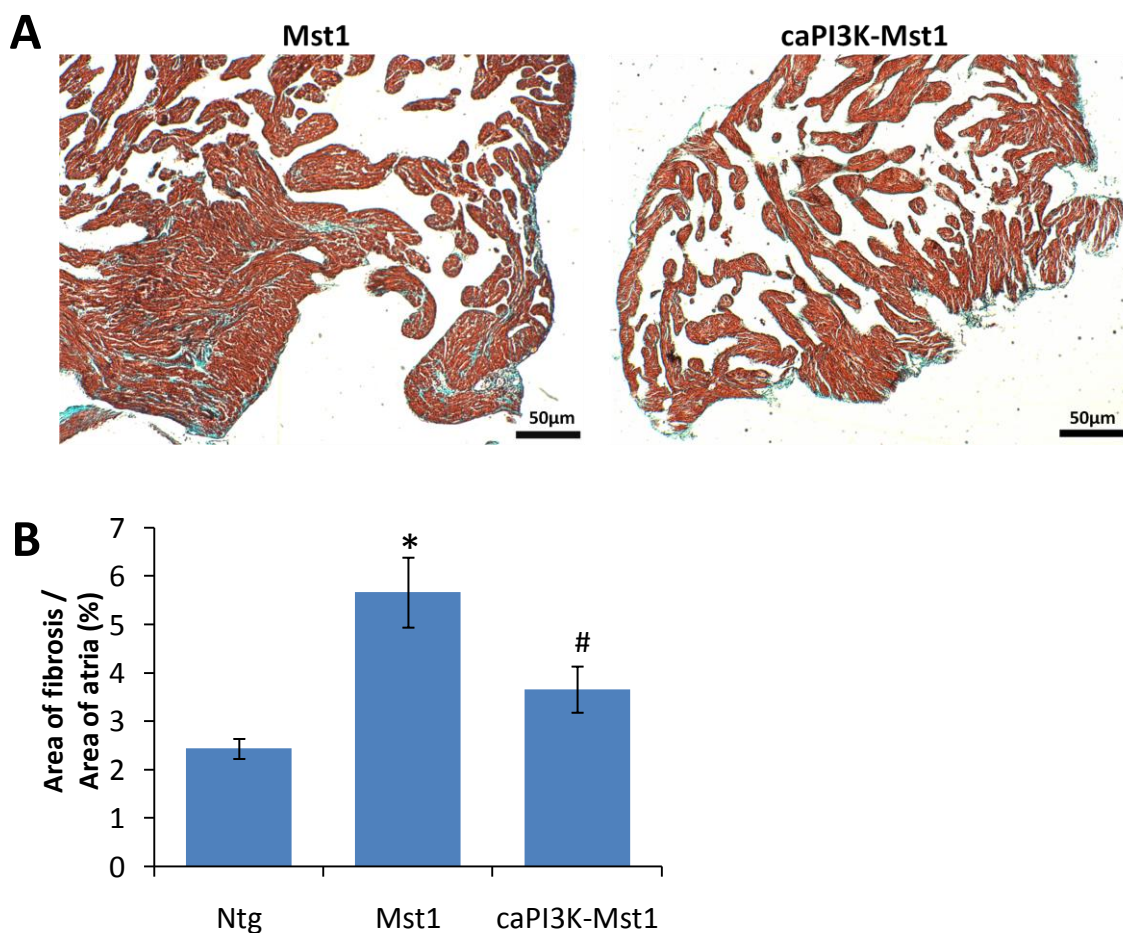


Figure 63. Atrial fibrosis in Ntg, Mst1 and caPI3K-Mst1 mice.

A: Representative left atria showing fibrosis (blue staining, Masson's trichrome, 40 X magnification). **B:** Quantitative analysis of area of fibrosis relative to area of atria in Ntg (n=8), Mst1 (n=7) and caPI3K-Mst1 (n=4) mice. * $p < 0.05$ compared with Ntg, and # $p < 0.05$ compared with Mst1.

4.4. Discussion

4.4.1. Summary of major findings

In this chapter I investigated whether a reduction in PI3K (p110 α) activity leads to cardiac conduction abnormalities in an *in vivo* mouse model of dilated cardiomyopathy. I have shown that reduced PI3K (p110 α) activity in a setting of HF induced an increase in atrial chamber dimensions which was associated with increased fibrosis, particularly in the left atrium of the heart. Structural changes associated with fibrosis of the left atrium also induced the formation of atrial thrombi, and genes associated with ECM remodelling and collagen deposition were increased in the atria of dnPI3K-Mst1 mice. Reduced PI3K (p110 α) activity in a setting of HF induced varying degrees of AVB, which occurred as a result of delayed conduction between the SA node and the bundle of His. Reduced PI3K (p110 α) activity also made the heart more susceptible to develop AF, with all dnPI3K-Mst1 mice displaying AF when ECG recordings were examined for 24 hours by telemetry. Potassium channel and metabolism genes associated with AF in humans were up-regulated in atria from mice that develop AF. Importantly, this study also suggests that reduced PI3K (p110 α) activity may be relevant in patients with AF, as PI3K (p110 α) activity was lower in atrial appendages of patients with acute or chronic AF. Collectively, these novel findings described in this chapter indicate that PI3K (p110 α) protects the heart against cardiac conduction abnormalities and AF in a setting of dilated cardiomyopathy.

4.4.2. Reduced PI3K (p110 α) activity induces cardiac conduction abnormalities and makes the heart more susceptible to atrial fibrillation

HF is a risk factor for the development of AF, but the molecular mechanisms responsible are not well understood (Corradi *et al.*, 2008; Nishida *et al.*, 2010). Numerous genetically modified mouse models develop HF, but only a relatively small number of these models develop AF [see Table 6, page 57; (Adam *et al.*, 2007; Hagendorff *et al.*, 1999; Kehat *et al.*, 2006; Ogata *et al.*, 2008; Saba *et al.*, 2005; Sah *et al.*, 1999; Temple *et al.*, 2005; Xiao *et al.*, 2004)]. Consequently, a better understanding of the molecular mechanisms responsible for the link between HF and AF, as well as

the generation of genetic models of AF to test therapeutic interventions is clearly needed. To date there has been no clear link between PI3K (p110 α) activity and the development of AF, but risk factors for the development of AF (including aging, obesity, and diabetes) are all associated with insulin resistance that could lead to depressed or defective PI3K (p110 α) signalling (Fink *et al.*, 1983; Kahn and Flier, 2000; Tsang *et al.*, 2005). The results described in this chapter indicate that reducing PI3K (p110 α) activity in the hearts of mice with dilated cardiomyopathy (dnPI3K-Mst1) accelerated the progression of HF and induced the spontaneous onset of AF.

Previous clinical and experimental evidence has suggested that atrial enlargement and fibrosis are important histopathological substrates for AF (Osranek *et al.*, 2005; Roberts, 2006). Both atrial chamber dilation and fibrosis were seen in the dnPI3K-Mst1 mice (Figure 48; Figure 49), which would increase the likelihood of re-entry and contribute to AF. The increased levels of fibrosis were associated with up-regulation of genes associated with fibrosis and remodelling of the ECM in the atria of the dnPI3K-Mst1 mice (Figure 50). Chronic atrial thrombi were present in almost 50% of the mice (Figure 51). Pathophysiological changes that can lead to the formation of thrombi include anatomical and structural changes, abnormal changes in blood constituents, or blood stasis due to HF (Esmon, 2009). In the current study there was no difference in blood constituents (Figure 52) between the different transgenic mice, and blood constituents did not contribute to atrial and left ventricular disarrangement by activating pro-MMPs to MMPs (Figure 53). It is therefore likely that structural changes associated with the increased fibrosis in the atria contribute to blood stasis, which leads to thrombus formation.

By ECG, all dnPI3K-Mst1 mice displayed varying degrees of AVB with severely depressed R- and P- amplitudes (Figure 54; Figure 55 A-C), and this could not be reversed by β -adrenergic stimulation (Figure 55 D), indicating that the AVB has a histopathological pathogenesis. Further examination showed that the cardiac conduction blockade was due to a blockade between the atrial potential and the His potential (Figure 56). Under anaesthesia, AF was observed in 40% of dnPI3K-Mst1 mice, but ambulatory telemetry studies suggest that the incidence of AF is higher (since AF was detected in 100% of mice when examined for 24 hours; Figure 57; Figure 58). As reduced PI3K (p110 α) activity was associated with increased atrial fibrosis and

the up-regulation of collagen and ECM related genes in the atria of the dnPI3K-Mst1 mice (Figure 50), it is likely that the dnPI3K transgene may increase the likelihood of AF in the Mst1 mice by increasing fibrosis, suggesting that reduced PI3K (p110 α) activity is a primary cause of AF development rather than a consequence.

The initial characterisation of the Mst1 mice showed that dilated cardiomyopathy occurred from approximately 2 months of age, due to progressive myocyte apoptosis (Yamamoto *et al.*, 2003). The authors did not report an arrhythmic phenotype, but ECG studies were not performed (Yamamoto *et al.*, 2003). Mst1 mice at 4.5 months displayed AVB with reduced R- and P- amplitudes, but these changes were less severe than in the dnPI3K-Mst1 mice (Table 27), and no AF was detected in the Mst1 mice. As it could be argued that the HF phenotype was simply accelerated in the dnPI3K-Mst1 mice because the expression of PI3K (p110 α) (a cardioprotective kinase) was reduced in a setting of dilated cardiomyopathy, the phenotype of aged Mst1 mice was also examined. Aged Mst1 mice (approximately 15 months of age) had a similar HF phenotype compared with dnPI3K-Mst1 mice (approximately 4.5 months of age; Table 28), but AF was still not detected in the aged Mst1 mice. Furthermore, another mouse model of dilated cardiomyopathy (due to over-expression of the β_2 -adrenergic receptor) had a similar cardiac phenotype to the dnPI3K-Mst1 mice (including marked fibrosis and atrial dilation), but did not develop AF (Du *et al.*, 2000b).

Reduced PI3K (p110 α) activity appears to have a significant contribution to the development of AF, as the dnPI3K transgene alone significantly affected the P-R interval in aged mice (Table 28). Additionally, there were also changes in the expression of potassium channels and metabolism genes in atria of dnPI3K mice (Figure 61). Previous studies have linked the modification of potassium channels and genes associated with energy metabolism to animal and human models of AF, and a tight relationship between myocardial energetic dynamics and cardiac electrical activity has also been shown (Ausma *et al.*, 2000; Carrasco *et al.*, 2001; Kalifa *et al.*, 2008; Mihm *et al.*, 2001; Tsai *et al.*, 2008). Additionally, connexin 46 has been identified in the SA node of mice and other mammals (Bruzzzone *et al.*, 1996; Coppen *et al.*, 1999; van der Velden *et al.*, 2000a; Verheijck *et al.*, 2001), suggesting that it may play a role in cardiac conduction. While both the dnPI3K and the Mst1 transgenes alone had a significant effect on gene expression of the potassium channels and

metabolism genes, the changes were even greater in the dnPI3K-Mst1 mice (Figure 60; Figure 61). Unfortunately protein expression data to confirm these gene expression changes could not be performed due to the small size of mouse atria. However, other studies using larger animal models have reported good correlations between protein and gene expression of the Kv4.3 (encoded by *Kcnd3*, Figure 61) potassium channel, and down-regulation of Kv4.3 is associated with AF in humans and dogs (Borlak and Thum, 2003; Brundel *et al.*, 2001; Grammer *et al.*, 2000; Yue *et al.*, 1999). Further studies are necessary to examine the functional consequences of the gene alterations in dnPI3K-Mst1 mice.

4.4.3. Advantages of the atrial fibrillation mouse model

The AF model described in this chapter has several advantages over some previously described AF mouse models, particularly because the dnPI3K-Mst1 mice survive for 4.5 months (see Chapter 3, Figure 27) which provides time to follow disease progression. A previously described AF mouse model due to over-expression of RhoA in the heart develop atrial arrhythmias with dilated, fibrotic atria, but die by 6 weeks of age (Sah *et al.*, 1999), precluding detailed mechanistic investigation. Another AF model [*Rac1*, (Adam *et al.*, 2007)] required approximately 1.5 years to develop AF. The dnPI3K-Mst1 mouse model will enable further biochemical and electrophysiological studies to explore the mechanisms responsible for inducing AF. Additionally, the mice are generated by the crossing of two transgenic models that have less severe or no disease at baseline, making it less likely that the AF phenotype could be lost due to breeding complications.

4.4.4. Potential role of PI3K (p110 α) in human atrial fibrillation

Finally, to examine whether reduced PI3K (p110 α) activity was a feature associated with AF in humans, PI3K (p110 α) activity was assessed in atrial appendages from patients who either had acute or chronic AF compared with patients in sinus rhythm. Up to 50% of patients who undergo cardiothoracic surgery develop paroxysmal AF post-operatively (Aranki *et al.*, 1996; Chandy *et al.*, 2004; Dogan *et al.*, 2007). PI3K (p110 α) activity was reduced in coronary artery bypass graft surgery patients that

developed AF post-operatively compared with patients in sinus rhythm (Figure 62). Additionally, patients who had chronic AF due to mitral valve disease also had reduced PI3K (p110 α) activity (Figure 62). Together, these results suggest that reduced PI3K (p110 α) activity may be an important clinical predictor for the development of AF. It could be speculated that CABG surgery may trigger AF in patients who already have reduced PI3K (p110 α) activity under basal conditions (possibly due to aging or inactivity). This would be consistent with the dnPI3K mice that have normal cardiac function under basal conditions, but develop HF more rapidly in response to cardiac stress (McMullen *et al.*, 2003; McMullen *et al.*, 2007).

4.4.5. Increased PI3K (p110 α) activity can protect the stressed heart from cardiac conduction abnormalities

Both the animal and human studies suggested that decreased PI3K (p110 α) activity may predispose the heart to AF. To assess whether increased PI3K (p110 α) activity could also protect the stressed heart from the development of cardiac conduction abnormalities associated with AF observed in the dnPI3K-Mst1 mice, the electrophysiological characteristics of the caPI3K-Mst1 mice were compared with Mst1 mice alone. Since AF was not present in the Mst1 mice, even in aged mice, the direct effect of increased PI3K (p110 α) activity on AF incidence could not be assessed. However, in caPI3K-Mst1 mice, atrial fibrosis (a substrate often associated with the development of AF) was reduced by 34% compared with Mst1 mice (see Figure 63, page 177), and the mean P-R interval (indicative of cardiac conduction blockade) was reduced by 15% compared with Mst1 mice (see Section 4.3.6.). Taken together, these studies suggest that increased PI3K (p110 α) activity can protect the stressed heart from cardiac conduction abnormalities.

4.5. Conclusion

In conclusion, this chapter describes the generation of a genetic mouse model of AF that is associated with HF and overt atrial remodelling, simulating the clinical situation. The results demonstrate that a reduction of PI3K (p110 α) signalling accelerates HF in a setting of dilated cardiomyopathy and makes the heart susceptible to AF (summarised in Figure 64). A reduction of PI3K (p110 α) activity (a critical effector of insulin signalling) can potentially explain the link between risk factors such as aging, diabetes, and obesity with AF. Strategies that could activate PI3K (p110 α) specifically in the heart may represent a potential therapeutic intervention for HF and AF.

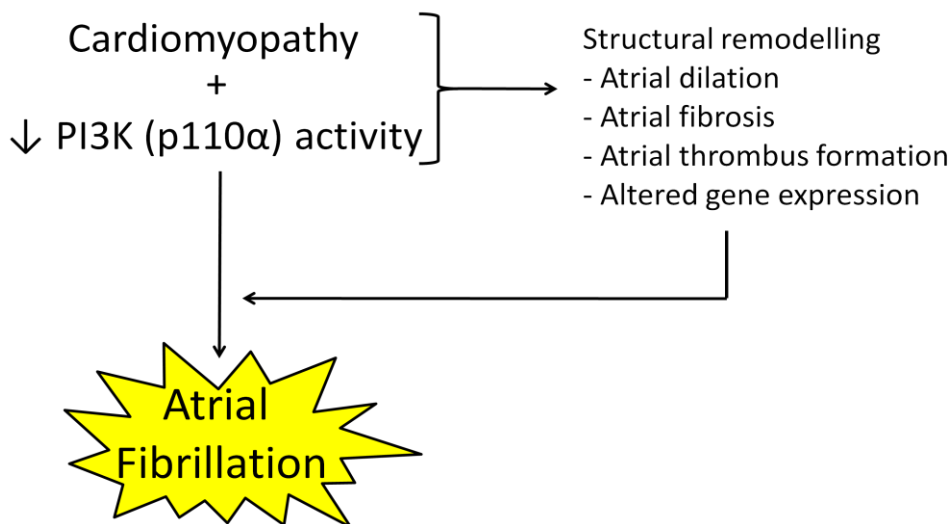


Figure 64. Mechanism of increased susceptibility to AF induced by the reduction of PI3K (p110 α) activity.

Chapter 5 – Role of PI3K (p110 α) in estrogen mediated cardioprotection

5.1. Introduction

As previously discussed (see Section 1.3.7.), males and females often respond differently in a setting of cardiac stress [extensively reviewed by (Du *et al.*, 2006) and (Luczak and Leinwand, 2009)]. Thus, there is a clear need for a more comprehensive understanding of gender-specific differences in a setting of cardiac disease. Pre-menopausal women are generally more protected against cardiovascular disease than aged-matched men and this protection has been attributed to the actions of estrogen (Mikkola and Clarkson, 2002; Sullivan, 2003). Interestingly, settings of diabetes and hypertension are associated with greater risk of cardiovascular disease in women compared with men (Regitz-Zagrosek, 2006) and PI3K (p110 α) signalling can be defective in these settings (Chen *et al.*, 2005; Hansen *et al.*, 2001; Kim *et al.*, 1999; Mauvais-Jarvis *et al.*, 2002; Ohanian and Heagerty, 1992). Previous studies have linked estrogen with the PI3K (p110 α)-Akt pathway. Estrogen can activate Akt in cardiac myocytes through a direct non-nuclear pathway involving the regulatory subunit of PI3K (i.e. p85) (Simoncini *et al.*, 2000), and it is known that female hearts have increased levels of Akt compared with males (Camper-Kirby *et al.*, 2001). Studies described in Chapter 3 of this thesis showed that female mice with depressed cardiac PI3K (p110 α) in a setting of dilated cardiomyopathy developed more severe disease than their male counterparts (see Figure 28, Figure 31, Figure 32, and Figure 33 pages 110-127). This suggested that the cardioprotection seen in females may be mediated through an interaction between PI3K (p110 α) and estrogen. As such, the final aim of this thesis was to examine the contribution of PI3K (p110 α) in mediating the cardioprotection attributed to estrogen. It was hypothesised that there would be an association between PI3K (p110 α) and ER α in the heart, and that this association would be critical for mediating the cardioprotective properties of estrogen in females.

5.2. Methods

5.2.1 Techniques used in this study

The following techniques were used for the studies described in this chapter:

- Transgenic mouse model generation (as described in Chapter 2, pages 63)
- Transgenic mouse model genotyping (as described in Chapter 2, pages 66-68)
- Ovariectomy surgery and estrogen replacement therapy (as described in Chapter 2, pages 77-79)
- Echocardiography (as described in Chapter 2, page 68)
- Tissue harvesting and tibia length measurement (as described in Chapter 2, page 80)
- Protein extraction, measurement of protein concentration, immunoprecipitation, and Western blotting (as described in Chapter 2, pages 81-87)

5.2.2. Animals

All animals used in the studies described in this chapter were female Ntg, caPI3K, dnPI3K, Mst1, caPI3K-Mst1 and dnPI3K-Mst1 mice at 3-4.5 months of age (dnPI3K-Mst1 mice have a mean lifespan of 4.5 months; see Section 3.3.1.). Animals underwent either ovariectomy or a sham operation (as described in Section 2.5.), and differences associated with ovariectomy are shown in comparison to sham-operated control mice of the same genotype. Due to breeding difficulties, only four dnPI3K mice were available for this study. All four dnPI3K mice were ovariectomised. Since no sham-operated mice were available for comparison, all measurements were shown in comparison with non-operated control female dnPI3K mice at 4.5 months of age (as previously characterised in Chapter 3, see pages 117-127).

A subset of mice was also subjected to estrogen replacement therapy or placebo treatment (as described in Section 2.5.) at the time of ovariectomy or the sham operation. Differences associated with estrogen replacement therapy are shown in comparison to mice that underwent either the ovariectomy operation alone or the sham-operation alone.

5.3. Results

5.3.1. Interaction between the regulatory subunit of PI3K (p110 α) and estrogen receptor α in the heart

To determine whether PI3K interacts with ER α in the adult heart, immunoprecipitation experiments were performed as previously described (see Section 2.7.5.). Control heart (Ntg) samples were immunoprecipitated with a PI3K p85 antibody and then probed with an ER α antibody (see Table 11, page 85). Detection of ER α in those samples immunoprecipitated with a PI3K (p85) antibody indicates that PI3K associates with ER α in the adult heart (Figure 65).

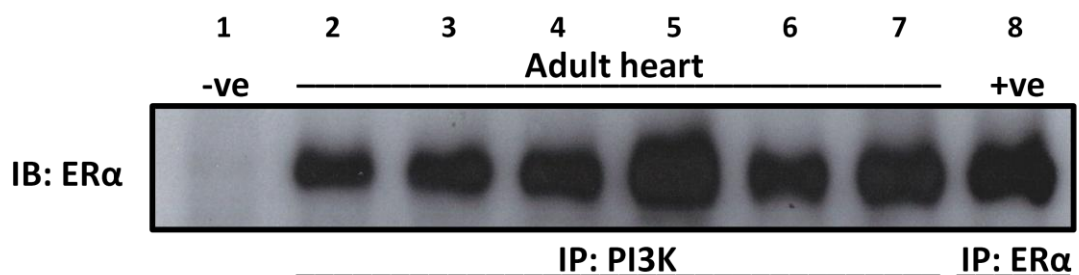


Figure 65. Estrogen receptor α is associated with the regulatory subunit of phosphoinositide 3-kinase (p110 α) in the heart.

Phosphoinositide 3-kinase (p110 α) (PI3K) interacts with estrogen receptor α (ER α) in the adult heart (non-transgenic mice; n=6). Lane 1: negative (-ve) control (heart lysate without antibody), Lanes 2-7: heart lysate (cytosolic fraction) from 6 different non-transgenic mice immunoprecipitated with an antibody against the p85 regulatory subunit of PI3K, and Lane 8: positive (+ve) control (heart sample immunoprecipitated with 1 μ l of ER α antibody). IP: immunoprecipitate, and IB: immunoblot.

5.3.2. Effectiveness of ovariectomy surgery

Uterus weight was measured to confirm that the ovariectomy operation had been successful (Figure 66). Uterus weight [expressed as uterus weight to tibia length ratio (UW/TL)] was significantly decreased (91% decrease) in mice that underwent ovariectomy surgery compared with sham-operated mice (Figure 66).

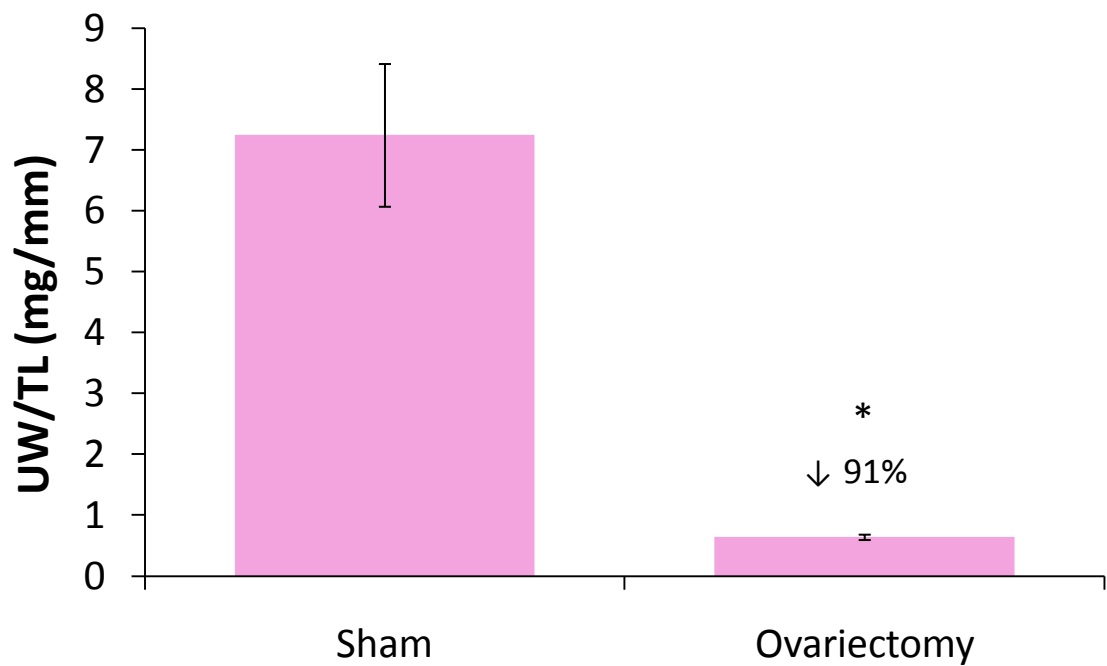


Figure 66. Uterus weight of ovariectomised and sham-operated mice.

Ovariectomised Ntg mice ($n=12$) have a 91% reduction in uterus weight / tibia length ratio (UW/TL) compared with sham-operated Ntg mice ($n=11$), confirming the effectiveness of the ovariectomy surgery. * $p<0.0001$ compared with sham.

5.3.3. Phenotype of ovariectomised mice

5.3.3.1. Cardiac chamber dimensions and systolic function

Cardiac chamber dimensions and wall thicknesses were assessed from echocardiographic images as described earlier (see Section 2.4.1.). Tibia lengths and heart rates were comparable between all groups (Table 29). Sham-operated Mst1, caPI3K-Mst1 and dnPI3K-Mst1 mice had significantly larger LVESD compared with Ntg, caPI3K or dnPI3K mice (Table 29), as previously shown in non-operated mice (see Chapter 3). Ovariectomy tended to decrease LVESD in the Mst1 mice ($p=0.16$) compared with sham-operated controls, but did not affect LVESD in any of the other groups (Table 29). No significant difference was seen in LVEDD or wall thicknesses in any of the groups following ovariectomy (Table 29).

Systolic function was assessed as previously described (see Section 2.4.1.). As previously shown in Chapter 3 (see Table 16 and Figure 29, pages 112 and 115), Mst1 mice had depressed fractional shortening compared with Ntg mice under control/sham conditions. caPI3K-Mst1 mice had improved fractional shortening, while dnPI3K-Mst1 mice had reduced fractional shortening, compared with Mst1 mice alone (see Chapter 3, Table 16). While statistically insignificant (due to small numbers in the caPI3K-Mst1 sham group; $n=4$), similar differences/trends were seen in the sham-operated caPI3K-Mst1 and dnPI3K-Mst1 mice (Table 29). Interestingly, there was a small but significant improvement in fractional shortening in the ovariectomised Mst1 mice (Table 29, Figure 67). Ovariectomy had no significant effect on fractional shortening in any of the other groups (Table 29, Figure 67).

5.3.3.2. Morphology

Increased body weight following ovariectomy was reported by Holt and colleagues (Holt *et al.*, 1936), and has since been well documented in other studies [reviewed in (Butera, 2010)]. Similar to previous studies, there was also a significant increase in body weight following ovariectomy in the current study (Figure 68, Table 30).

Organ weights at autopsy (4-4.5 months of age) were assessed and are shown in Table 30. UW/TL was significantly reduced in all ovariectomised groups

Table 29. Effect of ovariectomy on cardiac chamber dimensions and left ventricular wall thicknesses at 4-4.5 months of age.

LVEDS: left ventricular end-systolic dimension; LVEDD: left ventricular end-diastolic dimension; LVPW: left ventricular posterior wall thickness; and IVS: interventricular septal width; Non-op: non-operated control. ~ $p < 0.05$ compared with sham of the same genotype; * $p < 0.05$ compared with Ntg that underwent the same procedure; ‡ $p < 0.05$ compared with caPI3K that underwent the same procedure; ^ $p < 0.05$ compared with dnPI3K that underwent the same procedure; # $p < 0.05$ compared with Mst1 that underwent the same procedure; § $p = 0.09$ compared with Mst1 that underwent the same procedure; and † $p < 0.05$ compared with caPI3K-Mst1 that underwent the same procedure.

	Procedure	N	Tibia Length (mm)	Heart Rate (beats per minute)	LVEDS (mm)	LVEDD (mm)	LVPW (mm)	IVS (mm)	Fractional shortening (%)
Ntg	Sham	5	17.1 ± 0.1	536 ± 4	1.88 ± 0.12	3.77 ± 0.21	0.74 ± 0.07	0.93 ± 0.03	50 ± 1
	Ovariectomy	5	16.9 ± 0.3	535 ± 19	1.66 ± 0.14	3.56 ± 0.08	0.76 ± 0.04	0.95 ± 0.04	54 ± 3
caPI3K	Sham	4	17.2 ± 0.1	532 ± 6	1.86 ± 0.04	4.08 ± 0.08	0.78 ± 0.11	1.02 ± 0.11	54 ± 0.2
	Ovariectomy	5	17.0 ± 0.1	543 ± 11	1.77 ± 0.12	3.88 ± 0.12	0.76 ± 0.08	1.10 ± 0.07	54 ± 2
dnPI3K	Non-op	8	17.4 ± 0.1	502 ± 11	1.89 ± 0.09	3.71 ± 0.12	0.54 ± 0.03 *‡	0.70 ± 0.05 *‡	49 ± 2
	Ovariectomy	4	17.0 ± 0.3	505 ± 20	1.76 ± 0.12	3.50 ± 0.18	0.59 ± 0.07 *‡	0.63 ± 0.04 *‡	50 ± 2
Mst1	Sham	5	17.3 ± 0.1	504 ± 22	2.83 ± 0.13 *‡^	4.10 ± 0.13 *^	0.73 ± 0.05 ^	0.66 ± 0.09 *‡	31 ± 1 *‡^
	Ovariectomy	7	17.1 ± 0.2	523 ± 14	2.65 ± 0.17 *‡^	4.19 ± 0.19 *^	0.77 ± 0.05 ^	0.68 ± 0.07 *‡	37 ± 2 ~*‡^
caPI3K-Mst1	Sham	4	17.2 ± 0.1 (n=3)	491 ± 4	2.88 ± 0.20 *‡^	4.54 ± 0.26 *^	0.75 ± 0.11 ^	0.80 ± 0.13	37 ± 2 *‡^
	Ovariectomy	3	17.1 ± 0.2	547 ± 19	2.76 ± 0.14 *‡^	4.21 ± 0.17 *^	0.86 ± 0.07 ^	0.73 ± 0.11 *‡	34 ± 1 *‡^
dnPI3K-Mst1	Sham	5	17.1 ± 0.2	503 ± 16	3.59 ± 0.29 *‡^#†	4.80 ± 0.16 *‡^#	0.54 ± 0.07 *‡#†	0.60 ± 0.07 *‡†	26 ± 4 *‡^§†
	Ovariectomy	4	17.6 ± 0.1	528 ± 11	3.28 ± 0.31 *‡^#	4.63 ± 0.29 *‡^#	0.50 ± 0.05 *‡#†	0.67 ± 0.08 *‡	30 ± 2 *‡^#

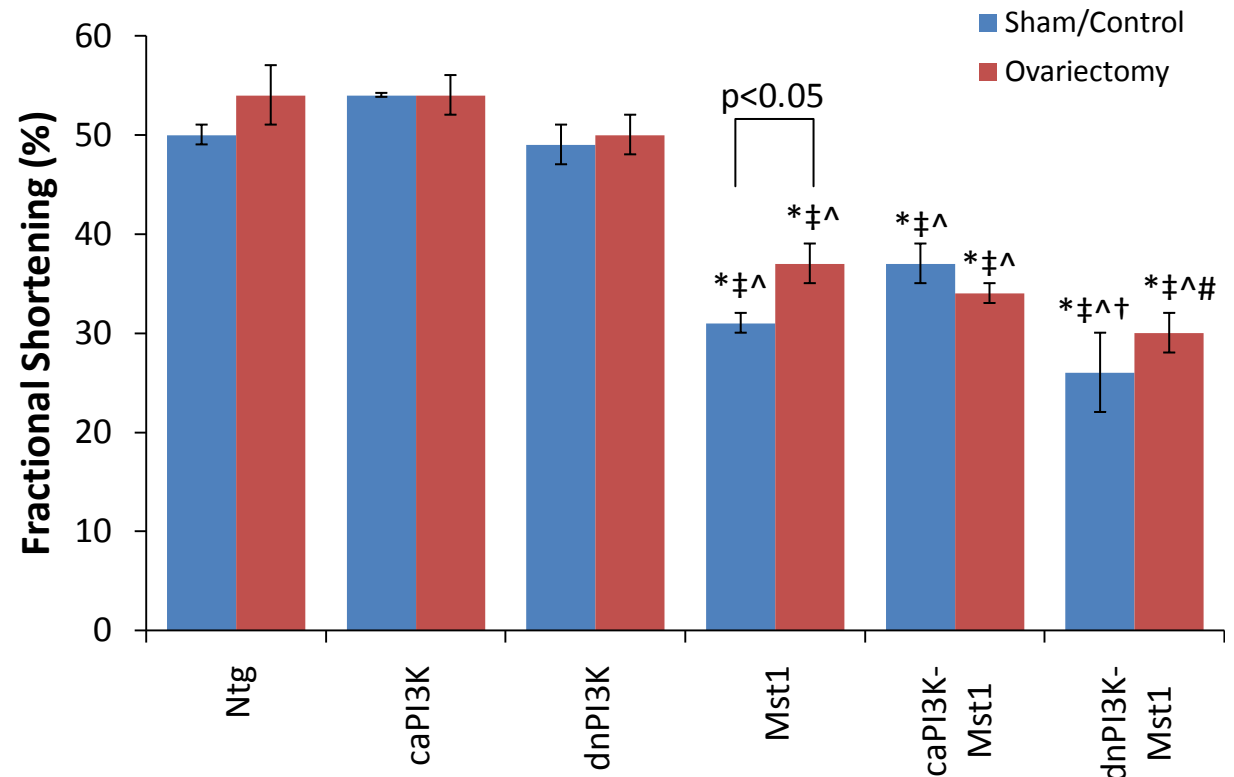
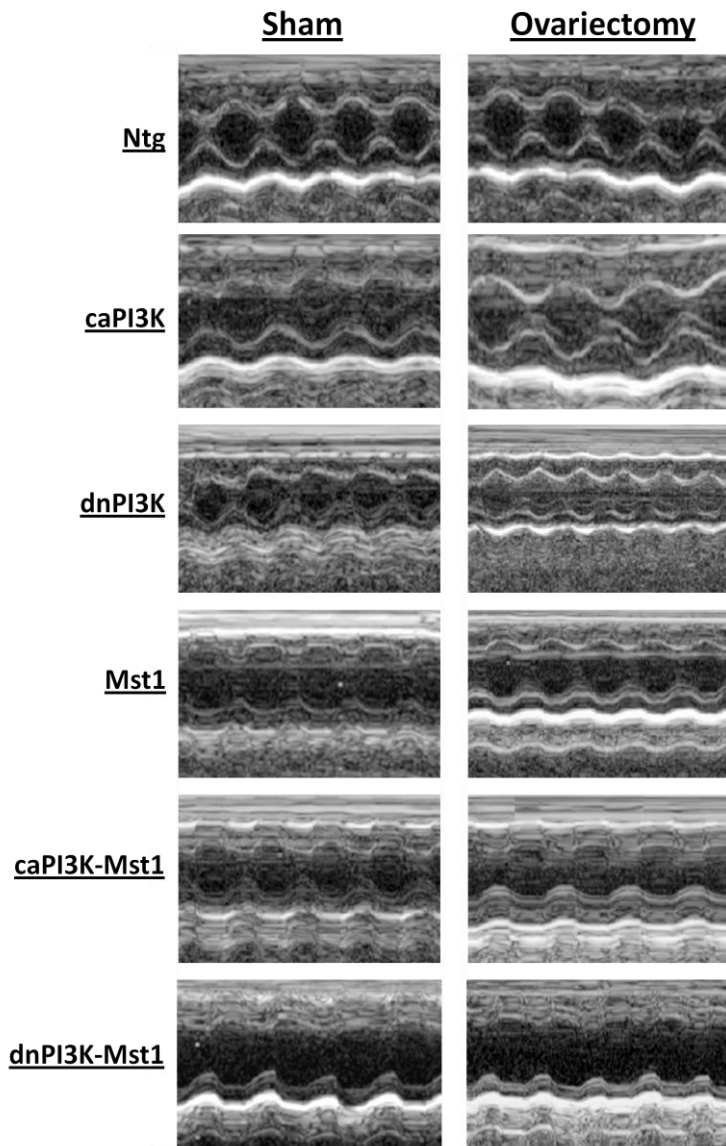


Figure 67. Fractional shortening in transgenic mice at 4-4.5 months of age that underwent ovariectomy or a sham operation.

* $p < 0.05$ compared with Ntg that underwent the same procedure; † $p < 0.05$ compared with caPI3K that underwent the same procedure; ^ $p < 0.05$ compared with dnPI3K that underwent the same procedure; # $p < 0.05$ compared with Mst1 that underwent the same procedure; and † $p < 0.05$ compared with caPI3K-Mst1 that underwent the same procedure. $n = 3-8$ in each group.

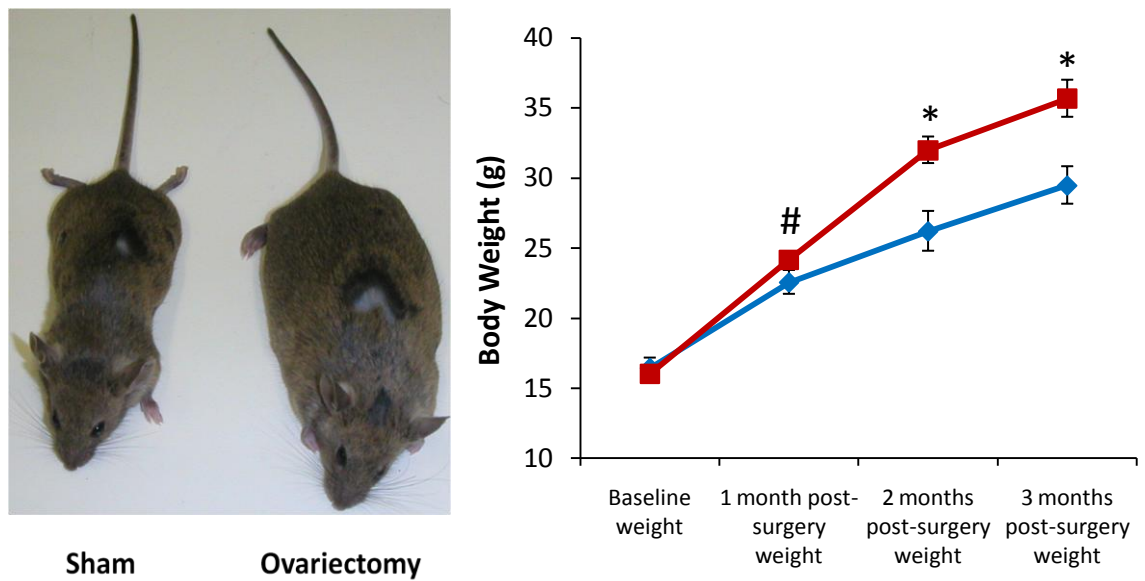


Figure 68. Body weight gain in mice following ovariectomy.

Left panel: An ovariectomised non-transgenic mouse displayed increased body weight compared with a sham-operated non-transgenic littermate. **Right panel:** Quantitative analysis of body weight from Ntg mice at 3.5-4 weeks of age (baseline weight), and at monthly intervals following ovariectomy ($n=13$, red) or sham ($n=11$, blue) surgery (1 month post-surgery weight, 2 months post-surgery weight, and 3 months post-surgery weight). * $p<0.05$ compared with sham-operated mice of the same age, and # $p=0.08$ compared with sham-operated mice of the same age.

Table 30. Effect of ovariectomy on organ weights of transgenic mice at 4-4.5 months of age.

OVX: ovariectomy (4-4.5 months of age); Non-op: non-operated control (4 months of age); N/A: not assessed; BW - Start: body weight prior to surgery; BW – End: body weight at end of study; TL: tibia length; HW/BW: heart weight/body weight ratio; HW/TL: heart weight/tibia length ratio; AW/TL: atrial weight/tibia length ratio; LW/TL: lung weight/tibia length ratio; and UW/TL: uterus weight/tibia length ratio. For simplicity this table highlights significant differences with Ntg mice that underwent the same procedure (* $p<0.05$), and significant differences of ovariectomised mice compared with sham or non-operated control mice (~ $p<0.05$). A table showing all significant differences is presented in Appendix 1.

	Proce- dure	N	BW – Start (g)	BW – End (g)	TL (mm)	Heart weight (mg)	HW/TL (mg/mm)	Atrial weight (mg)	AW/TL (mg/mm)	Lung weight (mg)	LW/TL (mg/mm)	Uterus weight (mg)	UW/TL (mg/mm)
Ntg	Sham	11	16.4±0.7	29.2±1.4	17.0±0.1	116.6±2.9	6.84±0.15	6.4±0.3	0.38±0.02	154.0±3.9	9.04±0.21	122.1±16.5	7.17±0.97
	OVX	13	16.0±0.6	35.6±1.5~	17.1±0.1	112.9±3.5	6.59±0.17	5.6±0.2	0.33±0.01	153.0±3.5	8.93±0.16	11.0±0.7~	0.64±0.04~
caPI3K	Sham	7	15.2±0.5	26.3±0.8	17.0±0.1	137.3±2.4*	8.07±0.12*	5.9±0.3	0.35±0.02	154.2±5.6	9.07±0.31	92.2±10.8*	5.43±0.64*
	OVX	5	14.9±0.5	34.8±1.4~	16.9±0.1	131.9±3.3*	7.80±0.16*	5.9±0.4	0.35±0.02	150.5±2.6	8.90±0.13	9.2±0.8~	0.54±0.05~
dnPI3K	Non-op	10	N/A	25.2±0.3	17.0±0.1	88.6±1.2*	5.21±0.06*	4.2±0.2	0.25±0.01	143.1±1.7	8.42±0.12	N/A	N/A
	OVX	4	15.8±0.5	31.8±2.2~	17.0±0.3	80.9±1.5*	4.76±0.06*	3.9±0.5	0.23±0.03	148.5±6.8	8.73±0.28	10.7±1.4	0.63±0.09
Mst1	Sham	5	17.3±1.1	30.4±1.3	17.3±0.1	136.1±2.8*	7.89±0.14*	14.4±1.5*	0.83±0.09*	180.7±7.6*	10.48±0.43*	106.6±8.1	6.18±0.46
	OVX	9	15.4±0.6	35.5±1.7~	17.2±0.2	122.2±4.9~	7.08±0.23~*	12.6±0.9*	0.73±0.05*	161.8±8.2~	9.38±0.43~	12.4±1.2~	0.72±0.07~
caPI3K- Mst1	Sham	3	15.7±1.2	27.2±0.7	17.2±0.1	132.3±2.1*	7.69±0.12*	13.5±0.5*	0.79±0.03*	172.8±2.9*	10.05±0.23*	83.1±4.6*	4.84±0.30*
	OVX	6	15.5±0.7	34.7±2.0~	17.2±0.1	125.9±5.1*	7.33±0.28*	12.3±0.6*	0.72±0.04*	166.1±4.2	9.68±0.23	8.4±1.2~	0.49±0.07~
dnPI3K- Mst1	Sham	5	16.0±1.0	27.3±0.9	17.1±0.2	125.0±5.8	7.29±0.27	14.6±1.6*	0.85±0.08*	182.8±10.3*	10.67±0.52*	128.6±6.8	7.51±0.38
	OVX	7	16.4±0.7	39.1±1.9~	17.5±0.1	130.1±6.9*	7.42±0.37*	16.5±1.7*	0.94±0.09*	176.9±6.6*	10.10±0.35*	13.7±1.5~	0.78±0.08~

(Table 30). Ovariectomy did not significantly alter HW/TL, AW/TL, or LW/TL in Ntg, caPI3K or dnPI3K mice (Table 30). Ovariectomy improved fractional shortening in the Mst1 mice (see Figure 67), and this was associated with a decrease in HW/TL, LW/TL, and a trend for a decrease in AW/TL (Figure 69, Table 30). Ovariectomy had no significant effect on HW/TL, AW/TL, or LW/TL in caPI3K-Mst1 or dnPI3K-Mst1 mice (Table 30).

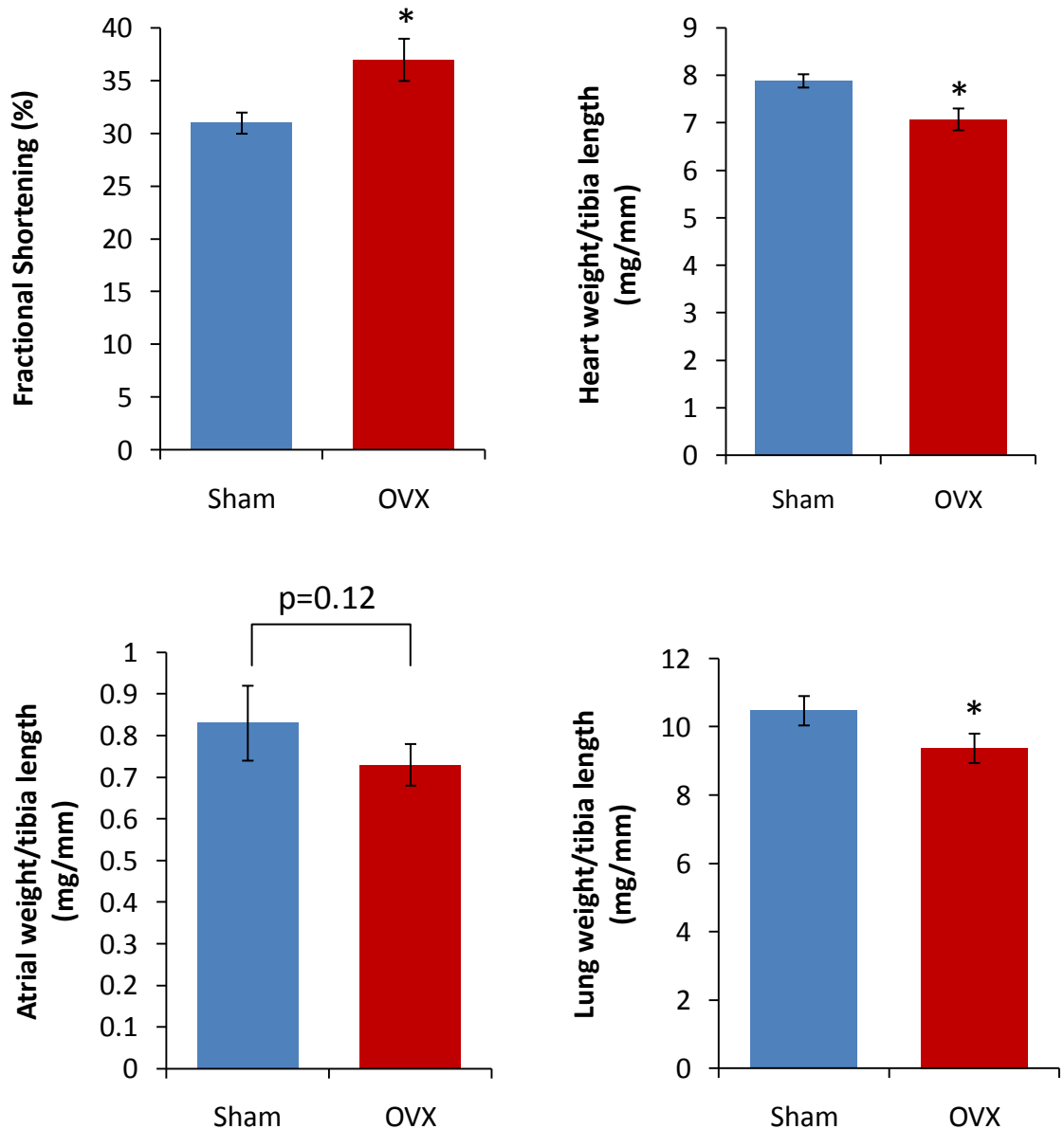


Figure 69. Mst1 mice show an improved cardiac phenotype following ovariectomy.

Mst1 mice that underwent ovariectomy (OVX, n=7-9) have improved systolic function (fractional shortening) and displayed reduced heart weight, and lung weight, as well as a trend for decreased atrial weight, compared with Mst1 mice that underwent a sham operation (n=5).

* $p < 0.05$ compared with Mst1 sham; and § $p = 0.12$ compared with Mst1 Sham.

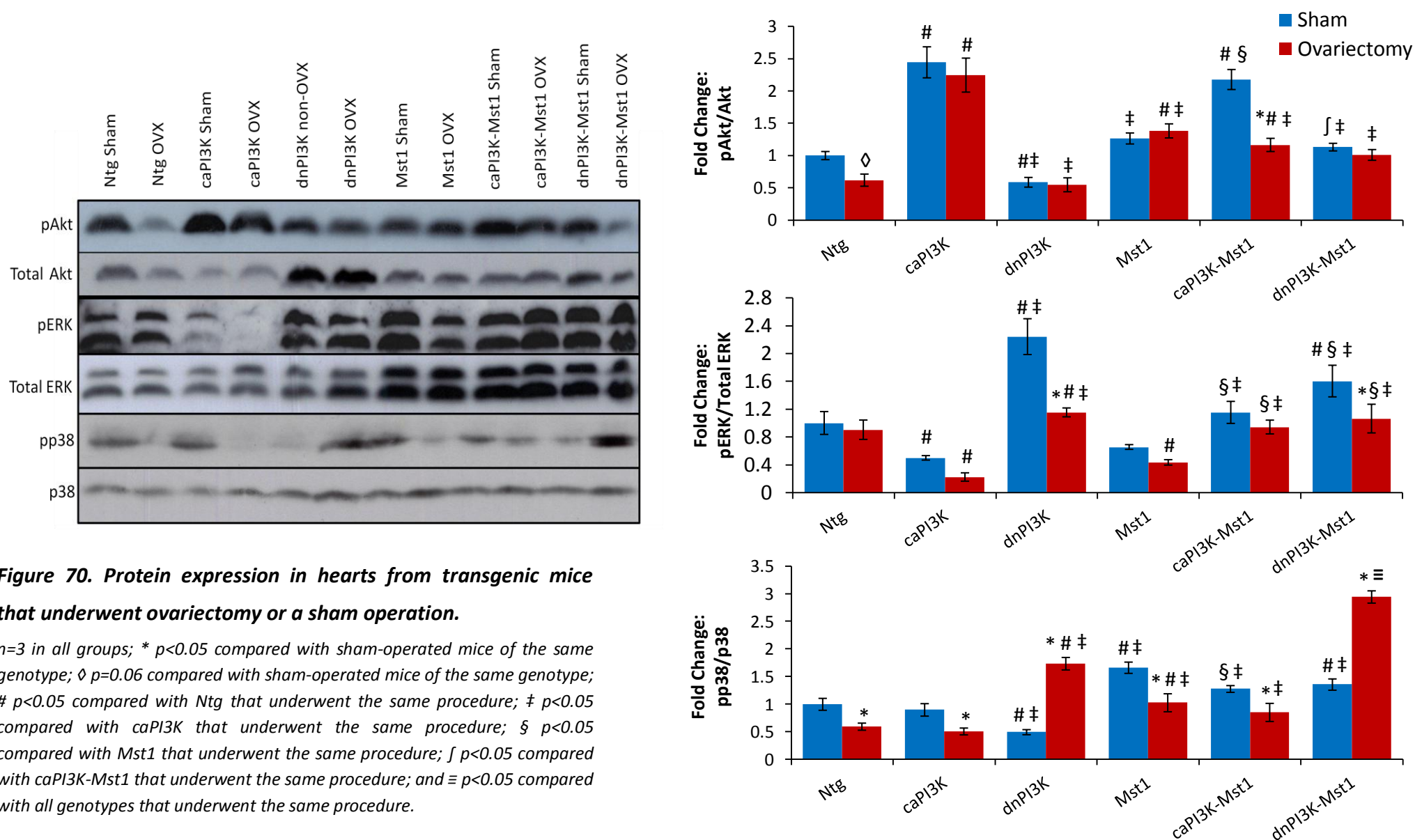
5.3.4. Protein expression in heart tissue following ovariectomy

Heart tissue was obtained from ovariectomised or sham-operated transgenic mice and protein expression of pAkt, pERK, and pp38 was analysed as previously described (see Section 2.7.). There was a strong trend for a decrease in pAkt expression between sham-operated and ovariectomised Ntg mice ($p=0.06$; Figure 70). As seen with the initial characterisation of the transgenic mice (see Figure 43, page 139), sham-operated caPI3K and caPI3K-Mst1 mice showed a significant increase in pAkt expression compared with sham-operated Ntg mice (Figure 70). Non-operated dnPI3K mice had decreased pAkt expression compared with sham-operated Ntg mice (Figure 70). There was no difference in pAkt expression between sham-operated Ntg, Mst1, and dnPI3K-Mst1 mice (Figure 70). Ovariectomy did not affect pAkt expression in the caPI3K, dnPI3K, Mst1, or dnPI3K-Mst1 mice compared with sham-operated mice (Figure 70). Interestingly, there was a reduction in pAkt expression in the ovariectomised caPI3K-Mst1 mice compared with sham-operated caPI3K-Mst1 mice (Figure 70).

There was no difference in pERK expression between sham-operated or ovariectomised Ntg mice (Figure 70). As previously found (see Figure 43, page 139), sham-operated caPI3K mice displayed decreased pERK expression compared with sham-operated Ntg mice, while non-operated dnPI3K mice had increased pERK expression compared with sham-operated Ntg mice (Figure 70). Sham-operated dnPI3K-Mst1 had greater pERK expression compared with sham-operated Ntg mice (Figure 70). Ovariectomy reduced pERK expression in the dnPI3K mice and dnPI3K-Mst1 mice (Figure 70).

As observed with the initial characterisation of the transgenic mice (see Figure 43, page 139), sham-operated Mst1 and dnPI3K-Mst1 mice had increased pp38 expression compared with sham-operated Ntg mice (Figure 70). Ovariectomy reduced pp38 in hearts of Ntg, caPI3K, Mst1, and caPI3K-Mst1 mice (Figure 70). In contrast, ovariectomy increased pp38 in hearts of dnPI3K and dnPI3K-Mst1 mice (Figure 70).

The significance of the changes in protein expression is currently unclear. The relationship between expression of signalling proteins in the hearts of ovariectomised Mst1 mice with the observed improvement in cardiac parameters (Figure 69) is complex and will require further investigation.



5.3.5. Effect of estrogen replacement following ovariectomy

To determine whether estrogen replacement could reverse the effects of ovariectomy, a subset of transgenic mice were subjected to ovariectomy and estrogen replacement therapy simultaneously, as previously described (see Section 2.5.).

5.3.5.1. Effectiveness of estrogen replacement

To confirm that estrogen replacement had been successful, uterus weights from sham-operated Ntg mice that received a placebo pellet were compared with ovariectomised Ntg mice that received estrogen pellets (Figure 71). Uterus weight was not different between the two groups (Figure 71).

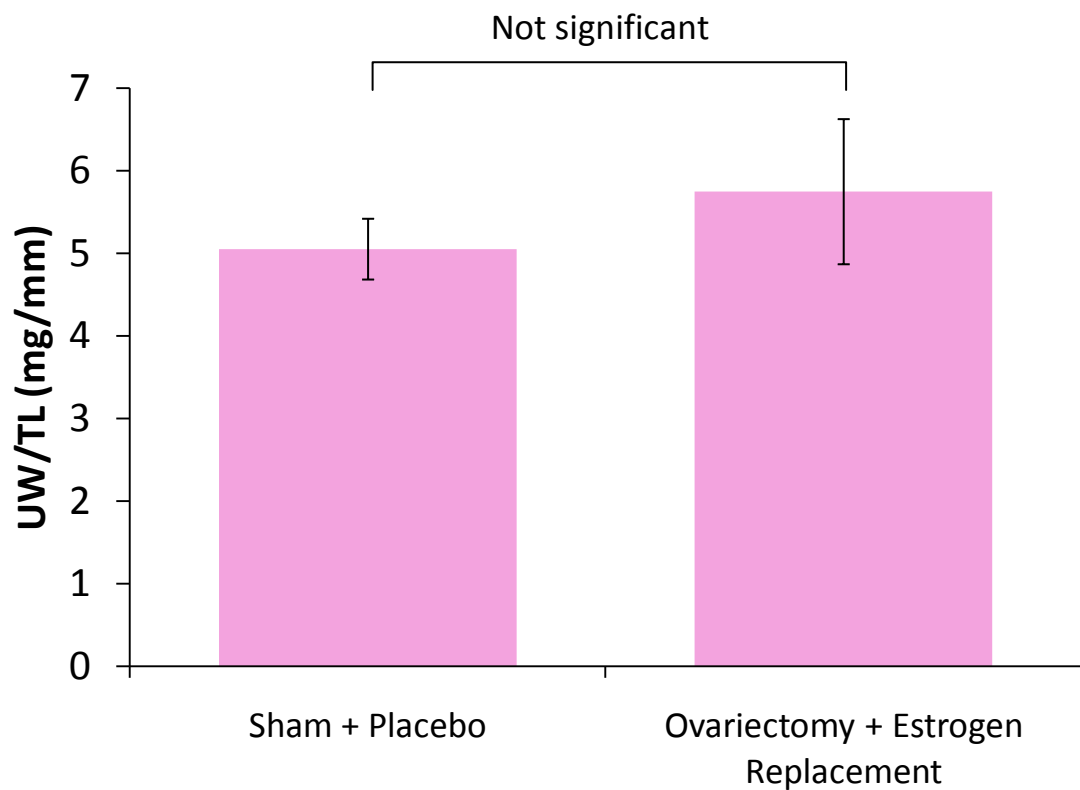


Figure 71. Uterus weight/tibia length in sham-operated mice that received placebo pellets compared with ovariectomised mice that received estrogen pellets.

No difference in uterus weight/tibia length (UW/TL) was observed between sham-operated mice that received placebo treatment ($n=4$) and ovariectomised mice that received estrogen replacement ($n=4$).

5.3.5.2. Unexpected adverse effect of estrogen replacement therapy

Estrogen replacement at the time of ovariectomy induced unexpected side effects in the transgenic mice. Initially, a dose of 27.8 μ g/day 17 β -estradiol (90-day pellet, 2.5mg) was administered subcutaneously as had previously been reported (Cavasin *et al.*, 2003; Lekgabe *et al.*, 2006). At approximately 4 months of age (3 months following ovariectomy surgery and estrogen replacement), it was observed that 3 of 9 mice had swollen abdomens and appeared to be in some discomfort. Upon autopsy, swelling of the bladder due to urinary retention was found in all of the mice. These side-effects have only been previously reported in immune compromised mice (Pearse *et al.*, 2009; Walker *et al.*, 1992) or mice receiving estrogen pellets for over 4 months (Levin-Allerhand *et al.*, 2003).

Since the supra-physiological concentration of 17 β -estradiol was suspected to be the cause of the observed side-effects, the dose was halved in a subsequent subset of mice. Six mice in a cohort of 17 were ovariectomised and received the half estrogen dose (1.25mg, 90-day release 17 β -estradiol pellet; dose restored uterus weights to sham values). The other 11 mice in the cohort served as controls (included ovariectomy alone, sham mice, and ovariectomy plus placebo pellet). At 3 months of age (2 months following surgery) bladder enlargement was identified by palpitation and echocardiography. At autopsy, 5 of the 6 mice that had been ovariectomised and received half an estrogen pellet had noticeably enlarged bladders. Based on pathology results, this did not lead to abnormal pathology of the bladder or back pressure on the kidney. However, if these mice had been left for the time frame proposed in my studies (approximately 3 months) abnormal pathology may have developed. The Ntg mice that received a placebo pellet following sham surgery did not develop any of the above-noted side effects. As a result of these side effects and to remain compliant with the Alfred Medical Research and Education Precinct Animal Ethics Committee it was necessary to cease the estrogen replacement study. Consequently, mouse numbers in these experimental groups are lower than initially planned. Furthermore, comparison between the estrogen replacement and ovariectomy mice is not ideal, because the majority of the estrogen replacement mice were dissected at 3-3.5 months of age, whereas the majority of the ovariectomy mice were dissected at 4-4.5 months of age.

5.3.5.3. Cardiac chamber dimensions and fractional shortening following estrogen replacement

Tibia lengths were smaller in the mice that underwent ovariectomy and received estrogen replacement, but this can be explained by the younger age of these mice (3-3.5 months compared with 4-4.5 months; see Table 34 in Appendix 3). As previously shown, ovariectomy seemed to improve LVESD and fractional shortening in Mst1 mice (Table 29), but had no significant impact in any other group. Estrogen replacement appeared to reverse the effect of ovariectomy in the Mst1 mice, leading to a cardiac phenotype similar to sham-operated Mst1 mice (Figure 72). Estrogen replacement had no apparent effect on the cardiac phenotype of the Ntg, caPI3K-Mst1, or dnPI3K-Mst1 mice (see Table 34 in Appendix 3).

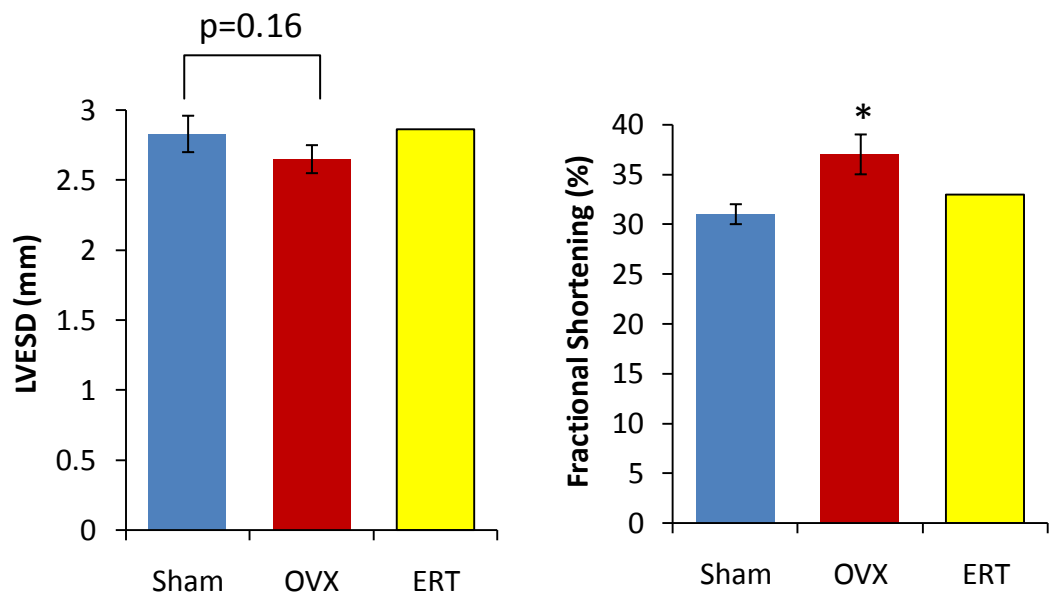


Figure 72. Mst1 mice show improved cardiac function following ovariectomy, which appears to be reversed by estrogen replacement.

Mst1 mice that underwent ovariectomy (OVX, red colour, n=7) tended to have reduced left ventricular end systolic dimension (LVESD, see Table 29) and had improved systolic function (fractional shortening) compared with Mst1 mice that underwent a sham operation (Sham, blue colour, n=5). Estrogen replacement (ERT, yellow colour, n=2) appeared to reverse these effects. * $p < 0.05$ compared with sham.

5.3.5.4. Morphology of ovariectomised mice with or without estrogen replacement

The effect of estrogen replacement on organ weights of ovariectomised mice is presented in Table 31. Of note, due to the complications associated with administration of estrogen pellets, the sham and ovariectomised mice are approximately 4-4.5 months of age. In contrast, the ovariectomised mice that received estrogen pellets were approximately 3 months of age. Furthermore, numbers are low in the ovariectomy plus estrogen replacement groups. Consequently, interpretation of this data is complicated and should be examined with caution, but provides some insight for future studies (as discussed in Section 5.5.).

A subset of Ntg mice were subjected to the sham operation and received placebo pellets. There was no difference in cardiac function or organ weights in these mice compared with Ntg sham operated mice without a pellet. Estrogen replacement significantly increased UW/TL ratios compared with ovariectomised mice (Table 31). Interestingly, estrogen replacement was less effective in the dnPI3K-Mst1 mice in terms of restoring uterus weight (Table 31). The reason for this is unclear. Despite the ovariectomy plus estrogen replacement groups being younger than sham or ovariectomised mice alone, estrogen pellets seemed to prevent the weight gain observed in ovariectomised mice (Table 31). Differences in tibial length can be explained by the different ages of the mice (Table 31).

In Mst1 mice, ovariectomy decreased HW/TL, AW/TL, and LW/TL (Table 31, see also Appendix 2). Estrogen replacement seemed to reverse this effect (Table 31, Figure 73). Though, this data should be treated with some caution because there were only two mice in the ovariectomy plus estrogen replacement Mst1 group. Neither ovariectomy nor estrogen replacement therapy altered the cardiac phenotype of the caPI3K-Mst1 or dnPI3K-Mst1 mice (see Table 31, Appendix 2, and Appendix 3).

Table 31. Effect of estrogen replacement on organ weights of ovariectomised transgenic mice.

OVX: ovariectomy (4-4.5 months of age); OVX+ERT: ovariectomy followed by estrogen replacement therapy (3-3.5 months of age); N/A: not assessed; BW - Start: body weight prior to surgery; BW – End: body weight at end of study; TL: tibia length; HW/BW: heart weight/body weight ratio; HW/TL: heart weight/tibia length ratio; AW/TL: atrial weight/tibia length ratio; LW/TL: lung weight/tibia length ratio; and UW/TL: uterus weight/tibia length ratio. ~ $p < 0.05$ compared with sham; and § $p < 0.05$ compared with OVX. The statistics for the Mst1 OVX group are the same as in Table 30, as a comparison with the Mst1 OVX+ERT group could not be made ($n=2$). For simplicity this table only highlights significant differences compared with sham-operated, OVX, and OVX+ERT mice. A table showing all significant differences is presented in Appendix 2.

	Proce- dure	N	BW – Start (g)	BW – End (g)	TL (mm)	Heart weight (mg)	HW/TL (mg/mm)	Atrial weight (mg)	AW/TL (mg/mm)	Lung weight (mg)	LW/TL (mg/mm)	Uterus weight (mg)	UW/TL (mg/mm)
Ntg	Sham	11	16.4±0.7	29.2±1.4	17.0±0.1	116.6±2.9	6.84±0.15	6.4±0.3	0.38±0.02	154.0±3.9	9.04±0.21	122.1±16.5	7.17±0.97
	OVX	13	16.0±0.6	35.6±1.5~	17.1±0.1	112.9±3.5	6.59±0.17	5.6±0.2	0.33±0.01	153.0±3.5	8.93±0.16	11.0±0.7~	0.64±0.04~
	OVX+ERT	3	16.2±0.7	21.5±0.8~§	15.5±0.1~§	88.1±2.7~§	5.69±0.12	5.2±0.9	0.33±0.06	124.0±4.7~§	8.02±0.23	84.0±18.1§	5.42±1.15§
Mst1	Sham	5	17.3±1.1	30.4±1.3	17.3±0.1	136.1±2.8	7.89±0.14	14.4±1.5	0.83±0.09	180.7±7.6	10.48±0.43	106.6±8.1	6.18±0.46
	OVX	9	15.4±0.6	35.5±1.7~	17.2±0.2	122.2±4.9~	7.08±0.23~	12.6±0.9	0.73±0.05	161.8±8.2~	9.38±0.43~	12.4±1.2~	0.72±0.07~
	OVX+ERT	2	16.8	25.9	15.9	134.5	8.50	15.1	0.94	196.6	12.44	95.6	5.95
caPI3K- Mst1	Sham	3	15.7±1.2	27.2±0.7	17.2±0.1	132.3±2.1	7.69±0.12	13.5±0.5	0.79±0.03	172.8±2.9	10.05±0.23	83.1±4.6	4.84±0.30
	OVX	6	15.5±0.7	34.7±2.0~	17.2±0.1	125.9±5.1	7.33±0.28	12.3±0.6	0.72±0.04	166.1±4.2	9.68±0.23	8.4±1.2~	0.49±0.07~
	OVX+ERT	6	14.4±1.1	22.6±0.6§	15.4±0.3~§	111.1±4.2	7.22±0.23	11.7±0.8	0.76±0.05	142.2±4.6~§	9.24±0.23	96.6±21.0§	6.27±1.53§
dnPI3K- Mst1	Sham	5	16.0±1.0	27.3±0.9	17.1±0.2	125.0±5.8	7.29±0.27	14.6±1.6	0.85±0.08	182.8±10.3	10.67±0.52	128.6±6.8	7.51±0.38
	OVX	7	16.4±0.7	39.1±1.9~	17.5±0.1	130.1±6.9	7.42±0.37	16.5±1.7	0.94±0.09	176.9±6.6	10.10±0.35	13.7±1.5~	0.78±0.08~
	OVX+ERT	4	18.3±1.5	23.0±0.8§	15.7±0.2~§	141.1±18.5	9.01±1.19	21.3±7.1	1.35±0.43	165.3±16.5	10.53±0.96	54.1±4.2~§	3.45±0.24~§

Note: Data for sham and OVX mice from each group are the same as shown in Table 30.

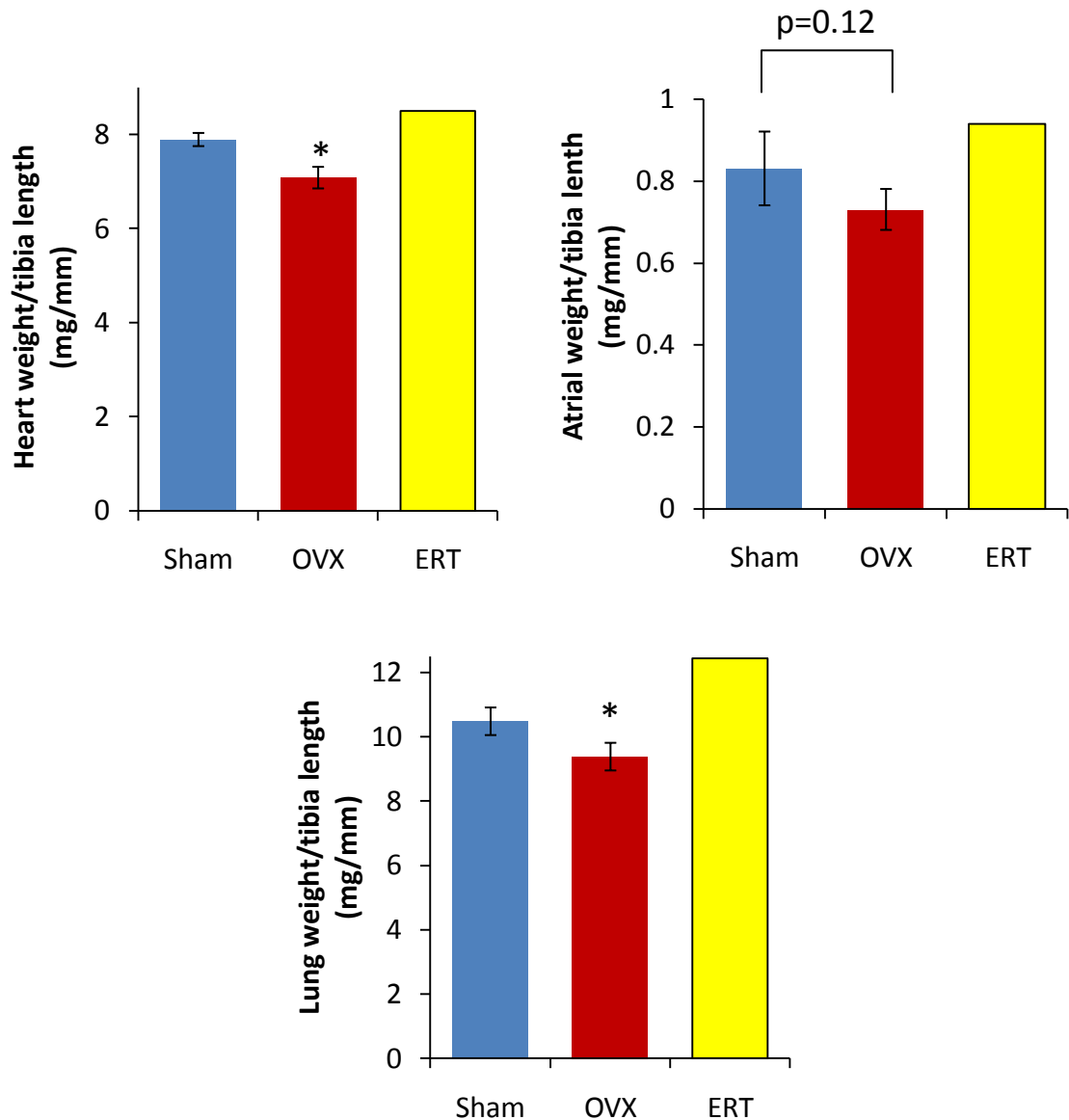


Figure 73. *Mst1* mice show an improved cardiac phenotype following ovariectomy, which appears to be reversed by estrogen replacement.

Mst1 mice that underwent ovariectomy (OVX, red colour, $n=9$) have reduced heart weight, atrial weight, and lung weight compared with *Mst1* mice that underwent a sham operation (Sham, blue colour, $n=5$). Estrogen replacement (ERT, yellow colour, $n=2$) appeared to reverse these effects. * $p<0.05$ compared with sham.

5.4. Discussion

5.4.1. Summary of major findings

Experiments in this chapter were designed to investigate the role of an interaction between estrogen and PI3K (p110 α) in mediating cardioprotection in the female heart in a setting of dilated cardiomyopathy. I was able to demonstrate that the regulatory subunit of PI3K (p110 α) complexes with ER α in the adult mouse heart. The initial hypothesis was that ovariectomy would have an adverse effect on cardiac parameters in Mst1 mice. In contrast, ovariectomy improved cardiac function in the Mst1 mice and estrogen replacement seemed to reverse this effect. It was also hypothesised that if the effects of estrogen were largely mediated via PI3K (p110 α), ovariectomy and estrogen replacement would have little effect in the caPI3K-Mst1 or dnPI3K-Mst1 mice, because PI3K (p110 α) is already constitutively activated or depressed, respectively. Consistent with this hypothesis, ovariectomy with or without estrogen replacement had no significant effect in caPI3K-Mst1 or dnPI3K-Mst1 mice. This suggests the phenotype observed in ovariectomised Mst1 mice was dependent on PI3K (p110 α).

5.4.2. Interaction between estrogen receptor α and PI3K (p110 α) in the adult heart

An unanticipated and novel finding from Chapter 3 of this thesis showed that female mice with depressed cardiac PI3K (p110 α) in a setting of HF developed more severe cardiac disease compared with their male counterparts. As previously described (see Section 1.5.7.2.), settings of diabetes and hypertension are associated with increased cardiovascular risk in females (Regitz-Zagrosek, 2006), and both conditions can be associated with depressed or defective PI3K (p110 α) signalling (Chen *et al.*, 2005; Hansen *et al.*, 2001; Kim *et al.*, 1999; Mauvais-Jarvis *et al.*, 2002; Ohanian and Heagerty, 1992). Previous investigators have shown that estrogen can activate Akt in neonatal rat cardiac myocytes (Patten and Karas, 2006; Simoncini *et al.*, 2000), and that female hearts have increased Akt expression (Camper-Kirby *et al.*, 2001). These studies suggest that cardioprotection in females may be mediated through an interaction between estrogen and the PI3K (p110 α) – Akt pathway.

To assess a possible link between ER α and PI3K (p110 α), immunoprecipitation experiments were performed. I was able to show that ER α associates with the regulatory subunit of PI3K (p110 α) in the heart of the adult mouse (i.e. p85; Figure 65). *In vitro* studies using human endothelial cells previously demonstrated that ER α can activate the PI3K signalling pathway (Patten and Karas, 2006; Simoncini *et al.*, 2000). To assess the functional significance of the ER α -PI3K interaction in the heart in an *in vivo* model, ovariectomy surgery was performed in the PI3K (p110 α), Mst1 and double-transgenic mice. It was hypothesised that PI3K (p110 α) plays a critical role in mediating the cardioprotective properties of estrogen via an interaction with ER α in the female heart (Figure 74).

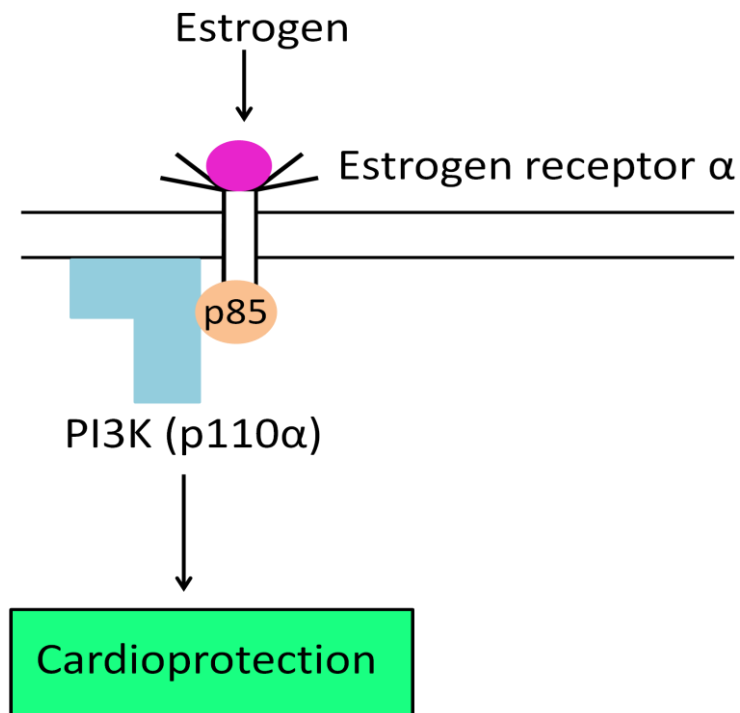


Figure 74. Possible mechanism via which an interaction between ER α and PI3K (p110 α) mediates cardioprotection in females.

5.4.3. Impact of ovariectomy and estrogen replacement in Mst1 mice with or without manipulation of PI3K (p110 α)

Numerous studies have demonstrated that ovariectomy in cardiac disease models has an adverse effect on cardiac function in female mice (Bhuiyan *et al.*, 2007; Du *et al.*,

2006; Lekgabe *et al.*, 2006; Mendelsohn and Karas, 1999; Sharkey *et al.*, 1998; Shinmura *et al.*, 2008; Xu *et al.*, 2003). Thus, it was hypothesised that ovariectomy would have an adverse effect in the Mst1 mice. Interestingly however, ovariectomy improved the cardiac phenotype of the Mst1 mice compared with sham-operated Mst1 mice (improved systolic function, reduced heart weight, atrial weight and lung weight, see Figure 73). Furthermore, estrogen replacement therapy appeared to reverse this effect (see Figure 73). The mechanisms for this apparent benefit of ovariectomy remain unclear. One previous study showed improved lifespan following ovariectomy in β 2-adrenergic receptor over-expressing female mice (Gao *et al.*, 2003b). Further investigation of the molecular mechanisms responsible for the apparent benefit of ovariectomy in the Mst1 mice is warranted. The unexpected improvement in Mst1 mice after ovariectomy was not observed in either ovariectomised caPI3K-Mst1 or dnPI3K-Mst1 mice. Thus, constitutive activation or depressed activation of PI3K (p110 α) in a setting of Mst1 over-expression appears to prevent the occurrence of an ovariectomy-induced phenotype in the Mst1 mice.

5.5. Limitations and future studies

Due to unexpected complications with the estrogen replacement studies, further experiments examining the interaction of ER α and PI3K (p110 α) signalling will be required. The observed side effects with estrogen pellets (i.e. urine retention) were also observed in a study by Levin-Allarhand and colleagues. These investigators showed that use of subcutaneous 17 β -estradiol pellets resulted in urine retention, and ultimately premature death (Levin-Allerhand *et al.*, 2003). In contrast, a supraphysiological or physiological dose (1000nM and 200nM, respectively) in the drinking water was shown to be effective and free of the observed side-effects (Levin-Allerhand *et al.*, 2003). The authors were unable to totally explain why administration via the drinking water was safer than via a subcutaneous pellet (with similar increases in uterus weight with estrogen treatment). However, the authors commented that possible reasons may be associated with different pharmacokinetics of the oral versus subcutaneously administered 17 β -estradiol (with oral administration susceptible to first-pass clearance by the liver, thereby suppressing estrogen levels sufficiently to

prevent urine retention but still yield a uterotrophic response), the production of biologically active estrogen catabolites, or the more fluctuating pattern of 17 β -estradiol administration using drinking water as opposed to pellets. In future studies, it would be advisable to administer estrogen via the drinking water.

Given the unexpected protection observed in ovariectomised Mst1 mice, it would be interesting to conduct ovariectomy studies in another cardiac disease model (such as pressure overload), in which ovariectomy has previously been shown to have an adverse effect (Bhuiyan *et al.*, 2007). Additionally, the interaction of PI3K (p110 α) and ER α will also be investigated in our laboratory via the generation and characterisation of cardiac-specific ER α knockout mice utilising the Cre-lox-based conditional knockout approach. ER α floxed mice have previously been characterised (Feng *et al.*, 2007). ER α will be deleted specifically from adult cardiac myocytes by crossing the ER α floxed mice with cardiac-specific Cre recombinase transgenic mice using the α -MHC promoter, allowing for the examination of the role of ER α specifically in the heart. These ER α knockout mice will be crossed with the PI3K (p110 α) transgenic mice (i.e. caPI3K or dnPI3K) to further examine ER α -mediated PI3K (p110 α) activation in the male and female heart.

5.6. Conclusion

Results from this chapter further highlight the complexities and limited knowledge surrounding signalling mechanisms in males and females, and the relationship with sex hormones. In contrast to the majority of studies in the literature, ovariectomy had a beneficial impact in Mst1 mice and estrogen had an adverse effect. Studies investigating the functional significance of the ER α – PI3K (p110 α) interaction in the heart should improve our general understanding of signalling mechanisms responsible for mediating cardiac protection in different cardiac disease models and genders.

Chapter 6 - General discussion

The three main aims of my thesis were to:

1. To investigate the protective effects of PI3K (p110 α) in an *in vivo* mouse model of dilated cardiomyopathy and to elucidate the mechanisms responsible.
2. To assess whether reduced activation of PI3K (p110 α) makes the compromised heart more susceptible to cardiac conduction abnormalities and AF.
3. To examine the contribution of PI3K (p110 α) in mediating cardioprotection induced by estrogen in the adult heart.

A summary of the overall findings of my thesis are presented in Figure 75. This thesis showed that increased PI3K (p110 α) activity is beneficial in a setting of dilated cardiomyopathy (Mst1 mouse model), while decreased PI3K (p110 α) activity accelerated the heart failure phenotype (Figure 75). The Mst1 mouse model is associated with a reduction in lifespan, a fall in cardiac function, lung congestion, cardiac fibrosis, increased apoptosis and ECG abnormalities (Figure 75). Expression of the caPI3K transgene in the Mst1 mice (i.e. caPI3K-Mst1) was able to improve all these parameters, partly through the action of Akt (Figure 75). In contrast, expression of the dnPI3K transgene in the Mst1 mice (i.e. dnPI3K-Mst1) further reduced lifespan as well as cardiac function, and increased lung congestion, fibrosis, apoptosis, and ECG abnormalities (Figure 75). Furthermore, the reduced PI3K (p110 α) activity in the Mst1 mice increased the heart's susceptibility to atrial fibrillation (Figure 75). Finally, there were gender differences associated with the accelerated heart failure phenotype of the dnPI3K-Mst1 mice. Female dnPI3K-Mst1 mice displayed a more severe phenotype compared with males, indicated by increased atrial weight and lung weight, as well as reduced lifespan and cardiac function (Figure 75).

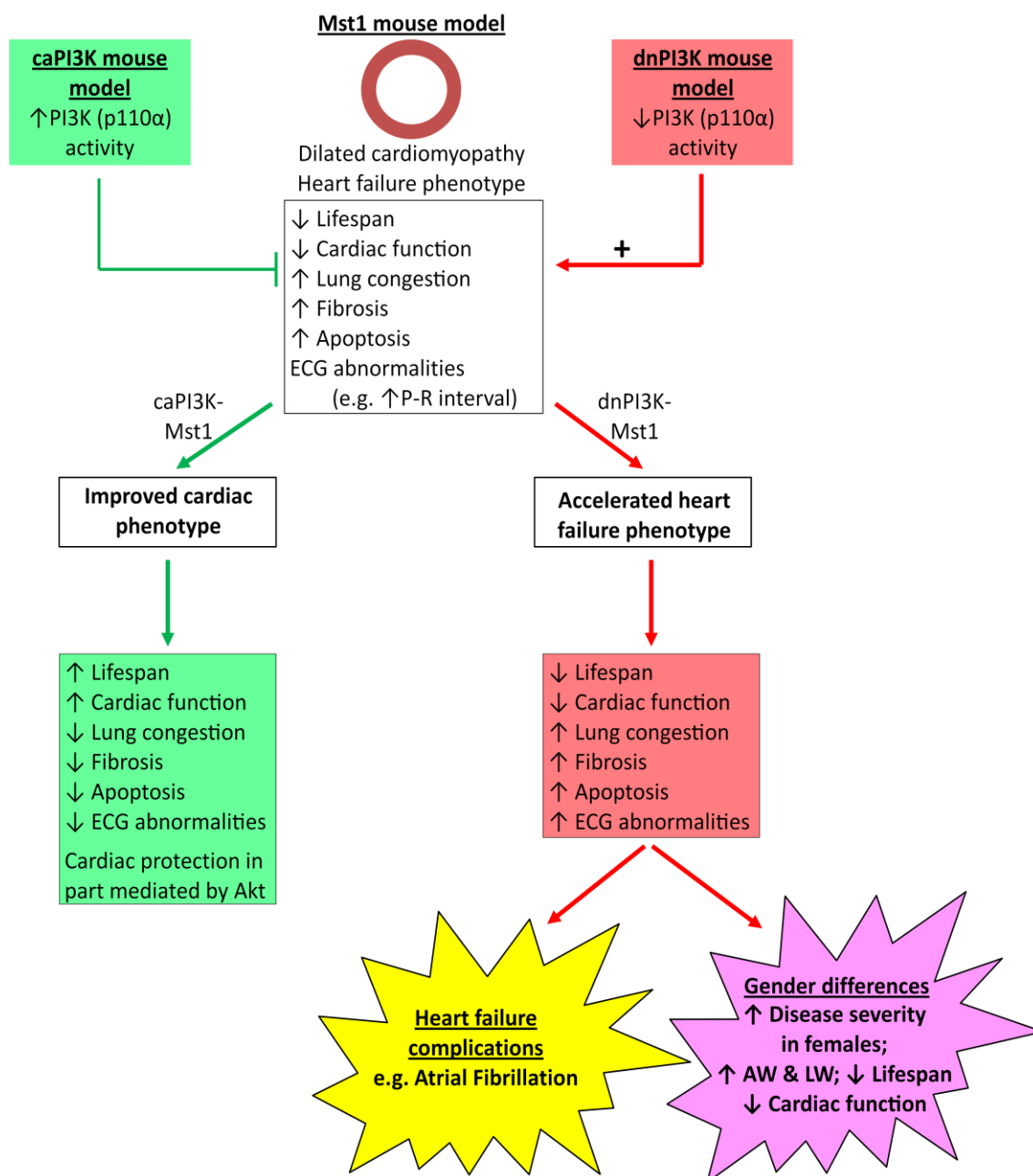


Figure 75. Summary of the novel findings from my PhD project.

Mice over-expressing mammalian sterile 20-like kinase 1 [*Mst1*] develop dilated cardiomyopathy and a heart failure phenotype. Increasing PI3K (p110α) activity [by using the constitutively active PI3K (p110α) (*caPI3K*) mouse] improved the cardiac phenotype in the *Mst1* mice (*caPI3K-Mst1*). In contrast, reducing PI3K (p110α) activity [by using the dominant negative PI3K (p110α) (*dnPI3K*) mouse] accelerated the heart failure phenotype and increased the heart's susceptibility to atrial fibrillation in the *Mst1* mice (*dnPI3K-Mst1*). Gender differences were observed in the *dnPI3K-Mst1* mice, with female mice showing increased atrial weight (AW) and lung weight (LW), as well as reduced lifespan and cardiac function compared with males.

6.1. Research approaches leading to the experimental findings

Approaches to specifically manipulate PI3K (p110 α) activity in the heart

The studies described in this thesis used caPI3K and dnPI3K transgenic mouse models [previously described by Shioi and colleagues (Shioi *et al.*, 2000)], that allowed for detailed examination of the role of PI3K (p110 α) activity specifically in cardiac myocytes [transgene expression driven by the α -MHC promoter (Gulick *et al.*, 1991)]. caPI3K transgenic mice have increased cardiac PI3K (p110 α) activity (6.5-fold), and enlarged hearts (physiological hypertrophy). In contrast, dnPI3K transgenics have decreased cardiac PI3K (p110 α) activity (reduced by approximately 77%), and small hearts (Shioi *et al.*, 2000). Together, these models (gain of function and loss/reduction of function) represent a powerful approach to accurately assess the role of PI3K (p110 α) in the heart under different settings. In general, studies utilising transgenic mouse models in which signalling proteins have been activated and inhibited (e.g. caPI3K and dnPI3K) have not been common. Rather, studies often focus on a single manipulation of a gene of interest (Cook *et al.*, 2009; Molkenin and Robbins, 2009). The distinct advantage of the approach used in this study is that PI3K (p110 α) – regulated processes of functional significance should present as opposite phenotypes in the two models (caPI3K and dnPI3K).

This thesis describes the generation of two unique double-transgenic mouse models with altered PI3K (p110 α) activity. caPI3K-Mst1 and dnPI3K-Mst1 mice were generated by crossing the PI3K (p110 α) transgenic mice [i.e. caPI3K or dnPI3K (Shioi *et al.*, 2000)] with mice over-expressing Mst1 (Yamamoto *et al.*, 2003). The caPI3K-Mst1 mice had increased PI3K (p110 α) activity in a setting of cardiac stress (dilated cardiomyopathy). Conversely, the dnPI3K-Mst1 mice had decreased PI3K (p110 α) activity in a setting of dilated cardiomyopathy. This cardiac-specific gene complementation approach proved a powerful tool for examining the role of PI3K (p110 α) in a disease setting. Increasing PI3K (p110 α) activity improved the phenotype of Mst1 mice, whereas decreasing PI3K (p110 α) activity made the phenotype worse.

Integrated measurements to assess the phenotype of transgenic mice

The phenotypes of the double-transgenic mice were determined using a variety of integrated physiological and molecular approaches. Cardiac function was assessed

using echocardiography and catheterisation. Echocardiography provides a measure of systolic function (fractional shortening) as well as an indication of gross cardiac morphology (e.g. remodelling), while catheterisation provides detailed measures of cardiac function and ventricular pressures. Additionally, electrophysiology parameters were examined in anaesthetised mice (ECG and ECG catheterisation), as well as conscious ambulatory mice (telemetry). Importantly, cardiac function parameters were also correlated with morphological and biomolecular markers of pathology. Assessment of fibrosis and apoptosis (characteristic of cardiac disease) was performed through histology staining, as well as microarray analysis of gene expression. Hypertrophy was correlated with hypertrophic and heart failure gene expression markers, (including ANP, BNP, β -MHC, and α -skeletal actin), as well as protein expression changes associated with hypertrophy (Akt, ERK, p38). The identification of differential protein expression in the transgenic models provided a means to assess the functional significance of targets downstream of PI3K (p110 α). The increased phosphorylation of Akt in caPI3K and caPI3K-Mst1 mice in comparison with Ntg mice, together with decreased phosphorylation of Akt in the dnPI3K mice lead to the generation of caPI3K-Mst1-kdAkt mice. These studies demonstrated that Akt is only in part responsible for the cardioprotection induced by caPI3K in the Mst1 mice. Together, these physiological and molecular approaches allowed for a comprehensive examination of the cardiac phenotype of the transgenic mice.

6.2. PI3K (p110 α) as a potential therapeutic target

Translation of mouse studies to the clinical setting

Results from the dnPI3K-Mst1 mouse studies suggested that reduced PI3K (p110 α) activity increased the susceptibility of the stressed heart to AF. To examine whether this laboratory finding has the potential to be translated into a clinical setting, tissue biopsies from patients with or without AF were analysed for PI3K (p110 α) activity. Findings showed that both acute and chronic AF patients had reduced activity of PI3K (p110 α) activity in their atrial appendages. These results suggest there may be therapeutic potential of targeting the PI3K (p110 α) pathway in a clinical setting.

Previous studies have demonstrated that translation of findings from mouse studies to human clinical studies is possible (Araujo *et al.*, 2005; Hilfiker-Kleiner *et al.*, 2007). Female mice with cardiac-specific deletion of Stat3 developed postpartum cardiomyopathy, and this was associated with increased presence of the hormone prolactin (Hilfiker-Kleiner *et al.*, 2007). Treatment of the Stat3 knockout mice with an inhibitor of prolactin secretion (normally used to stop lactation postpartum in patients) prevented postpartum cardiomyopathy, while increased prolactin generation by over-expressing the enzyme Cathepsin D (a key enzyme required to cleave prolactin into its active form) recapitulated the postpartum cardiomyopathy phenotype (Hilfiker-Kleiner *et al.*, 2007). Preliminary studies in postpartum cardiomyopathy patients showed reduced Stat3 expression and increased presence of prolactin compared with control patients (Hilfiker-Kleiner *et al.*, 2007), suggesting that inhibition of prolactin release may be of therapeutic benefit in these patients. As a result of these findings, and the fact that the prolactin inhibitor had previously been shown to be safe in patients, the authors were able to start a small-scale clinical trial (extensive experimentation using larger pre-clinical animal models was not required). The investigators were able to show that the inhibitor of prolactin secretion in addition to standard heart failure treatment was successful in preventing the recurrence of postpartum cardiomyopathy in patients who had previously developed postpartum cardiomyopathy after delivery [improved cardiac function and dimensions and 100% survival (Hilfiker-Kleiner *et al.*, 2007)]. In contrast, those patients receiving only standard heart failure treatment had reduced cardiac function and a 50% mortality rate (Hilfiker-Kleiner *et al.*, 2007).

In another study, mice with a genetic mutation for cardiac troponin T developed hypertrophic cardiomyopathy, characterised by marked increases in interstitial fibrosis (Lim *et al.*, 2001). The level of interstitial fibrosis is a major predictor of sudden death in patients with hypertrophic cardiomyopathy (Lim *et al.*, 2001). Lim and colleagues showed that treatment with the ARB, losartan, reversed interstitial fibrosis in cardiac troponin T mutant mice (Lim *et al.*, 2001). As a result of these findings, and the fact that losartan has been shown to be safe in patients, the therapeutic benefit of losartan in human non-obstructive hypertrophic cardiomyopathy was assessed in a small-scale clinical trial by Araujo and colleagues

(Araujo *et al.*, 2005). The investigators were able to show that administration of losartan for a six-month period significantly improved left ventricular diastolic function in patients with non-obstructive hypertrophic cardiomyopathy (Araujo *et al.*, 2005). A subsequent randomised controlled trial showed that treatment of patients with non-obstructive hypertrophic cardiomyopathy with losartan for a period of one year reduced left ventricular mass in these patients (Yamazaki *et al.*, 2007). Losartan is currently in Phase 2 clinical trials for the treatment of patients with hypertrophic non-obstructive cardiomyopathy, but results have not yet been reported (see <http://clinicaltrials.gov/ct2/show/study/NCT01150461>).

Rationale for the concept that PI3K (p110 α) could be a therapeutic target for heart disease

Results presented in this thesis and previous studies (see Section 1.5.1.4.) have suggested that activation of the IGF1-PI3K-Akt signalling pathway can be beneficial in a setting of cardiac disease, while decreased PI3K (p110 α) or Akt1 activity has an adverse effect (see Table 5, page 38). The studies described in Chapter 3 of this thesis clearly demonstrate that increased PI3K (p110 α) activity specifically in the heart is beneficial in a setting of dilated cardiomyopathy, improving lifespan and cardiac function, while decreasing fibrosis and apoptosis. In contrast, reducing PI3K (p110 α) activity specifically in the heart was detrimental in a setting of dilated cardiomyopathy, reducing lifespan and cardiac function, while increasing fibrosis and apoptosis. Additionally, in Chapter 4 of this thesis, it was shown that decreased PI3K (p110 α) activity increased the susceptibility to AF in a setting of dilated cardiomyopathy. Taken together, these studies suggest that targeting PI3K (p110 α) may be a therapeutic target in the treatment of HF and AF.

Potential risk factors associated with PI3K (p110 α) therapeutics

The major challenge in targeting PI3K (p110 α), arises from the diverse actions of PI3K (p110 α) in numerous cell types, leading to potential off-target effects (McMullen and Jay, 2007). Studies suggest that mutations in PI3K (p110 α) play critical roles in two of the six essential physiological changes required for the development of cancer (namely

self-sufficiency in growth signals, and evasion of apoptosis) (Hanahan and Weinberg, 2000). Additionally, mutations leading to increased PI3K (p110 α) activity have been associated with a diverse range of cancers (Campbell *et al.*, 2004; Li *et al.*, 1997a; Liaw *et al.*, 1997; Samuels *et al.*, 2004). Consequently, activation of PI3K (p110 α) to treat cardiac disease may lead to increased cancer risk in other tissues.

Conversely, while inhibition of PI3K (p110 α) may be beneficial in a setting of cancer, it is important to consider the heart when devising therapeutic strategies. Expression of the dnPI3K transgene in the transgenic mouse did not affect cardiac function or lifespan under basal conditions (Shioi *et al.*, 2000), suggesting that inhibitors of the PI3K (p110 α) signalling pathway may be safe in the heart under normal conditions. However, previous studies in mice (McMullen *et al.*, 2003; McMullen *et al.*, 2007) and the studies described in Chapters 3 and 4 of this thesis raise concerns regarding the use of PI3K (p110 α) or tyrosine kinase inhibitors as anticancer agents, particularly in patients with underlying cardiac conditions. Results presented in this thesis suggest that decreased PI3K (p110 α) activity increases the susceptibility to the development of HF and AF. A recent clinical trial of lapatinib, a novel tyrosine kinase inhibitor that acts in part by inhibiting PI3K (p110 α), showed increased incidence of AF (Blackwell *et al.*, 2009). Similarly, there has also been a reported association of HF in cancer patients given the tyrosine kinase inhibitors trastuzumab or imatinib mesylate (Crone *et al.*, 2002; Kerkela *et al.*, 2006). Thus, it would be important to minimise any additional stress on the heart (such as hypertension or drugs that have cardiotoxic effects) when patients are given PI3K (p110 α) or tyrosine kinase inhibitors.

Technical approaches for targeting PI3K (p110 α)

The diverse actions of PI3K (p110 α) in various tissues makes the development of treatment strategies difficult. As such, it would be of interest to identify downstream targets regulated by PI3K (p110 α) that may represent more cardiac-specific therapeutic targets. Recent studies in our laboratory have identified several cardiac-selective mRNAs and microRNAs that are regulated by PI3K (p110 α) (Lin *et al.*, 2010). It is thought that these targets may be a useful tool to target PI3K (p110 α) signalling directly in the heart.

Another approach would be to specifically increase PI3K (p110 α) in the heart by combining gene therapy with novel delivery systems. Cardiac surgical procedures and novel delivery systems that allow efficient vector delivery to the heart alone have been successful in large animals *in vivo* (Bridges *et al.*, 2005; Byrne *et al.*, 2008; Kaye *et al.*, 2007). Kaye and colleagues have developed a novel V-Focus circuit and catheter system that provides safe, efficient, and targeted delivery of therapeutics to the beating heart of a conscious patient. This device was shown to substantially improve heart function in the failing heart of animals when a virus was used to deliver the SERCA-2a gene (Byrne *et al.*, 2008; Kaye *et al.*, 2007), and has now entered pre-clinical trials. As such, it is applicable to gene therapy.

6.3. Conclusion

Cardiac hypertrophy can be classified as either physiological or pathological. Recognition of the distinct mechanisms responsible for these two forms of hypertrophy has provided new therapeutic targets for HF. This thesis presents compelling data to support further investigation of the pharmacological potential of activating components of the PI3K (p110 α) pathway in a setting of cardiac stress. Increased PI3K (p110 α) activity protected the heart against cardiac dysfunction, increased lifespan, and reduced the pathological consequences of HF. In contrast, reduced PI3K (p110 α) activity further reduced cardiac function and lifespan, and increased the pathological consequences of HF. Reduced PI3K (p110 α) activity also predisposed the stressed heart to cardiac conduction abnormalities and AF. While a better understanding of the mechanisms responsible for gender differences in cardiac hypertrophy and HF is required, the data presented in this thesis suggests that the PI3K (p110 α) pathway plays a particularly important role in mediating cardioprotection in females. Taken together, these studies support further investigation of the potential therapeutic benefit of increasing PI3K (p110 α) activity in a setting of HF.

References

Abdelhadi, R.H., Gurm, H.S., Van Wagoner, D.R., and Chung, M.K. (2004). Relation of an exaggerated rise in white blood cells after coronary bypass or cardiac valve surgery to development of atrial fibrillation postoperatively. *American Journal of Cardiology* *93*, 1176-1178.

ACE-Inhibitor-Myocardial-Infarction-Collaborative-Group (1998). Indications for ACE inhibitors in the early treatment of acute myocardial infarction: systematic overview of individual data from 100,000 patients in randomized trials. *Circulation* *97*, 2202-2212.

Adabag, A.S., Maron, B.J., Appelbaum, E., Harrigan, C.J., Buros, J.L., Gibson, C.M., Lesser, J.R., Hanna, C.A., Udelson, J.E., Manning, W.J., and Maron, M.S. (2008). Occurrence and frequency of arrhythmias in hypertrophic cardiomyopathy in relation to delayed enhancement on cardiovascular magnetic resonance. *Journal of the American College of Cardiology* *51*, 1369-1374.

Adam, O., Frost, G., Custodis, F., Sussman, M.A., Schafers, H.J., Bohm, M., and Laufs, U. (2007). Role of Rac1 GTPase activation in atrial fibrillation. *Journal of the American College of Cardiology* *50*, 359-367.

Adams, T.E., Epa, V.C., Garrett, T.P., and Ward, C.W. (2000). Structure and function of the type 1 insulin-like growth factor receptor. *Cellular & Molecular Life Sciences* *57*, 1050-1093.

Adorisio, R., De Luca, L., Rossi, J., and Gheorghide, M. (2006). Pharmacological treatment of chronic heart failure. *Heart Failure Reviews* *11*, 109-123.

Afzal, A.R., Mandal, K., Nyamweya, S., Foteinos, G., Poloniecki, J., Camm, A.J., Jahangiri, M., and Xu, Q. (2008). Association of Met439Thr substitution in heat shock protein 70 gene with postoperative atrial fibrillation and serum HSP70 protein levels. *Cardiology* *110*, 45-52.

Agmon, Y., Khandheria, B.K., Gentile, F., and Seward, J.B. (2002). Clinical and echocardiographic characteristics of patients with left atrial thrombus and sinus rhythm: experience in 20 643 consecutive transesophageal echocardiographic examinations. *Circulation* 105, 27-31.

AIHW (2004). Heart, stroke and vascular diseases - Australian facts 2004. A report from the Heart Foundation and the Australian Institute of Health and Welfare. *Cardiovascular Disease Series* 22, 1-152.

AIHW (2008). Australia's Health 2008. The eleventh biennial health report of the Australian Institute of Health and Welfare.

Akazawa, H., and Komuro, I. (2003). Roles of cardiac transcription factors in cardiac hypertrophy. *Circulation Research* 92, 1079-1088.

Akhter, S.A., Luttrell, L.M., Rockman, H.A., Iaccarino, G., Lefkowitz, R.J., and Koch, W.J. (1998). Targeting the receptor-Gq interface to inhibit in vivo pressure overload myocardial hypertrophy. *Science* 280, 574-577.

Akki, A., Smith, K., and Seymour, A.M. (2008). Compensated cardiac hypertrophy is characterised by a decline in palmitate oxidation. *Molecular & Cellular Biochemistry* 311, 215-224.

Albertazzi, P., and Purdie, D. (2002). The nature and utility of the phytoestrogens: a review of the evidence. *Maturitas* 42, 173-185.

Allard, M.F., Schonekess, B.O., Henning, S.L., English, D.R., and Lopaschuk, G.D. (1994). Contribution of oxidative metabolism and glycolysis to ATP production in hypertrophied hearts. *American Journal of Physiology* 267, H742-750.

Allen, D.L., Harrison, B.C., Maass, A., Bell, M.L., Byrnes, W.C., and Leinwand, L.A. (2001). Cardiac and skeletal muscle adaptations to voluntary wheel running in the mouse. *Journal of Applied Physiology: Respiratory, Environmental & Exercise Physiology* 90, 1900-1908.

Alpert, N.R., and Mulieri, L.A. (1982). Increased myothermal economy of isometric force generation in compensated cardiac hypertrophy induced by pulmonary artery constriction in the rabbit. A characterization of heat liberation in normal and hypertrophied right ventricular papillary muscles. *Circulation Research* 50, 491-500.

Alwine, J.C., Kemp, D.J., and Stark, G.R. (1977). Method for detection of specific RNAs in agarose gels by transfer to diazobenzyloxymethyl-paper and hybridization with DNA probes. *Proceedings of the National Academy of Sciences of the United States of America* 74, 5350-5354.

Amiodarone-Investigators (1997). Effect of prophylactic amiodarone on mortality after acute myocardial infarction and in congestive heart failure: meta-analysis of individual data from 6500 patients in randomised trials. *Amiodarone Trials Meta-Analysis Investigators. Lancet* 350, 1417-1424.

Ammash, N.M., Seward, J.B., Bailey, K.R., Edwards, W.D., and Tajik, A.J. (2000). Clinical profile and outcome of idiopathic restrictive cardiomyopathy. *Circulation* 101, 2490-2496.

Aoki, H., and Izumo, S. (2001). Signal transduction of cardiac myocyte hypertrophy. In *Heart physiology and pathology* (4th edition), N. Sperelakis, Y. Kurachi, A. Terzic, and M.V. Cohen, eds. (San Diego, Academic Press), pp. 1065-1086.

Aoyagi, T., Yonekura, K., Eto, Y., Matsumoto, A., Yokoyama, I., Sugiura, S., Momomura, S., Hirata, Y., Baker, D.L., and Periasamy, M. (1999). The sarcoplasmic reticulum Ca²⁺-ATPase (SERCA2) gene promoter activity is decreased in response to severe left

ventricular pressure-overload hypertrophy in rat hearts. *Journal of Molecular & Cellular Cardiology* 31, 919-926.

Arai, M., Otsu, K., MacLennan, D.H., and Periasamy, M. (1992). Regulation of sarcoplasmic reticulum gene expression during cardiac and skeletal muscle development. *American Journal of Physiology* 262, C614-620.

Arai, M., Alpert, N.R., MacLennan, D.H., Barton, P., and Periasamy, M. (1993). Alterations in sarcoplasmic reticulum gene expression in human heart failure. A possible mechanism for alterations in systolic and diastolic properties of the failing myocardium. *Circulation Research* 72, 463-469.

Arai, M., Suzuki, T., and Nagai, R. (1996). Sarcoplasmic reticulum genes are upregulated in mild cardiac hypertrophy but downregulated in severe cardiac hypertrophy induced by pressure overload. *Journal of Molecular & Cellular Cardiology* 28, 1583-1590.

Aranki, S.F., Shaw, D.P., Adams, D.H., Rizzo, R.J., Couper, G.S., VanderVliet, M., Collins, J.J., Jr., Cohn, L.H., and Burstin, H.R. (1996). Predictors of atrial fibrillation after coronary artery surgery. Current trends and impact on hospital resources. *Circulation* 94, 390-397.

Araujo, A.Q., Arteaga, E., Ianni, B.M., Buck, P.C., Rabello, R., and Mady, C. (2005). Effect of Losartan on left ventricular diastolic function in patients with nonobstructive hypertrophic cardiomyopathy. *American Journal of Cardiology* 96, 1563-1567.

Asahi, M., Nakayama, H., Tada, M., and Otsu, K. (2003). Regulation of sarco(endo)plasmic reticulum Ca²⁺ adenosine triphosphatase by phospholamban and sarcolipin: implication for cardiac hypertrophy and failure. *Trends in Cardiovascular Medicine* 13, 152-157.

Assayag, P., Carre, F., Chevalier, B., Delcayre, C., Mansier, P., and Swynghedauw, B. (1997). Compensated cardiac hypertrophy: arrhythmogenicity and the new myocardial phenotype. *Cardiovascular Research* 34, 439-444.

Atchley, A.E., Jr., and Douglas, P.S. (2007). Left ventricular hypertrophy in athletes: morphologic features and clinical correlates. *Cardiology Clinics* 25, 371-382, v.

Aurigemma, G.P., and Gaasch, W.H. (1995). Gender differences in older patients with pressure-overload hypertrophy of the left ventricle. *Cardiology* 86, 310-317.

Ausma, J., Wijffels, M., van Eys, G., Koide, M., Ramaekers, F., Allessie, M., and Borgers, M. (1997). Dedifferentiation of atrial cardiomyocytes as a result of chronic atrial fibrillation. *American Journal of Pathology* 151, 985-997.

Ausma, J., Coumans, W.A., Duimel, H., Van der Vusse, G.J., Allessie, M.A., and Borgers, M. (2000). Atrial high energy phosphate content and mitochondrial enzyme activity during chronic atrial fibrillation. *Cardiovascular Research* 47, 788-796.

Babiker, F.A., De Windt, L.J., van Eickels, M., Grohe, C., Meyer, R., and Doevendans, P.A. (2002). Estrogenic hormone action in the heart: regulatory network and function. *Cardiovascular Research* 53, 709-719.

Backs, J., Backs, T., Neef, S., Kreusser, M.M., Lehmann, L.H., Patrick, D.M., Grueter, C.E., Qi, X., Richardson, J.A., Hill, J.A., Katus, H.A., Bassel-Duby, R., Maier, L.S., and Olson, E.N. (2009). The delta isoform of CaM kinase II is required for pathological cardiac hypertrophy and remodeling after pressure overload. *Proceedings of the National Academy of Sciences of the United States of America* 106, 2342-2347.

Baines, C.P., and Molkenin, J.D. (2005). STRESS signaling pathways that modulate cardiac myocyte apoptosis. *Journal of Molecular & Cellular Cardiology* 38, 47-62.

Baker, D.W., and Wright, R.F. (1994). Management of heart failure. IV. Anticoagulation for patients with heart failure due to left ventricular systolic dysfunction. *Journal Of the American Medical Association* 272, 1614-1618.

Barany, M. (1967). ATPase activity of myosin correlated with speed of muscle shortening. *Journal of General Physiology* 50, Suppl:197-218.

Bassi, R., Heads, R., Marber, M.S., and Clark, J.E. (2008). Targeting p38-MAPK in the ischaemic heart: kill or cure? *Current Opinion in Pharmacology* 8, 141-146.

Batista, R.J., Verde, J., Nery, P., Bocchino, L., Takeshita, N., Bhayana, J.N., Bergsland, J., Graham, S., Houck, J.P., and Salerno, T.A. (1997). Partial left ventriculectomy to treat end-stage heart disease. *Annals of Thoracic Surgery* 64, 634-638.

Benjamin, E.J., Levy, D., Vaziri, S.M., D'Agostino, R.B., Belanger, A.J., and Wolf, P.A. (1994). Independent risk factors for atrial fibrillation in a population-based cohort. The Framingham Heart Study. *Journal Of the American Medical Association* 271, 840-844.

Benjamin, E.J., Wolf, P.A., D'Agostino, R.B., Silbershatz, H., Kannel, W.B., and Levy, D. (1998). Impact of atrial fibrillation on the risk of death: the Framingham Heart Study. *Circulation* 98, 946-952.

Bernardo, B.C., Weeks, K.L., Pretorius, L., and McMullen, J.R. (2010). Molecular distinction between physiological and pathological cardiac hypertrophy: experimental findings and therapeutic strategies. *Pharmacology & Therapeutics* 128, 191-227.

Bernstein, S.A., and Morley, G.E. (2006). Gap junctions and propagation of the cardiac action potential. *Adv Cardiol* 42, 71-85.

Bers, D.M. (2002). Cardiac excitation-contraction coupling. *Nature* 415, 198-205.

Bertola, L.D., Ott, E.B., Griepma, S., Vonk, F.J., and Bagowski, C.P. (2008). Developmental expression of the alpha-skeletal actin gene. *BMC Evolutionary Biology* 8, 166.

Bertrand, L., Horman, S., Beauloye, C., and Vanoverschelde, J.L. (2008). Insulin signalling in the heart. *Cardiovascular Research* 79, 238-248.

Bhuiyan, M.S., Shioda, N., and Fukunaga, K. (2007). Ovariectomy augments pressure overload-induced hypertrophy associated with changes in Akt and nitric oxide synthase signaling pathways in female rats. *American Journal of Physiology - Endocrinology and Metabolism* 293, E1606-1614.

Blackwell, K.L., Pegram, M.D., Tan-Chiu, E., Schwartzberg, L.S., Arbushites, M.C., Maltzman, J.D., Forster, J.K., Rubin, S.D., Stein, S.H., and Burstein, H.J. (2009). Single-agent lapatinib for HER2-overexpressing advanced or metastatic breast cancer that progressed on first- or second-line trastuzumab-containing regimens. *Annals of Oncology* 20, 1026-1031.

Bleumink, G.S., Knetsch, A.M., Sturkenboom, M.C.J.M., Straus, S.M.J.M., Hofman, A., Deckers, J.W., Witteman, J.C.M., and Stricker, B.H.C. (2004). Quantifying the heart failure epidemic: prevalence, incidence rate, lifetime risk and prognosis of heart failure The Rotterdam Study. *European Heart Journal* 25, 1614-1619.

Blinderman, C.D., Homel, P., Billings, J.A., Portenoy, R.K., and Tennstedt, S.L. (2008). Symptom distress and quality of life in patients with advanced congestive heart failure. *Journal of Pain & Symptom Management* 35, 594-603.

Boehmer, J.P. (2003). Device therapy for heart failure. *American Journal of Cardiology* 91, 53D-59D.

Bogoyevitch, M.A., Gillespie-Brown, J., Ketterman, A.J., Fuller, S.J., Ben-Levy, R., Ashworth, A., Marshall, C.J., and Sugden, P.H. (1996). Stimulation of the stress-activated mitogen-activated protein kinase subfamilies in perfused heart. p38/RK mitogen-activated protein kinases and c-Jun N-terminal kinases are activated by ischemia/reperfusion. *Circulation Research* 79, 162-173.

Boheler, K.R., Carrier, L., de la Bastie, D., Allen, P.D., Komajda, M., Mercadier, J.J., and Schwartz, K. (1991). Skeletal actin mRNA increases in the human heart during ontogenic development and is the major isoform of control and failing adult hearts. *Journal of Clinical Investigation* 88, 323-330.

Boixel, C., Fontaine, V., Rucker-Martin, C., Milliez, P., Louedec, L., Michel, J.B., Jacob, M.P., and Hatem, S.N. (2003). Fibrosis of the left atria during progression of heart failure is associated with increased matrix metalloproteinases in the rat. *Journal of the American College of Cardiology* 42, 336-344.

Bolling, S.F., Pagani, F.D., Deeb, G.M., and Bach, D.S. (1998). Intermediate-term outcome of mitral reconstruction in cardiomyopathy. *Journal of Thoracic and Cardiovascular Surgery* 115, 381-388.

Borlak, J., and Thum, T. (2003). Hallmarks of ion channel gene expression in end-stage heart failure. *FASEB Journal* 17, 1592-1608.

Bosch, R.F., Zeng, X., Grammer, J.B., Popovic, K., Mewis, C., and Kuhlkamp, V. (1999). Ionic mechanisms of electrical remodeling in human atrial fibrillation. *Cardiovascular Research* 44, 121-131.

Bossuyt, J., Helmstadter, K., Wu, X., Clements-Jewery, H., Haworth, R.S., Avkiran, M., Martin, J.L., Pogwizd, S.M., and Bers, D.M. (2008). Ca²⁺/calmodulin-dependent protein kinase II δ and protein kinase D overexpression reinforce the histone deacetylase 5 redistribution in heart failure. *Circulation Research* 102, 695-702.

Bourdoncle, A., Labesse, G., Margueron, R., Castet, A., Cavailles, V., and Royer, C.A. (2005). The nuclear receptor coactivator PGC-1 α exhibits modes of interaction with the estrogen receptor distinct from those of SRC-1. *Journal of Molecular Biology* *347*, 921-934.

Bourne, G.H. (1953). Enzymes of the intercalated disks of heart muscle fibres. *Nature* *172*, 588-589.

Bowman, J.C., Steinberg, S.F., Jiang, T., Geenen, D.L., Fishman, G.I., and Buttrick, P.M. (1997). Expression of protein kinase C beta in the heart causes hypertrophy in adult mice and sudden death in neonates. *Journal of Clinical Investigation* *100*, 2189-2195.

Bradford, M.M. (1976). A rapid and sensitive method for the quantitation of microgram quantities of protein utilizing the principle of protein-dye binding. *Analytical Biochemistry* *72*, 248-254.

Braz, J.C., Bueno, O.F., Liang, Q., Wilkinson, D., Dai, Z.K., Parsons, S., Braunwart, J., Glascock, B.J., Klevitsky, R., Kimball, T.F., Hewett, T.E., and Molkentin, J.D. (2003). Targeted inhibition of p38 MAPK promotes hypertrophic cardiomyopathy through upregulation of calcineurin-NFAT signaling. *Journal of Clinical Investigation* *111*, 1475-1486.

Bridges, C.R., Gopal, K., Holt, D.E., Yarnall, C., Cole, S., Anderson, R.B., Yin, X., Nelson, A., Kozyak, B.W., Wang, Z., Lesniewski, J., Su, L.T., Thesier, D.M., Sundar, H., and Stedman, H.H. (2005). Efficient myocyte gene delivery with complete cardiac surgical isolation in situ. *Journal of Thoracic and Cardiovascular Surgery* *130*, 1364.

Bridgman, P., Aronovitz, M.A., Kakkar, R., Oliverio, M.I., Coffman, T.M., Rand, W.M., Konstam, M.A., Mendelsohn, M.E., and Patten, R.D. (2005). Gender-specific patterns of left ventricular and myocyte remodeling following myocardial infarction in mice

deficient in the angiotensin II type 1a receptor. *American Journal of Physiology - Heart & Circulatory Physiology* 289, H586-592.

Bristow, M.R. (2000a). Beta-adrenergic receptor blockade in chronic heart failure. *Circulation* 101, 558-569.

Bristow, M.R. (2000b). Mechanistic and clinical rationales for using beta-blockers in heart failure. *Journal of Cardiac Failure* 6, 8-14.

Brown, L. (2005). Cardiac extracellular matrix: a dynamic entity. *American Journal of Physiology - Heart & Circulatory Physiology* 289, H973-974.

Brown, R.D., Ambler, S.K., Mitchell, M.D., and Long, C.S. (2005). The cardiac fibroblast: therapeutic target in myocardial remodeling and failure. *Annual Review of Pharmacology and Toxicology* 45, 657-687.

Brundel, B.J., van Gelder, I.C., Henning, R.H., Tuinenburg, A.E., Deelman, L.E., Tieleman, R.G., Grandjean, J.G., van Gilst, W.H., and Crijns, H.J. (1999). Gene expression of proteins influencing the calcium homeostasis in patients with persistent and paroxysmal atrial fibrillation. *Cardiovascular Research* 42, 443-454.

Brundel, B.J., Van Gelder, I.C., Henning, R.H., Tuinenburg, A.E., Wietes, M., Grandjean, J.G., Wilde, A.A., Van Gilst, W.H., and Crijns, H.J. (2001). Alterations in potassium channel gene expression in atria of patients with persistent and paroxysmal atrial fibrillation: differential regulation of protein and mRNA levels for K⁺ channels. *Journal of the American College of Cardiology* 37, 926-932.

Brundel, B.J., Henning, R.H., Kampinga, H.H., Van Gelder, I.C., and Crijns, H.J. (2002). Molecular mechanisms of remodeling in human atrial fibrillation. *Cardiovascular Research* 54, 315-324.

Brundel, B.J., Kampinga, H.H., and Henning, R.H. (2004). Calpain inhibition prevents pacing-induced cellular remodeling in a HL-1 myocyte model for atrial fibrillation. *Cardiovascular Research* 62, 521-528.

Brunet, A., Bonni, A., Zigmond, M.J., Lin, M.Z., Juo, P., Hu, L.S., Anderson, M.J., Arden, K.C., Blenis, J., and Greenberg, M.E. (1999). Akt promotes cell survival by phosphorylating and inhibiting a Forkhead transcription factor. *Cell* 96, 857-868.

Bruzzone, R., White, T.W., and Paul, D.L. (1996). Connections with connexins: the molecular basis of direct intercellular signaling. *European Journal of Biochemistry* 238, 1-27.

Bueno, O.F., De Windt, L.J., Tymitz, K.M., Witt, S.A., Kimball, T.R., Klevitsky, R., Hewett, T.E., Jones, S.P., Lefer, D.J., Peng, C.F., Kitsis, R.N., and Molkenin, J.D. (2000). The MEK1-ERK1/2 signaling pathway promotes compensated cardiac hypertrophy in transgenic mice. *EMBO Journal* 19, 6341-6350.

Bueno, O.F., and Molkenin, J.D. (2002). Involvement of extracellular signal-regulated kinases 1/2 in cardiac hypertrophy and cell death. *Circulation Research* 91, 776-781.

Bueno, O.F., Wilkins, B.J., Tymitz, K.M., Glascock, B.J., Kimball, T.F., Lorenz, J.N., and Molkenin, J.D. (2002). Impaired cardiac hypertrophic response in Calcineurin Abeta - deficient mice. *Proceedings of the National Academy of Sciences of the United States of America* 99, 4586-4591.

Buerger, A., Rozhitskaya, O., Sherwood, M.C., Dorfman, A.L., Bisping, E., Abel, E.D., Pu, W.T., Izumo, S., and Jay, P.Y. (2006). Dilated cardiomyopathy resulting from high-level myocardial expression of Cre-recombinase. *Journal of Cardiac Failure* 12, 392-398.

Buelle, Y., Wambolt, R.B., Grist, M., Parsons, H.L., Chow, J.C., Antler, C., Bonen, A., Keller, A., Dunaway, G.A., Popov, K.M., Hochachka, P.W., and Allard, M.F. (2004).

Regular exercise is associated with a protective metabolic phenotype in the rat heart. *American Journal of Physiology - Heart & Circulatory Physiology* 287, H1055-1063.

Burgering, B.M., and Coffey, P.J. (1995). Protein kinase B (c-Akt) in phosphatidylinositol-3-OH kinase signal transduction. *Nature* 376, 599-602.

Burnette, W.N. (1981). "Western blotting": electrophoretic transfer of proteins from sodium dodecyl sulfate-polyacrylamide gels to unmodified nitrocellulose and radiographic detection with antibody and radioiodinated protein A. *Analytical Biochemistry* 112, 195-203.

Burnier, M. (2001). Angiotensin II type 1 receptor blockers. *Circulation* 103, 904-912.

Burstein, B., and Nattel, S. (2008). Atrial fibrosis: mechanisms and clinical relevance in atrial fibrillation. *Journal of the American College of Cardiology* 51, 802-809.

Butera, P.C. (2010). Estradiol and the control of food intake. *Physiology & Behavior* 99, 175-180.

Byrne, M.J., Power, J.M., Prevolos, A., Mariani, J.A., Hajjar, R.J., and Kaye, D.M. (2008). Recirculating cardiac delivery of AAV2/1SERCA2a improves myocardial function in an experimental model of heart failure in large animals. *Gene Therapy* 15, 1550-1557.

Campbell, I.G., Russell, S.E., Choong, D.Y., Montgomery, K.G., Ciavarella, M.L., Hooi, C.S., Cristiano, B.E., Pearson, R.B., and Phillips, W.A. (2004). Mutation of the PIK3CA gene in ovarian and breast cancer. *Cancer Research* 64, 7678-7681.

Campbell, N.A., and Reece, J.B. (2002). *Biology* 6th Edition (San Francisco, Benjamin Cummings).

Camper-Kirby, D., Welch, S., Walker, A., Shiraishi, I., Setchell, K.D., Schaefer, E., Kajstura, J., Anversa, P., and Sussman, M.A. (2001). Myocardial Akt activation and gender: increased nuclear activity in females versus males. *Circulation Research* *88*, 1020-1027.

Cantley, L.C. (2002). The phosphoinositide 3-kinase pathway. *Science* *296*, 1655-1657.

Cardin, S., Libby, E., Pelletier, P., Le Bouter, S., Shiroshita-Takeshita, A., Le Meur, N., Leger, J., Demolombe, S., Ponton, A., Glass, L., and Nattel, S. (2007). Contrasting gene expression profiles in two canine models of atrial fibrillation. *Circulation Research* *100*, 425-433.

Carrasco, A.J., Dzeja, P.P., Alekseev, A.E., Pucar, D., Zingman, L.V., Abraham, M.R., Hodgson, D., Bienengraeber, M., Puceat, M., Janssen, E., Wieringa, B., and Terzic, A. (2001). Adenylate kinase phosphotransfer communicates cellular energetic signals to ATP-sensitive potassium channels. *Proceedings of the National Academy of Sciences of the United States of America* *98*, 7623-7628.

Carrier, L., Boheler, K.R., Chassagne, C., de la Bastie, D., Wisnewsky, C., Lakatta, E.G., and Schwartz, K. (1992). Expression of the sarcomeric actin isogenes in the rat heart with development and senescence. *Circulation Research* *70*, 999-1005.

Cavasin, M.A., Sankey, S.S., Yu, A.L., Menon, S., and Yang, X.P. (2003). Estrogen and testosterone have opposing effects on chronic cardiac remodeling and function in mice with myocardial infarction. *American Journal of Physiology - Heart & Circulatory Physiology* *284*, H1560-1569.

Cavasin, M.A., Tao, Z., Menon, S., and Yang, X.-P. (2004). Gender differences in cardiac function during early remodeling after acute myocardial infarction in mice. *Life Sciences* *75*, 2181-2192.

CDC (2006). Health, United States, with chartbook on trends in the health of Americans (Hyattsville, MD, Centers for Disease Control and Prevention & National Center for Health Statistics).

Cecchi, F., Olivotto, I., Monteregegi, A., Santoro, G., Dolara, A., and Maron, B.J. (1995). Hypertrophic cardiomyopathy in Tuscany: clinical course and outcome in an unselected regional population. *Journal of the American College of Cardiology* 26, 1529-1536.

Chandy, J., Nakai, T., Lee, R.J., Bellows, W.H., Dzankic, S., and Leung, J.M. (2004). Increases in P-wave dispersion predict postoperative atrial fibrillation after coronary artery bypass graft surgery. *Anesthesia & Analgesia* 98, 303-310.

Chelu, M.G., and Wehrens, X.H. (2007). Sarcoplasmic reticulum calcium leak and cardiac arrhythmias. *Biochemical Society Transactions* 35, 952-956.

Chelu, M.G., Sarma, S., Sood, S., Wang, S., van Oort, R.J., Skapura, D.G., Li, N., Santonastasi, M., Muller, F.U., Schmitz, W., Schotten, U., Anderson, M.E., Valderrabano, M., Dobrev, D., and Wehrens, X.H. (2009). Calmodulin kinase II-mediated sarcoplasmic reticulum Ca²⁺ leak promotes atrial fibrillation in mice. *Journal of Clinical Investigation* 119, 1940-1951.

Chen, S., Yan, W., Huang, J., Ge, D., Yao, Z., and Gu, D. (2005). Association analysis of the variant in the regulatory subunit of phosphoinositide 3-kinase (p85alpha) with Type 2 diabetes mellitus and hypertension in the Chinese Han population. *Diabetic Medicine* 22, 737-743.

Chen, S.A., Hsieh, M.H., Tai, C.T., Tsai, C.F., Prakash, V.S., Yu, W.C., Hsu, T.L., Ding, Y.A., and Chang, M.S. (1999). Initiation of atrial fibrillation by ectopic beats originating from the pulmonary veins: electrophysiological characteristics, pharmacological responses, and effects of radiofrequency ablation. *Circulation* 100, 1879-1886.

Chien, K.R., Zhu, H., Knowlton, K.U., Miller-Hance, W., Van-Bilsen, M., O'Brien, T.X., and Evans, S.M. (1993). Transcriptional regulation during cardiac growth and development. *Annual Review of Physiology* 55, 77-95.

Cho, H., Thorvaldsen, J.L., Chu, Q., Feng, F., and Birnbaum, M.J. (2001). Akt1/PKB α is required for normal growth but dispensable for maintenance of glucose homeostasis in mice. *Journal of Biological Chemistry* 276, 38349-38352.

Choukroun, G., Hajjar, R., Kyriakis, J.M., Bonventre, J.V., Rosenzweig, A., and Force, T. (1998). Role of the stress-activated protein kinases in endothelin-induced cardiomyocyte hypertrophy. *Journal of Clinical Investigation* 102, 1311-1320.

Choukroun, G., Hajjar, R., Fry, S., del Monte, F., Haq, S., Guerrero, J.L., Picard, M., Rosenzweig, A., and Force, T. (1999). Regulation of cardiac hypertrophy in vivo by the stress-activated protein kinases/c-Jun NH(2)-terminal kinases. *Journal of Clinical Investigation* 104, 391-398.

Christe, M.E., and Rodgers, R.L. (1994). Altered glucose and fatty acid oxidation in hearts of the spontaneously hypertensive rat. *Journal of Molecular & Cellular Cardiology* 26, 1371-1375.

Chung, M.K., Martin, D.O., Sprecher, D., Wazni, O., Kanderian, A., Carnes, C.A., Bauer, J.A., Tchou, P.J., Niebauer, M.J., Natale, A., and Van Wagoner, D.R. (2001). C-reactive protein elevation in patients with atrial arrhythmias: inflammatory mechanisms and persistence of atrial fibrillation. *Circulation* 104, 2886-2891.

Chung, T.H., Wang, S.M., and Wu, J.C. (2004). 17 β -estradiol reduces the effect of metabolic inhibition on gap junction intercellular communication in rat cardiomyocytes via the estrogen receptor. *Journal of Molecular & Cellular Cardiology* 37, 1013-1022.

CIBISII-Investigators (1999). The Cardiac Insufficiency Bisoprolol Study II (CIBIS-II): a randomised trial. *Lancet* 353, 9-13.

Clark, J.E., Sarafraz, N., and Marber, M.S. (2007). Potential of p38-MAPK inhibitors in the treatment of ischaemic heart disease. *Pharmacology & Therapeutics* 116, 192-206.

Clark, R.A., McLennan, S., Dawson, A., Wilkinson, D., and Stewart, S. (2004). Uncovering a hidden epidemic: a study of the current burden of heart failure in Australia. *Heart, Lung & Circulation* 13, 266-273.

Cleland, J.G., Daubert, J.C., Erdmann, E., Freemantle, N., Gras, D., Kappenberger, L., and Tavazzi, L. (2005). The effect of cardiac resynchronization on morbidity and mortality in heart failure. *New England Journal of Medicine* 352, 1539-1549.

Clerk, A., Bogoyevitch, M.A., Anderson, M.B., and Sugden, P.H. (1994). Differential activation of protein kinase C isoforms by endothelin-1 and phenylephrine and subsequent stimulation of p42 and p44 mitogen-activated protein kinases in ventricular myocytes cultured from neonatal rat hearts. *Journal of Biological Chemistry* 269, 32848-32857.

Clerk, A., Michael, A., and Sugden, P.H. (1998). Stimulation of the p38 mitogen-activated protein kinase pathway in neonatal rat ventricular myocytes by the G protein-coupled receptor agonists, endothelin-1 and phenylephrine: a role in cardiac myocyte hypertrophy? *Journal of Cell Biology* 142, 523-535.

Coats, A.J. (2000). Exercise training in heart failure. *Current Controlled Trials in Cardiovascular Medicine* 1, 155-160.

Cohn, J.N., Bristow, M.R., Chien, K.R., Colucci, W.S., Frazier, O.H., Leinwand, L.A., Lorell, B.H., Moss, A.J., Sonnenblick, E.H., Walsh, R.A., Mockrin, S.C., and Reinlib, L. (1997).

Report of the National Heart, Lung, and Blood Institute Special Emphasis Panel on Heart Failure Research. *Circulation* 95, 766-770.

Cohn, J.N., Ferrari, R., and Sharpe, N. (2000). Cardiac remodeling-concepts and clinical implications: a consensus paper from an international forum on cardiac remodeling. *Journal of the American College of Cardiology* 35, 569-582.

Cohn, J.N., and Tognoni, G. (2001). A randomized trial of the angiotensin-receptor blocker valsartan in chronic heart failure. *New England Journal of Medicine* 345, 1667-1675.

Condorelli, G., Drusco, A., Stassi, G., Bellacosa, A., Roncarati, R., Iaccarino, G., Russo, M.A., Gu, Y., Dalton, N., Chung, C., Latronico, M.V.G., Napoli, C., Sadoshima, J., Croce, C.M., and Ross, J., Jr. (2002). Akt induces enhanced myocardial contractility and cell size in vivo in transgenic mice. *Proceedings of the National Academy of Sciences of the United States of America* 99, 12333-12338.

Cook, S.A., Sugden, P.H., and Clerk, A. (1999). Activation of c-Jun N-terminal kinases and p38-mitogen-activated protein kinases in human heart failure secondary to ischaemic heart disease. *Journal of Molecular & Cellular Cardiology* 31, 1429-1434.

Cook, S.A., Clerk, A., and Sugden, P.H. (2009). Are transgenic mice the 'alkahest' to understanding myocardial hypertrophy and failure? *Journal of Molecular & Cellular Cardiology* 46, 118-129.

Cooper, G. (1987). Cardiocyte adaptation to chronically altered load. *Annual Review of Physiology* 49, 501-518.

Coppen, S.R., Kodama, I., Boyett, M.R., Dobrzynski, H., Takagishi, Y., Honjo, H., Yeh, H.I., and Severs, N.J. (1999). Connexin45, a major connexin of the rabbit sinoatrial

node, is co-expressed with connexin43 in a restricted zone at the nodal-crista terminalis border. *Journal of Histochemistry and Cytochemistry* 47, 907-918.

Corradi, D., Callegari, S., Benussi, S., Nascimbene, S., Pastori, P., Calvi, S., Maestri, R., Astorri, E., Pappone, C., and Alfieri, O. (2004). Regional left atrial interstitial remodeling in patients with chronic atrial fibrillation undergoing mitral-valve surgery. *Virchows Archiv* 445, 498-505.

Corradi, D., Callegari, S., Benussi, S., Maestri, R., Pastori, P., Nascimbene, S., Bosio, S., Dorigo, E., Grassani, C., Rusconi, R., Vettori, M.V., Alinovi, R., Astorri, E., Pappone, C., and Alfieri, O. (2005). Myocyte changes and their left atrial distribution in patients with chronic atrial fibrillation related to mitral valve disease. *Hum Pathol* 36, 1080-1089.

Corradi, D., Callegari, S., Maestri, R., Benussi, S., and Alfieri, O. (2008). Structural remodeling in atrial fibrillation. *Nature Clinical Practice Cardiovascular Medicine* 5, 782-796.

Cowie, M.R., Wood, D.A., Coats, A.J., Thompson, S.G., Suresh, V., Poole-Wilson, P.A., and Sutton, G.C. (2000). Survival of patients with a new diagnosis of heart failure: a population based study. *Heart* 83, 505-510.

Crone, S.A., Zhao, Y.Y., Fan, L., Gu, Y., Minamisawa, S., Liu, Y., Peterson, K.L., Chen, J., Kahn, R., Condorelli, G., Ross, J., Jr., Chien, K.R., and Lee, K.F. (2002). ErbB2 is essential in the prevention of dilated cardiomyopathy. *Nature Medicine* 8, 459-465.

D'Angelo, D.D., Sakata, Y., Lorenz, J.N., Boivin, G.P., Walsh, R.A., Liggett, S.B., and Dorn, G.W., 2nd (1997). Transgenic Galphaq overexpression induces cardiac contractile failure in mice. *Proceedings of the National Academy of Sciences of the United States of America* 94, 8121-8126.

Daitoku, H., and Fukamizu, A. (2007). FOXO transcription factors in the regulatory networks of longevity. *Journal of Biochemistry* *141*, 769-774.

Dan, I., Watanabe, N.M., and Kusumi, A. (2001). The Ste20 group kinases as regulators of MAP kinase cascades. *Trends in Cell Biology* *11*, 220-230.

Daniels, A., van Bilsen, M., Goldschmeding, R., van der Vusse, G.J., and van Nieuwenhoven, F.A. (2009). Connective tissue growth factor and cardiac fibrosis. *Acta Physiol (Oxf)* *195*, 321-338.

Datta, S.R., Dudek, H., Tao, X., Masters, S., Fu, H., Gotoh, Y., and Greenberg, M.E. (1997). Akt phosphorylation of BAD couples survival signals to the cell-intrinsic death machinery. *Cell* *91*, 231-241.

Davies, M., Hobbs, F., Davis, R., Kenkre, J., Roalfe, A.K., Hare, R., Wosornu, D., and Lancashire, R.J. (2001). Prevalence of left-ventricular systolic dysfunction and heart failure in the Echocardiographic Heart of England Screening study: a population based study. *Lancet* *358*, 439-444.

Davila-Roman, V.G., Vedala, G., Herrero, P., de las Fuentes, L., Rogers, J.G., Kelly, D.P., and Gropler, R.J. (2002). Altered myocardial fatty acid and glucose metabolism in idiopathic dilated cardiomyopathy. *Journal of the American College of Cardiology* *40*, 271-277.

De Caterina, R. (2009). The current role of anticoagulants in cardiovascular medicine. *J Cardiovasc Med (Hagerstown)* *10*, 595-604.

de Jager, T., Pelzer, T., Muller-Botz, S., Imam, A., Muck, J., and Neyses, L. (2001). Mechanisms of estrogen receptor action in the myocardium. Rapid gene activation via the ERK1/2 pathway and serum response elements. *Journal of Biological Chemistry* *276*, 27873-27880.

de Simone, G., Devereux, R.B., Daniels, S.R., and Meyer, R.A. (1995). Gender differences in left ventricular growth. *Hypertension* 26, 979-983.

de Simone, G., Palmieri, V., Koren, M.J., Mensah, G.A., Roman, M.J., and Devereux, R.B. (2001). Prognostic implications of the compensatory nature of left ventricular mass in arterial hypertension. *Journal of Hypertension* 19, 119-125.

de Simone, G., Kitzman, D.W., Palmieri, V., Liu, J.E., Oberman, A., Hopkins, P.N., Bella, J.N., Rao, D.C., Arnett, D.K., and Devereux, R.B. (2004). Association of inappropriate left ventricular mass with systolic and diastolic dysfunction: the HyperGEN study. *American Journal of Hypertension* 17, 828-833.

de Simone, G., Gottdiener, J.S., Chinali, M., and Maurer, M.S. (2008). Left ventricular mass predicts heart failure not related to previous myocardial infarction: the Cardiovascular Health Study. *European Heart Journal* 29, 741-747.

DeBosch, B., Sambandam, N., Weinheimer, C., Courtois, M., and Muslin, A.J. (2006a). Akt2 regulates cardiac metabolism and cardiomyocyte survival. *Journal of Biological Chemistry* 281, 32841-32851.

DeBosch, B., Treskov, I., Lupu, T.S., Weinheimer, C., Kovacs, A., Courtois, M., and Muslin, A.J. (2006b). Akt1 is required for physiological cardiac growth. *Circulation* 113, 2097-2104.

Dec, G.W. (2004). Management of heart failure: crossing boundary over to the surgical country. *Surgical Clinics of North America* 84, 1-25.

Deedwania, P.C., Singh, B.N., Ellenbogen, K., Fisher, S., Fletcher, R., and Singh, S.N. (1998). Spontaneous conversion and maintenance of sinus rhythm by amiodarone in patients with heart failure and atrial fibrillation: observations from the veterans affairs

congestive heart failure survival trial of antiarrhythmic therapy (CHF-STAT). The Department of Veterans Affairs CHF-STAT Investigators. *Circulation* 98, 2574-2579.

del Monte, F., Harding, S.E., Schmidt, U., Matsui, T., Kang, Z.B., Dec, G.W., Gwathmey, J.K., Rosenzweig, A., and Hajjar, R.J. (1999). Restoration of contractile function in isolated cardiomyocytes from failing human hearts by gene transfer of SERCA2a. *Circulation* 100, 2308-2311.

Delaughter, M.C., Taffet, G.E., Fiorotto, M.L., Entman, M.L., and Schwartz, R.J. (1999). Local insulin-like growth factor I expression induces physiologic, then pathologic, cardiac hypertrophy in transgenic mice. *FASEB Journal* 13, 1923-1929.

Dernellis, J., and Panaretou, M. (2001). C-reactive protein and paroxysmal atrial fibrillation: evidence of the implication of an inflammatory process in paroxysmal atrial fibrillation. *Acta Cardiologica* 56, 375-380.

Dernellis, J., and Panaretou, M. (2005). Effect of C-reactive protein reduction on paroxysmal atrial fibrillation. *American Heart Journal* 150, 1064.

Deroo, B.J., and Korach, K.S. (2006). Estrogen receptors and human disease. *Journal of Clinical Investigation* 116, 561-570.

Deschamps, A.M., and Murphy, E. (2009). Activation of a novel estrogen receptor, GPER, is cardioprotective in male and female rats. *American Journal of Physiology - Heart & Circulatory Physiology* 297, H1806-1813.

Di Napoli, P., Taccardi, A.A., Grilli, A., Felaco, M., Balbone, A., Angelucci, D., Gallina, S., Calafiore, A.M., De Caterina, R., and Barsotti, A. (2003). Left ventricular wall stress as a direct correlate of cardiomyocyte apoptosis in patients with severe dilated cardiomyopathy. *American Heart Journal* 146, 1105-1111.

Dinanian, S., Boixel, C., Juin, C., Hulot, J.S., Coulombe, A., Rucker-Martin, C., Bonnet, N., Le Grand, B., Slama, M., Mercadier, J.J., and Hatem, S.N. (2008). Downregulation of the calcium current in human right atrial myocytes from patients in sinus rhythm but with a high risk of atrial fibrillation. *European Heart Journal* 29, 1190-1197.

Dogan, S.M., Buyukates, M., Kandemir, O., Aydin, M., Gursurer, M., Acikgoz, S., Yavuzer, R., Cam, F., and Dursun, A. (2007). Predictors of atrial fibrillation after coronary artery bypass surgery. *Coronary Artery Disease* 18, 327-331.

Donaldson, C., Eder, S., Baker, C., Aronovitz, M.J., Weiss, A.D., Hall-Porter, M., Wang, F., Ackerman, A., Karas, R.H., Molkenin, J.D., and Patten, R.D. (2009). Estrogen attenuates left ventricular and cardiomyocyte hypertrophy by an estrogen receptor-dependent pathway that increases calcineurin degradation. *Circulation Research* 104, 265-275.

Dor, V., Sabatier, M., Di Donato, M., Montiglio, F., Toso, A., and Maioli, M. (1998). Efficacy of endoventricular patch plasty in large postinfarction akinetic scar and severe left ventricular dysfunction: comparison with a series of large dyskinetic scars. *Journal of Thoracic and Cardiovascular Surgery* 116, 50-59.

Dorn, G.W., 2nd, Robbins, J., Ball, N., and Walsh, R.A. (1994). Myosin heavy chain regulation and myocyte contractile depression after LV hypertrophy in aortic-banded mice. *American Journal of Physiology* 267, H400-405.

Douglas, P.S., Katz, S.E., Weinberg, E.O., Chen, M.H., Bishop, S.P., and Lorell, B.H. (1998). Hypertrophic remodeling: gender differences in the early response to left ventricular pressure overload. *Journal of the American College of Cardiology* 32, 1118-1125.

Doval, H.C., Nul, D.R., Grancelli, H.O., Perrone, S.V., Bortman, G.R., and Curiel, R. (1994). Randomised trial of low-dose amiodarone in severe congestive heart failure.

Grupo de Estudio de la Sobrevida en la Insuficiencia Cardiaca en Argentina (GESICA). *Lancet* *344*, 493-498.

Du, X.-J., Samuel, C.S., Gao, X.-M., Zhao, L., Parry, L.J., and Tregear, G.W. (2003). Increased myocardial collagen and ventricular diastolic dysfunction in relaxin deficient mice: a gender-specific phenotype. *Cardiovascular Research* *57*, 395-404.

Du, X.J., Autelitano, D.J., Dilley, R.J., Wang, B., Dart, A.M., and Woodcock, E.A. (2000a). Beta(2)-adrenergic receptor overexpression exacerbates development of heart failure after aortic stenosis. *Circulation* *101*, 71-77.

Du, X.J., Gao, X.M., Wang, B., Jennings, G.L., Woodcock, E.A., and Dart, A.M. (2000b). Age-dependent cardiomyopathy and heart failure phenotype in mice overexpressing beta(2)-adrenergic receptors in the heart. *Cardiovascular Research* *48*, 448-454.

Du, X.J., Fang, L., and Kiriazis, H. (2006). Sex dimorphism in cardiac pathophysiology: experimental findings, hormonal mechanisms, and molecular mechanisms. *Pharmacology & Therapeutics* *111*, 434-475.

Ducharme, A., Swedberg, K., Pfeffer, M.A., Cohen-Solal, A., Granger, C.B., Maggioni, A.P., Michelson, E.L., McMurray, J.J., Olsson, L., Rouleau, J.L., Young, J.B., Olofsson, B., Puu, M., and Yusuf, S. (2006). Prevention of atrial fibrillation in patients with symptomatic chronic heart failure by candesartan in the Candesartan in Heart failure: Assessment of Reduction in Mortality and morbidity (CHARM) program. *American Heart Journal* *152*, 86-92.

Duffy, H.S., and Wit, A.L. (2008). Is there a role for remodeled connexins in AF? No simple answers. *Journal of Molecular & Cellular Cardiology* *44*, 4-13.

Dupont, E., Ko, Y., Rothery, S., Coppen, S.R., Baghai, M., Haw, M., and Severs, N.J. (2001a). The gap-junctional protein connexin40 is elevated in patients susceptible to postoperative atrial fibrillation. *Circulation* 103, 842-849.

Dupont, E., Matsushita, T., Kaba, R.A., Voizzi, C., Coppen, S.R., Khan, N., Kaprielian, R., Yacoub, M.H., and Severs, N.J. (2001b). Altered connexin expression in human congestive heart failure. *Journal of Molecular & Cellular Cardiology* 33, 359-371.

Eapen, Z., and Rogers, J.G. (2009). Strategies to attenuate pathological remodeling in heart failure. *Current Opinion in Cardiology* 24, 223-229.

Earnest, D.L., and Hurst, J.W. (1970). Exophthalmos, stare, increase in intraocular pressure and systolic propulsion of the eyeballs due to congestive heart failure. *American Journal of Cardiology* 26, 351-354.

Edwards, D.P. (2005). Regulation of signal transduction pathways by estrogen and progesterone. *Annu Rev Physiol* 67, 335-376.

el Alaoui-Talibi, Z., Landormy, S., Loireau, A., and Moravec, J. (1992). Fatty acid oxidation and mechanical performance of volume-overloaded rat hearts. *American Journal of Physiology* 262, H1068-1074.

Elfgang, C., Eckert, R., Lichtenberg-Frate, H., Butterweck, A., Traub, O., Klein, R.A., Hulser, D.F., and Willecke, K. (1995). Specific permeability and selective formation of gap junction channels in connexin-transfected HeLa cells. *Journal of Cell Biology* 129, 805-817.

Esmon, C.T. (2009). Basic mechanisms and pathogenesis of venous thrombosis. *Blood Reviews* 23, 225-229.

Exton, J.H. (1996). Regulation of phosphoinositide phospholipases by hormones, neurotransmitters, and other agonists linked to G proteins. *Annual Review of Pharmacology & Toxicology* 36, 481-509.

Fagard, R.H. (1997). Impact of different sports and training on cardiac structure and function. *Cardiol Clin* 15, 397-412.

Falk, R.H. (1998). Etiology and complications of atrial fibrillation: insights from pathology studies. *American Journal of Cardiology* 82, 10N-17N.

Fananapazir, L., Tracy, C.M., Leon, M.B., Winkler, J.B., Cannon, R.O., 3rd, Bonow, R.O., Maron, B.J., and Epstein, S.E. (1989). Electrophysiologic abnormalities in patients with hypertrophic cardiomyopathy. A consecutive analysis in 155 patients. *Circulation* 80, 1259-1268.

Fareh, S., Villemaire, C., and Nattel, S. (1998). Importance of refractoriness heterogeneity in the enhanced vulnerability to atrial fibrillation induction caused by tachycardia-induced atrial electrical remodeling. *Circulation* 98, 2202-2209.

Feinberg, W.M., Blackshear, J.L., Laupacis, A., Kronmal, R., and Hart, R.G. (1995). Prevalence, age distribution, and gender of patients with atrial fibrillation. Analysis and implications. *Archives of Internal Medicine* 155, 469-473.

Feng, Y., Manka, D., Wagner, K.U., and Khan, S.A. (2007). Estrogen receptor-alpha expression in the mammary epithelium is required for ductal and alveolar morphogenesis in mice. *Proceedings of the National Academy of Sciences of the United States of America* 104, 14718-14723.

Ferrans, V.J. (1984). Cardiac hypertrophy: morphological aspects. In *Growth of the heart in health and disease*, R. Zak, ed. (New York, Raven Press), pp. 187-239.

Ferreira-Cornwell, M.C., Luo, Y., Narula, N., Lenox, J.M., Lieberman, M., and Radice, G.L. (2002). Remodeling the intercalated disc leads to cardiomyopathy in mice misexpressing cadherins in the heart. *Journal of Cell Science* *115*, 1623-1634.

Filice, E., Recchia, A.G., Pellegrino, D., Angelone, T., Maggiolini, M., and Cerra, M.C. (2009). A new membrane G protein-coupled receptor (GPR30) is involved in the cardiac effects of 17beta-estradiol in the male rat. *Journal of Physiology and Pharmacology* *60*, 3-10.

Fink, R.I., Kolterman, O.G., Griffin, J., and Olefsky, J.M. (1983). Mechanisms of insulin resistance in aging. *Journal of Clinical Investigation* *71*, 1523-1535.

Fiorotto, M.L., Schwartz, R.J., and Delaughter, M.C. (2003). Persistent IGF-I overexpression in skeletal muscle transiently enhances DNA accretion and growth. *FASEB Journal* *17*, 59-60.

Flesch, M., Schwinger, R.H., Schnabel, P., Schiffer, F., van Gelder, I., Bavendiek, U., Sudkamp, M., Kuhn-Regnier, F., and Bohm, M. (1996). Sarcoplasmic reticulum Ca²⁺-ATPase and phospholamban mRNA and protein levels in end-stage heart failure due to ischemic or dilated cardiomyopathy. *Journal of Molecular Medicine* *74*, 321-332.

Flynn, K.E., Pina, I.L., Whellan, D.J., Lin, L., Blumenthal, J.A., Ellis, S.J., Fine, L.J., Howlett, J.G., Keteyian, S.J., Kitzman, D.W., Kraus, W.E., Miller, N.H., Schulman, K.A., Spertus, J.A., O'Connor, C.M., and Weinfurt, K.P. (2009). Effects of exercise training on health status in patients with chronic heart failure: HF-ACTION randomized controlled trial. *Journal Of the American Medical Association* *301*, 1451-1459.

Frank, K., Bolck, B., Bavendiek, U., and Schwinger, R.H. (1998). Frequency dependent force generation correlates with sarcoplasmic calcium ATPase activity in human myocardium. *Basic Research in Cardiology* *93*, 405-411.

Franke, T.F., Kaplan, D.R., and Cantley, L.C. (1997). Direct regulation of the Akt proto-oncogene product by phosphatidylinositol-3,4-bisphosphate. *Science* 275, 665-668.

Freeman, W.D., and Aguilar, M.I. (2008). Stroke prevention in atrial fibrillation and other major cardiac sources of embolism. *Neurologic Clinics* 26, 1129-1160, x-xi.

Freude, B., Masters, T.N., Robicsek, F., Fokin, A., Kostin, S., Zimmermann, R., Ullmann, C., Lorenz-Meyer, S., and Schaper, J. (2000). Apoptosis is initiated by myocardial ischemia and executed during reperfusion. *Journal of Molecular & Cellular Cardiology* 32, 197-208.

Frey, N., Katus, H.A., Olson, E.N., and Hill, J.A. (2004). Hypertrophy of the heart: a new therapeutic target? *Circulation* 109, 1580-1589.

Fruman, D.A., Meyers, R.E., and Cantley, L.C. (1998). Phosphoinositide kinases. *Annual Review of Biochemistry* 67, 481-507.

Frustaci, A., Chimenti, C., Bellocci, F., Morgante, E., Russo, M.A., and Maseri, A. (1997). Histological substrate of atrial biopsies in patients with lone atrial fibrillation. *Circulation* 96, 1180-1184.

Furnary, A.P., Jessup, F.M., and Moreira, L.P. (1996). Multicenter trial of dynamic cardiomyoplasty for chronic heart failure. The American Cardiomyoplasty Group. *Journal of the American College of Cardiology* 28, 1175-1180.

Fuster, V., Ryden, L.E., Asinger, R.W., Cannom, D.S., Crijns, H.J., Frye, R.L., Halperin, J.L., Kay, G.N., Klein, W.W., Levy, S., McNamara, R.L., Prystowsky, E.N., Wann, L.S., Wyse, D.G., Gibbons, R.J., Antman, E.M., Alpert, J.S., Faxon, D.P., Gregoratos, G., Hiratzka, L.F., Jacobs, A.K., Russell, R.O., Smith, S.C., Alonso-Garcia, A., Blomstrom-Lundqvist, C., De Backer, G., Flather, M., Hradec, J., Oto, A., Parkhomenko, A., Silber, S., and Torbicki, A. (2001). ACC/AHA/ESC guidelines for the management of patients with atrial

fibrillation: executive summary. A Report of the American College of Cardiology/American Heart Association Task Force on Practice Guidelines and the European Society of Cardiology Committee for Practice Guidelines and Policy Conferences (Committee to Develop Guidelines for the Management of Patients With Atrial Fibrillation): developed in Collaboration With the North American Society of Pacing and Electrophysiology. *Journal of the American College of Cardiology* 38, 1231-1266.

Fuster, V., Ryden, L.E., Cannom, D.S., Crijns, H.J., Curtis, A.B., Ellenbogen, K.A., Halperin, J.L., Le Heuzey, J.Y., Kay, G.N., Lowe, J.E., Olsson, S.B., Prystowsky, E.N., Tamargo, J.L., Wann, S., Smith, S.C., Jr., Jacobs, A.K., Adams, C.D., Anderson, J.L., Antman, E.M., Hunt, S.A., Nishimura, R., Ornato, J.P., Page, R.L., Riegel, B., Priori, S.G., Blanc, J.J., Budaj, A., Camm, A.J., Dean, V., Deckers, J.W., Despres, C., Dickstein, K., Lekakis, J., McGregor, K., Metra, M., Morais, J., Osterspey, A., and Zamorano, J.L. (2006). ACC/AHA/ESC 2006 guidelines for the management of patients with atrial fibrillation - executive summary: a report of the American College of Cardiology/American Heart Association Task Force on Practice Guidelines and the European Society of Cardiology Committee for Practice Guidelines (Writing Committee to Revise the 2001 Guidelines for the Management of Patients With Atrial Fibrillation). *Journal of the American College of Cardiology* 48, 854-906.

Gabel, S.A., Walker, V.R., London, R.E., Steenbergen, C., Korach, K.S., and Murphy, E. (2005). Estrogen receptor beta mediates gender differences in ischemia/reperfusion injury. *Journal of Molecular & Cellular Cardiology* 38, 289-297.

Galinska, A., Hatch, V., Craig, R., Murphy, A.M., Van Eyk, J.E., Wang, C.L., Lehman, W., and Foster, D.B. (2010). The C terminus of cardiac troponin I stabilizes the Ca²⁺-activated state of tropomyosin on actin filaments. *Circulation Research* 106, 705-711.

Gao, X.-M., Agrotis, A., Autelitano, D.J., Percy, E., Woodcock, E.A., Jennings, G.L., Dart, A.M., and Du, X.-J. (2003a). Sex hormones and cardiomyopathic phenotype induced by cardiac beta 2-adrenergic receptor overexpression. *Endocrinology* 144, 4097-4105.

Gao, X.M., Dart, A.M., Dewar, E., Jennings, G., and Du, X.J. (2000). Serial echocardiographic assessment of left ventricular dimensions and function after myocardial infarction in mice. *Cardiovascular Research* 45, 330-338.

Gao, X.M., Agrotis, A., Autelitano, D.J., Percy, E., Woodcock, E.A., Jennings, G.L., Dart, A.M., and Du, X.J. (2003b). Sex hormones and cardiomyopathic phenotype induced by cardiac beta 2-adrenergic receptor overexpression. *Endocrinology* 144, 4097-4105.

Gaspo, R., Bosch, R.F., Talajic, M., and Nattel, S. (1997). Functional mechanisms underlying tachycardia-induced sustained atrial fibrillation in a chronic dog model. *Circulation* 96, 4027-4035.

Gavrieli, Y., Sherman, Y., and Ben-Sasson, S.A. (1992). Identification of programmed cell death in situ via specific labeling of nuclear DNA fragmentation. *Journal of Cell Biology* 119, 493-501.

Gehlbach, B.K., and Geppert, E. (2004). The pulmonary manifestations of left heart failure. *Chest* 125, 669-682.

Gellersen, B., Fernandes, M.S., and Brosens, J.J. (2009). Non-genomic progesterone actions in female reproduction. *Human Reproduction Update* 15, 119-138.

Gerdes, A.M., Onodera, T., Wang, X., and McCune, S.A. (1996). Myocyte remodeling during the progression to failure in rats with hypertension. *Hypertension* 28, 609-614.

Girard, J., Ferre, P., Pegorier, J.P., and Duee, P.H. (1992). Adaptations of glucose and fatty acid metabolism during perinatal period and suckling-weaning transition. *Physiological Reviews* 72, 507-562.

Giuberti, K., Pereira, R.B., Bianchi, P.R., Paigel, A.S., Vassallo, D.V., and Stefanon, I. (2007). Influence of ovariectomy in the right ventricular contractility in heart failure rats. *Archives of Medical Research* 38, 170-175.

Gomori, G. (1950). A rapid one-step trichrome stain. *American Journal of Clinical Pathology* 20, 661-664.

Goodyear, L.J., Giorgino, F., Sherman, L.A., Carey, J., Smith, R.J., and Dohm, G.L. (1995). Insulin receptor phosphorylation, insulin receptor substrate-1 phosphorylation, and phosphatidylinositol 3-kinase activity are decreased in intact skeletal muscle strips from obese subjects. *Journal of Clinical Investigation* 95, 2195-2204.

Grady, D., Herrington, D., Bittner, V., Blumenthal, R., Davidson, M., Hlatky, M., Hsia, J., Hulley, S., Herd, A., Khan, S., Newby, L.K., Waters, D., Vittinghoff, E., and Wenger, N. (2002). Cardiovascular disease outcomes during 6.8 years of hormone therapy: Heart and Estrogen/progestin Replacement Study follow-up (HERS II). *Journal Of the American Medical Association* 288, 49-57.

Grammer, J.B., Bosch, R.F., Kuhlkamp, V., and Seipel, L. (2000). Molecular remodeling of Kv4.3 potassium channels in human atrial fibrillation. *Journal of Cardiovascular Electrophysiology* 11, 626-633.

Grandi, A.M., Venco, A., Barzizza, F., Scalise, F., Pantaleo, P., and Finardi, G. (1992). Influence of age and sex on left ventricular anatomy and function in normals. *Cardiology* 81, 8-13.

Granelli-Piperno, A., and Reich, E. (1978). A study of proteases and protease-inhibitor complexes in biological fluids. *Journal of Experimental Medicine* 148, 223-234.

Greenberg, B., Quinones, M.A., Koilpillai, C., Limacher, M., Shindler, D., Benedict, C., and Shelton, B. (1995). Effects of long-term enalapril therapy on cardiac structure and

function in patients with left ventricular dysfunction. Results of the SOLVD echocardiography substudy. *Circulation* *91*, 2573-2581.

Gregorevic, P., Blankinship, M.J., Allen, J.M., Crawford, R.W., Meuse, L., Miller, D.G., Russell, D.W., and Chamberlain, J.S. (2004). Systemic delivery of genes to striated muscles using adeno-associated viral vectors. *Nature Medicine* *10*, 828-834.

Greiser, M., Neuberger, H.R., Harks, E., El-Armouche, A., Boknik, P., de Haan, S., Verheyen, F., Verheule, S., Schmitz, W., Ravens, U., Nattel, S., Allessie, M.A., Dobrev, D., and Schotten, U. (2009). Distinct contractile and molecular differences between two goat models of atrial dysfunction: AV block-induced atrial dilatation and atrial fibrillation. *Journal of Molecular & Cellular Cardiology* *46*, 385-394.

Grodstein, F., Manson, J.E., Colditz, G.A., Willett, W.C., Speizer, F.E., and Stampfer, M.J. (2000). A prospective, observational study of postmenopausal hormone therapy and primary prevention of cardiovascular disease. *Annals of Internal Medicine* *133*, 933-941.

Grohe, C., Kahlert, S., Lobbert, K., and Vetter, H. (1998). Expression of oestrogen receptor alpha and beta in rat heart: role of local oestrogen synthesis. *J Endocrinol* *156*, R1-7.

Gulick, J., Subramaniam, A., Neumann, J., and Robbins, J. (1991). Isolation and characterization of the mouse cardiac myosin heavy chain genes. *Journal of Biological Chemistry* *266*, 9180-9185.

Gunasinghe, S.K., and Spinale, F.G. (2004). Myocardial basis of heart failure: role of the cardiac interstitium. In *Heart Failure*, D.L. Mann, ed. (Philadelphia, Saunders), pp. 57-70.

Gunning, P., Ponte, P., Blau, H., and Kedes, L. (1983). Alpha-skeletal and alpha-cardiac actin genes are coexpressed in adult human skeletal muscle and heart. *Molecular & Cellular Biology* 3, 1985-1995.

Gutstein, D.E., Liu, F.Y., Meyers, M.B., Choo, A., and Fishman, G.I. (2003). The organization of adherens junctions and desmosomes at the cardiac intercalated disc is independent of gap junctions. *Journal of Cell Science* 116, 875-885.

Guyton, A.C., and Hall, J.E. (2000). *Textbook of Medical Physiology Tenth Edition* (Sydney, W.B. Saunders Company).

Haefliger, J.A., Bruzzone, R., Jenkins, N.A., Gilbert, D.J., Copeland, N.G., and Paul, D.L. (1992). Four novel members of the connexin family of gap junction proteins. Molecular cloning, expression, and chromosome mapping. *Journal of Biological Chemistry* 267, 2057-2064.

Hagendorff, A., Schumacher, B., Kirchhoff, S., Luderitz, B., and Willecke, K. (1999). Conduction disturbances and increased atrial vulnerability in Connexin40-deficient mice analyzed by transesophageal stimulation. *Circulation* 99, 1508-1515.

Haissaguerre, M., Jais, P., Shah, D.C., Takahashi, A., Hocini, M., Quiniou, G., Garrigue, S., Le Mouroux, A., Le Metayer, P., and Clementy, J. (1998). Spontaneous initiation of atrial fibrillation by ectopic beats originating in the pulmonary veins. *New England Journal of Medicine* 339, 659-666.

Hajjar, R.J., Schmidt, U., Matsui, T., Guerrero, J.L., Lee, K.H., Gwathmey, J.K., Dec, G.W., Semigran, M.J., and Rosenzweig, A. (1998). Modulation of ventricular function through gene transfer in vivo. *Proceedings of the National Academy of Sciences of the United States of America* 95, 5251-5256.

Hall, J.M., Couse, J.F., and Korach, K.S. (2001). The multifaceted mechanisms of estradiol and estrogen receptor signaling. *Journal of Biological Chemistry* 276, 36869-36872.

Hanahan, D., and Weinberg, R.A. (2000). The hallmarks of cancer. *Cell* 100, 57-70.

Hannigan, G.E., Coles, J.G., and Dedhar, S. (2007). Integrin-linked kinase at the heart of cardiac contractility, repair, and disease. *Circulation Research* 100, 1408-1414.

Hansen, L., Zethelius, B., Berglund, L., Reneland, R., Hansen, T., Berne, C., Lithell, H., Hemmings, B.A., and Pedersen, O. (2001). In vitro and in vivo studies of a naturally occurring variant of the human p85alpha regulatory subunit of the phosphoinositide 3-kinase: inhibition of protein kinase B and relationships with type 2 diabetes, insulin secretion, glucose disappearance constant, and insulin sensitivity. *Diabetes* 50, 690-693.

Harris, I.S., Zhang, S., Treskov, I., Kovacs, A., Weinheimer, C., and Muslin, A.J. (2004). Raf-1 kinase is required for cardiac hypertrophy and cardiomyocyte survival in response to pressure overload. *Circulation* 110, 718-723.

Harris, P., Nagy, S., and Vardaxi, N. (2006). *Mosby's Dictionary of Medicine, Nursing & Health Professions* (Sydney, Elsevier Australia).

Hasenfuss, G., Reinecke, H., Studer, R., Meyer, M., Pieske, B., Holtz, J., Holubarsch, C., Posival, H., Just, H., and Drexler, H. (1994). Relation between myocardial function and expression of sarcoplasmic reticulum Ca(2+)-ATPase in failing and nonfailing human myocardium. *Circulation Research* 75, 434-442.

Hasenfuss, G. (1998). Alterations of calcium-regulatory proteins in heart failure. *Cardiovascular Research* 37, 279-289.

Hasenfuss, G., and Pieske, B. (2002). Calcium cycling in congestive heart failure. *Journal of Molecular & Cellular Cardiology* 34, 951-969.

Hayakawa, Y., Chandra, M., Miao, W., Shirani, J., Brown, J.H., Dorn, G.W., 2nd, Armstrong, R.C., and Kitsis, R.N. (2003). Inhibition of cardiac myocyte apoptosis improves cardiac function and abolishes mortality in the peripartum cardiomyopathy of Galpha(q) transgenic mice. *Circulation* 108, 3036-3041.

Healey, J.S., Baranchuk, A., Crystal, E., Morillo, C.A., Garfinkle, M., Yusuf, S., and Connolly, S.J. (2005). Prevention of atrial fibrillation with angiotensin-converting enzyme inhibitors and angiotensin receptor blockers: a meta-analysis. *Journal of the American College of Cardiology* 45, 1832-1839.

Heeringa, J., van der Kuip, D.A., Hofman, A., Kors, J.A., van Herpen, G., Stricker, B.H., Stijnen, T., Lip, G.Y., and Witteman, J.C. (2006). Prevalence, incidence and lifetime risk of atrial fibrillation: the Rotterdam study. *European Heart Journal* 27, 949-953.

Heiat, A., Gross, C.P., and Krumholz, H.M. (2002). Representation of the elderly, women, and minorities in heart failure clinical trials. *Archives of Internal Medicine* 162, 1682-1688.

Heist, E.K., and Ruskin, J.N. (2006). Atrial fibrillation and congestive heart failure: risk factors, mechanisms, and treatment. *Progress in Cardiovascular Diseases* 48, 256-269.

Hewett, T.E., Grupp, I.L., Grupp, G., and Robbins, J. (1994). Alpha-skeletal actin is associated with increased contractility in the mouse heart. *Circulation Research* 74, 740-746.

Higginbotham, M.B., Morris, K.G., Coleman, R.E., and Cobb, F.R. (1984). Sex-related differences in the normal cardiac response to upright exercise. *Circulation* 70, 357-366.

Hilfiker-Kleiner, D., Kaminski, K., Podewski, E., Bonda, T., Schaefer, A., Sliwa, K., Forster, O., Quint, A., Landmesser, U., Doerries, C., Luchtefeld, M., Poli, V., Schneider, M.D., Balligand, J.L., Desjardins, F., Ansari, A., Struman, I., Nguyen, N.Q., Zschemisch, N.H., Klein, G., Heusch, G., Schulz, R., Hilfiker, A., and Drexler, H. (2007). A cathepsin D-cleaved 16 kDa form of prolactin mediates postpartum cardiomyopathy. *Cell* 128, 589-600.

Hisamoto, K., and Bender, J.R. (2005). Vascular cell signaling by membrane estrogen receptors. *Steroids* 70, 382-387.

Hobai, I.A., and O'Rourke, B. (2001). Decreased sarcoplasmic reticulum calcium content is responsible for defective excitation-contraction coupling in canine heart failure. *Circulation* 103, 1577-1584.

Hoch, B., Meyer, R., Hetzer, R., Krause, E.G., and Karczewski, P. (1999). Identification and expression of delta-isoforms of the multifunctional Ca²⁺/calmodulin-dependent protein kinase in failing and nonfailing human myocardium. *Circulation Research* 84, 713-721.

Hofmann, T., Obukhov, A.G., Schaefer, M., Harteneck, C., Gudermann, T., and Schultz, G. (1999). Direct activation of human TRPC6 and TRPC3 channels by diacylglycerol. *Nature* 397, 259-263.

Hoh, J.F., McGrath, P.A., and Hale, P.T. (1978). Electrophoretic analysis of multiple forms of rat cardiac myosin: effects of hypophysectomy and thyroxine replacement. *Journal of Molecular & Cellular Cardiology* 10, 1053-1076.

Holt, H., Keeton, R.W., and Vennesland, B. (1936). The effect of gonadectomy on body structure and body weight in albino rats. *American Journal of Physiology* 114, 515-522.

Holubarsch, C., Goulette, R.P., Litten, R.Z., Martin, B.J., Mulieri, L.A., and Alpert, N.R. (1985). The economy of isometric force development, myosin isoenzyme pattern and myofibrillar ATPase activity in normal and hypothyroid rat myocardium. *Circulation Research* 56, 78-86.

Hong, C.S., Cho, M.C., Kwak, Y.G., Song, C.H., Lee, Y.H., Lim, J.S., Kwon, Y.K., Chae, S.W., and Kim, D.H. (2002). Cardiac remodeling and atrial fibrillation in transgenic mice overexpressing junctin. *FASEB Journal* 16, 1310-1312.

Hong, C.S., Kwon, S.J., Cho, M.C., Kwak, Y.G., Ha, K.C., Hong, B., Li, H., Chae, S.W., Chai, O.H., Song, C.H., Li, Y., Kim, J.C., Woo, S.H., Lee, S.Y., Lee, C.O., and D.H., K. (2008). Overexpression of junctate induces cardiac hypertrophy and arrhythmia via altered calcium handling. *Journal of Molecular & Cellular Cardiology* 44, 672-682.

Hu, Q., Klippel, A., Muslin, A.J., Fantl, W.J., and Williams, L.T. (1995). Ras-dependent induction of cellular responses by constitutively active phosphatidylinositol-3 kinase. *Science* 268, 100-102.

Hulley, S., Grady, D., Bush, T., Furberg, C., Herrington, D., Riggs, B., and Vittinghoff, E. (1998). Randomized trial of estrogen plus progestin for secondary prevention of coronary heart disease in postmenopausal women. Heart and Estrogen/progestin Replacement Study (HERS) Research Group. *Journal Of the American Medical Association* 280, 605-613.

Hunt, S.A., and Frazier, O.H. (1998). Mechanical circulatory support and cardiac transplantation. *Circulation* 97, 2079-2090.

Hunt, S.A., Abraham, W.T., Chin, M.H., Feldman, A.M., Francis, G.S., Ganiats, T.G., Jessup, M., Konstam, M.A., Mancini, D.M., Michl, K., Oates, J.A., Rahko, P.S., Silver, M.A., Stevenson, L.W., and Yancy, C.W. (2009). 2009 focused update incorporated into the ACC/AHA 2005 Guidelines for the Diagnosis and Management of Heart Failure in

Adults: a report of the American College of Cardiology Foundation/American Heart Association Task Force on Practice Guidelines: developed in collaboration with the International Society for Heart and Lung Transplantation. *Circulation* 119, e391-479.

Hunter, J.J., and Chien, K.R. (1999). Signaling pathways for cardiac hypertrophy and failure. *New England Journal of Medicine* 341, 1276-1283.

Huynh, K., McMullen, J.R., Julius, T.L., Tan, J.W., Love, J.E., Cemerlang, N., Kiriazis, H., Du, X.J., and Ritchie, R.H. (2010). Cardiac-specific IGF-1 receptor transgenic expression protects against cardiac fibrosis and diastolic dysfunction in a mouse model of diabetic cardiomyopathy. *Diabetes* 59, 1512-1520.

Iemitsu, M., Miyauchi, T., Maeda, S., Sakai, S., Kobayashi, T., Fujii, N., Miyazaki, H., Matsuda, M., and Yamaguchi, I. (2001). Physiological and pathological cardiac hypertrophy induce different molecular phenotypes in the rat. *American Journal of Physiology - Regulatory, Integrative and Comparative Physiology* 281, R2029-R2036.

Ikeda, Y., Aihara, K., Sato, T., Akaike, M., Yoshizumi, M., Suzaki, Y., Izawa, Y., Fujimura, M., Hashizume, S., Kato, M., Yagi, S., Tamaki, T., Kawano, H., Matsumoto, T., Azuma, H., and Kato, S. (2005). Androgen receptor gene knockout male mice exhibit impaired cardiac growth and exacerbation of angiotensin II-induced cardiac fibrosis. *Journal of Biological Chemistry* 280, 29661-29666.

Ikeda, Y., Aihara, K., Yoshida, S., Sato, T., Yagi, S., Iwase, T., Sumitomo, Y., Ise, T., Ishikawa, K., Azuma, H., Akaike, M., Kato, S., and Matsumoto, T. (2009). Androgen-androgen receptor system protects against angiotensin II-induced vascular remodeling. *Endocrinology* 150, 2857-2864.

Ikeda, Y., Aihara, K., Akaike, M., Sato, T., Ishikawa, K., Ise, T., Yagi, S., Iwase, T., Ueda, Y., Yoshida, S., Azuma, H., Walsh, K., Tamaki, T., Kato, S., and Matsumoto, T. (2010).

Androgen receptor counteracts Doxorubicin-induced cardiotoxicity in male mice. *Molecular Endocrinology* 24, 1338-1348.

Ilkovski, B., Clement, S., Sewry, C., North, K.N., and Cooper, S.T. (2005). Defining alpha-skeletal and alpha-cardiac actin expression in human heart and skeletal muscle explains the absence of cardiac involvement in ACTA1 nemaline myopathy. *Neuromuscular Disorders* 15, 829-835.

Itoi, T., and Lopaschuk, G.D. (1993). The contribution of glycolysis, glucose oxidation, lactate oxidation, and fatty acid oxidation to ATP production in isolated biventricular working hearts from 2-week-old rabbits. *Pediatr Res* 34, 735-741.

Izumo, S., Lompre, A.M., Matsuoka, R., Koren, G., Schwartz, K., Nadal-Ginard, B., and Mahdavi, V. (1987). Myosin heavy chain messenger RNA and protein isoform transitions during cardiac hypertrophy. Interaction between hemodynamic and thyroid hormone-induced signals. *Journal of Clinical Investigation* 79, 970-977.

Izumo, S., Nadal-Ginard, B., and Mahdavi, V. (1988). Protooncogene induction and reprogramming of cardiac gene expression produced by pressure overload. *Proceedings of the National Academy of Sciences of the United States of America* 85, 339-343.

Jain, M., Liao, R., Podesser, B.K., Ngoy, S., Apstein, C.S., and Eberli, F.R. (2002). Influence of gender on the response to hemodynamic overload after myocardial infarction. *American Journal of Physiology - Heart & Circulatory Physiology* 283, H2544-2550.

Jalil, J.E., Doering, C.W., Janicki, J.S., Pick, R., Shroff, S.G., and Weber, K.T. (1989). Fibrillar collagen and myocardial stiffness in the intact hypertrophied rat left ventricle. *Circulation Research* 64, 1041-1050.

Jang, S.W., Yang, S.J., Srinivasan, S., and Ye, K. (2007). Akt phosphorylates Mst1 and prevents its proteolytic activation, blocking FOXO3 phosphorylation and nuclear translocation. *Journal of Biological Chemistry* 282, 30836-30844.

Janicki, J.S., and Brower, G.L. (2002). The role of myocardial fibrillar collagen in ventricular remodeling and function. *Journal of Cardiac Failure* 8, S319-325.

Jankowski, M., Wang, D., Mukaddam-Daher, S., and Gutkowska, J. (2005). Pregnancy alters nitric oxide synthase and natriuretic peptide systems in the rat left ventricle. *J Endocrinol* 184, 209-217.

Jayatileke, A., and Rockman, H.A. (2005). Animal models of dilated cardiomyopathy and relevance to human disease. In *Molecular mechanisms of cardiac hypertrophy and failure*, R.A. Walsh, ed. (London, Taylor and Francis Group), pp. 667-692.

Jennings, G., Nelson, L., Nestel, P., Esler, M., Korner, P., Burton, D., and Bazelmans, J. (1986). The effects of changes in physical activity on major cardiovascular risk factors, hemodynamics, sympathetic function, and glucose utilization in man: a controlled study of four levels of activity. *Circulation* 73, 30-40.

Ji, Y., Lalli, M.J., Babu, G.J., Xu, Y., Kirkpatrick, D.L., Liu, L.H., Chiamvimonvat, N., Walsh, R.A., Shull, G.E., and Periasamy, M. (2000). Disruption of a single copy of the SERCA2 gene results in altered Ca²⁺ homeostasis and cardiomyocyte function. *Journal of Biological Chemistry* 275, 38073-38080.

Jiang, C., Poole-Wilson, P.A., Sarrel, P.M., Mochizuki, S., Collins, P., and MacLeod, K.T. (1992). Effect of 17 beta-oestradiol on contraction, Ca²⁺ current and intracellular free Ca²⁺ in guinea-pig isolated cardiac myocytes. *Br J Pharmacol* 106, 739-745.

Jiang, Y., Gram, H., Zhao, M., New, L., Gu, J., Feng, L., Di Padova, F., Ulevitch, R.J., and Han, J. (1997). Characterization of the structure and function of the fourth member of

p38 group mitogen-activated protein kinases, p38delta. *Journal of Biological Chemistry* 272, 30122-30128.

John, R., Kamdar, F., Liao, K., Colvin-Adams, M., Boyle, A., and Joyce, L. (2008). Improved survival and decreasing incidence of adverse events with the HeartMate II left ventricular assist device as bridge-to-transplant therapy. *Annals of Thoracic Surgery* 86, 1227-1234; discussion 1234-1225.

Johnson, G.L., Dohlman, H.G., and Graves, L.M. (2005). MAPK kinase kinases (MKKKs) as a target class for small-molecule inhibition to modulate signaling networks and gene expression. *Current Opinion in Chemical Biology* 9, 325-331.

Johnson, N.L., Gardner, A.M., Diener, K.M., Lange-Carter, C.A., Gleavy, J., Jarpe, M.B., Minden, A., Karin, M., Zon, L.I., and Johnson, G.L. (1996). Signal transduction pathways regulated by mitogen-activated/extracellular response kinase kinase kinase induce cell death. *Journal of Biological Chemistry* 271, 3229-3237.

Jugdutt, B.I. (2003). Ventricular remodeling after infarction and the extracellular collagen matrix: when is enough enough? *Circulation* 108, 1395-1403.

Kadambi, V.J., and Kranias, E.G. (1998). Genetically engineered mice: model systems for left ventricular failure. *Journal of Cardiac Failure* 4, 349-361.

Kahn, B.B., and Flier, J.S. (2000). Obesity and insulin resistance. *Journal of Clinical Investigation* 106, 473-481.

Kajantie, E., Fall, C.H., Seppala, M., Koistinen, R., Dunkel, L., Yliharsila, H., Osmond, C., Andersson, S., Barker, D.J., Forsen, T., Holt, R.I., Phillips, D.I., and Eriksson, J. (2003). Serum insulin-like growth factor (IGF)-I and IGF-binding protein-1 in elderly people: relationships with cardiovascular risk factors, body composition, size at birth, and childhood growth. *Journal of Clinical Endocrinology & Metabolism* 88, 1059-1065.

Kajstura, J., Fiordaliso, F., Andreoli, A.M., Li, B., Chimenti, S., Medow, M.S., Limana, F., Nadal-Ginard, B., Leri, A., and Anversa, P. (2001). IGF-1 overexpression inhibits the development of diabetic cardiomyopathy and angiotensin II-mediated oxidative stress. *Diabetes* *50*, 1414-1424.

Kalifa, J., Maixent, J.M., Chalvidan, T., Dalmasso, C., Colin, D., Cozma, D., Laurent, P., Deharo, J.C., Djiane, P., Cozzone, P., and Bernard, M. (2008). Energetic metabolism during acute stretch-related atrial fibrillation. *Molecular & Cellular Biochemistry* *317*, 69-75.

Kallergis, E.M., Manios, E.G., Kanoupakis, E.M., Mavrikakis, H.E., Kolyvaki, S.G., Lyrarakis, G.M., Chlouverakis, G.I., and Vardas, P.E. (2008). The role of the post-cardioversion time course of hs-CRP levels in clarifying the relationship between inflammation and persistence of atrial fibrillation. *Heart* *94*, 200-204.

Kamei, Y., Ohizumi, H., Fujitani, Y., Nemoto, T., Tanaka, T., Takahashi, N., Kawada, T., Miyoshi, M., Ezaki, O., and Kakizuka, A. (2003). PPARgamma coactivator 1beta/ERR ligand 1 is an ERR protein ligand, whose expression induces a high-energy expenditure and antagonizes obesity. *Proceedings of the National Academy of Sciences of the United States of America* *100*, 12378-12383.

Kamkin, A., Kiseleva, I., Lozinsky, I., and Scholz, H. (2005). Electrical interaction of mechanosensitive fibroblasts and myocytes in the heart. *Basic Research in Cardiology* *100*, 337-345.

Kampinga, H.H., Henning, R.H., van Gelder, I.C., and Brundel, B.J. (2007). Beat shock proteins and atrial fibrillation. *Cell Stress Chaperones* *12*, 97-100.

Kanagaratnam, P., Rothery, S., Patel, P., Severs, N.J., and Peters, N.S. (2002). Relative expression of immunolocalized connexins 40 and 43 correlates with human atrial conduction properties. *Journal of the American College of Cardiology* *39*, 116-123.

Kang, P.M., Haunstetter, A., Aoki, H., Usheva, A., and Izumo, S. (2000). Morphological and molecular characterization of adult cardiomyocyte apoptosis during hypoxia and reoxygenation. *Circulation Research* 87, 118-125.

Kang, P.M., and Izumo, S. (2000). Apoptosis and heart failure: A critical review of the literature. *Circulation Research* 86, 1107-1113.

Kanoh, M., Takemura, G., Misao, J., Hayakawa, Y., Aoyama, T., Nishigaki, K., Noda, T., Fujiwara, T., Fukuda, K., Minatoguchi, S., and Fujiwara, H. (1999). Significance of myocytes with positive DNA in situ nick end-labeling (TUNEL) in hearts with dilated cardiomyopathy: not apoptosis but DNA repair. *Circulation* 99, 2757-2764.

Kanter, H.L., Saffitz, J.E., and Beyer, E.C. (1992). Cardiac myocytes express multiple gap junction proteins. *Circulation Research* 70, 438-444.

Kato, S., Endoh, H., Masuhiro, Y., Kitamoto, T., Uchiyama, S., Sasaki, H., Masushige, S., Gotoh, Y., Nishida, E., Kawashima, H., Metzger, D., and Chambon, P. (1995). Activation of the estrogen receptor through phosphorylation by mitogen-activated protein kinase. *Science* 270, 1491-1494.

Kawase, Y., Ly, H.Q., Prunier, F., Lebeche, D., Shi, Y., Jin, H., Hadri, L., Yoneyama, R., Hoshino, K., Takewa, Y., Sakata, S., Peluso, R., Zsebo, K., Gwathmey, J.K., Tardif, J.C., Tanguay, J.F., and Hajjar, R.J. (2008). Reversal of cardiac dysfunction after long-term expression of SERCA2a by gene transfer in a pre-clinical model of heart failure. *Journal of the American College of Cardiology* 51, 1112-1119.

Kaye, D.M., Prevolos, A., Marshall, T., Byrne, M., Hoshijima, M., Hajjar, R., Mariani, J.A., Pepe, S., Chien, K.R., and Power, J.M. (2007). Percutaneous cardiac recirculation-mediated gene transfer of an inhibitory phospholamban peptide reverses advanced heart failure in large animals. *Journal of the American College of Cardiology* 50, 253-260.

Ke, L., Qi, X.Y., Dijkhuis, A.J., Chartier, D., Nattel, S., Henning, R.H., Kampinga, H.H., and Brundel, B.J. (2008). Calpain mediates cardiac troponin degradation and contractile dysfunction in atrial fibrillation. *Journal of Molecular & Cellular Cardiology* 45, 685-693.

Kehat, I., Heinrich, R., Ben-Izhak, O., Miyazaki, H., Gutkind, J.S., and Aronheim, A. (2006). Inhibition of basic leucine zipper transcription is a major mediator of atrial dilatation. *Cardiovascular Research* 70, 543-554.

Keller, H., Givel, F., Perroud, M., and Wahli, W. (1995). Signaling cross-talk between peroxisome proliferator-activated receptor/retinoid X receptor and estrogen receptor through estrogen response elements. *Molecular Endocrinology* 9, 794-804.

Kerkela, R., Grazette, L., Yacobi, R., Iliescu, C., Patten, R., Beahm, C., Walters, B., Shevtsov, S., Pesant, S., Clubb, F.J., Rosenzweig, A., Salomon, R.N., Van Etten, R.A., Alroy, J., Durand, J.B., and Force, T. (2006). Cardiotoxicity of the cancer therapeutic agent imatinib mesylate. *Nature Medicine* 12, 908-916.

Khan, R., and Sheppard, R. (2006). Fibrosis in heart disease: understanding the role of transforming growth factor-beta in cardiomyopathy, valvular disease and arrhythmia. *Immunology* 118, 10-24.

Kiatchosakun, S., Kirkpatrick, D., and Hoit, B.D. (2001). Effects of tribromoethanol anesthesia on echocardiographic assessment of left ventricular function in mice. *Comparative Medicine* 51, 26-29.

Kim, A.M., Tingen, C.M., and Woodruff, T.K. (2010). Sex bias in trials and treatment must end. *Nature* 465, 688-689.

Kim, J., Wende, A.R., Sena, S., Theobald, H.A., Soto, J., Sloan, C., Wayment, B.E., Litwin, S.E., Holzenberger, M., LeRoith, D., and Abel, E.D. (2008). Insulin-like growth factor I

receptor signaling is required for exercise-induced cardiac hypertrophy. *Molecular Endocrinology* 22, 2531-2543.

Kim, J.K., Pedram, A., Razandi, M., and Levin, E.R. (2006). Estrogen prevents cardiomyocyte apoptosis through inhibition of reactive oxygen species and differential regulation of p38 kinase isoforms. *Journal of Biological Chemistry* 281, 6760-6767.

Kim, Y.B., Nikoulina, S.E., Ciaraldi, T.P., Henry, R.R., and Kahn, B.B. (1999). Normal insulin-dependent activation of Akt/protein kinase B, with diminished activation of phosphoinositide 3-kinase, in muscle in type 2 diabetes. *Journal of Clinical Investigation* 104, 733-741.

Kirchhefer, U., Schmitz, W., Scholz, H., and Neumann, J. (1999). Activity of cAMP-dependent protein kinase and Ca²⁺/calmodulin-dependent protein kinase in failing and nonfailing human hearts. *Cardiovascular Research* 42, 254-261.

Kirchhoff, S., Nelles, E., Hagendorff, A., Kruger, O., Traub, O., and Willecke, K. (1998). Reduced cardiac conduction velocity and predisposition to arrhythmias in connexin40-deficient mice. *Current Biology* 8, 299-302.

Klein, G., Schroder, F., Vogler, D., Schaefer, A., Haverich, A., Schieffer, B., Korte, T., and Drexler, H. (2003). Increased open probability of single cardiac L-type calcium channels in patients with chronic atrial fibrillation: role of phosphatase 2A. *Cardiovascular Research* 59, 37-45.

Klein, L.W., and Horowitz, L.N. (1988). Familial right ventricular dilated cardiomyopathy associated with supraventricular arrhythmias. *American Journal of Cardiology* 62, 482-483.

Klippel, A., Kavanaugh, W.M., Pot, D., and Williams, L.T. (1997). A specific product of phosphatidylinositol 3-kinase directly activates the protein kinase Akt through its pleckstrin homology domain. *Molecular & Cellular Biology* 17, 338-344.

Komuro, I., Kudo, S., Yamazaki, T., Zou, Y., Shiojima, I., and Yazaki, Y. (1996). Mechanical stretch activates the stress-activated protein kinases in cardiac myocytes. *FASEB Journal* 10, 631-636.

Konertz, W.F., Shapland, J.E., Hotz, H., Dushe, S., Braun, J.P., Stantke, K., and Kleber, F.X. (2001). Passive containment and reverse remodeling by a novel textile cardiac support device. *Circulation* 104, 1270-275.

Kong, S.W., Bodyak, N., Yue, P., Liu, Z., Brown, J., Izumo, S., and Kang, P.M. (2005). Genetic expression profiles during physiological and pathological cardiac hypertrophy and heart failure in rats. *Physiological Genomics* 21, 34-42.

Konhilas, J.P., Maass, A.H., Luckey, S.W., Stauffer, B.L., Olson, E.N., and Leinwand, L.A. (2004). Sex modifies exercise and cardiac adaptation in mice. *American Journal of Physiology - Heart & Circulatory Physiology* 287, H2768-2776.

Konhilas, J.P., Watson, P.A., Maass, A., Boucek, D.M., Horn, T., Stauffer, B.L., Luckey, S.W., Rosenberg, P., and Leinwand, L.A. (2006). Exercise can prevent and reverse the severity of hypertrophic cardiomyopathy. *Circulation Research* 98, 540-548.

Konhilas, J.P., and Leinwand, L.A. (2007). The effects of biological sex and diet on the development of heart failure. *Circulation* 116, 2747-2759.

Kops, G.J., and Burgering, B.M. (1999). Forkhead transcription factors: new insights into protein kinase B (c-akt) signaling. *Journal of Molecular Medicine* 77, 656-665.

Korantzopoulos, P., Kolettis, T.M., Galaris, D., and Goudevenos, J.A. (2007). The role of oxidative stress in the pathogenesis and perpetuation of atrial fibrillation. *International Journal of Cardiology* 115, 135-143.

Kostin, S., Klein, G., Szalay, Z., Hein, S., Bauer, E.P., and Schaper, J. (2002). Structural correlate of atrial fibrillation in human patients. *Cardiovascular Research* 54, 361-379.

Kravtsov, G.M., Kam, K.W., Liu, J., Wu, S., and Wong, T.M. (2007). Altered Ca(2+) handling by ryanodine receptor and Na(+)-Ca(2+) exchange in the heart from ovariectomized rats: role of protein kinase A. *Am J Physiol Cell Physiol* 292, C1625-1635.

Krum, H., and Abraham, W.T. (2009). Heart failure. *Lancet* 373, 941-955.

Kubota, T., McTiernan, C.F., Frye, C.S., Slawson, S.E., Lemster, B.H., Koretsky, A.P., Demetris, A.J., and Feldman, A.M. (1997). Dilated cardiomyopathy in transgenic mice with cardiac-specific overexpression of tumor necrosis factor-alpha. *Circulation Research* 81, 627-635.

Kulesh, D.A., Clive, D.R., Zarlenga, D.S., and Greene, J.J. (1987). Identification of interferon-modulated proliferation-related cDNA sequences. *Proceedings of the National Academy of Sciences of the United States of America* 84, 8453-8457.

Kumagai, K., Khrestian, C., and Waldo, A.L. (1997). Simultaneous multisite mapping studies during induced atrial fibrillation in the sterile pericarditis model. Insights into the mechanism of its maintenance. *Circulation* 95, 511-521.

Kumar, N.M., and Gilula, N.B. (1996). The gap junction communication channel. *Cell* 84, 381-388.

Kumar, R., and Thompson, E.B. (2003). Transactivation functions of the N-terminal domains of nuclear hormone receptors: protein folding and coactivator interactions. *Molecular Endocrinology* 17, 1-10.

Kumar, V., Abbas, A.K., and Fausto, N. (2005). *Robbins and Cotran's Pathologic Basis of Disease* (Philadelphia, Elsevier/Saunders).

Lai, L.P., Su, M.J., Lin, J.L., Lin, F.Y., Tsai, C.H., Chen, Y.S., Huang, S.K., Tseng, Y.Z., and Lien, W.P. (1999). Down-regulation of L-type calcium channel and sarcoplasmic reticular Ca(2+)-ATPase mRNA in human atrial fibrillation without significant change in the mRNA of ryanodine receptor, calsequestrin and phospholamban: an insight into the mechanism of atrial electrical remodeling. *Journal of the American College of Cardiology* 33, 1231-1237.

Lee, P.Y., Alexander, K.P., Hammill, B.G., Pasquali, S.K., and Peterson, E.D. (2001). Representation of elderly persons and women in published randomized trials of acute coronary syndromes. *Journal Of the American Medical Association* 286, 708-713.

Lehtinen, M.K., Yuan, Z., Boag, P.R., Yang, Y., Villen, J., Becker, E.B., DiBacco, S., de la Iglesia, N., Gygi, S., Blackwell, T.K., and Bonni, A. (2006). A conserved MST-FOXO signaling pathway mediates oxidative-stress responses and extends life span. *Cell* 125, 987-1001.

Lekgabe, E.D., Kiriazis, H., Zhao, C., Xu, Q., Moore, X.L., Su, Y., Bathgate, R.A., Du, X.J., and Samuel, C.S. (2005). Relaxin reverses cardiac and renal fibrosis in spontaneously hypertensive rats. *Hypertension* 46, 412-418.

Lekgabe, E.D., Royce, S.G., Hewitson, T.D., Tang, M.L., Zhao, C., Moore, X.L., Tregear, G.W., Bathgate, R.A., Du, X.J., and Samuel, C.S. (2006). The effects of relaxin and estrogen deficiency on collagen deposition and hypertrophy of nonreproductive organs. *Endocrinology* 147, 5575-5583.

Lemke, L.E., Bloem, L.J., Fouts, R., Esterman, M., Sandusky, G., and Vlahos, C.J. (2001). Decreased p38 MAPK activity in end-stage failing human myocardium: p38 MAPK alpha is the predominant isoform expressed in human heart. *Journal of Molecular & Cellular Cardiology* 33, 1527-1540.

Levick, S.P., and Brower, G.L. (2008). Regulation of matrix metalloproteinases is at the heart of myocardial remodeling. *American Journal of Physiology - Heart & Circulatory Physiology* 295, H1375-1376.

Levin-Allerhand, J.A., Sokol, K., and Smith, J.D. (2003). Safe and effective method for chronic 17beta-estradiol administration to mice. *Contemporary Topics in Laboratory Animal Science* 42, 33-35.

Levin, E.R. (2001). Cell localization, physiology, and nongenomic actions of estrogen receptors. *Journal of Applied Physiology: Respiratory, Environmental & Exercise Physiology* 91, 1860-1867.

Levy, D., Garrison, R.J., Savage, D.D., Kannel, W.B., and Castelli, W.P. (1990). Prognostic implications of echocardiographically determined left ventricular mass in the Framingham Heart Study. *New England Journal of Medicine* 322, 1561-1566.

Levy, D., Kenchaiah, S., Larson, M.G., Benjamin, E.J., Kupka, M.J., Ho, K.K., Murabito, J.M., and Vasan, R.S. (2002). Long-term trends in the incidence of and survival with heart failure. *New England Journal of Medicine* 347, 1397-1402.

Lewinter, M.M., Popper, J., McNabb, M., Nyland, L., Bell, S.B., and Granzier, H. (2010). Extensible behavior of titin in the miniswine left ventricle. *Circulation* 121, 768-774.

Li, D., Fareh, S., Leung, T.K., and Nattel, S. (1999). Promotion of atrial fibrillation by heart failure in dogs: atrial remodeling of a different sort. *Circulation* 100, 87-95.

Li, J., Yen, C., Liaw, D., Podsypanina, K., Bose, S., Wang, S.I., Puc, J., Miliareis, C., Rodgers, L., McCombie, R., Bigner, S.H., Giovanella, B.C., Ittmann, M., Tycko, B., Hibshoosh, H., Wigler, M.H., and Parsons, R. (1997a). PTEN, a putative protein tyrosine phosphatase gene mutated in human brain, breast, and prostate cancer. *Science* 275, 1943-1947.

Li, J., McLerie, M., and Lopatin, A.N. (2004a). Transgenic upregulation of IK1 in the mouse heart leads to multiple abnormalities of cardiac excitability. *American Journal of Physiology - Heart & Circulatory Physiology* 287, H2790-2802.

Li, Q., Li, B., Wang, X., Leri, A., Jana, K.P., Liu, Y., Kajstura, J., Baserga, R., and Anversa, P. (1997b). Overexpression of insulin-like growth factor-1 in mice protects from myocyte death after infarction, attenuating ventricular dilation, wall stress, and cardiac hypertrophy. *Journal of Clinical Investigation* 100, 1991-1999.

Li, W., Mital, S., Ojaimi, C., Csiszar, A., Kaley, G., and Hintze, T.H. (2004b). Premature death and age-related cardiac dysfunction in male eNOS-knockout mice. *Journal of Molecular & Cellular Cardiology* 37, 671-680.

Li, W.G., Zaheer, A., Coppey, L., and Oskarsson, H.J. (1998). Activation of JNK in the remote myocardium after large myocardial infarction in rats. *Biochemical & Biophysical Research Communications* 246, 816-820.

Li, Y., Kishimoto, I., Saito, Y., Harada, M., Kuwahara, K., Izumi, T., Hamanaka, I., Takahashi, N., Kawakami, R., Tanimoto, K., Nakagawa, Y., Nakanishi, M., Adachi, Y., Garbers, D.L., Fukamizu, A., and Nakao, K. (2004c). Androgen contributes to gender-related cardiac hypertrophy and fibrosis in mice lacking the gene encoding guanylyl cyclase-A. *Endocrinology* 145, 951-958.

Liang, Q., Bueno, O.F., Wilkins, B.J., Kuan, C.Y., Xia, Y., and Molkentin, J.D. (2003). c-Jun N-terminal kinases (JNK) antagonize cardiac growth through cross-talk with calcineurin-NFAT signaling. *EMBO Journal* 22, 5079-5089.

Liao, P., Georgakopoulos, D., Kovacs, A., Zheng, M., Lerner, D., Pu, H., Saffitz, J., Chien, K., Xiao, R.P., Kass, D.A., and Wang, Y. (2001). The in vivo role of p38 MAP kinases in cardiac remodeling and restrictive cardiomyopathy. *Proceedings of the National Academy of Sciences of the United States of America* 98, 12283-12288.

Liaw, D., Marsh, D.J., Li, J., Dahia, P.L., Wang, S.I., Zheng, Z., Bose, S., Call, K.M., Tsou, H.C., Peacocke, M., Eng, C., and Parsons, R. (1997). Germline mutations of the PTEN gene in Cowden disease, an inherited breast and thyroid cancer syndrome. *Nature Genetics* 16, 64-67.

Liberatore, G.T., Samson, A., Bladin, C., Schleuning, W.D., and Medcalf, R.L. (2003). Vampire bat salivary plasminogen activator (desmoteplase): a unique fibrinolytic enzyme that does not promote neurodegeneration. *Stroke* 34, 537-543.

Lilly, L.S. (2007). *Pathophysiology of heart disease: a collaborative project of medical students and faculty*, 4th Edition. (Sydney, Lippincott Williams & Wilkins).

Lim, D.S., Lutucuta, S., Bachireddy, P., Youker, K., Evans, A., Entman, M., Roberts, R., and Marian, A.J. (2001). Angiotensin II blockade reverses myocardial fibrosis in a transgenic mouse model of human hypertrophic cardiomyopathy. *Circulation* 103, 789-791.

Lin, R.C., Weeks, K.L., Gao, X.M., Williams, R.B., Bernardo, B.C., Kiriazis, H., Matthews, V.B., Woodcock, E.A., Bouwman, R.D., Mollica, J.P., Speirs, H.J., Dawes, I.W., Daly, R.J., Shioi, T., Izumo, S., Febbraio, M.A., Du, X.J., and McMullen, J.R. (2010). PI3K(p110 alpha) protects against myocardial infarction-induced heart failure: identification of

PI3K-regulated miRNA and mRNA. *Arteriosclerosis, Thrombosis, and Vascular Biology* 30, 724-732.

Ling, H., Zhang, T., Pereira, L., Means, C.K., Cheng, H., Gu, Y., Dalton, N.D., Peterson, K.L., Chen, J., Bers, D., and Heller Brown, J. (2009). Requirement for Ca²⁺/calmodulin-dependent kinase II in the transition from pressure overload-induced cardiac hypertrophy to heart failure in mice. *Journal of Clinical Investigation* 119, 1230-1240.

Lip, G.Y., and Gibbs, C.R. (1999). Does heart failure confer a hypercoagulable state? Virchow's triad revisited. *Journal of the American College of Cardiology* 33, 1424-1426.

Lip, G.Y., and Varughese, G.I. (2005). Diabetes mellitus and atrial fibrillation: perspectives on epidemiological and pathophysiological links. *International Journal of Cardiology* 105, 319-321.

Lip, G.Y., and Tse, H.F. (2007). Management of atrial fibrillation. *Lancet* 370, 604-618.

Liu, F., Levin, M.D., Petrenko, N.B., Lu, M.M., Wang, T., Yuan, L.J., Stout, A.L., Epstein, J.A., and Patel, V.V. (2008). Histone-deacetylase inhibition reverses atrial arrhythmia inducibility and fibrosis in cardiac hypertrophy independent of angiotensin. *Journal of Molecular & Cellular Cardiology* 45, 715-723.

Liu, H., Pedram, A., and Kim, J.K. (2010). Estrogen prevents cardiomyocyte apoptosis by suppressing p38(alpha)-mediated p53 and by downregulating p53 inhibition on p38(beta). *Cardiovascular Research* *In press*.

Liu, J., Sadoshima, J., Zhai, P., Hong, C., Yang, G., Chen, W., Yan, L., Wang, Y., Vatner, S.F., and Vatner, D.E. (2006). Pressure overload induces greater hypertrophy and mortality in female mice with p38alpha MAPK inhibition. *Journal of Molecular & Cellular Cardiology* 41, 680-688.

Liu, T., Li, G., Li, L., and Korantzopoulos, P. (2007). Association between C-reactive protein and recurrence of atrial fibrillation after successful electrical cardioversion: a meta-analysis. *Journal of the American College of Cardiology* 49, 1642-1648.

Liu, W., Zi, M., Jin, J., Prehar, S., Oceandy, D., Kimura, T.E., Lei, M., Neyses, L., Weston, A.H., Cartwright, E.J., and Wang, X. (2009). Cardiac-specific deletion of *mkk4* reveals its role in pathological hypertrophic remodeling but not in physiological cardiac growth. *Circulation Research* 104, 905-914.

Lloyd-Jones, D., Adams, R.J., Brown, T.M., Carnethon, M., Dai, S., De Simone, G., Ferguson, T.B., Ford, E., Furie, K., Gillespie, C., Go, A., Greenlund, K., Haase, N., Hailpern, S., Ho, P.M., Howard, V., Kissela, B., Kittner, S., Lackland, D., Lisabeth, L., Marelli, A., McDermott, M.M., Meigs, J., Mozaffarian, D., Mussolino, M., Nichol, G., Roger, V.L., Rosamond, W., Sacco, R., Sorlie, P., Thom, T., Wasserthiel-Smoller, S., Wong, N.D., and Wylie-Rosett, J. (2010). Heart disease and stroke statistics-2010 update: a report from the American Heart Association. *Circulation* 121, e46-e215.

Lompre, A.M., Nadal-Ginard, B., and Mahdavi, V. (1984). Expression of the cardiac ventricular alpha- and beta-myosin heavy chain genes is developmentally and hormonally regulated. *Journal of Biological Chemistry* 259, 6437-6446.

Lopaschuk, G.D., Spafford, M.A., and Marsh, D.R. (1991). Glycolysis is predominant source of myocardial ATP production immediately after birth. *American Journal of Physiology* 261, H1698-1705.

Lopaschuk, G.D., Collins-Nakai, R.L., and Itoi, T. (1992). Developmental changes in energy substrate use by the heart. *Cardiovascular Research* 26, 1172-1180.

Lorell, B.H., and Carabello, B.A. (2000). Left ventricular hypertrophy: pathogenesis, detection, and prognosis. *Circulation* 102, 470-479.

Lorenz, K., Schmitt, J.P., Schmitteckert, E.M., and Lohse, M.J. (2009). A new type of ERK1/2 autophosphorylation causes cardiac hypertrophy. *Nature Medicine* *15*, 75-83.

Lu, Z., Scherlag, B.J., Lin, J., Niu, G., Fung, K.M., Zhao, L., Ghias, M., Jackman, W.M., Lazzara, R., Jiang, H., and Po, S.S. (2008). Atrial fibrillation begets atrial fibrillation: autonomic mechanism for atrial electrical remodeling induced by short-term rapid atrial pacing. *Circulation: Arrhythmia and Electrophysiology* *1*, 184-192.

Lu, Z., Jiang, Y.P., Wang, W., Xu, X.H., Mathias, R.T., Entcheva, E., Ballou, L.M., Cohen, I.S., and Lin, R.Z. (2009). Loss of cardiac phosphoinositide 3-kinase p110 alpha results in contractile dysfunction. *Circulation* *120*, 318-325.

Luczak, E.D., and Leinwand, L.A. (2009). Sex-based cardiac physiology. *Annual Review of Physiology* *71*, 1-18.

Luo, J., McMullen, J.R., Sobkiw, C.L., Zhang, L., Dorfman, A.L., Sherwood, M.C., Logsdon, M.N., Horner, J.W., DePinho, R.A., Izumo, S., and Cantley, L.C. (2005). Class IA phosphoinositide 3-kinase regulates heart size and physiological cardiac hypertrophy. *Molecular & Cellular Biology* *25*, 9491-9502.

Lyons, G.E., Schiaffino, S., Sassoon, D., Barton, P., and Buckingham, M. (1990). Developmental regulation of myosin gene expression in mouse cardiac muscle. *Journal of Cell Biology* *111*, 2427-2436.

Ma, H., Sprecher, H.W., and Kolattukudy, P.E. (1998). Estrogen-induced production of a peroxisome proliferator-activated receptor (PPAR) ligand in a PPARgamma-expressing tissue. *Journal of Biological Chemistry* *273*, 30131-30138.

Maceira, A.M., Barba, J., Beloqui, O., and Diez, J. (2002). Ultrasonic backscatter and diastolic function in hypertensive patients. *Hypertension* *40*, 239-243.

MacKenna, D., Summerour, S.R., and Villarreal, F.J. (2000). Role of mechanical factors in modulating cardiac fibroblast function and extracellular matrix synthesis. *Cardiovascular Research* 46, 257-263.

MacLellan, W.R., and Schneider, M.D. (2000). Genetic dissection of cardiac growth control pathways. *Annual Review of Physiology* 62, 289-319.

Maggioni, A.P., Latini, R., Carson, P.E., Singh, S.N., Barlera, S., Glazer, R., Masson, S., Cere, E., Tognoni, G., and Cohn, J.N. (2005). Valsartan reduces the incidence of atrial fibrillation in patients with heart failure: results from the Valsartan Heart Failure Trial (Val-HeFT). *American Heart Journal* 149, 548-557.

Mahesh, V.B., Brann, D.W., and Hendry, L.B. (1996). Diverse modes of action of progesterone and its metabolites. *Journal of Steroid Biochemistry & Molecular Biology* 56, 209-219.

Mahmoodzadeh, S., Eder, S., Nordmeyer, J., Ehler, E., Huber, O., Martus, P., Weiske, J., Pregla, R., Hetzer, R., Regitz-Zagrosek, V., Mahmoodzadeh, S., Eder, S., Nordmeyer, J., Ehler, E., Huber, O., Martus, P., Weiske, J., Pregla, R., Hetzer, R., and Regitz-Zagrosek, V. (2006). Estrogen receptor alpha up-regulation and redistribution in human heart failure. *FASEB Journal* 20, 926-934.

Manabe, I., Shindo, T., and Nagai, R. (2002). Gene expression in fibroblasts and fibrosis: involvement in cardiac hypertrophy. *Circulation Research* 91, 1103-1113.

Mancarella, S., Yue, Y., Karnabi, E., Qu, Y., El-Sherif, N., and Boutjdir, M. (2008). Impaired Ca²⁺ homeostasis is associated with atrial fibrillation in the alpha1D L-type Ca²⁺ channel KO mouse. *American Journal of Physiology - Heart & Circulatory Physiology* 295, H2017-2024.

Mandal, K., Torsney, E., Poloniecki, J., Camm, A.J., Xu, Q., and Jahangiri, M. (2005). Association of high intracellular, but not serum, heat shock protein 70 with postoperative atrial fibrillation. *Annals of Thoracic Surgery* 79, 865-871.

Mandapati, R., Skanes, A., Chen, J., Berenfeld, O., and Jalife, J. (2000). Stable microreentrant sources as a mechanism of atrial fibrillation in the isolated sheep heart. *Circulation* 101, 194-199.

Mangelsdorf, D.J., Thummel, C., Beato, M., Herrlich, P., Schutz, G., Umesono, K., Blumberg, B., Kastner, P., Mark, M., Chambon, P., and Evans, R.M. (1995). The nuclear receptor superfamily: the second decade. *Cell* 83, 835-839.

Manson, J.E., Hsia, J., Johnson, K.C., Rossouw, J.E., Assaf, A.R., Lasser, N.L., Trevisan, M., Black, H.R., Heckbert, S.R., Detrano, R., Strickland, O.L., Wong, N.D., Crouse, J.R., Stein, E., and Cushman, M. (2003). Estrogen plus progestin and the risk of coronary heart disease. *New England Journal of Medicine* 349, 523-534.

Marks, A.R., Reiken, S., and Marx, S.O. (2002). Progression of heart failure: is protein kinase a hyperphosphorylation of the ryanodine receptor a contributing factor? *Circulation* 105, 272-275.

Maron, B.J., Gohman, T.E., and Aeppli, D. (1998). Prevalence of sudden cardiac death during competitive sports activities in Minnesota high school athletes. *Journal of the American College of Cardiology* 32, 1881-1884.

Maron, B.J., Casey, S.A., Poliac, L.C., Gohman, T.E., Almquist, A.K., and Aeppli, D.M. (1999). Clinical course of hypertrophic cardiomyopathy in a regional United States cohort. *Journal Of the American Medical Association* 281, 650-655.

Maron, B.J., Shen, W.K., Link, M.S., Epstein, A.E., Almquist, A.K., Daubert, J.P., Bardy, G.H., Favale, S., Rea, R.F., Boriani, G., Estes, N.A., 3rd, and Spirito, P. (2000). Efficacy of

implantable cardioverter-defibrillators for the prevention of sudden death in patients with hypertrophic cardiomyopathy. *New England Journal of Medicine* 342, 365-373.

Maron, B.J., Olivotto, I., Bellone, P., Conte, M.R., Cecchi, F., Flygenring, B.P., Casey, S.A., Gohman, T.E., Bongioanni, S., and Spirito, P. (2002). Clinical profile of stroke in 900 patients with hypertrophic cardiomyopathy. *Journal of the American College of Cardiology* 39, 301-307.

Maron, B.J., and Pelliccia, A. (2006). The heart of trained athletes: cardiac remodeling and the risks of sports, including sudden death. *Circulation* 114, 1633-1644.

Marsh, J.D., Lehmann, M.H., Ritchie, R.H., Gwathmey, J.K., Green, G.E., and Schiebinger, R.J. (1998). Androgen receptors mediate hypertrophy in cardiac myocytes. *Circulation* 98, 256-261.

Martin, S.S., Haruta, T., A.J., M., Klippel, A., Williams, L.T., and Olefsky, J.M. (1996). Activated phosphatidylinositol 3-kinase is sufficient to mediate actin rearrangement and GLUT4 translocation in 3T3-L1 adipocytes. *Journal of Biological Chemistry* 271, 17605-17608.

Masson, P.J. (1929). Some histological methods. Trichrome stainings and their preliminary technique. *Journal of Technical Methods* 12, 75-90.

Mathew, S.T., Patel, J., and Joseph, S. (2009). Atrial fibrillation: mechanistic insights and treatment options. *European Journal of Internal Medicine* 20, 672-681.

Matsui, H., MacLennan, D.H., Alpert, N.R., and Periasamy, M. (1995). Sarcoplasmic reticulum gene expression in pressure overload-induced cardiac hypertrophy in rabbit. *American Journal of Physiology* 268, C252-258.

Matsui, T., Li, L., Wu, J.C., Cook, S.A., Nagoshi, T., Picard, M.H., Liao, R., and Rosenzweig, A. (2002). Phenotypic spectrum caused by transgenic overexpression of activated Akt in the heart. *Journal of Biological Chemistry* 277, 22896-22901.

Matsui, T., and Rosenzweig, A. (2005). Convergent signal transduction pathways controlling cardiomyocyte survival and function: the role of PI 3-kinase and Akt. *Journal of Molecular & Cellular Cardiology* 38, 63-71.

Mauvais-Jarvis, F., Ueki, K., Fruman, D.A., Hirshman, M.F., Sakamoto, K., Goodyear, L.J., Iannaccone, M., Accili, D., Cantley, L.C., and Kahn, C.R. (2002). Reduced expression of the murine p85alpha subunit of phosphoinositide 3-kinase improves insulin signaling and ameliorates diabetes. *Journal of Clinical Investigation* 109, 141-149.

Mayer, Y., Czosnek, H., Zeelon, P.E., Yaffe, D., and Nudel, U. (1984). Expression of the genes coding for the skeletal muscle and cardiac actions in the heart. *Nucleic Acids Research* 12, 1087-1100.

McKenna, N.J., and O'Malley, B.W. (2002). Combinatorial control of gene expression by nuclear receptors and coregulators. *Cell* 108, 465-474.

McKenna, W.J., and Behr, E.R. (2002). Hypertrophic cardiomyopathy: management, risk stratification, and prevention of sudden death. *Heart* 87, 169-176.

McMullen, J.R., Shioi, T., Zhang, L., Tarnavski, O., Sherwood, M.C., Kang, P.M., and Izumo, S. (2003). Phosphoinositide 3-kinase(p110alpha) plays a critical role for the induction of physiological, but not pathological, cardiac hypertrophy. *Proceedings of the National Academy of Sciences of the United States of America* 100, 12355-12360.

McMullen, J.R., Shioi, T., Huang, W.Y., Zhang, L., Tarnavski, O., Bisping, E., Schinke, M., Kong, S., Sherwood, M.C., Brown, J., Riggi, L., Kang, P.M., and Izumo, S. (2004). The insulin-like growth factor 1 receptor induces physiological heart growth via the

phosphoinositide 3-kinase(p110alpha) pathway. *Journal of Biological Chemistry* 279, 4782-4793.

McMullen, J.R., Sadoshima, J., and Izumo, S. (2005). Physiological versus pathological cardiac hypertrophy. In *Molecular Mechanisms of Cardiac Hypertrophy and Failure*, R.A. Walsh, ed. (London, Taylor and Francis Group), pp. 117-136.

McMullen, J.R., Amirahmadi, F., Woodcock, E.A., Schinke-Braun, M., Bouwman, R.D., Hewitt, K.A., Mollica, J.P., Zhang, L., Zhang, Y., Shioi, T., Buerger, A., Izumo, S., Jay, P.Y., and Jennings, G.L. (2007). Protective effects of exercise and phosphoinositide 3-kinase(p110alpha) signaling in dilated and hypertrophic cardiomyopathy. *Proceedings of the National Academy of Sciences of the United States of America* 104, 612-617.

McMullen, J.R., and Jay, P.Y. (2007). PI3K(p110alpha) inhibitors as anti-cancer agents: minding the heart. *Cell Cycle* 6, 910-913.

McMullen, J.R., and Jennings, G.L. (2007). Differences between pathological and physiological cardiac hypertrophy: novel therapeutic strategies to treat heart failure. *Clinical & Experimental Pharmacology & Physiology* 34, 255-262.

McMurray, J., and Pfeffer, M.A. (2002). New therapeutic options in congestive heart failure: Parts I & II. *Circulation* 105, 2099-2106 & 2223-2228.

McNamara, D.M., Holubkov, R., Janosko, K., Palmer, A., Wang, J.J., MacGowan, G.A., Murali, S., Rosenblum, W.D., London, B., and Feldman, A.M. (2001). Pharmacogenetic interactions between beta-blocker therapy and the angiotensin-converting enzyme deletion polymorphism in patients with congestive heart failure. *Circulation* 103, 1644-1648.

Mehta, P.K., and Griendling, K.K. (2007). Angiotensin II cell signaling: physiological and pathological effects in the cardiovascular system. *American Journal of Physiology - Cell Physiology* 292, C82-97.

Melloni, C., Berger, J.S., Wang, T.Y., Gunes, F., Stebbins, A., Pieper, K.S., Dolor, R.J., Douglas, P.S., Mark, D.B., and Newby, L.K. (2010). Representation of women in randomized clinical trials of cardiovascular disease prevention. *Circulation: Cardiovascular Quality and Outcomes* 3, 135-142.

Mendelsohn, M.E., and Karas, R.H. (1999). The protective effects of estrogen on the cardiovascular system. *New England Journal of Medicine* 340, 1801-1811.

Mendelsohn, M.E., and Karas, R.H. (2005). Molecular and cellular basis of cardiovascular gender differences. *Science* 308, 1583-1587.

Mercadier, J.J., Lompre, A.M., Duc, P., Boheler, K.R., Fraysse, J.B., Wisnewsky, C., Allen, P.D., Komajda, M., and Schwartz, K. (1990). Altered sarcoplasmic reticulum Ca²⁺-ATPase gene expression in the human ventricle during end-stage heart failure. *Journal of Clinical Investigation* 85, 305-309.

Mihm, M.J., Yu, F., Carnes, C.A., Reiser, P.J., McCarthy, P.M., Van Wagoner, D.R., and Bauer, J.A. (2001). Impaired myofibrillar energetics and oxidative injury during human atrial fibrillation. *Circulation* 104, 174-180.

Mikkola, T.S., and Clarkson, T.B. (2002). Estrogen replacement therapy, atherosclerosis, and vascular function. *Cardiovascular Research* 53, 605-619.

Minamino, T., Yujiri, T., Terada, N., Taffet, G.E., Michael, L.H., Johnson, G.L., and Schneider, M.D. (2002). MEKK1 is essential for cardiac hypertrophy and dysfunction induced by Gq. *Proceedings of the National Academy of Sciences of the United States of America* 99, 3866-3871.

Miner, E.C., and Miller, W.L. (2006). A look between the cardiomyocytes: the extracellular matrix in heart failure. *Mayo Clinic Proceedings* 81, 71-76.

Mitchell, J.H., Cawood, E., Kinniburgh, D., Provan, A., Collins, A.R., and Irvine, D.S. (2001). Effect of a phytoestrogen food supplement on reproductive health in normal males. *Clinical Science* 100, 613-618.

Miyamoto, M.I., del Monte, F., Schmidt, U., DiSalvo, T.S., Kang, Z.B., Matsui, T., Guerrero, J.L., Gwathmey, J.K., Rosenzweig, A., and Hajjar, R.J. (2000). Adenoviral gene transfer of SERCA2a improves left-ventricular function in aortic-banded rats in transition to heart failure. *Proceedings of the National Academy of Sciences of the United States of America* 97, 793-798.

Molkentin, J.D., Lu, J.R., Antos, C.L., Markham, B., Richardson, J., Robbins, J., Grant, S.R., and Olson, E.N. (1998). A calcineurin-dependent transcriptional pathway for cardiac hypertrophy. *Cell* 93, 215-228.

Molkentin, J.D., and Dorn, G.W., 2nd (2001). Cytoplasmic signaling pathways that regulate cardiac hypertrophy. *Annual Review of Physiology* 63, 391-426.

Molkentin, J.D., and Robbins, J. (2009). With great power comes great responsibility: using mouse genetics to study cardiac hypertrophy and failure. *Journal of Molecular & Cellular Cardiology* 46, 130-136.

Montserrat, L., Elliott, P.M., Gimeno, J.R., Sharma, S., Penas-Lado, M., and McKenna, W.J. (2003). Non-sustained ventricular tachycardia in hypertrophic cardiomyopathy: an independent marker of sudden death risk in young patients. *Journal of the American College of Cardiology* 42, 873-879.

Morkin, E. (2000). Control of cardiac myosin heavy chain gene expression. *Microscopy Research and Technique* 50, 522-531.

Morton, J.B., Byrne, M.J., Power, J.M., Raman, J., and Kalman, J.M. (2002). Electrical remodeling of the atrium in an anatomic model of atrial flutter: relationship between substrate and triggers for conversion to atrial fibrillation. *Circulation* 105, 258-264.

Mosterd, A., and Hoes, A.W. (2007). Clinical epidemiology of heart failure. *Heart* 93, 1137-1146.

Muller, F.U., Lewin, G., Baba, H.A., Boknik, P., Fabritz, L., Kirchhefer, U., Kirchhof, P., Loser, K., Matus, M., Neumann, J., Riemann, B., and Schmitz, W. (2005). Heart-directed expression of a human cardiac isoform of cAMP-response element modulator in transgenic mice. *Journal of Biological Chemistry* 280, 6906-6914.

Mulrow, J.P., Healy, M.J., and McKenna, W.J. (1986). Variability of ventricular arrhythmias in hypertrophic cardiomyopathy and implications for treatment. *American Journal of Cardiology* 58, 615-618.

Munch, G., Bolck, B., Brixius, K., Reuter, H., Mehlhorn, U., Bloch, W., and Schwinger, R.H. (2000). SERCA2a activity correlates with the force-frequency relationship in human myocardium. *American Journal of Physiology - Heart & Circulatory Physiology* 278, H1924-1932.

Mureddu, G.F., Pasanisi, F., Palmieri, V., Celentano, A., Contaldo, F., and de Simone, G. (2001). Appropriate or inappropriate left ventricular mass in the presence or absence of prognostically adverse left ventricular hypertrophy. *Journal of Hypertension* 19, 1113-1119.

Muslin, A.J. (2008). MAPK signalling in cardiovascular health and disease: molecular mechanisms and therapeutic targets. *Clinical Science* 115, 203-218.

Nag, A.C. (1980). Study of non-muscle cells of the adult mammalian heart: a fine structural analysis and distribution. *Cytobios* 28, 41-61.

Nahrendorf, M., Frantz, S., Hu, K., von zur Muhlen, C., Tomaszewski, M., Scheuermann, H., Kaiser, R., Jazbutyte, V., Beer, S., Bauer, W., Neubauer, S., Ertl, G., Allolio, B., and Callies, F. (2003). Effect of testosterone on post-myocardial infarction remodeling and function. *Cardiovascular Research* 57, 370-378.

Nakagawa, M., Hamaoka, K., Hattori, T., and Sawada, T. (1988). Postnatal DNA synthesis in hearts of mice: autoradiographic and cytofluorometric investigations. *Cardiovascular Research* 22, 575-583.

Nakajima, H., Nakajima, H.O., Salcher, O., Dittie, A.S., Dembowski, K., Jing, S., and Field, L.J. (2000). Atrial but not ventricular fibrosis in mice expressing a mutant transforming growth factor-beta(1) transgene in the heart. *Circulation Research* 86, 571-579.

Namba, T., Tsutsui, H., Tagawa, H., Takahashi, M., Saito, K., Kozai, T., Usui, M., Imanaka-Yoshida, K., Imaizumi, T., and Takeshita, A. (1997). Regulation of fibrillar collagen gene expression and protein accumulation in volume-overloaded cardiac hypertrophy. *Circulation* 95, 2448-2454.

Nanas, J.N., Kontoyannis, D.A., Alexopoulos, G.P., Anastasiou-Nana, M.I., Tsagalou, E.P., Stamatelopoulos, S.F., and Moulopoulos, S.D. (2001). Long-term intermittent dobutamine infusion combined with oral amiodarone improves the survival of patients with severe congestive heart failure. *Chest* 119, 1173-1178.

Nao, T., Ohkusa, T., Hisamatsu, Y., Inoue, N., Matsumoto, T., Yamada, J., Shimizu, A., Yoshiga, Y., Yamagata, T., Kobayashi, S., Yano, M., Hamano, K., and Matsuzaki, M. (2003). Comparison of expression of connexin in right atrial myocardium in patients with chronic atrial fibrillation versus those in sinus rhythm. *American Journal of Cardiology* 91, 678-683.

Narula, J., Haider, N., Virmani, R., DiSalvo, T.G., Kolodgie, F.D., Hajjar, R.J., Schmidt, U., Semigran, M.J., Dec, G.W., and Khaw, B.A. (1996). Apoptosis in myocytes in end-stage heart failure. *New England Journal of Medicine* 335, 1182-1189.

Nattel, S. (1999). Ionic determinants of atrial fibrillation and Ca²⁺ channel abnormalities : cause, consequence, or innocent bystander? *Circulation Research* 85, 473-476.

Nattel, S., and Li, D. (2000). Ionic remodeling in the heart: pathophysiological significance and new therapeutic opportunities for atrial fibrillation. *Circulation Research* 87, 440-447.

Nattel, S. (2002). New ideas about atrial fibrillation 50 years on. *Nature* 415, 219-226.

Nattel, S., Burstein, B., and Dobrev, D. (2008). Atrial remodeling and atrial fibrillation: mechanisms and implications. *Circulation: Arrhythmia and Electrophysiology* 1, 62-73.

Neer, E.J. (1995). Heterotrimeric G proteins: organizers of transmembrane signals. *Cell* 80, 249-257.

Nelson, L., Jennings, G.L., Esler, M.D., and Korner, P.I. (1986). Effect of changing levels of physical activity on blood-pressure and haemodynamics in essential hypertension. *Lancet* 2, 473-476.

Neri Serneri, G.G., Boddi, M., Cecioni, I., Vanni, S., Coppo, M., Papa, M.L., Bandinelli, B., Bertolozzi, I., Polidori, G., Toscano, T., Maccherini, M., and Modesti, P.A. (2001a). Cardiac angiotensin II formation in the clinical course of heart failure and its relationship with left ventricular function. *Circulation Research* 88, 961-968.

Neri Serneri, G.G., Boddi, M., Modesti, P.A., Cecioni, I., Coppo, M., Padeletti, L., Michelucci, A., Colella, A., and Galanti, G. (2001b). Increased cardiac sympathetic

activity and insulin-like growth factor-I formation are associated with physiological hypertrophy in athletes. *Circulation Research* 89, 977-982.

Neubauer, S. (2007). The failing heart-an engine out of fuel. *New England Journal of Medicine* 356, 1140-1151.

NHF (2005). The shifting burden of cardiovascular disease in Australia. A report prepared for the National Heart Foundation by Access Economics.

NHF (2007). The Burden of Cardiovascular Disease in Australia for the Year 2003. A report prepared by the National Heart Foundation of Australia.

Nicol, R.L., Frey, N., Pearson, G., Cobb, M., Richardson, J., and Olson, E.N. (2001). Activated MEK5 induces serial assembly of sarcomeres and eccentric cardiac hypertrophy. *EMBO Journal* 20, 2757-2767.

Niessen, C.M. (2007). Tight junctions/adherens junctions: basic structure and function. *Journal of Investigative Dermatology* 127, 2525-2532.

Nishida, K., Yamaguchi, O., Hirotsani, S., Hikoso, S., Higuchi, Y., Watanabe, T., Takeda, T., Osuka, S., Morita, T., Kondoh, G., Uno, Y., Kashiwase, K., Taniike, M., Nakai, A., Matsumura, Y., Miyazaki, J., Sudo, T., Hongo, K., Kusakari, Y., Kurihara, S., Chien, K.R., Takeda, J., Hori, M., and Otsu, K. (2004). p38alpha mitogen-activated protein kinase plays a critical role in cardiomyocyte survival but not in cardiac hypertrophic growth in response to pressure overload. *Molecular & Cellular Biology* 24, 10611-10620.

Nishida, K., Michael, G., Dobrev, D., and Nattel, S. (2010). Animal models for atrial fibrillation: clinical insights and scientific opportunities. *Europace* 12, 160-172.

Nissen, S.E., Tuzcu, E.M., Libby, P., Thompson, P.D., Ghali, M., Garza, D., Berman, L., Shi, H., Buebendorf, E., and Topol, E.J. (2004). Effect of antihypertensive agents on

cardiovascular events in patients with coronary disease and normal blood pressure: the CAMELOT study, a randomized controlled trial. *Journal Of the American Medical Association* *292*, 2217-2225.

Noorman, M., van der Heyden, M.A., van Veen, T.A., Cox, M.G., Hauer, R.N., de Bakker, J.M., and van Rijen, H.V. (2009). Cardiac cell-cell junctions in health and disease: electrical versus mechanical coupling. *Journal of Molecular & Cellular Cardiology* *47*, 23-31.

Nordmeyer, J., Eder, S., Mahmoodzadeh, S., Martus, P., Fielitz, J., Bass, J., Bethke, N., Zurbrugg, H.R., Pregla, R., Hetzer, R., and Regitz-Zagrosek, V. (2004). Upregulation of myocardial estrogen receptors in human aortic stenosis. *Circulation* *110*, 3270-3275.

Nunez, S.B., Medin, J.A., Braissant, O., Kemp, L., Wahli, W., Ozato, K., and Segars, J.H. (1997). Retinoid X receptor and peroxisome proliferator-activated receptor activate an estrogen responsive gene independent of the estrogen receptor. *Molecular and Cellular Endocrinology* *127*, 27-40.

O'Connell, T.D., Ishizaka, S., Nakamura, A., Swigart, P.M., Rodrigo, M.C., Simpson, G.L., Cotecchia, S., Rokosh, D.G., Grossman, W., Foster, E., and Simpson, P.C. (2003). The alpha(1A/C)- and alpha(1B)-adrenergic receptors are required for physiological cardiac hypertrophy in the double-knockout mouse. *Journal of Clinical Investigation* *111*, 1783-1791.

Odashima, M., Usui, S., Takagi, H., Hong, C., Liu, J., Yokota, M., and Sadoshima, J. (2007). Inhibition of endogenous Mst1 prevents apoptosis and cardiac dysfunction without affecting cardiac hypertrophy after myocardial infarction. *Circulation Research* *100*, 1344-1352.

Ogata, T., Ueyama, T., Isodono, K., Tagawa, M., Takehara, N., Kawashima, T., Harada, K., Takahashi, T., Shioi, T., Matsubara, H., and Oh, H. (2008). MURC, a muscle-restricted

coiled-coil protein that modulates the Rho/ROCK pathway, induces cardiac dysfunction and conduction disturbance. *Molecular & Cellular Biology* 28, 3424-3436.

Ogawa, Y., Tamura, N., Chusho, H., and Nakao, K. (2001). Brain natriuretic peptide appears to act locally as an antifibrotic factor in the heart. *Canadian Journal of Physiology and Pharmacology* 79, 723-729.

Ohanian, J., and Heagerty, A.M. (1992). The phosphoinositide signaling system and hypertension. *Current Opinion in Nephrology & Hypertension* 1, 73-82.

Ohkusa, T., Ueyama, T., Yamada, J., Yano, M., Fujumura, Y., Esato, K., and Matsuzaki, M. (1999). Alterations in cardiac sarcoplasmic reticulum Ca²⁺ regulatory proteins in the atrial tissue of patients with chronic atrial fibrillation. *Journal of the American College of Cardiology* 34, 255-263.

Ohno, M., Takemura, G., Ohno, A., Misao, J., Hayakawa, Y., Minatoguchi, S., Fujiwara, T., and Fujiwara, H. (1998). "Apoptotic" myocytes in infarct area in rabbit hearts may be oncotic myocytes with DNA fragmentation: analysis by immunogold electron microscopy combined with in situ nick end-labeling. *Circulation* 98, 1422-1430.

Olgin, J.E., and Verheule, S. (2002). Transgenic and knockout mouse models of atrial arrhythmias. *Cardiovascular Research* 54, 280-286.

Oliver, P.M., Fox, J.E., Kim, R., Rockman, H.A., Kim, H.S., Reddick, R.L., Pandey, K.N., Milgram, S.L., Smithies, O., and Maeda, N. (1997). Hypertension, cardiac hypertrophy, and sudden death in mice lacking natriuretic peptide receptor A. *Proceedings of the National Academy of Sciences of the United States of America* 94, 14730-14735.

Olivetti, G., Giordano, G., Corradi, D., Melissari, M., Lagrasta, C., Gambert, S.R., and Anversa, P. (1995). Gender differences and aging: effects on the human heart. *Journal of the American College of Cardiology* 26, 1068-1079.

Olivetti, G., Abbi, R., Quaini, F., Kajstura, J., Cheng, W., Nitahara, J.A., Quaini, E., Di Loreto, C., Beltrami, C.A., Krajewski, S., Reed, J.C., and Anversa, P. (1997). Apoptosis in the failing human heart. *New England Journal of Medicine* 336, 1131-1141.

Olivotto, I., Cecchi, F., Casey, S.A., Dolaro, A., Traverse, J.H., and Maron, B.J. (2001). Impact of atrial fibrillation on the clinical course of hypertrophic cardiomyopathy. *Circulation* 104, 2517-2524.

Olson, E.N., and Williams, R.S. (2000). Calcineurin signaling and muscle remodeling. *Cell* 101, 689-692.

Olson, E.N. (2004). A decade of discoveries in cardiac biology. *Nature Medicine* 10, 467-474.

Osorio, J.C., Stanley, W.C., Linke, A., Castellari, M., Diep, Q.N., Panchal, A.R., Hintze, T.H., Lopaschuk, G.D., and Recchia, F.A. (2002). Impaired myocardial fatty acid oxidation and reduced protein expression of retinoid X receptor-alpha in pacing-induced heart failure. *Circulation* 106, 606-612.

Osranek, M., Bursi, F., Bailey, K.R., Grossardt, B.R., Brown, R.D., Jr., Kopecky, S.L., Tsang, T.S., and Seward, J.B. (2005). Left atrial volume predicts cardiovascular events in patients originally diagnosed with lone atrial fibrillation: three-decade follow-up. *European Heart Journal* 26, 2556-2561.

Ostadal, B., Ostadalova, I., and Dhalla, N.S. (1999). Development of cardiac sensitivity to oxygen deficiency: comparative and ontogenetic aspects. *Physiological Reviews* 79, 635-659.

Owen, K.L., Pretorius, L., and McMullen, J.R. (2009). The protective effects of exercise and phosphoinositide 3-kinase (p110alpha) in the failing heart. *Clinical Science* 116, 365-375.

Packer, M., Colucci, W.S., Sackner-Bernstein, J.D., Liang, C.S., Goldscher, D.A., Freeman, I., Kukin, M.L., Kinhal, V., Udelson, J.E., Klapholz, M., Gottlieb, S.S., Pearle, D., Cody, R.J., Gregory, J.J., Kantrowitz, N.E., LeJemtel, T.H., Young, S.T., Lukas, M.A., and Shusterman, N.H. (1996). Double-blind, placebo-controlled study of the effects of carvedilol in patients with moderate to severe heart failure. The PRECISE Trial. Prospective Randomized Evaluation of Carvedilol on Symptoms and Exercise. *Circulation* 94, 2793-2799.

Packer, M., and Cohn, J.N. (1999). Consensus recommendations for the management of chronic heart failure. On behalf of the membership of the advisory council to improve outcomes nationwide in heart failure. *American Journal of Cardiology* 83, 1A-38A.

Packer, M., Poole-Wilson, P.A., Armstrong, P.W., Cleland, J.G., Horowitz, J.D., Massie, B.M., Ryden, L., Thygesen, K., and Uretsky, B.F. (1999). Comparative effects of low and high doses of the angiotensin-converting enzyme inhibitor, lisinopril, on morbidity and mortality in chronic heart failure. ATLAS Study Group. *Circulation* 100, 2312-2318.

Packer, M., Coats, A.J., Fowler, M.B., Katus, H.A., Krum, H., Mohacsi, P., Rouleau, J.L., Tendera, M., Castaigne, A., Roecker, E.B., Schultz, M.K., and DeMets, D.L. (2001). Effect of carvedilol on survival in severe chronic heart failure. *New England Journal of Medicine* 344, 1651-1658.

Pasumarthi, K.B., and Field, L.J. (2002). Cardiomyocyte cell cycle regulation. *Circulation Research* 90, 1044-1054.

Patel, J.B., Valencik, M.L., Pritchett, A.M., Burnett, J.C., Jr., McDonald, J.A., and Redfield, M.M. (2005). Cardiac-specific attenuation of natriuretic peptide A receptor activity accentuates adverse cardiac remodeling and mortality in response to pressure overload. *American Journal of Physiology - Heart & Circulatory Physiology* 289, H777-784.

Patten, R.D., and Karas, R.H. (2006). Estrogen replacement and cardiomyocyte protection. *Trends in Cardiovascular Medicine* 16, 69-75.

Pearse, G., Frith, J., Randall, K.J., and Klinowska, T. (2009). Urinary retention and cystitis associated with subcutaneous estradiol pellets in female nude mice. *Toxicologic Pathology* 37, 227-234.

Pearson, G., Robinson, F., Gibson, T.B., Xu, B.E., Karandikar, M., Berman, K., and Cobb, M.H. (2001). Mitogen-activated protein (MAP) kinase pathways: regulation and physiological functions. *Endocrine Reviews* 22, 153-183.

Pedersen, O.D., Bagger, H., Kober, L., and Torp-Pedersen, C. (1999). Trandolapril reduces the incidence of atrial fibrillation after acute myocardial infarction in patients with left ventricular dysfunction. *Circulation* 100, 376-380.

Pelzer, T., Shamim, A., and Neyses, L. (1996). Estrogen effects in the heart. *Molecular & Cellular Biochemistry* 160-161, 307-313.

Pelzer, T., Loza, P.A., Hu, K., Bayer, B., Dienesch, C., Calvillo, L., Couse, J.F., Korach, K.S., Neyses, L., and Ertl, G. (2005). Increased mortality and aggravation of heart failure in estrogen receptor-beta knockout mice after myocardial infarction. *Circulation* 111, 1492-1498.

Periasamy, M., Reed, T.D., Liu, L.H., Ji, Y., Loukianov, E., Paul, R.J., Nieman, M.L., Riddle, T., Duffy, J.J., Doetschman, T., Lorenz, J.N., and Shull, G.E. (1999). Impaired cardiac performance in heterozygous mice with a null mutation in the sarco(endo)plasmic reticulum Ca²⁺ ATPase isoform 2 (SERCA2) gene. *Journal of Biological Chemistry* 274, 2556-2562.

Periasamy, M., and Huke, S. (2001). SERCA pump level is a critical determinant of Ca(2+)homeostasis and cardiac contractility. *Journal of Molecular & Cellular Cardiology* 33, 1053-1063.

Periasamy, M., and Kalyanasundaram, A. (2007). SERCA pump isoforms: their role in calcium transport and disease. *Muscle & Nerve* 35, 430-442.

Peter, P.S., Brady, J.E., Yan, L., Chen, W., Engelhardt, S., Wang, Y., Sadoshima, J., Vatner, S.F., and Vatner, D.E. (2007). Inhibition of p38 alpha MAPK rescues cardiomyopathy induced by overexpressed beta 2-adrenergic receptor, but not beta 1-adrenergic receptor. *Journal of Clinical Investigation* 117, 1335-1343.

Petrich, B.G., Molkenin, J.D., and Wang, Y. (2003). Temporal activation of c-Jun N-terminal kinase in adult transgenic heart via cre-loxP-mediated DNA recombination. *FASEB Journal* 17, 749-751.

Petrich, B.G., and Wang, Y. (2004). Stress-activated MAP kinases in cardiac remodeling and heart failure; new insights from transgenic studies. *Trends in Cardiovascular Medicine* 14, 50-55.

Pfeffer, J.M., Pfeffer, M.A., Mirsky, I., and Braunwald, E. (1982). Regression of left ventricular hypertrophy and prevention of left ventricular dysfunction by captopril in the spontaneously hypertensive rat. *Proceedings of the National Academy of Sciences of the United States of America* 79, 3310-3314.

Pfeffer, M.A., Lamas, G.A., Vaughan, D.E., Parisi, A.F., and Braunwald, E. (1988). Effect of captopril on progressive ventricular dilatation after anterior myocardial infarction. *New England Journal of Medicine* 319, 80-86.

Piacentino, V., 3rd, Weber, C.R., Chen, X., Weisser-Thomas, J., Margulies, K.B., Bers, D.M., and Houser, S.R. (2003). Cellular basis of abnormal calcium transients of failing human ventricular myocytes. *Circulation Research* *92*, 651-658.

Pina, I.L., Apstein, C.S., Balady, G.J., Belardinelli, R., Chaitman, B.R., Duscha, B.D., Fletcher, B.J., Fleg, J.L., Myers, J.N., and Sullivan, M.J. (2003). Exercise and heart failure: A statement from the American Heart Association Committee on exercise, rehabilitation, and prevention. *Circulation* *107*, 1210-1225.

Platzer, J., Engel, J., Schrott-Fischer, A., Stephan, K., Bova, S., Chen, H., Zheng, H., and Striessnig, J. (2000). Congenital deafness and sinoatrial node dysfunction in mice lacking class D L-type Ca²⁺ channels. *Cell* *102*, 89-97.

Pluim, B.M., Zwinderman, A.H., van der Laarse, A., and van der Wall, E.E. (2000). The athlete's heart. A meta-analysis of cardiac structure and function. *Circulation* *101*, 336-344.

Podesser, B.K., Jain, M., Ngoy, S., Apstein, C.S., and Eberli, F.R. (2007). Unveiling gender differences in demand ischemia: a study in a rat model of genetic hypertension. *European Journal of Cardio-Thoracic Surgery* *31*, 298-304.

Poole-Wilson, P.A., Uretsky, B.F., Thygesen, K., Cleland, J.G., Massie, B.M., and Ryden, L. (2003). Mode of death in heart failure: findings from the ATLAS trial. *Heart* *89*, 42-48.

Popescu, L.M., Gherghiceanu, M., Hinescu, M.E., Cretoiu, D., Ceafalan, L., Regalia, T., Popescu, A.C., Ardeleanu, C., and Mandache, E. (2006). Insights into the interstitium of ventricular myocardium: interstitial Cajal-like cells (ICLC). *Journal of Cellular and Molecular Medicine* *10*, 429-458.

Prasad, V., Okunade, G.W., Miller, M.L., Shull, G.E., Prasad, V., Okunade, G.W., Miller, M.L., and Shull, G.E. (2004). Phenotypes of SERCA and PMCA knockout mice. *Biochemical & Biophysical Research Communications* 322, 1192-1203.

Pretorius, L., Owen, K.L., Jennings, G.L., and McMullen, J.R. (2008). Promoting physiological hypertrophy in the failing heart. *Clinical & Experimental Pharmacology & Physiology* 35, 438-441.

Pretorius, L., Du, X.J., Woodcock, E.A., Kiriazis, H., Lin, R.C., Marasco, S., Medcalf, R.L., Ming, Z., Head, G.A., Tan, J.W., Cemerlang, N., Sadoshima, J., Shioi, T., Izumo, S., Lukoshkova, E.V., Dart, A.M., Jennings, G.L., and McMullen, J.R. (2009). Reduced phosphoinositide 3-kinase (p110alpha) activation increases the susceptibility to atrial fibrillation. *American Journal of Pathology* 175, 998-1009.

Prossnitz, E.R., Arterburn, J.B., Smith, H.O., Oprea, T.I., Sklar, L.A., and Hathaway, H.J. (2008). Estrogen signaling through the transmembrane G protein-coupled receptor GPR30. *Annual Review of Physiology* 70, 165-190.

Pu, M., Gao, Z., Li, J., Sinoway, L., and Davidson, W.R., Jr. (2005). Development of a new animal model of chronic mitral regurgitation in rats under transesophageal echocardiographic guidance. *Journal of the American Society of Echocardiography* 18, 468-474.

Purcell, N.H., Wilkins, B.J., York, A., Saba-El-Leil, M.K., Meloche, S., Robbins, J., and Molkentin, J.D. (2007). Genetic inhibition of cardiac ERK1/2 promotes stress-induced apoptosis and heart failure but has no effect on hypertrophy in vivo. *Proceedings of the National Academy of Sciences of the United States of America* 104, 14074-14079.

Qi, X.Y., Yeh, Y.H., Xiao, L., Burstein, B., Maguy, A., Chartier, D., Villeneuve, L.R., Brundel, B.J., Dobrev, D., and Nattel, S. (2008). Cellular signaling underlying atrial tachycardia remodeling of L-type calcium current. *Circulation Research* 103, 845-854.

Ramirez, M.T., Sah, V.P., Zhao, X.L., Hunter, J.J., Chien, K.R., and Brown, J.H. (1997). The MEKK-JNK pathway is stimulated by alpha1-adrenergic receptor and ras activation and is associated with in vitro and in vivo cardiac hypertrophy. *Journal of Biological Chemistry* 272, 14057-14061.

Recchia, F.A., McConnell, P.I., Bernstein, R.D., Vogel, T.R., Xu, X., and Hintze, T.H. (1998). Reduced nitric oxide production and altered myocardial metabolism during the decompensation of pacing-induced heart failure in the conscious dog. *Circulation Research* 83, 969-979.

Reed, K.E., Westphale, E.M., Larson, D.M., Wang, H.Z., Veenstra, R.D., and Beyer, E.C. (1993). Molecular cloning and functional expression of human connexin37, an endothelial cell gap junction protein. *Journal of Clinical Investigation* 91, 997-1004.

Regitz-Zagrosek, V. (2006). Therapeutic implications of the gender-specific aspects of cardiovascular disease. *Nature Reviews Drug Discovery* 5, 425-438.

Reiss, K., Cheng, W., Ferber, A., Kajstura, J., Li, P., Li, B., Olivetti, G., Homcy, C.J., Baserga, R., and Anversa, P. (1996). Overexpression of insulin-like growth factor-1 in the heart is coupled with myocyte proliferation in transgenic mice. *Proceedings of the National Academy of Sciences of the United States of America* 93, 8630-8635.

Reisz-Porszasz, S., Bhasin, S., Artaza, J.N., Shen, R., Sinha-Hikim, I., Hogue, A., Fielder, T.J., and Gonzalez-Cadavid, N.F. (2003). Lower skeletal muscle mass in male transgenic mice with muscle-specific overexpression of myostatin. *American Journal of Physiology - Endocrinology and Metabolism* 285, E876-888.

Revankar, C.M., Cimino, D.F., Sklar, L.A., Arterburn, J.B., and Prossnitz, E.R. (2005). A transmembrane intracellular estrogen receptor mediates rapid cell signaling. *Science* 307, 1625-1630.

Rhoades, R.A., and Bell, D.R. (2009). *Medical physiology: principles for clinical medicine* 3rd edition. (Philadelphia, Lippincott Williams & Wilkins).

Rigor, D.L., Bodyak, N., Bae, S., Choi, J.H., Zhang, L., Ter-Ovanesyan, D., He, Z., McMullen, J.R., Shioi, T., Izumo, S., King, G.L., and Kang, P.M. (2009). Phosphoinositide 3-kinase Akt signaling pathway interacts with protein kinase C β 2 in the regulation of physiologic developmental hypertrophy and heart function. *American Journal of Physiology - Heart & Circulatory Physiology* 296, H566-572.

Rimbaud, S., Sanchez, H., Garnier, A., Fortin, D., Bigard, X., Veksler, V., and Ventura-Clapier, R. (2009). Stimulus specific changes of energy metabolism in hypertrophied heart. *Journal of Molecular & Cellular Cardiology* 46, 952-959.

Ritchie, R.H., and Delbridge, L.M. (2006). Cardiac hypertrophy, substrate utilization and metabolic remodelling: cause or effect? *Clinical & Experimental Pharmacology & Physiology* 33, 159-166.

Roberts, R. (2006). Genomics and cardiac arrhythmias. *Journal of the American College of Cardiology* 47, 9-21.

Roger, V.L., Weston, S.A., Redfield, M.M., Hellermann-Homan, J.P., Killian, J., Yawn, B.P., and Jacobsen, S.J. (2004). Trends in heart failure incidence and survival in a community-based population. *Journal Of the American Medical Association* 292, 344-350.

Rohr, S. (2004). Role of gap junctions in the propagation of the cardiac action potential. *Cardiovascular Research* 62, 309-322.

Rondinone, C.M., Wang, L.M., Lonroth, P., Wesslau, C., Pierce, J.H., and Smith, U. (1997). Insulin receptor substrate (IRS) 1 is reduced and IRS-2 is the main docking protein for phosphatidylinositol 3-kinase in adipocytes from subjects with non-insulin-

dependent diabetes mellitus. *Proceedings of the National Academy of Sciences of the United States of America* 94, 4171-4175.

Rose, E.A., Gelijns, A.C., Moskowitz, A.J., Heitjan, D.F., Stevenson, L.W., Dembitsky, W., Long, J.W., Ascheim, D.D., Tierney, A.R., Levitan, R.G., Watson, J.T., Meier, P., Ronan, N.S., Shapiro, P.A., Lazar, R.M., Miller, L.W., Gupta, L., Frazier, O.H., Desvigne-Nickens, P., Oz, M.C., and Poirier, V.L. (2001). Long-term mechanical left ventricular assistance for end-stage heart failure. *New England Journal of Medicine* 345, 1435-1443.

Rossi, M.A. (1998). Pathologic fibrosis and connective tissue matrix in left ventricular hypertrophy due to chronic arterial hypertension in humans. *Journal of Hypertension* 16, 1031-1041.

Rossouw, J.E., Anderson, G.L., Prentice, R.L., LaCroix, A.Z., Kooperberg, C., Stefanick, M.L., Jackson, R.D., Beresford, S.A., Howard, B.V., Johnson, K.C., Kotchen, J.M., and Ockene, J. (2002). Risks and benefits of estrogen plus progestin in healthy postmenopausal women: principal results from the Women's Health Initiative randomized controlled trial. *Journal Of the American Medical Association* 288, 321-333.

Rossouw, J.E., Prentice, R.L., Manson, J.E., Wu, L., Barad, D., Barnabei, V.M., Ko, M., LaCroix, A.Z., Margolis, K.L., and Stefanick, M.L. (2007). Postmenopausal hormone therapy and risk of cardiovascular disease by age and years since menopause. *Journal Of the American Medical Association* 297, 1465-1477.

Rostock, T., Steven, D., Lutomsky, B., Servatius, H., Drewitz, I., Klemm, H., Mullerleile, K., Ventura, R., Meinertz, T., and Willems, S. (2008). Atrial fibrillation begets atrial fibrillation in the pulmonary veins on the impact of atrial fibrillation on the electrophysiological properties of the pulmonary veins in humans. *Journal of the American College of Cardiology* 51, 2153-2160.

Saba, S., Janczewski, A.M., Baker, L.C., Shusterman, V., Gursoy, E.C., Feldman, A.M., Salama, G., McTiernan, C.F., and London, B. (2005). Atrial contractile dysfunction, fibrosis, and arrhythmias in a mouse model of cardiomyopathy secondary to cardiac-specific overexpression of tumor necrosis factor-(alpha). *American Journal of Physiology - Heart & Circulatory Physiology* 289, H1456-1467.

Sadoshima, J., Montagne, O., Wang, Q., Yang, G., Warden, J., Liu, J., Takagi, G., Karoor, V., Hong, C., Johnson, G.L., Vatner, D.E., and Vatner, S.F. (2002). The MEKK1-JNK pathway plays a protective role in pressure overload but does not mediate cardiac hypertrophy. *Journal of Clinical Investigation* 110, 271-279.

Sah, V.P., Minamisawa, S., Tam, S.P., Wu, T.H., Dorn, G.W., 2nd, Ross, J., Jr., Chien, K.R., and Brown, J.H. (1999). Cardiac-specific overexpression of RhoA results in sinus and atrioventricular nodal dysfunction and contractile failure. *Journal of Clinical Investigation* 103, 1627-1634.

Sak, K., and Everaus, H. (2004). Nongenomic effects of 17beta-estradiol--diversity of membrane binding sites. *J Steroid Biochem Mol Biol* 88, 323-335.

Sakata, Y., Hoit, B.D., Liggett, S.B., Walsh, R.A., and Dorn, G.W., 2nd (1998). Decompensation of pressure-overload hypertrophy in G alpha q-overexpressing mice. *Circulation* 97, 1488-1495.

Sambrook, J., and Russel, D.W. (2001). *Molecular cloning: a laboratory manual* (volume 1). 3 edn (New York, Cold Spring Harbor Laboratory Press).

Samuels, Y., Wang, Z., Bardelli, A., Silliman, N., Ptak, J., Szabo, S., Yan, H., Gazdar, A., Powell, S.M., Riggins, G.J., Willson, J.K., Markowitz, S., Kinzler, K.W., Vogelstein, B., and Velculescu, V.E. (2004). High frequency of mutations of the PIK3CA gene in human cancers. *Science* 304, 554.

Sancho, V., Nuche, B., Arnes, L., Cancelas, J., Gonzalez, N., Diaz-Miguel, M., Martin-Duce, A., Valverde, I., and Villanueva-Penacarrillo, M.L. (2007). The action of GLP-1 and exendins upon glucose transport in normal human adipocytes, and on kinase activity as compared to morbidly obese patients. *International Journal of Molecular Medicine* 19, 961-966.

Santen, R.J., Allred, D.C., Ardoin, S.P., Archer, D.F., Boyd, N., Braunstein, G.D., Burger, H.G., Colditz, G.A., Davis, S.R., Gambacciani, M., Gower, B.A., Henderson, V.W., Jarjour, W.N., Karas, R.H., Kleerekoper, M., Lobo, R.A., Manson, J.E., Marsden, J., Martin, K.A., Martin, L., Pinkerton, J.V., Rubinow, D.R., Teede, H., Thiboutot, D.M., and Utian, W.H. (2010). Postmenopausal hormone therapy: an Endocrine Society scientific statement. *Journal of Clinical Endocrinology & Metabolism* 95, s1-s66.

Saraste, A., Pulkki, K., Kallajoki, M., Henriksen, K., Parvinen, M., and Voipio-Pulkki, L.M. (1997). Apoptosis in human acute myocardial infarction. *Circulation* 95, 320-323.

Satoh, T., and Zipes, D.P. (1996). Unequal atrial stretch in dogs increases dispersion of refractoriness conducive to developing atrial fibrillation. *Journal of Cardiovascular Electrophysiology* 7, 833-842.

Saumarez, R.C., Camm, A.J., Panagos, A., Gill, J.S., Stewart, J.T., de Belder, M.A., Simpson, I.A., and McKenna, W.J. (1992). Ventricular fibrillation in hypertrophic cardiomyopathy is associated with increased fractionation of paced right ventricular electrograms. *Circulation* 86, 467-474.

Savelieva, I., and Camm, J. (2008). Statins and polyunsaturated fatty acids for treatment of atrial fibrillation. *Nature Clinical Practice Cardiovascular Medicine* 5, 30-41.

Saxon, L.A., and De Marco, T. (2002). Arrhythmias associated with dilated cardiomyopathy. *Cardiac Electrophysiology Review* 6, 18-25.

Schachinger, V., Assmus, B., Britten, M.B., Honold, J., Lehmann, R., Teupe, C., Abolmaali, N.D., Vogl, T.J., Hofmann, W.K., Martin, H., Dimmeler, S., and Zeiher, A.M. (2004). Transplantation of progenitor cells and regeneration enhancement in acute myocardial infarction: final one-year results of the TOPCARE-AMI Trial. *Journal of the American College of Cardiology* 44, 1690-1699.

Schaible, T.F., and Scheuer, J. (1979). Effects of physical training by running or swimming on ventricular performance of rat hearts. *Journal of Applied Physiology: Respiratory, Environmental & Exercise Physiology* 46, 854-860.

Schaible, T.F., Penpargkul, S., and Scheuer, J. (1981). Cardiac responses to exercise training in male and female rats. *Journal of Applied Physiology: Respiratory, Environmental & Exercise Physiology* 50, 112-117.

Schaible, T.F., and Scheuer, J. (1981). Cardiac function in hypertrophied hearts from chronically exercised female rats. *Journal of Applied Physiology: Respiratory, Environmental & Exercise Physiology* 50, 1140-1145.

Schaible, T.F., and Scheuer, J. (1984). Response of the heart to exercise training. In *Growth of the heart in health and disease*, R. Zak, ed. (New York, Raven Press), pp. 381-420.

Schena, M., Shalon, D., Davis, R.W., and Brown, P.O. (1995). Quantitative monitoring of gene expression patterns with a complementary DNA microarray. *Science* 270, 467-470.

Scheuer, J., Malhotra, A., Hirsch, C., Capasso, J., and Schaible, T.F. (1982). Physiologic cardiac hypertrophy corrects contractile protein abnormalities associated with pathologic hypertrophy in rats. *Journal of Clinical Investigation* 70, 1300-1305.

Scheuer, J., and Buttrick, P. (1987). The cardiac hypertrophic responses to pathologic and physiologic loads. *Circulation* 75 (suppl 1), I-63 - I-68.

Schiaffino, S., Samuel, J.L., Sassoon, D., Lompre, A.M., Garner, I., Marotte, F., Buckingham, M., Rappaport, L., and Schwartz, K. (1989a). Nonsynchronous accumulation of alpha-skeletal actin and beta-myosin heavy chain mRNAs during early stages of pressure-overload-induced cardiac hypertrophy demonstrated by in situ hybridization. *Circulation Research* 64, 937-948.

Schiaffino, S., Samuel, J.L., Sassoon, D., Lompre, A.M., Garner, I., Marotte, F., Buckingham, M., Rappaport, L., and Schwartz, K. (1989b). Nonsynchronous accumulation of alpha-skeletal actin and beta-myosin heavy chain mRNAs during early stages of pressure-overload--induced cardiac hypertrophy demonstrated by in situ hybridization. *Circulation Research* 64, 937-948.

Schocken, D.D., Benjamin, E.J., Fonarow, G.C., Krumholz, H.M., Levy, D., Mensah, G.A., Narula, J., Shor, E.S., Young, J.B., and Hong, Y. (2008). Prevention of heart failure: a scientific statement from the American Heart Association Councils on Epidemiology and Prevention, Clinical Cardiology, Cardiovascular Nursing, and High Blood Pressure Research; Quality of Care and Outcomes Research Interdisciplinary Working Group; and Functional Genomics and Translational Biology Interdisciplinary Working Group. *Circulation* 117, 2544-2565.

Schotten, U., Neuberger, H.R., and Allessie, M.A. (2003). The role of atrial dilatation in the domestication of atrial fibrillation. *Progress in Biophysics and Molecular Biology* 82, 151-162.

Schreiber, S.N., Knutti, D., Brogli, K., Uhlmann, T., and Kralli, A. (2003). The transcriptional coactivator PGC-1 regulates the expression and activity of the orphan nuclear receptor estrogen-related receptor alpha (ERRalpha). *Journal of Biological Chemistry* 278, 9013-9018.

Schreiber, S.N., Emter, R., Hock, M.B., Knutti, D., Cardenas, J., Podvinec, M., Oakeley, E.J., and Kralli, A. (2004). The estrogen-related receptor alpha (ERRalpha) functions in PPARgamma coactivator 1alpha (PGC-1alpha)-induced mitochondrial biogenesis. *Proceedings of the National Academy of Sciences of the United States of America* *101*, 6472-6477.

Schultz, J.E.J., Glascock, B.J., Witt, S.A., Nieman, M.L., Nattamai, K.J., Liu, L.H., Lorenz, J.N., Shull, G.E., Kimball, T.R., and Periasamy, M. (2004). Accelerated onset of heart failure in mice during pressure overload with chronically decreased SERCA2 calcium pump activity. *American Journal of Physiology - Heart & Circulatory Physiology* *286*, H1146-1153.

Schwartz, K., Lecarpentier, Y., Martin, J.L., Lompre, A.M., Mercadier, J.J., and Swynghedauw, B. (1981). Myosin isoenzymic distribution correlates with speed of myocardial contraction. *Journal of Molecular & Cellular Cardiology* *13*, 1071-1075.

Schwartz, K., de la Bastie, D., Bouveret, P., Oliviero, P., Alonso, S., and Buckingham, M. (1986). Alpha-skeletal muscle actin mRNA's accumulate in hypertrophied adult rat hearts. *Circulation Research* *59*, 551-555.

Semsarian, C., and Maron, B.J. (2002). Sudden cardiac death in the young. *Medical Journal of Australia* *176*, 148-149.

Setchell, K.D. (1998). Phytoestrogens: the biochemistry, physiology, and implications for human health of soy isoflavones. *American Journal of Clinical Nutrition* *68*, 1333S-1346S.

Severs, N.J., Bruce, A.F., Dupont, E., and Rothery, S. (2008). Remodelling of gap junctions and connexin expression in diseased myocardium. *Cardiovascular Research* *80*, 9-19.

Shannon, T.R., Ginsburg, K.S., and Bers, D.M. (2002). Quantitative assessment of the SR Ca²⁺ leak-load relationship. *Circulation Research* 91, 594-600.

Sharkey, L.C., Holycross, B.J., Park, S., McCune, S.A., Hoversland, R., and Radin, M.J. (1998). Effect of ovariectomy in heart failure-prone SHHF/Mcc-facp rats. *American Journal of Physiology* 275, R1968-1976.

Sharov, V.G., Sabbah, H.N., Shimoyama, H., Goussev, A.V., Lesch, M., and Goldstein, S. (1996). Evidence of cardiocyte apoptosis in myocardium of dogs with chronic heart failure. *American Journal of Pathology* 148, 141-149.

Shiels, H.A., and White, E. (2008). The Frank-Starling mechanism in vertebrate cardiac myocytes. *Journal of Experimental Biology* 211, 2005-2013.

Shinmura, K., Nagai, M., Tamaki, K., and Bolli, R. (2008). Loss of ischaemic preconditioning in ovariectomized rat hearts: possible involvement of impaired protein kinase C epsilon phosphorylation. *Cardiovascular Research* 79, 387-394.

Shioi, T., Kang, P.M., Douglas, P.S., Hampe, J., Yballe, C.M., Lawitts, J., Cantley, L.C., and Izumo, S. (2000). The conserved phosphoinositide 3-kinase pathway determines heart size in mice. *EMBO Journal* 19, 2537-2548.

Shioi, T., McMullen, J.R., Kang, P.M., Douglas, P.S., Obata, T., Franke, T.F., Cantley, L.C., and Izumo, S. (2002). Akt/protein kinase B promotes organ growth in transgenic mice. *Molecular & Cellular Biology* 22, 2799-2809.

Shiraishi, I., Melendez, J., Ahn, Y., Skavdahl, M., Murphy, E., Welch, S., Schaefer, E., Walsh, K., Rosenzweig, A., Torella, D., Nurzynska, D., Kajstura, J., Leri, A., Anversa, P., and Sussman, M.A. (2004). Nuclear targeting of Akt enhances kinase activity and survival of cardiomyocytes. *Circulation Research* 94, 884-891.

Shiroshita-Takeshita, A., Schram, G., Lavoie, J., and Nattel, S. (2004). Effect of simvastatin and antioxidant vitamins on atrial fibrillation promotion by atrial-tachycardia remodeling in dogs. *Circulation* *110*, 2313-2319.

Shlipak, M.G., Angeja, B.G., Go, A.S., Frederick, P.D., Canto, J.G., and Grady, D. (2001). Hormone therapy and in-hospital survival after myocardial infarction in postmenopausal women. *Circulation* *104*, 2300-2304.

Siedner, S., Kruger, M., Schroeter, M., Metzler, D., Roell, W., Fleischmann, B.K., Hescheler, J., Pfitzer, G., and Stehle, R. (2003). Developmental changes in contractility and sarcomeric proteins from the early embryonic to the adult stage in the mouse heart. *Journal of Physiology* *548*, 493-505.

Silverman, J., Powers, J., Stromberg, P., Pultz, J.A., and Kent, S. (1989). Effects on C3H mouse mammary cancer of changing from a high fat to a low fat diet before, at, or after puberty. *Cancer Research* *49*, 3857-3860.

Simoncini, T., Hafezi-Moghadam, A., Brazil, D.P., Ley, K., Chin, W.W., and Liao, J.K. (2000). Interaction of oestrogen receptor with the regulatory subunit of phosphatidylinositol-3-OH kinase. *Nature* *407*, 538-541.

Singal, P.K., and Iliskovic, N. (1998). Doxorubicin-induced cardiomyopathy. *New England Journal of Medicine* *339*, 900-905.

Singh, S.N., Fletcher, R.D., Fisher, S.G., Singh, B.N., Lewis, H.D., Deedwania, P.C., Massie, B.M., Colling, C., and Lazzeri, D. (1995). Amiodarone in patients with congestive heart failure and asymptomatic ventricular arrhythmia. Survival Trial of Antiarrhythmic Therapy in Congestive Heart Failure. *New England Journal of Medicine* *333*, 77-82.

Skavdahl, M., Steenbergen, C., Clark, J., Myers, P., Demianenko, T., Mao, L., Rockman, H.A., Korach, K.S., and Murphy, E. (2005). Estrogen receptor-beta mediates male-female differences in the development of pressure overload hypertrophy. *American Journal of Physiology - Heart & Circulatory Physiology* 288, H469-476.

Smith, P.J., Ornatsky, O., Stewart, D.J., Picard, P., Dawood, F., Wen, W.H., Liu, P.P., Webb, D.J., and Monge, J.C. (2000). Effects of estrogen replacement on infarct size, cardiac remodeling, and the endothelin system after myocardial infarction in ovariectomized rats. *Circulation* 102, 2983-2989.

Solti, F., Vecsey, T., Kekesi, V., and Juhasz-Nagy, A. (1989). The effect of atrial dilatation on the genesis of atrial arrhythmias. *Cardiovascular Research* 23, 882-886.

Song, G., Ouyang, G., and Bao, S. (2005). The activation of Akt/PKB signaling pathway and cell survival. *Journal of Cellular and Molecular Medicine* 9, 59-71.

Soonpaa, M.H., Kim, K.K., Pajak, L., Franklin, M., and Field, L.J. (1996). Cardiomyocyte DNA synthesis and binucleation during murine development. *American Journal of Physiology* 271, H2183-2189.

Sossalla, S., Fluschnik, N., Schotola, H., Ort, K.R., Neef, S., Schulte, T., Wittkopper, K., Renner, A., Schmitto, J.D., Gummert, J., El-Armouche, A., Hasenfuss, G., and Maier, L.S. (2010). Inhibition of elevated Ca²⁺/Calmodulin-dependent protein kinase II improves contractility in human failing myocardium. *Circulation Research* *In press*.

Soti, C., Nagy, E., Gircz, Z., Vigh, L., Csermely, P., and Ferdinandy, P. (2005). Heat shock proteins as emerging therapeutic targets. *British Journal of Clinical Pharmacology* 146, 769-780.

Spinale, F.G. (2007). Myocardial matrix remodeling and the matrix metalloproteinases: influence on cardiac form and function. *Physiological Reviews* 87, 1285-1342.

Spirito, P., Watson, R.M., and Maron, B.J. (1987). Relation between extent of left ventricular hypertrophy and occurrence of ventricular tachycardia in hypertrophic cardiomyopathy. *American Journal of Cardiology* 60, 1137-1142.

Srivastava, D., and Yu, S. (2006). Stretching to meet needs: integrin-linked kinase and the cardiac pump. *Genes & Development* 20, 2327-2331.

St Rammos, K., Koullias, G.J., Hassan, M.O., Argyrakis, N.P., Voucharas, C.G., Scarupa, S.J., and Cowte, T.G. (2002). Low preoperative HSP70 atrial myocardial levels correlate significantly with high incidence of postoperative atrial fibrillation after cardiac surgery. *Cardiovascular Surgery* 10, 228-232.

Stamm, C., Westphal, B., Kleine, H.D., Petzsch, M., Kittner, C., Klinge, H., Schumichen, C., Nienaber, C.A., Freund, M., and Steinhoff, G. (2003). Autologous bone-marrow stem-cell transplantation for myocardial regeneration. *Lancet* 361, 45-46.

Stanley, W.C., Recchia, F.A., and Lopaschuk, G.D. (2005). Myocardial substrate metabolism in the normal and failing heart. *Physiological Reviews* 85, 1093-1129.

Starling, R.C., Jessup, M., Oh, J.K., Sabbah, H.N., Acker, M.A., Mann, D.L., and Kubo, S.H. (2007). Sustained benefits of the CorCap Cardiac Support Device on left ventricular remodeling: three year follow-up results from the Acorn clinical trial. *Annals of Thoracic Surgery* 84, 1236-1242.

Stewart, S., MacIntyre, K., Capewell, S., and McMurray, J.J. (2003). Heart failure and the aging population: an increasing burden in the 21st century? *Heart* 89, 49-53.

Strauer, B.E., Brehm, M., Zeus, T., Kostering, M., Hernandez, A., Sorg, R.V., Kogler, G., and Wernet, P. (2002). Repair of infarcted myocardium by autologous intracoronary mononuclear bone marrow cell transplantation in humans. *Circulation* 106, 1913-1918.

Streit, S., Michalski, C.W., Erkan, M., Kleeff, J., and Friess, H. (2009). Northern blot analysis for detection and quantification of RNA in pancreatic cancer cells and tissues. *Nature Protocols* 4, 37-43.

Studer, R., Reinecke, H., Bilger, J., Eschenhagen, T., Bohm, M., Hasenfuss, G., Just, H., Holtz, J., and Drexler, H. (1994). Gene expression of the cardiac Na(+)-Ca²⁺ exchanger in end-stage human heart failure. *Circulation Research* 75, 443-453.

Sugden, P.H., and Clerk, A. (1998). Cellular mechanisms of cardiac hypertrophy. *Journal of Molecular Medicine* 76, 725-746.

Sullivan, J.L. (2003). Are menstruating women protected from heart disease because of, or in spite of, estrogen? Relevance to the iron hypothesis. *American Heart Journal* 145, 190-194.

Sullivan, M.J., Cobb, F.R., and Higginbotham, M.B. (1991). Stroke volume increases by similar mechanisms during upright exercise in normal men and women. *American Journal of Cardiology* 67, 1405-1412.

Sun, H., Chartier, D., Leblanc, N., and Nattel, S. (2001). Intracellular calcium changes and tachycardia-induced contractile dysfunction in canine atrial myocytes. *Cardiovascular Research* 49, 751-761.

Suurmeijer, A.J., Clement, S., Francesconi, A., Bocchi, L., Angelini, A., Van Veldhuisen, D.J., Spagnoli, L.G., Gabbiani, G., and Orlandi, A. (2003). Alpha-actin isoform distribution in normal and failing human heart: a morphological, morphometric, and biochemical study. *Journal of Pathology* 199, 387-397.

Suzuki, K., Imajoh, S., Emori, Y., Kawasaki, H., Minami, Y., and Ohno, S. (1987). Calcium-activated neutral protease and its endogenous inhibitor. Activation at the cell membrane and biological function. *FEBS Lett* 220, 271-277.

Swynghedauw, B. (1986). Developmental and functional adaptation of contractile proteins in cardiac and skeletal muscles. *Physiological Reviews* 66, 710-771.

Tachibana, H., Perrino, C., Takaoka, H., Davis, R.J., Naga Prasad, S.V., and Rockman, H.A. (2006). JNK1 is required to preserve cardiac function in the early response to pressure overload. *Biochemical & Biophysical Research Communications* 343, 1060-1066.

Takahashi, J., Kagaya, Y., Kato, I., Ohta, J., Isoyama, S., Miura, M., Sugai, Y., Hirose, M., Wakayama, Y., Ninomiya, M., Watanabe, J., Takasawa, S., Okamoto, H., and Shirato, K. (2003). Deficit of CD38/cyclic ADP-ribose is differentially compensated in hearts by gender. *Biochemical & Biophysical Research Communications* 312, 434-440.

Takeishi, Y., Ping, P., Bolli, R., Kirkpatrick, D.L., Hoit, B.D., and Walsh, R.A. (2000). Transgenic overexpression of constitutively active protein kinase C epsilon causes concentric cardiac hypertrophy. *Circulation Research* 86, 1218-1223.

Takeishi, Y., Huang, Q., Abe, J., Glassman, M., Che, W., Lee, J.D., Kawakatsu, H., Lawrence, E.G., Hoit, B.D., Berk, B.C., and Walsh, R.A. (2001). Src and multiple MAP kinase activation in cardiac hypertrophy and congestive heart failure under chronic pressure-overload: comparison with acute mechanical stretch. *Journal of Molecular & Cellular Cardiology* 33, 1637-1648.

Tamura, T., Said, S., and Gerdes, A.M. (1999). Gender-related differences in myocyte remodeling in progression to heart failure. *Hypertension* 33, 676-680.

Tanaka, M., Chen, Z., Bartunkova, S., Yamasaki, N., and Izumo, S. (1999). The cardiac homeobox gene *Csx/Nkx2.5* lies genetically upstream of multiple genes essential for heart development. *Development* 126, 1269-1280.

Tang, R.B., Liu, X.H., Kalifa, J., Li, Z.A., Dong, J.Z., Yang, Y., Liu, X.P., Long, D.Y., Yu, R.H., and Ma, C.S. (2009). Body mass index and risk of left atrial thrombus in patients with atrial fibrillation. *American Journal of Cardiology* 104, 1699-1703.

Tardiff, J.C., Hewett, T.E., Factor, S.M., Vikstrom, K.L., Robbins, J., and Leinwand, L.A. (2000). Expression of the beta (slow)-isoform of MHC in the adult mouse heart causes dominant-negative functional effects. *American Journal of Physiology - Heart & Circulatory Physiology* 278, H412-419.

Tavi, P., Han, C., and Weckstrom, M. (1998). Mechanisms of stretch-induced changes in $[Ca^{2+}]_i$ in rat atrial myocytes: role of increased troponin C affinity and stretch-activated ion channels. *Circulation Research* 83, 1165-1177.

Taylor, A.H., and Al-Azzawi, F. (2000). Immunolocalisation of oestrogen receptor beta in human tissues. *J Mol Endocrinol* 24, 145-155.

Taylor, D.A., Atkins, B.Z., Hungspreugs, P., Jones, T.R., Reedy, M.C., Hutcheson, K.A., Glower, D.D., and Kraus, W.E. (1998). Regenerating functional myocardium: improved performance after skeletal myoblast transplantation. *Nature Medicine* 4, 929-933.

Tcherepanova, I., Puigserver, P., Norris, J.D., Spiegelman, B.M., and McDonnell, D.P. (2000). Modulation of estrogen receptor-alpha transcriptional activity by the coactivator PGC-1. *Journal of Biological Chemistry* 275, 16302-16308.

Teiger, E., Than, V.D., Richard, L., Wisnewsky, C., Tea, B.S., Gaboury, L., Tremblay, J., Schwartz, K., and Hamet, P. (1996). Apoptosis in pressure overload-induced heart hypertrophy in the rat. *Journal of Clinical Investigation* 97, 2891-2897.

Temple, J., Frias, P., Rottman, J., Yang, T., Wu, Y., Verheijck, E.E., Zhang, W., Siprachanh, C., Kanki, H., Atkinson, J.B., King, P., Anderson, M.E., Kupersmidt, S., and

Roden, D.M. (2005). Atrial fibrillation in KCNE1-null mice. *Circulation Research* 97, 62-69.

Tepass, U., Truong, K., Godt, D., Ikura, M., and Peifer, M. (2000). Cadherins in embryonic and neural morphogenesis. *Nature Reviews Molecular Cell Biology* 1, 91-100.

Thom, T., Haase, N., Rosamond, W., Howard, V.J., Rumsfeld, J., Manolio, T., Zheng, Z.J., Flegal, K., O'Donnell, C., Kittner, S., Lloyd-Jones, D., Goff, D.C., Jr., Hong, Y., Adams, R., Friday, G., Furie, K., Gorelick, P., Kissela, B., Marler, J., Meigs, J., Roger, V., Sidney, S., Sorlie, P., Steinberger, J., Wasserthiel-Smoller, S., Wilson, M., Wolf, P., American Heart Association Statistics, C., and Stroke Statistics, S. (2006). Heart disease and stroke statistics--2006 update: a report from the American Heart Association Statistics Committee and Stroke Statistics Subcommittee. *Circulation* 113, 14.

Thomas, W.G., Brandenburger, Y., Autelitano, D.J., Pham, T., Qian, H., and Hannan, R.D. (2002). Adenoviral-directed expression of the type 1A angiotensin receptor promotes cardiomyocyte hypertrophy via transactivation of the epidermal growth factor receptor. *Circulation Research* 90, 135-142.

Thorburn, A., Thorburn, J., Chen, S.Y., Powers, S., Shubeita, H.E., Feramisco, J.R., and Chien, K.R. (1993). HRas-dependent pathways can activate morphological and genetic markers of cardiac muscle cell hypertrophy. *Journal of Biological Chemistry* 268, 2244-2249.

Thrall, G., Lane, D., Carroll, D., and Lip, G.Y. (2006). Quality of life in patients with atrial fibrillation: a systematic review. *American Journal of Medicine* 119, 448 e441-419.

Tobimatsu, T., and Fujisawa, H. (1989). Tissue-specific expression of four types of rat calmodulin-dependent protein kinase II mRNAs. *Journal of Biological Chemistry* 264, 17907-17912.

Toker, A., and Cantley, L.C. (1997). Signalling through the lipid products of phosphoinositide-3-OH kinase. *Nature* 387, 673-676.

Trombitas, K., Redkar, A., Centner, T., Wu, Y., Labeit, S., and Granzier, H. (2000). Extensibility of isoforms of cardiac titin: variation in contour length of molecular subsegments provides a basis for cellular passive stiffness diversity. *Biophysical Journal* 79, 3226-3234.

Tsai, C.T., Lai, L.P., Hwang, J.J., Lin, J.L., and Chiang, F.T. (2008). Molecular genetics of atrial fibrillation. *Journal of the American College of Cardiology* 52, 241-250.

Tsai, M.J., and O'Malley, B.W. (1994). Molecular mechanisms of action of steroid/thyroid receptor superfamily members. *Annu Rev Biochem* 63, 451-486.

Tsang, A., Hausenloy, D.J., Mocanu, M.M., Carr, R.D., and Yellon, D.M. (2005). Preconditioning the diabetic heart: the importance of Akt phosphorylation. *Diabetes* 54, 2360-2364.

Umana, E., Solares, C.A., and Alpert, M.A. (2003). Tachycardia-induced cardiomyopathy. *American Journal of Medicine* 114, 51-55.

Ura, S., Masuyama, N., Graves, J.D., and Gotoh, Y. (2001). MST1-JNK promotes apoptosis via caspase-dependent and independent pathways. *Genes to Cells* 6, 519-530.

Vaccarino, V., Krumholz, H.M., Yarzebski, J., Gore, J.M., and Goldberg, R.J. (2001). Sex differences in 2-year mortality after hospital discharge for myocardial infarction. *Annals of Internal Medicine* 134, 173-181.

van Bilsen, M., van Nieuwenhoven, F.A., and van der Vusse, G.J. (2009). Metabolic remodelling of the failing heart: beneficial or detrimental? *Cardiovascular Research* *81*, 420-428.

Van Der Heide, L.P., Hoekman, M.F., and Smidt, M.P. (2004). The ins and outs of FoxO shuttling: mechanisms of FoxO translocation and transcriptional regulation. *Biochemical Journal* *380*, 297-309.

van der Hooft, C.S., Heeringa, J., van Herpen, G., Kors, J.A., Kingma, J.H., and Stricker, B.H. (2004). Drug-induced atrial fibrillation. *Journal of the American College of Cardiology* *44*, 2117-2124.

van der Velden, H.M., Ausma, J., Rook, M.B., Hellemons, A.J., van Veen, T.A., Allessie, M.A., and Jongsma, H.J. (2000a). Gap junctional remodeling in relation to stabilization of atrial fibrillation in the goat. *Cardiovascular Research* *46*, 476-486.

van der Velden, H.M., van der Zee, L., Wijffels, M.C., van Leuven, C., Dorland, R., Vos, M.A., Jongsma, H.J., and Allessie, M.A. (2000b). Atrial fibrillation in the goat induces changes in monophasic action potential and mRNA expression of ion channels involved in repolarization. *Journal of Cardiovascular Electrophysiology* *11*, 1262-1269.

van der Vusse, G.J., Glatz, J.F., Stam, H.C., and Reneman, R.S. (1992). Fatty acid homeostasis in the normoxic and ischemic heart. *Physiological Reviews* *72*, 881-940.

van Eickels, M., Grohe, C., Cleutjens, J.P., Janssen, B.J., Wellens, H.J., and Doevendans, P.A. (2001). 17beta-estradiol attenuates the development of pressure-overload hypertrophy. *Circulation* *104*, 1419-1423.

Van Wagoner, D.R., Pond, A.L., Lamorgese, M., Rossie, S.S., McCarthy, P.M., and Nerbonne, J.M. (1999). Atrial L-type Ca²⁺ currents and human atrial fibrillation. *Circulation Research* *85*, 428-436.

Vandekerckhove, J., and Weber, K. (1979). The complete amino acid sequence of actins from bovine aorta, bovine heart, bovine fast skeletal muscle, and rabbit slow skeletal muscle. A protein-chemical analysis of muscle actin differentiation. *Differentiation* 14, 123-133.

Vandekerckhove, J., Bugaisky, G., and Buckingham, M. (1986). Simultaneous expression of skeletal muscle and heart actin proteins in various striated muscle tissues and cells. A quantitative determination of the two actin isoforms. *Journal of Biological Chemistry* 261, 1838-1843.

Vanhaesebroeck, B., Leeyers, S.J., Panayotou, G., and Waterfield, M.D. (1997). Phosphoinositide 3-kinases: a conserved family of signal transducers. *Trends in Biochemical Sciences* 22, 267-272.

Vasan, R.S., Sullivan, L.M., D'Agostino, R.B., Roubenoff, R., Harris, T., Sawyer, D.B., Levy, D., and Wilson, P.W. (2003). Serum insulin-like growth factor I and risk for heart failure in elderly individuals without a previous myocardial infarction: the Framingham Heart Study. *Annals of Internal Medicine* 139, 642-648.

Verheij, M., Bose, R., Lin, X.H., Yao, B., Jarvis, W.D., Grant, S., Birrer, M.J., Szabo, E., Zon, L.I., Kyriakis, J.M., Haimovitz-Friedman, A., Fuks, Z., and Kolesnick, R.N. (1996). Requirement for ceramide-initiated SAPK/JNK signalling in stress-induced apoptosis. *Nature* 380, 75-79.

Verheijck, E.E., van Kempen, M.J., Veereschild, M., Lurvink, J., Jongasma, H.J., and Bouman, L.N. (2001). Electrophysiological features of the mouse sinoatrial node in relation to connexin distribution. *Cardiovascular Research* 52, 40-50.

Verheule, S., van Kempen, M.J., te Welscher, P.H., Kwak, B.R., and Jongasma, H.J. (1997). Characterization of gap junction channels in adult rabbit atrial and ventricular myocardium. *Circulation Research* 80, 673-681.

Verheule, S., Sato, T., Everett, T., Engle, S.K., Otten, D., Rubart-von der Lohe, M., Nakajima, H.O., Nakajima, H., Field, L.J., and Olgin, J.E. (2004). Increased vulnerability to atrial fibrillation in transgenic mice with selective atrial fibrosis caused by overexpression of TGF-beta1. *Circulation Research* 94, 1458-1465.

Vermes, E., Tardif, J.C., Bourassa, M.G., Racine, N., Levesque, S., White, M., Guerra, P.G., and Ducharme, A. (2003). Enalapril decreases the incidence of atrial fibrillation in patients with left ventricular dysfunction: insight from the Studies Of Left Ventricular Dysfunction (SOLVD) trials. *Circulation* 107, 2926-2931.

Wakasaki, H., Koya, D., Schoen, F.J., Jirousek, M.R., D.K., W., B.D., H., Walsh, R.A., and G.L., K. (1997). Targeted overexpression of protein kinase C B2 isoform in myocardium causes cardiomyopathy. *Proceedings of the National Academy of Sciences of the United States of America* 94, 9320-9325.

Walker, S.E., McMurray, R.W., Besch-Williford, C.L., and Keisler, D.H. (1992). Premature death with bladder outlet obstruction and hyperprolactinemia in New Zealand black X New Zealand white mice treated with ethinyl estradiol and 17 beta-estradiol. *Arthritis & Rheumatism* 35, 1387-1392.

Wang, L., Gout, I., and Proud, C.G. (2001). Cross-talk between the ERK and p70 S6 kinase (S6K) signaling pathways. MEK-dependent activation of S6K2 in cardiomyocytes. *Journal of Biological Chemistry* 276, 32670-32677.

Wang, T.J., Parise, H., Levy, D., D'Agostino, R.B., Sr., Wolf, P.A., Vasan, R.S., and Benjamin, E.J. (2004). Obesity and the risk of new-onset atrial fibrillation. *Journal Of the American Medical Association* 292, 2471-2477.

Wang, Y., Huang, S., Sah, V.P., Ross, J., Jr., Brown, J.H., Han, J., and Chien, K.R. (1998a). Cardiac muscle cell hypertrophy and apoptosis induced by distinct members of the p38

mitogen-activated protein kinase family. *Journal of Biological Chemistry* 273, 2161-2168.

Wang, Y., Su, B., Sah, V.P., Brown, J.H., Han, J., and Chien, K.R. (1998b). Cardiac hypertrophy induced by mitogen-activated protein kinase kinase 7, a specific activator for c-Jun NH2-terminal kinase in ventricular muscle cells. *Journal of Biological Chemistry* 273, 5423-5426.

Wang, Y. (2007). Mitogen-activated protein kinases in heart development and diseases. *Circulation* 116, 1413-1423.

Wankerl, M., and Schwartz, K. (1995). Calcium transport proteins in the nonfailing and failing heart: gene expression and function. *Journal of Molecular Medicine* 73, 487-496.

Watanabe, K., Nair, P., Labeit, D., Kellermayer, M.S., Greaser, M., Labeit, S., and Granzier, H. (2002). Molecular mechanics of cardiac titin's PEVK and N2B spring elements. *Journal of Biological Chemistry* 277, 11549-11558.

Weber, K.T., Janicki, J.S., Shroff, S.G., Pick, R., Chen, R.M., and Bashey, R.I. (1988). Collagen remodeling of the pressure-overloaded, hypertrophied nonhuman primate myocardium. *Circulation Research* 62, 757-765.

Weber, K.T. (1989). Cardiac interstitium in health and disease: the fibrillar collagen network. *Journal of the American College of Cardiology* 13, 1637-1652.

Weber, K.T., Brilla, C.G., and Janicki, J.S. (1993). Myocardial fibrosis: functional significance and regulatory factors. *Cardiovascular Research* 27, 341-348.

Weinberg, E.O., Thienelt, C.D., Katz, S.E., Bartunek, J., Tajima, M., Rohrbach, S., Douglas, P.S., and Lorell, B.H. (1999). Gender differences in molecular remodeling in

pressure overload hypertrophy. *Journal of the American College of Cardiology* 34, 264-273.

Weiss, R.G., Gerstenblith, G., and Bottomley, P.A. (2005). ATP flux through creatine kinase in the normal, stressed, and failing human heart. *Proceedings of the National Academy of Sciences of the United States of America* 102, 808-813.

Welch, S., Plank, D., Witt, S., Glascock, B., Schaefer, E., Chimenti, S., Andreoli, A.M., Limana, F., Leri, A., Kajstura, J., Anversa, P., and Sussman, M.A. (2002). Cardiac-specific IGF-1 expression attenuates dilated cardiomyopathy in tropomodulin-overexpressing transgenic mice. *Circulation Research* 90, 641-648.

Wellens, H.J. (2000). Pulmonary vein ablation in atrial fibrillation: hype or hope? *Circulation* 102, 2562-2564.

Wencker, D., Chandra, M., Nguyen, K., Miao, W., Garantziotis, S., Factor, S.M., Shirani, J., Armstrong, R.C., and Kitsis, R.N. (2003). A mechanistic role for cardiac myocyte apoptosis in heart failure. *Journal of Clinical Investigation* 111, 1497-1504.

Wettschureck, N., Rutten, H., Zywietz, A., Gehring, D., Wilkie, T.M., Chen, J., Chien, K.R., and Offermanns, S. (2001). Absence of pressure overload induced myocardial hypertrophy after conditional inactivation of Galphaq/Galphan1 in cardiomyocytes. *Nature Medicine* 7, 1236-1240.

Wheatley, W.B. (1951). A rapid staining procedure for intestinal amoebae and flagellates. *American Journal of Clinical Pathology* 21, 990-991.

Whitman, M., Downes, C.P., Keeler, M., Keller, T., and Cantley, L. (1988). Type I phosphatidylinositol kinase makes a novel inositol phospholipid, phosphatidylinositol-3-phosphate. *Nature* 332, 644-646.

Wijffels, M.C., Kirchhof, C.J., Dorland, R., and Allessie, M.A. (1995). Atrial fibrillation begets atrial fibrillation. A study in awake chronically instrumented goats. *Circulation* 92, 1954-1968.

Wilkins, B.J., Dai, Y.S., Bueno, O.F., Parsons, S.A., Xu, J., Plank, D.M., Jones, F., Kimball, T.R., and Molkenin, J.D. (2004). Calcineurin/NFAT coupling participates in pathological, but not physiological, cardiac hypertrophy. *Circulation Research* 94, 110-118.

Willenheimer, R., van Veldhuisen, D.J., Silke, B., Erdmann, E., Follath, F., Krum, H., Ponikowski, P., Skene, A., van de Ven, L., Verkenne, P., and Lechat, P. (2005). Effect on survival and hospitalization of initiating treatment for chronic heart failure with bisoprolol followed by enalapril, as compared with the opposite sequence: results of the randomized Cardiac Insufficiency Bisoprolol Study (CIBIS) III. *Circulation* 112, 2426-2435.

Wilson, E.M., and Spinale, F.G. (2001). Myocardial remodelling and matrix metalloproteinases in heart failure: turmoil within the interstitium. *Annals of Medicine* 33, 623-634.

Wilson, K.P., Fitzgibbon, M.J., Caron, P.R., Griffith, J.P., Chen, W., McCaffrey, P.G., Chambers, S.P., and Su, M.S. (1996). Crystal structure of p38 mitogen-activated protein kinase. *Journal of Biological Chemistry* 271, 27696-27700.

Winegrad, S., Wisnewsky, C., and Schwartz, K. (1990). Effect of thyroid hormone on the accumulation of mRNA for skeletal and cardiac alpha-actin in hearts from normal and hypophysectomized rats. *Proceedings of the National Academy of Sciences of the United States of America* 87, 2456-2460.

Wing, L.M., Reid, C.M., Ryan, P., Beilin, L.J., Brown, M.A., Jennings, G.L., Johnston, C.I., McNeil, J.J., Macdonald, G.J., Marley, J.E., Morgan, T.O., and West, M.J. (2003). A

comparison of outcomes with angiotensin-converting-enzyme inhibitors and diuretics for hypertension in the elderly. *New England Journal of Medicine* 348, 583-592.

Woessner, J.F., Jr. (1995). Quantification of matrix metalloproteinases in tissue samples. *Methods in Enzymology* 248, 510-528.

Wuytack, F., Raeymaekers, L., and Missiaen, L. (2002). Molecular physiology of the SERCA and SPCA pumps. *Cell Calcium* 32, 279-305.

Wynn, T.A. (2008). Cellular and molecular mechanisms of fibrosis. *Journal of Pathology* 214, 199-210.

Xia, Z., Dickens, M., Raingeaud, J., Davis, R.J., and Greenberg, M.E. (1995). Opposing effects of ERK and JNK-p38 MAP kinases on apoptosis. *Science* 270, 1326-1331.

Xiao, H.D., Fuchs, S., Campbell, D.J., Lewis, W., Dudley, S.C., Jr., Kasi, V.S., Hoit, B.D., Keshelava, G., Zhao, H., Capecchi, M.R., and Bernstein, K.E. (2004). Mice with cardiac-restricted angiotensin-converting enzyme (ACE) have atrial enlargement, cardiac arrhythmia, and sudden death. *American Journal of Pathology* 165, 1019-1032.

Xin, H.B., Senbonmatsu, T., Cheng, D.S., Wang, Y.X., Copello, J.A., Ji, G.J., Collier, M.L., Deng, K.Y., Jeyakumar, L.H., Magnuson, M.A., Inagami, T., Kotlikoff, M.I., and Fleischer, S. (2002). Oestrogen protects FKBP12.6 null mice from cardiac hypertrophy. *Nature* 416, 334-338.

Xu, J., Cui, G., Esmailian, F., Plunkett, M., Marelli, D., Ardehali, A., Odum, J., Laks, H., and Sen, L. (2004). Atrial extracellular matrix remodeling and the maintenance of atrial fibrillation. *Circulation* 109, 363-368.

Xu, Y., Arenas, I.A., Armstrong, S.J., and Davidge, S.T. (2003). Estrogen modulation of left ventricular remodeling in the aged heart. *Cardiovascular Research* 57, 388-394.

Yamamoto, S., Yang, G., Zablocki, D., Liu, J., Hong, C., Kim, S.J., Soler, S., Odashima, M., Thaisz, J., Yehia, G., Molina, C.A., Yatani, A., Vatner, D.E., Vatner, S.F., and Sadoshima, J. (2003). Activation of Mst1 causes dilated cardiomyopathy by stimulating apoptosis without compensatory ventricular myocyte hypertrophy. *Journal of Clinical Investigation* 111, 1463-1474.

Yamazaki, T., Suzuki, J., Shimamoto, R., Tsuji, T., Ohmoto-Sekine, Y., Ohtomo, K., and Nagai, R. (2007). A new therapeutic strategy for hypertrophic nonobstructive cardiomyopathy in humans. A randomized and prospective study with an Angiotensin II receptor blocker. *International Heart Journal* 48, 715-724.

Yaoita, H., and Maruyama, Y. (2008). Intervention for apoptosis in cardiomyopathy. *Heart Failure Reviews* 13, 181-191.

Yue, L., Melnyk, P., Gaspo, R., Wang, Z., and Nattel, S. (1999). Molecular mechanisms underlying ionic remodeling in a dog model of atrial fibrillation. *Circulation Research* 84, 776-784.

Zak, R. (1974). Development and proliferative capacity of cardiac muscle cells. *Circulation Research* 35, suppl II:17-26.

Zak, R. (1984). *Growth of the heart in health and disease* (New York, Raven Press).

Zannad, F., Briancon, S., Juilliere, Y., Mertes, P.M., Villemot, J.P., Alla, F., and Virion, J.M. (1999). Incidence, clinical and etiologic features, and outcomes of advanced chronic heart failure: the EPICAL Study. *Epidemiologie de l'Insuffisance Cardiaque Avancee en Lorraine. Journal of the American College of Cardiology* 33, 734-742.

Zannad, F., Agrinier, N., and Alla, F. (2009). Heart failure burden and therapy. *Europace* 11 Suppl 5, v1-9.

Zhai, P., Eurell, T.E., Cooke, P.S., Lubahn, D.B., and Gross, D.R. (2000). Myocardial ischemia-reperfusion injury in estrogen receptor-alpha knockout and wild-type mice. *American Journal of Physiology - Heart & Circulatory Physiology* 278, H1640-1647.

Zhang, C.L., McKinsey, T.A., Chang, S., Antos, C.L., Hill, J.A., and Olson, E.N. (2002). Class II histone deacetylases act as signal-responsive repressors of cardiac hypertrophy. *Cell* 110, 479-488.

Zhang, D., Gaussin, V., Taffet, G.E., Belaguli, N.S., Yamada, M., Schwartz, R.J., Michael, L.H., Overbeek, P.A., and Schneider, M.D. (2000). TAK1 is activated in the myocardium after pressure overload and is sufficient to provoke heart failure in transgenic mice. *Nature Medicine* 6, 556-563.

Zhang, R., Khoo, M.S., Wu, Y., Yang, Y., Grueter, C.E., Ni, G., Price, E.E., Jr., Thiel, W., Guatimosim, S., Song, L.S., Madu, E.C., Shah, A.N., Vishnivetskaya, T.A., Atkinson, J.B., Gurevich, V.V., Salama, G., Lederer, W.J., Colbran, R.J., and Anderson, M.E. (2005a). Calmodulin kinase II inhibition protects against structural heart disease. *Nature Medicine* 11, 409-417.

Zhang, S., Weinheimer, C., Courtois, M., Kovacs, A., Zhang, C.E., Cheng, A.M., Wang, Y., and Muslin, A.J. (2003a). The role of the Grb2-p38 MAPK signaling pathway in cardiac hypertrophy and fibrosis. *Journal of Clinical Investigation* 111, 833-841.

Zhang, T., Maier, L.S., Dalton, N.D., Miyamoto, S., Ross, J., Jr., Bers, D.M., and Brown, J.H. (2003b). The deltaC isoform of CaMKII is activated in cardiac hypertrophy and induces dilated cardiomyopathy and heart failure. *Circulation Research* 92, 912-919.

Zhang, X., Chen, S., Yoo, S., Chakrabarti, S., Zhang, T., Ke, T., Oberti, C., Yong, S.L., Fang, F., Li, L., de la Fuente, R., Wang, L., Chen, Q., and Wang, Q.K. (2008). Mutation in nuclear pore component NUP155 leads to atrial fibrillation and early sudden cardiac death. *Cell* 135, 1017-1027.

Zhang, Z., He, Y., Tuteja, D., Xu, D., Timofeyev, V., Zhang, Q., Glatzer, K.A., Xu, Y., Shin, H.S., Low, R., and Chiamvimonvat, N. (2005b). Functional roles of Cav1.3(alpha1D) calcium channels in atria: insights gained from gene-targeted null mutant mice. *Circulation* *112*, 1936-1944.

Zile, M.R., Green, G.R., Schuyler, G.T., Aurigemma, G.P., Miller, D.C., and Cooper, G. (2001). Cardiocyte cytoskeleton in patients with left ventricular pressure overload hypertrophy. *Journal of the American College of Cardiology* *37*, 1080-1084.

Zipes, D.P., Libby, P., Bonow, R.O., and Braunwald, E. (2005). *Braunwald's Heart Disease: A Textbook Of Cardiovascular Medicine Seventh Edition* (Philadelphia, Elsevier Saunders).

Zou, Y., Hiroi, Y., Uozumi, H., Takimoto, E., Toko, H., Zhu, W., Kudoh, S., Mizukami, M., Shimoyama, M., Shibasaki, F., Nagai, R., Yazaki, Y., and Komuro, I. (2001). Calcineurin plays a critical role in the development of pressure overload-induced cardiac hypertrophy. *Circulation* *104*, 97-101.

Appendix 1

Table 32. Effect of ovariectomy on organ weights of transgenic mice at 4-4.5 months of age (complete statistics presented).

OVX: ovariectomy (4-4.5 months of age); Non-op: non-operated control (4 months of age); N/A: not assessed; BW - Start: body weight prior to surgery; BW – End: body weight at end of study; TL: tibia length; HW/BW: heart weight/body weight ratio; HW/TL: heart weight/tibia length ratio; AW/TL: atrial weight/tibia length ratio; LW/TL: lung weight/tibia length ratio; and UW/TL: uterus weight/tibia length ratio. ~ $p < 0.05$ compared with sham or Non-op control; * $p < 0.05$ compared with Ntg that underwent the same procedure; ‡ $p < 0.05$ compared with caPI3K that underwent the same procedure; ^ $p < 0.05$ compared with dnPI3K Non-OVX control; ℓ $p < 0.05$ compared with dnPI3K OVX; # $p < 0.05$ compared with Mst1 that underwent the same procedure; and † $p < 0.05$ compared with caPI3K-Mst1 that underwent the same procedure.

	Proce- dure	N	BW – Start (g)	BW – End (g)	TL (mm)	Heart weight (mg)	HW/TL (mg/mm)	Atrial weight (mg)	AW/TL (mg/mm)	Lung weight (mg)	LW/TL (mg/mm)	Uterus weight (mg)	UW/TL (mg/mm)
Ntg	Sham	11	16.4±0.7	29.2±1.4	17.0±0.1	116.6±2.9	6.84±0.15	6.4±0.3	0.38±0.02	154.0±3.9	9.04±0.21	122.1±16.5	7.17±0.97
	OVX	13	16.0±0.6	35.6±1.5~	17.1±0.1	112.9±3.5	6.59±0.17	5.6±0.2	0.33±0.01	153.0±3.5	8.93±0.16	11.0±0.7~	0.64±0.04~
caPI3K	Sham	7	15.2±0.5	26.3±0.8	17.0±0.1	137.3±2.4*	8.07±0.12*	5.9±0.3	0.35±0.02	154.2±5.6	9.07±0.31	92.2±10.8*	5.43±0.64*
	OVX	5	14.9±0.5	34.8±1.4~	16.9±0.1	131.9±3.3*	7.80±0.16*	5.9±0.4	0.35±0.02	150.5±2.6	8.90±0.13	9.2±0.8~	0.54±0.05~
dnPI3K	Non- op	10	N/A	25.2±0.3	17.0±0.1	88.6±1.2*‡	5.21±0.06*‡	4.2±0.2	0.25±0.01	143.1±1.7	8.42±0.12	N/A	N/A
	OVX	4	15.8±0.5	31.8±2.2~	17.0±0.3	80.9±1.5*‡	4.76±0.06*‡	3.9±0.5	0.23±0.03	148.5±6.8	8.73±0.28	10.7±1.4	0.63±0.09
Mst1	Sham	5	17.3±1.1	30.4±1.3^	17.3±0.1	136.1±2.8*^	7.89±0.14*^	14.4±1.5*‡^	0.83±0.09*‡^	180.7±7.6*‡^	10.48±0.43*‡^	106.6±8.1	6.18±0.46
	OVX	9	15.4±0.6	35.5±1.7~	17.2±0.2	122.2±4.9~*ℓ	7.08±0.23~*ℓ	12.6±0.9§*‡ℓ	0.73±0.05§*‡ℓ	161.8±8.2~	9.38±0.43~	12.4±1.2~	0.72±0.07~
caPI3K- Mst1	Sham	3	15.7±1.2	27.2±0.7	17.2±0.1	132.3±2.1*^	7.69±0.12*^	13.5±0.5*‡^	0.79±0.03*‡^	172.8±2.9*‡^	10.05±0.23*‡^	83.1±4.6*	4.84±0.30*
	OVX	6	15.5±0.7	34.7±2.0~	17.2±0.1	125.9±5.1*ℓ	7.33±0.28*ℓ	12.3±0.6*‡ℓ	0.72±0.04*‡ℓ	166.1±4.2	9.68±0.23	8.4±1.2~	0.49±0.07~
dnPI3K- Mst1	Sham	5	16.0±1.0	27.3±0.9	17.1±0.2	125.0±5.8^	7.29±0.27‡^	14.6±1.6*‡^	0.85±0.08*‡^	182.8±10.3*‡^	10.67±0.52*‡^	128.6±6.8‡†	7.51±0.38‡†
	OVX	7	16.4±0.7	39.1±1.9~	17.5±0.1	130.1±6.9*^	7.42±0.37*^	16.5±1.7*‡ℓ	0.94±0.09*‡ℓ	176.9±6.6*‡ℓ	10.10±0.35*‡ℓ	13.7±1.5~	0.78±0.08~

Appendix 2

Table 33. Effect of estrogen replacement on organ weights of ovariectomised transgenic mice (complete statistics presented).

OVX: ovariectomy (4-4.5 months of age); OVX+ERT: ovariectomy followed by estrogen replacement therapy (3-3.5 months of age); N/A: not assessed; BW - Start: body weight prior to surgery; BW – End: body weight at end of study; TL: tibia length; HW/BW: heart weight/body weight ratio; HW/TL: heart weight/tibia length ratio; AW/TL: atrial weight/tibia length ratio; LW/TL: lung weight/tibia length ratio; and UW/TL: uterus weight/tibia length ratio. ~ $p < 0.05$ compared with sham; § $p < 0.05$ compared with OVX; * $p < 0.05$ compared with Ntg that underwent the same procedure; # $p < 0.05$ compared with Mst1 that underwent the same procedure; and † $p < 0.05$ compared with caPI3K-Mst1 that underwent the same procedure.

	Procedure	N	BW – Start (g)	BW – End (g)	TL (mm)	Heart weight (mg)	HW/TL (mg/mm)	Atrial weight (mg)	AW/TL (mg/mm)	Lung weight (mg)	LW/TL (mg/mm)	Uterus weight (mg)	UW/TL (mg/mm)
Ntg	Sham	11	16.4±0.7	29.2±1.4	17.0±0.1	116.6±2.9	6.84±0.15	6.4±0.3	0.38±0.02	154.0±3.9	9.04±0.21	122.1±16.5	7.17±0.97
	OVX	13	16.0±0.6	35.6±1.5~	17.1±0.1	112.9±3.5	6.59±0.17	5.6±0.2	0.33±0.01	153.0±3.5	8.93±0.16	11.0±0.7~	0.64±0.04~
	OVX+ERT	3	16.2±0.7	21.5±0.8~§	15.5±0.1~§	88.1±2.7~§	5.69±0.12	5.2±0.9	0.33±0.06	124.0±4.7~§	8.02±0.23	84.0±18.1§	5.42±1.15§
Mst1	Sham	5	17.3±1.1	30.4±1.3	17.3±0.1	136.1±2.8*	7.89±0.14*	14.4±1.5*	0.83±0.09*	180.7±7.6*	10.48±0.43*	106.6±8.1	6.18±0.46
	OVX	9	15.4±0.6	35.5±1.7~	17.2±0.2	122.2±4.9~*	7.08±0.23~	12.6±0.9*	0.73±0.05*	161.8±8.2~	9.38±0.43~	12.4±1.2~	0.72±0.07~
	OVX+ERT	2	16.8	25.9	15.9	134.5	8.50	15.1	0.94	196.6	12.44	95.6	5.95
caPI3K-Mst1	Sham	3	15.7±1.2	27.2±0.7	17.2±0.1	132.3±2.1*	7.69±0.12*	13.5±0.5*	0.79±0.03*	172.8±2.9*	10.05±0.23*	83.1±4.6*	4.84±0.30*
	OVX	6	15.5±0.7	34.7±2.0~	17.2±0.1	125.9±5.1*	7.33±0.28*	12.3±0.6*	0.72±0.04*	166.1±4.2	9.68±0.23	8.4±1.2~	0.49±0.07~
	OVX+ERT	6	14.4±1.1	22.6±0.6§	15.4±0.3~§	111.1±4.2	7.22±0.23*	11.7±0.8*	0.76±0.05*	142.2±4.6~§	9.24±0.23	96.6±21.0§	6.27±1.53§
dnPI3K-Mst1	Sham	5	16.0±1.0	27.3±0.9	17.1±0.2	125.0±5.8	7.29±0.27	14.6±1.6*	0.85±0.08*	182.8±10.3*	10.67±0.52*	128.6±6.8†	7.51±0.38†
	OVX	7	16.4±0.7	39.1±1.9~	17.5±0.1*	130.1±6.9*	7.42±0.37*	16.5±1.7*	0.94±0.09*	176.9±6.6*	10.10±0.35*	13.7±1.5~	0.78±0.08~
	OVX+ERT	4	18.3±1.5	23.0±0.8§	15.7±0.2~§	141.1±18.5*†	9.01±1.19*†	21.3±7.1*†	1.35±0.43*†	165.3±16.5*†	10.53±0.96*†	54.1±4.2~§†	3.45±0.24~§†

Note: Data for sham and OVX mice from each group are the same as shown in Table 30.

Appendix 3

Table 34. Cardiac chamber dimensions of transgenic mice following ovariectomy and estrogen replacement.

OVX: ovariectomy; OVX+ERT: ovariectomy followed by estrogen replacement therapy; LVESD: left ventricular end-systolic dimension; LVEDD: left ventricular end-diastolic dimension; LVPW: left ventricular posterior wall thickness; and IVS: interventricular septal width. ~ $p < 0.05$ compared with sham; § $p < 0.05$ compared with OVX; * $p < 0.05$ compared Ntg mice that underwent the same procedure; and † $p < 0.05$ compared with caPI3K-Mst1 that underwent the same procedure.

	Procedure	N	Tibia Length (mm)	Heart Rate (beats per minute)	LVESD (mm)	LVEDD (mm)	LVPW (mm)	IVS (mm)	Fractional shortening (%)
Ntg	Sham	5	17.1 ± 0.1	536 ± 4	1.88 ± 0.12	3.77 ± 0.21	0.74 ± 0.07	0.93 ± 0.03	50 ± 1
	OVX	5	16.9 ± 0.3	535 ± 19	1.66 ± 0.14	3.56 ± 0.08	0.76 ± 0.04	0.95 ± 0.04	54 ± 3
	OVX+ERT	3	15.9 ± 0.4 ~§	466 ± 17 ~§	1.91 ± 0.14	3.89 ± 0.14	0.87 ± 0.04	0.99 ± 0.02	51 ± 2
Mst1	Sham	5	17.3 ± 0.1	504 ± 22	2.83 ± 0.13 *	4.10 ± 0.13	0.73 ± 0.05	0.66 ± 0.09 *	31 ± 1 *
	OVX	7	17.1 ± 0.2	523 ± 14	2.65 ± 0.17 *	4.19 ± 0.19 *	0.77 ± 0.05	0.68 ± 0.07 *	37 ± 2 ~*
	OVX+ERT	2	15.9	351	2.86	4.29	0.63	0.63	33
caPI3K-Mst1	Sham	4	17.2 ± 0.1 (n=3)	491 ± 4	2.88 ± 0.20 *	4.54 ± 0.26 *	0.75 ± 0.11	0.80 ± 0.13	37 ± 2 *
	OVX	3	17.1 ± 0.2	547 ± 19	2.76 ± 0.14 *	4.21 ± 0.17 *	0.86 ± 0.07	0.73 ± 0.11 *	34 ± 1 *
	OVX+ERT	6	15.4 ± 0.3 ~§	377 ± 31 ~§	2.82 ± 0.05 *	4.47 ± 0.08 †	0.70 ± 0.05 *	0.65 ± 0.04 *	37 ± 1 *
dnPI3K-Mst1	Sham	5	17.1 ± 0.2	503 ± 16	3.59 ± 0.29 *†	4.80 ± 0.16 *	0.54 ± 0.07 *†	0.60 ± 0.07 *	26 ± 4 *†
	OVX	4	17.6 ± 0.1 *	528 ± 11	3.28 ± 0.31 *	4.63 ± 0.29 *	0.50 ± 0.05 *†	0.67 ± 0.08 *	30 ± 2 *
	OVX+ERT	2	15.1	408	3.57	4.82	0.33	0.30	26

Note: Data for sham and OVX mice from each group are the same as shown in Table 29.

Addendum

Page 90, Lines 13-15

The first 2 sentences of paragraph 2 are replaced with:

Chloroform (0.2ml per 1ml of Trizol) was added to each tube and the tubes shaken vigorously. The tubes were incubated at RT for 3 minutes and centrifuged at 4°C for 15 minutes at 10,000 rpm. The aqueous phase (containing the RNA) was transferred into a new tube (approximately 0.65ml per sample) and 0.5ml of isopropanol was added to each tube to precipitate the RNA. The tubes were incubated at RT for 10 minutes and centrifuged at 4°C for 10 minutes at 10,000 rpm.